# Influence of Succinimide Dispersants on Film Formation, Friction and Antiwear Properties of Zinc Dialkyl Dithiophosphate

by

## Jie Zhang

**A Thesis submitted to Imperial College London in fulfilment of the degree of Doctor of Philosophy and the diploma of Imperial College London**

**July 2010**

**Tribology Group**
**Department of Mechanical Engineering**
**The Imperial College of Science, Technology and Medicine**
**London**

**Abstract**

ZDDP (zinc dialkyldithiophosphate) is arguably the most successful antiwear additive ever employed in crankcase engine lubricants. It was originally used as an antioxidant and shortly afterwards recognized for its antiwear and extreme pressure properties. Unfortunately, another critical additive polyisobutylsuccinimide-polyamine (PIBSA-PAM), which is used as a dispersant in engine oils, is known to be antagonistic to ZDDP in terms of film formation, friction and wear. The mechanisms of this antagonism have been widely studied, but they are still not well understood. Furthermore, in order to protect engine exhaust catalysts from sulphated ash, phosphorus and sulphur (SAPS) and extend drain intervals of engine lubricants, a progressive reduction in ZDDP quantity but a growth in the use of PIBSA-PAM is required. The aim of this study is to explore the mechanisms and practical effects of the antagonism between ZDDP and PIBSA-PAM. Of particular interest is the impact on performance of the ratio of ZDDP to PIBSA-PAM, as measured by P:N ratio. Since ZDDP is a very effective antiwear additive, it produces only very low or "mild" rates of wear. To study this requires a new way to measure mild wear behaviour of formulated oils.

Several techniques have been applied in this study to investigate the film formation, friction and wear properties of ZDDP- and/or PIBSA-PAM-containing oils. These include a new mild wear testing method, which is tested and developed using a range of different types of additives.

It is found that the ratio of P:N plays a strong role in determining tribofilm formation and friction of ZDDP/PIBSA-PAM blends. However it plays a much weaker role in determining wear behaviour. It is found that some PIBSA-PAMs have considerable friction-reducing properties in their own right. The results suggest that PIBSA-PAM may interfere with the behaviour of ZDDP in several ways: by forming a ZDDP/ PIBSA-PAM complex at the metal surfaces to reduce the local activity of ZDDP; by PIBSA-PAM partially removing the ZDDP film; possibly also by PIBSA-PAM blocking ZDDP from metal surfaces. The newly-developed wear testing method can be used conveniently and effectively to study mild wear properties not just of ZDDP but of a wide range of other additives.

# Acknowledgements

First and foremost, I want to thank my supervisor Hugh Spikes, for everything he has done to support my research and thesis-writing. I would have been lost without his immense knowledge, patience, encouragement, sound advice. I would like to say that I am so honoured having this opportunity to work with you and I have learned so much from you indeed.

I also wish to express my warm and sincere thanks to all the academic staff in Tribology Group, Professor Andrew Olver, Dr. Richard Sayles, Dr. Daniele Dini, Dr. Philippa Cann and Dr. Janet Wong for important guidance and insightful comments. My sincere appreciation also goes to Chrissy Stevens and Paul Jobson for their supportive work.

In particular, I want to thank my sponsor, Chevron Oronite Company LLC. for the generous financial support. My keen appreciation goes to Professor Elaine Yamaguchi for your valuable instructions and suggestions that improved the quality of this study. I am also grateful to Chengbiao Wang, Danping Wei and Jiajun Liu, who have educated me and opened a door to academia for me when I was studying for my Master degree in China.

I am indebted to all labmates for providing me a friendly and stimulating environment in which to learn and enjoy. Thank you for every pleasant moment sporting, chatting, drinking and working together! I specially thank Tina for all your help, as well as too many others.

My deepest gratitude and love also give to my families.

# Table of Contents

# List of Figures

11

# List of Tables

# Chapter 1 Introduction

The automotive industry is facing increasingly rigorous government regulations on improving fuel economy and lowering emissions of engines. In order to tackle this, functional engine oil additives, which are formulated with base oil to form a complete package, need to be highly developed to meet the greater demands on the performance of engine lubricants.

Most of today's engine oils contain several critical lubricant additives, including an antiwear additive, dispersant, detergent, friction modifier, viscosity index improver and antioxidant. The most cost-effective antiwear additive is generally thought to be zinc dialkyl dithiophosphate (ZDDP) which forms boundary films on rubbing surfaces and thus protects engine components from wear. Polyisobutylsuccinimide-polyamine (PIBSA-PAM), which acts as a dispersant, is used to limit the agglomeration of engine soot by stabilizing soot particles in suspension in the lubricant. Unfortunately PIBSA-PAM is also known to be quite antagonistic to ZDDP in the latter's performance in engine lubrication.

In order to investigate the mechanisms of antagonism between ZDDP and PIBSA-PAM, several advanced techniques are used in this thesis to measure the influence of PIBSA-PAM on the film formation and friction properties of ZDDP. A new wear test method has also been developed to study the effects of PIBSA-PAM on the wear properties of ZDDP, as well as other additives under mild conditions.

Therefore, this research aims to study the influence of PIBSA-PAM on film formation, friction and wear properties of ZDDP; and to develop a new mild wear test method which can be applied to different lubricants. This can be formalised into the following objectives:

- To investigate the influence of different types of dispersants on the film formation and friction properties of ZDDP and explore the mechanisms of antagonism between ZDDP and dispersants

- To develop a new wear test under mild wear conditions and apply it to the study on the wear properties of ZDDP and dispersant-containing oils

- To apply this developed mild wear test method to study the wear properties of lubricants doped with several types of additives with and without ZDDP

This thesis begins in Chapter 2 with an introduction to boundary lubrication, which includes a description of current understanding of boundary lubrication and then outlines analytical methods for investigating boundary lubrication films. It then lists the additives used in engine lubricants to form boundary films.

Chapter 3 reviews our existing understanding of ZDDP and dispersant additives, following a review of the interactions between them. Chapter 4 focuses on wear tests methods - explains what mild wear is and the various methods of measuring (mild) wear.

In Chapter 5, the methods applied in this study are described in detail. MTM-SLIM, MTM-reciprocating, HFRR rigs and their use in this study are presented. This is followed by a brief introduction to two surface analysis tools – scanning white light interferometry (SWLI) and atomic force microscopy (AFM), and a list of the lubricants and additives tested in this study.

Chapter 6 describes, step by step, the development of a new mild wear test method. It explains why this study focuses on methods of measuring small amount of wear under pure sliding or mixed rolling/sliding conditions when thick ZDDP boundary film are present and also how to measure the small amount of wear.

Chapter 7 presents film forming and friction measurements using lubricant blends containing ZDDP and dispersants separately and in combination. It then investigates the influence of dispersants on the ZDDP boundary film in terms of film removal and friction. Chapter 8 describes a study on the wear properties of the solutions mostly tested in the previous chapter. The final results chapter, Chapter 9 describes the film formation and friction properties, and the application of the new mild wear test method to other functional lubricant additives such as detergents and friction modifiers, with and without ZDDP.

Chapter 10 discusses possible mechanisms for mechanisms of the antagonism between ZDDP and dispersant by summarizing the experimental results in combination with the literature. The results of wear tests are also summarized in this chapter which leads to the suggestions

for improving this wear test method. Finally in Chapter 11 it presents a brief list of the conclusions from the overall study and suggests some directions for the future research in this area.

# Chapter 2 Literature Review – Boundary Lubrication

Boundary lubrication occurs when rubbing systems are operating under relatively severe conditions, such as at low entrainment speed, with low viscosity oils or at a combination of high load and sliding speed. It is often associated with high friction and wear rates. Boundary additives, such as the additive ZDDP studied in this study, are capable of forming films on rubbing surfaces to reduce friction or resist wear. This chapter reviews the research on boundary lubrication, boundary additives, boundary films and various methods to study boundary lubrication.

## 2.1 Boundary Lubrication

### 2.1.1 Introduction

When two rubbing components are being lubricated by a liquid, three different regimes of lubrication can be observed, classified as fluid film lubrication, mixed lubrication and boundary lubrication [1]. Among these three main regimes, boundary lubrication generally occurs at relatively severe operating conditions, *e.g.* at very low entrainment speed, or at very high load or with very low viscosity fluids.

In boundary lubrication, lubricant additives play a key role since they contribute to the formation of boundary films. Additives acting on the surfaces to modify friction or improve surface durability during rubbing are described as 'boundary lubricating additives'. Both boundary additives and boundary films need to be characterized with a wide range of advanced techniques. The antiwear additive ZDDP of particular interest in this study is one type of boundary lubricating additive.

Over the last decade, boundary lubrication has been studied thoroughly but is still not very clearly understood. The main difficulties are: firstly, boundary lubrication involves the properties and variation of very thin layers, which are difficult to measure scientifically or analyze theoretically; secondly, boundary lubrication relates to so many factors, *e.g.* geometrical, physical and chemical nature of metal surface, impurity in lubricating oils, temperature, humidity, oxygen availability, *etc.*; thirdly, boundary lubrication usually involves several mechanisms which interact with each other.

Initially, analytical study carried out on boundary lubrication films was applied to rubbed surfaces which had been removed from rubbing contact, and the lubricating oil washed off. However there was a probability that some boundary lubricating films of interest would also be washed from rubbed surfaces using this type of approach. In the 1980s, more advanced methods were developed to study boundary films in-situ, either within rubbing contacts or at least submerged in the lubricant within which the film was formed.

## 2.1.2 Definition of Boundary Lubrication

Stribeck curve

The transitions between the different lubrication regimes, from fluid film lubrication to boundary lubrication, are often represented by the Stribeck curve [2]. In the classical form, as shown in Figure 2.1, friction coefficient is presented as a function of the service parameters that control fluid film thickness, including speed, load and lubricant viscosity. Nowadays, the term 'Stribeck curve' has been extended to describe any plot showing how friction coefficient varies with either fluid film thickness or the operating parameters that control it.
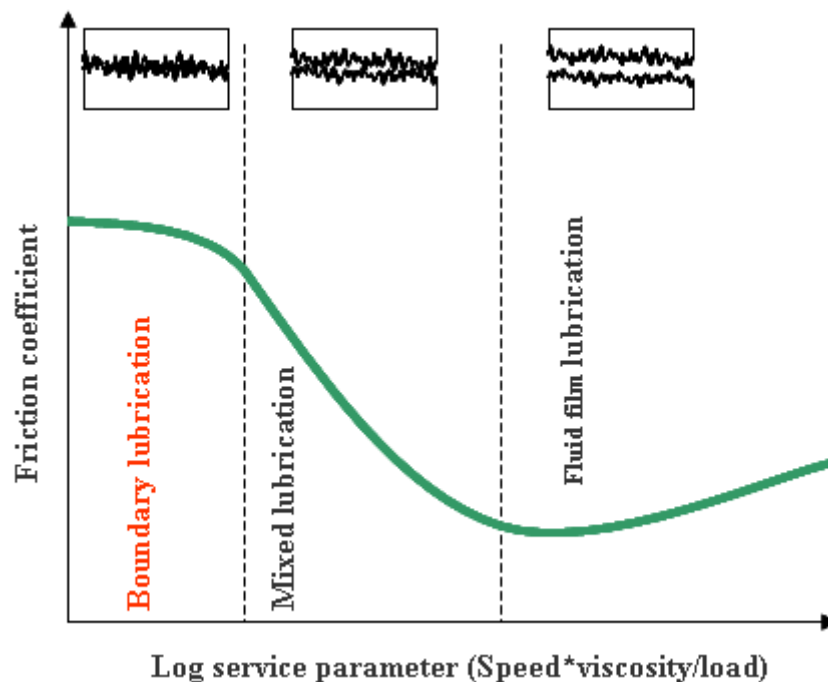


**Figure 2.1 Stribeck Curve**

Generally, rubbing systems that operate largely in the fluid film and mixed lubrication regimes show low friction and low wear because of little or no contact between rubbing surfaces. However, because of errors of manufacturing, or when the operating systems are in the initial starting or stopping stages or in high load conditions, systems can operate in the boundary lubrication regime. In such circumstances, boundary lubrication becomes crucial since its performance determines the values of the prevailing (and often high friction and wear), and thus determines the durability of the rubbing components. In order to characterize the friction and wear properties of the rubbing components fully, it is necessary to plot Stribeck curves, since this enables the regimes of boundary and mixed lubrication to be distinguished.

Definition of boundary lubrication

The earliest use of the term 'boundary lubrication' was in 1922 by Hardy [3]:

*'In what is often called complete lubrication, the kind of lubrication investigated by Towers and Osborne Reynolds, the solid surfaces are completely floated apart by the lubricant. There is, however, another kind of lubrication in which the solid faces are near enough to influence directly the physical properties of the lubricant. This is the condition found with 'dry' or 'greasy' surfaces. What Osborne Reynolds calls 'boundary conditions' then operate and the friction depends not only on the lubricant, but also on the chemical nature of the solid boundaries. Boundary lubrication differs so greatly from complete lubrication as to suggest that there is a discontinuity between the two states.'*

Hardy's concept defined boundary lubrication as a regime between hydrodynamic lubrication and dry contact. However, his definition is probably incomplete in view of the solid surfaces being improved by the lubricants and the existence of a protective boundary film [4].

After many years of research work on boundary lubrication applying a wide range of significantly developed techniques, in a review paper [4], Spikes defined boundary lubrication as '*a chemical or physical interaction between the rubbing surfaces and components of a liquid or vapour lubricant which results in localized surface films with physical properties different from both the rubbing surfaces and the bulk lubricant and which thereby influence friction, wear or seizure behaviour*'.

Boundary lubrication is now generally recognized to result from the adsorption or reaction of active chemical species from within the liquid lubricant on to solid surfaces to form low shear strength films. These films prevent, or at least reduce the direct contact of rubbing solid surfaces and thus limit the consequent formation of strongly adherent high friction metallic or ceramic junctions [5].

## 2.1.3 Historical Study on Boundary Lubrication

Shortly after the concept of hydrodynamic lubrication was developed and became a widely-accepted theory, it was found that castor oil and other "natural oil" derived from plants gave lower friction and smoother running compared to a good mineral oil with similar viscosity [6].

This was explained by a property called 'oiliness'. Oiliness was originally thought to be a property apart from viscosity, and it attracted many researchers' interest [6]-[10].

It was soon recognized that oiliness could be produced by adsorbed layers of surfactants and for almost 30 years such adsorption was considered to be the only mechanism of oiliness. During these 30 years, techniques such as solution concentration measurements [7], radiotracers [8] and contact potential methods [9], were applied to study this adsorption and it was shown that strongly adsorbed monolayers of surfactants with different structure or chain length could reduce friction to different extents [10].

A broader view of boundary lubrication developed in the late 1930s with the development of various types of lubricating additive to reduce friction and wear. Sulphur- and chlorine-containing extreme pressure (EP) additives [11] were found to reduce scuffing. These were considered capable of forming films on rubbing surfaces. However, arguments took place on the strength of films formed by EP additives, which were thought either to be strong in protection [12] or to be easily worn and thus reduce contact pressure [13]. There was also a wide range of research work carried out on phosphorus-containing additives. These additives were found to be very effective on wear protection and various mechanisms were suggested [14]. In the late 1940s, chemists made remarkable contributions to the development of additives based on the study of sulphur- and phosphorus-containing additives. The most successful example of these additives is widely accepted to be ZDDP which shows both EP and antiwear properties and is used in almost all engine oils even up to the present day.

In the 1950s and 1960s, research was guided by the availability of new analytical and experimental techniques. Geometrical and physical properties of rubbing surfaces, such as hardness, roughness and asperity properties firstly came into researchers' vision [15]. Then standardised friction and wear tests were widely used to investigate the performance of boundary films. Later, new surface analysis methods such as X-ray [16], and electron diffraction [17, 18], infrared analysis [19] and X-ray fluorescence [20] were applied to study these films. In the 1970s, other surface spectroscopic methods, *e.g.* XPS, Auger and SIMS, began to be used to study boundary films. These vacuum-based techniques require the analyzed samples to be removed from rubbing contact and cleaned properly, which could lead to time-consuming cleaning processes, inconvenient operation and damage to the formed films. Soon afterwards, several in-situ analysis techniques were developed to study boundary

lubrication. These techniques include the study of contacts between a transparent and a metal surface to permit direct observation into the contact [21], in-contact infrared spectroscopy [22], freezing of oil-covered, rubbed surfaces in liquid nitrogen so that surface films can then be examined on a cold-stage using SEM or SIMS [23], scanning tunnelling and atomic force microscopy [24], *etc.*

### 2.1.4 Boundary Films

There are several different types of boundary films, which have been systematically studied and categorised by Swalen [25] according to the aggregate state, chemical, physical properties and film thickness, as shown in Figure 2.2.
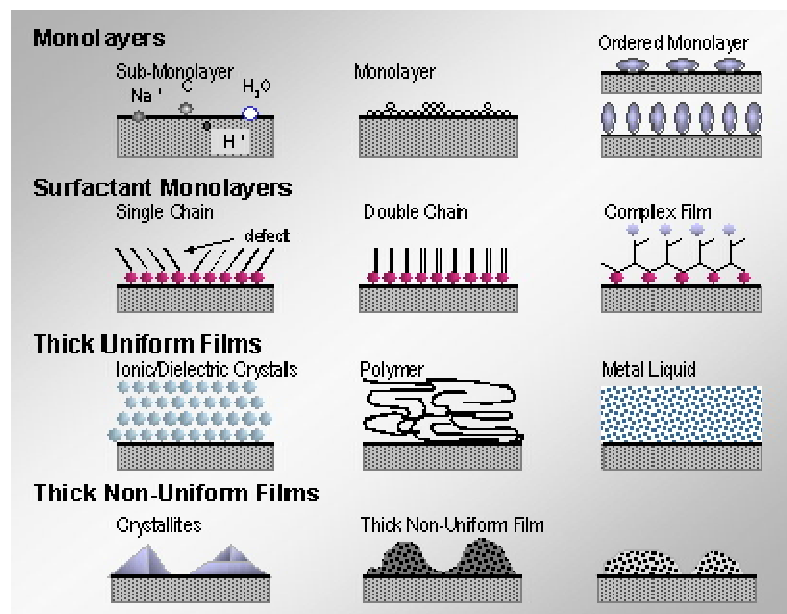


**Figure 2.2 Various Types of Films on Solid Surfaces [25]**

However, at a more practical level, boundary films can also be classified into two main types: solid-like boundary films and viscous or fluid-like boundary films [26]. The best way to differentiate these two types of boundary films is to look into their friction behaviour in Stribeck curves. As shown in Figure 2.3 and Figure 2.4, solid-like films reduce the friction coefficient at very low speeds while viscous, fluid-like film shift the Stribeck curve to the left. The friction coefficient reduction in boundary lubrication by solid-like films is due to the low shear strength of the asperities of the films and the reduction of adhesive junction. The viscous, liquid like films as a result of the formation of highly viscous surface layers, which

can be entrained at very low speed and therefore, make the mixed lubrication regime be reached at lower speed than in the absence of such layers.
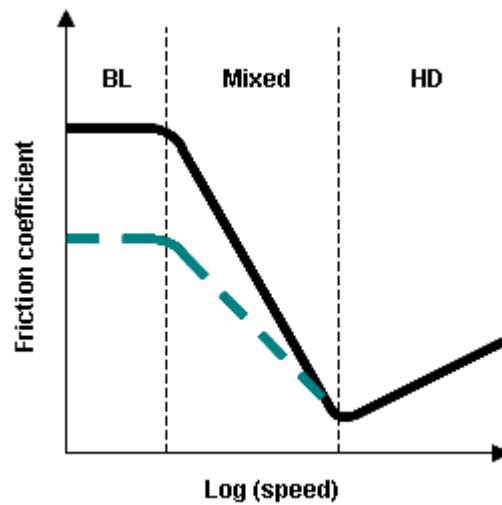


**Figure 2.3 Effect of Solid-like Boundary Film**
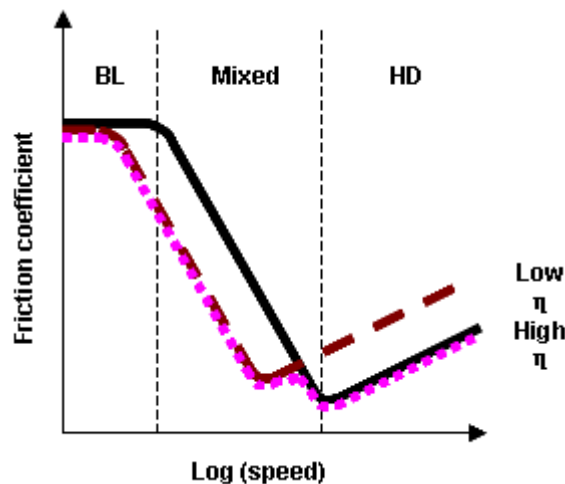


**Figure 2.4 Effect of Highly-viscous Boundary Film**

*2.1.4.1 Solid-like Boundary Films*

Most solid-like boundary films are formed through chemical reaction processes involving the boundary additives and the rubbing surfaces materials, controlled by environmental factors. These films are usually considered as sacrificial films because, during the rubbing operation, there is a dynamic equilibrium between the film formation by interaction between the surfaces and additives, and the removal by rubbing. These solid-like films include metal oxide film, surfactant monolayers, molybdenum disulphide films, phosphorus antiwear additive films, and sulphur and chlorine extreme pressure additive films.

Oxide films are metal oxide layers that are formed on most reactive metals including iron, which give moderately low friction coefficient, (lower than when bare metal surfaces are present), but tend to be abraded away at high contact pressures.

Surfactant monolayers are composed of long-chain surfactant molecules, which contain a polar group attached to a long, non-polar hydrocarbon chain. This polar end attaches to metal surfaces through Van der Waal attraction forces; meanwhile the long chain hydrocarbon group protruded from the surface and gives lower shear strength than metal or metal oxide on metal or metal oxide. This long chain structure reduces asperity adhesion, therefore reducing friction and wear. The disadvantage of using these surfactants is that these adsorbed monolayers can often be easily desorbed or melt at high temperatures.

Molybdenum disulphide films are formed by soluble, organo-molybdenum additives. These films are thin layers of $MoS_2$ with a layer lattice structure like graphite and are very easily sheared, which can result in very low friction coefficients. They appear to form only on the tops of the rubbing asperities and their formation is thus stimulated by rubbing.

Phosphorus antiwear additive films are formed by the reaction between phosphorus-containing antiwear additives and metal surfaces. ZDDP, which forms the basis of this study, can form quite thick layers of glass-like phosphate/polyphosphate. It will be further discussed in next chapter.

Sulphur and chlorine extreme pressure additive films serve in very severe conditions to prevent scuffing. In such conditions, these additives react with hot metal surfaces to form relatively low shear strength metal sulphide or chloride boundary films, which then protect the rubbing parts against seizure.

### *2.1.4.2 Viscous, Fluid-like Boundary Films*
When some polar viscosity index improver polymers added to mineral oils, they are adsorbed on metal surfaces to form monolayers with much higher concentration than the bulk solution. This boundary film effects friction at low speeds when the film thickness is more or less as the diameter of the polymer molecules, since the increased local viscosity entrains more fluid to help separate the rubbing surfaces in concentrated polymers.

Another type of viscous, fluid-like boundary film is formed by polar and non-polar components of different viscosity. Most polar components tend to be more strongly attracted to metal surfaces by Van der Waal forces and, if the polar component is the more viscous one, this forms a few nanometers of viscous boundary film. This phenomenon has been shown in friction studies [27] on mineral oil mixed with highly viscous polar ester.

## *2.1.4.3 Replenishment*

All boundary films mentioned above have a significant self replenishing characteristic, since these films can reform on rubbing surfaces by adsorption or reaction when they are damaged by rubbing. This is a key advantage of boundary lubrication compared to dry contact with solid coatings or treatments.

## 2.2 Boundary Additives

Most lubricants contain special additives to impact specific properties to the baseline oils to enhance performance and inhibit degradation. There are 10 major types of additives, categorized according to their functions: antiwear additives; dispersants; friction modifiers; extreme-pressure additives; detergents; antioxidants; corrosion inhibitors; pour-point depressants; foam inhibitors; and viscosity index improvers. There are also several other, less common additives such as tackiness agents, fatty oils, thickening agents, and colour stabilizers. The additives that act on the rubbing surfaces under boundary lubrication will be discussed below:

Antiwear additives

These additives are used to protect metal surfaces against wear by adsorbing and reacting with metal surfaces to form an easily shearable film. The most widely used are zinc dialkyldithiophosphates [28] and their derivatives. Other types of antiwear additives are acid phosphate, phosphites, sulphurized terpenes, sulphurized sperm oils, metal dithiocarbamates, and occasionally some sulphides. Since their function is to directly react or interact with other additives or metal surfaces, the additives may function on specified metal surfaces but not on others considering the compatibility between an antiwear additive and metal.

Dispersants

Dispersants are primarily additives used to disperse oxidized oil insoluble products like soot, water, or other contaminations. The most widely used dispersants are succinimides (like PIBSA-PAM) and Mannich reaction products. Succinimides are usually n-substituted long-chain alkenyl succinimides and Mannich reaction products are reaction products from polybutene and phenol which are treated with amines and boric acid. These additives do not contain metal in their molecules so that they are also called ashless dispersants. They are designed to have a polar head with basic amine and amide, and an attached long alkyl chain. Although designed to adsorb and stabilise carbonaceous material they are also attracted to metal surfaces where they can form viscous, fluid-like film under boundary lubrication.

Details of the mechanisms of how antiwear additives and dispersants work under boundary lubrication will be discussed in Chapter 3.

Detergents

Detergents are surfactants that adsorb on surfaces forming micelles around the insoluble materials formed by degradation of the oil. They are generally used in overbased form with calcium or magnesium carbonate added to form tiny cores in the surfactant micelles. This overbasing neutralizes acidic components from either the environment or oxidation of the lubricants. Commonly used detergents are metal sulfonates, metal salicylates, metal phenates and metal phophonates and thiophosphonates. Metals used in detergents are calcium, magnesium, barium and zinc, with the first two being the most common.

Friction Modifiers

Friction modifiers are used to lower the friction of the rubbing contacts under boundary lubrication conditions. There are two main types of friction modifier, organic and inorganic.

Originally most friction modifiers used were fatty oils such as sperm whale oil, lard oil, tallow, and blown rapeseed oil. These were probably largely effective due to their ability to release surface active long chain acids or partial esters during rubbing. They have now been largely replaced by custom-made surfactants such as olelyamide and glycerol monooleate.

The main inorganic friction modifiers are the soluble organomolybdenum compounds but materials such as finely dispersed graphite in oil and nanoparticulate additives such as inorganic fullerenes also fall into this category.

Extreme pressure additives are used under severe boundary conditions such as at very high load or high sliding speeds to prevent seizure, scuffing and welding. Most extreme pressure additives are sulphur-, chlorine- or phosphorus-containing compounds, such as chlorinated wax, sulphurized fatty oils, sulphurized mineral oils, chlorinated mineral oils, phophosulphurized fatty oils, benzyl and chlorobenzyl disulphides and some phosphites.

Viscosity index improvers are polymers ranging in molecular weight from ca 20000 (in transmission oils) to 100,000 or more (in engine oils). Most widely used viscosity index improvers are polymethacrylates, olefin copolymers, and polyisobutenes. The main function of these additives is to increase the viscosity of lubricants but to a greater proportionate extent at high temperature than low temperature.

Numerous antioxidants are used in lubricants to protect oils from oxidation by interrupting the oxidation chain reaction or passivating the metal surface with a protective film [29]. Antioxidants can interrupt the oxidation chain reaction in two ways, by reacting with free radicals (radical inhibitors) and by reacting with peroxides (peroxide decomposers). Extensively used antioxidants are hindered phenols, amines and sulphur and phosphorus compounds. ZDDP in this study also acts as a peroxide decomposing antioxidant, as will be discussed later in this thesis.

Corrosion inhibitors are additives which can form a close-packed film on the non-ferrous metal surfaces to protect them against attack from acidic contaminants in lubricants. Commonly used corrosion inhibitors are zinc dithiophosphate, zinc dithiocarbamate, sulphurized terpenes and phosphosulphurized terpenes. Rust inhibitors are a type of corrosion inhibitors which are specifically used to protect ferrous materials.

In this study, film formation and friction tests have been carried out mostly on antiwear additive (ZDDP) and dispersants (PIBSA-PAM), while the newly developed mild wear test method has been applied to study the wear resistance of ZDDP, dispersants, detergents and friction modifiers.

## 2.3 Methods to Study Boundary Lubrication

In the history of boundary lubrication research, one of the main drivers of progress has been the development and application of advanced analytical techniques. Basically, there are two main types of experimental methods to study boundary lubrication: behaviour testing and surface analysis.

Behaviour testing methods are used to investigate the variation of boundary lubrication performance, primarily friction, wear and scuffing, on operational parameters such as additive type, structure, concentration, test conditions of temperature and pressure and so on. Surface analysis is mainly applied to study the nature of boundary films such as chemical composition, thickness, roughness *etc.* The combination of these two types of methods has overcome many difficulties in studying boundary lubrication.

### 2.3.1 Historical Perspective

When Hardy [3] first defined boundary lubrication there were no advanced techniques to measure boundary films which were invisible and immeasurable by the laboratory methods of the time. Therefore, there were several early hypotheses on the nature of oiliness films.

In 1908, Kingsbury [30] assumed that the oiliness films were molecules preferentially to the metal surface. Wells [31] in 1920 suggested that the oiliness films reduced interfacial tension and thus increased the efficiency of lubrication. As mentioned above, Hardy [32] believed that the oiliness films composed of two molecular layers which slipped at their interface. However Deeley [33] thought the oiliness film was a compound of oil and metal and it was more than one molecule thick.

To study the effect of these oiliness films, researchers carried out several tests on their performance in the 1920s. Results showed that the oiliness films reduced friction coefficient to a value around 0.1 by the formation of monolayers of surfactants on the metallic surfaces [34], and this reduction was dependent on the chain length of the surfactants [3]. Further

work [35] showed that multilayers could also greatly enhance the films' durability, which was attributed to the replenishment of the film during rubbing.

From the 1940s to 1970s, the nature of adsorbed surfactant layers on the surfaces was widely studied. Researchers [36] demonstrated that the oiliness films were near-vertically oriented molecules of long chain polar surfactants and these films could be squeezed flat at high pressure conditions.

Although the concept of monolayer adsorption model of boundary lubrication was almost universally accepted, there was still consistent work showed that oiliness films were multilayer. Early in the 1920s, X-ray diffraction results showed hundreds of nanometers-thick films. There were also indications that lubricants may degrade chemically during rubbing to form polymerized, protective layers [37].

In the mid 1980s, several in-situ techniques made the study of boundary films more comprehensive and detailed. These techniques are described below:

### 2.3.2 Ultrathin Film Interferometry

Optical interferometry was applied originally in the 1960s to study the elastohydrodynamic film forming properties of lubricants [38]. A steel ball or cylinder is loaded in rolling or sliding against a glass flat. A beam of light is shone into the contact region through the glass flat from where it reflects back. Some of the light reflects from the underside of the glass while some passes through the oil film to be reflected back from the steel. As they emerge from the contact these two beams interfere so an interference fringe pattern is produced based on the oil film thickness distribution in the contact. By calculating the parameters of these fringes, the separation between the two rubbing surfaces can be obtained, which is the fluid film thickness formed between the two surfaces. As first developed, this method could not easily be applied to measure the very thin film thicknesses characteristic of boundary lubrication. Additionally, only certain, discrete thicknesses, spaced at least 50 nm apart could be determined. However at the end of the 1980s, this method was extended by adding a transparent solid spacer layer of around 100 nm to the glass flat. Interferometry could then be used to measure the combined thickness of both the lubricant film and the spacer layer and the lubricant film thickness calculated by subtracting the spacer layer thickness from the total

thickness, as shown in Figure 2.5. This method enabled successful measurements of films down to 2 to 5 nm as described in [39]. This paper presented measurements of the film forming properties of hexadecane and a solution of stearic acid in hexadecane. The results showed that these two solutions behave almost the same at high speeds, which conformed to the elastohydrodynamic behaviour; however at very low speeds the stearic acid tended to maintain a thin speed-independent separation which represents an oiliness film. Since this time the method has been gradually developed by Spikes and colleagues [40-44] and now it is widely used in studying oiliness films.

The spacer layer interference method has also been extended to map film thickness in lubricated contacts (SLIM) [39] and also of transparent, solid reaction films formed on surfaces during sliding/rolling (MTM/SLIM) [40, 41]. A detailed description of the latter and its application are presented in the Chapter 5.
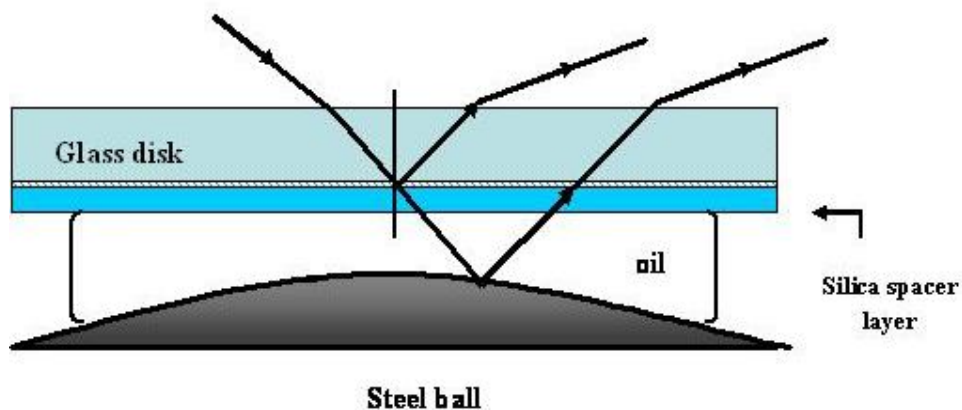


**Figure 2.5 Ultra Thin Film Interferometry [40]**

### 2.3.3 Scanning Tunneling Microscopy and Atomic Force Microscopy

There are two scanning probe microscopy techniques which have made significant contributions to the study of boundary films at the atomic and molecular level, scanning tunneling microscopy (STM) and atomic force microscopy (AFM). In the two techniques a tip interacts with the sample surface through a physical action such as attraction force, friction force and so on. The tip is scanned across sample surface and moved up and down to maintain constant the physical quantity being measured. The up/down motion, and also ancillary measurements such as lateral force, allows images of the studied surface to be constructed [45]. The basic principles of these two techniques are shown below:
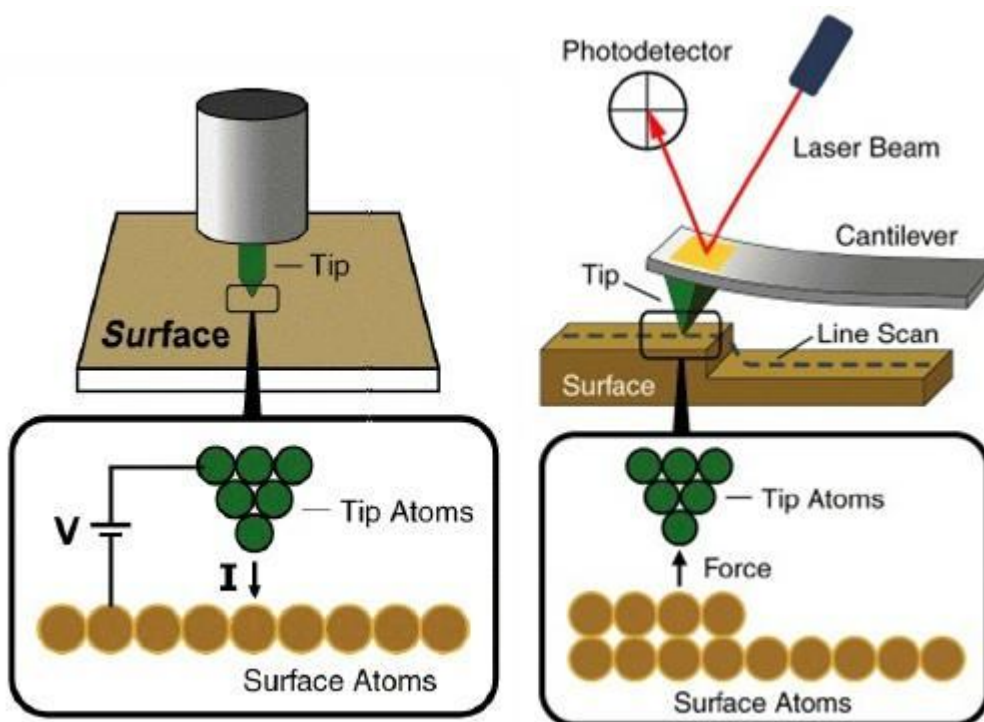
**Figure 2.6 Basic Principles of STM (left) and AFM (right) [46]**

The scanning tunneling microscopy was invented in 1982 by Binnig [46]. The tip of STM is manufactured to be very sharp, to a radius of nanometre scale. It traverses the surface, simultaneously moving up and down to maintain a constant tunneling current between the tip and surface. The distance of moving up and down is measured and combined with the horizontal distance moved to draw a height map of the surface. The drawback of this technique is that chemical variations of films formed on the surfaces may give varying tunneling current, which makes the height map not perfectly matched to the real topography of the surface. However, it does give considerable information of the surface, such as the alignment and even the mobility of molecular films [47].

AFM is introduced in Chapter 5. It has been used in current study to map the surface topography of rubbing specimens.

There are several other effective techniques to study boundary lubrication and boundary films. X-ray adsorption near edge structure technique (XANES) can be applied to study the molecular structure information of boundary films such as coordination number, bond distance and oxidation state of elements. Fuller [48] has used it to investigate thermal and

chemical reaction ZDDP boundary films of different forms, alkyl and aryl chain, primary and secondary. A film-freezing method [23] has been used to overcome the difficulties caused by those techniques which otherwise need samples to be thoroughly cleaned to remove volatile materials prior to analysis. The main feature of this method is that it takes out the rubbed specimens from a test rig and puts it into liquid nitrogen immediately, by which the specimens can be cooled down rapidly without damaging the film or the supernatant oil layers which will be scanned using cold stage SEM or SIMS. Other techniques like force balance apparatus [49], in-track ellipsometry [50] and in-contact visualisation [21] also play key role in the study of boundary lubrication and boundary films.

# Chapter 3 Literature review - ZDDP and dispersants

This chapter firstly reviews the current understanding on the nature, functions and properties of the individual additives ZDDP and succinimide-based dispersant, to obtain a general vision of how these additives act in lubricating oils. Then our understanding of interaction between these two additives is described, and the impact on this on the multifunctional performance of ZDDP and the dispersancy of dispersants.

## 3.1 Review of ZDDP

### 3.1.1 Background on ZDDP

ZDDP has been successfully used for many years in engine lubricating oils, not only because of its cost-effectiveness but also for its multifunctional behaviour, in which it acts as corrosion inhibitor, antioxidant, extreme pressure additive and antiwear additive. An enormous amount of research has been carried out to investigate the correlation between the nature of ZDDP and its performance in lubrication systems.

To protect engine exhaust catalysts from SAPS and maintain useful catalyst life, there has been, in recent years, a progressive reduction in the levels of permitted phosphorus (and sulphur) in engine oil which has lead to a reduction in the use of ZDDP. For example, in today's engine oils the ZDDP concentration is typically 0.8% wt. (≈0.08 P wt%) and this may be reduced further in future specifications. This has led to interest in searching for new antiwear additives which contains low/no SAPS and also designing new oil formulations with less ZDDP. Whichever approach is favoured, it must provide equivalent performance to existing ZDDP formulations. These two approaches have leaded a rapid growth in research on how ZDDP functions in engine oils in the last decade.

### 3.1.2 Nature of ZDDP

ZDDPs can be classified in various ways, for example in terms of acidity/basicity, molecular geometry *etc.* The overall chemical structure of ZDDP can be presented as in Figure 3.1. The R group dictates whether it is an alkyl- or aryl-dithiophosphate, and the alkyl groups can be a branched or linear alkane with usually between 1 and 14 carbons atoms. Typical examples in use include 2-butyl, n-pentyl, n-hexyl, 1, 3-dimethylbutyl, n-heptyl, n-octyl, isooctyl (2-ethylhexyl), 6-methylheptyl, 1-methylpropyl, dodecylphenyl, and others [51]. An important practical difference is between primary ZDDPs which have a primary alkyl group, *i.e.* with two H atoms on the α-carbon bonded to the oxygen and secondary ZDDP which have a secondary alkyl group with one H and one C bonded to the α-carbon (Figure 3.2).

Commercial ZDDPs are usually a mixture of neutral and basic salts and they can exist in monomeric and dimeric forms.
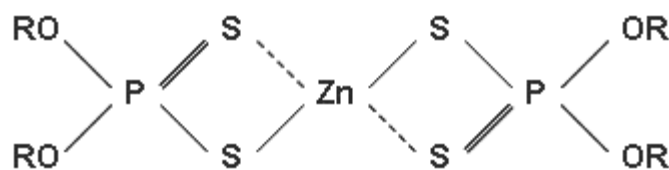

**Figure 3.1 Structure of ZDDP**
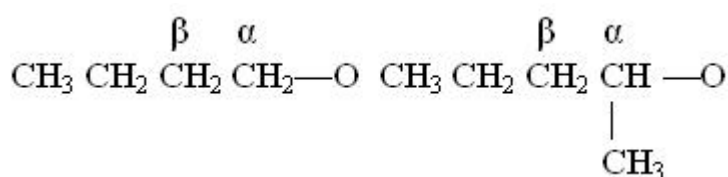

**Figure 3.2 ZDDP Alkyl Chain Types**

To compare the difference in stability and reactivity of neutral and basic ZDDPs, several advanced techniques have been applied both in air and in oils. Lawton and Kokotailo [52] examined dimer and monomer neutral ZDDPs using crystal X-ray diffraction, to determine the molecular geometry of these two forms. Several other researchers [53] investigated the basic form of ZDDP and hypothesised different reaction schemes and structures. Armstrong [54] found that basic ZDDP has higher molecular stability than neutral, and complexes having short S-O bonds are more stable. His investigation [55] of the reactivity of three forms of ZDDP, also confirmed that the most stable complexes are those in which a short S-O bond is formed, which suggested that the sulphur atoms in ZDDP are more likely to be point of attack. Harrison [56] suggested that the basic forms of ZDDP are less active in antiwear and antioxidant properties than neutral ones. However, Yamaguchi [57] and Fuller [58] applied XANES to investigate the antiwear films generated from neutral and basic ZDDPs, and suggested that the compositions (P and S) of tribofilms generated from neutral and basic ZDDPs were very comparable.

Gallopoulos [59] studied the structure of monomeric ZDDP with infrared spectra and suggested three possible structures – a covalent structure, an ionic hybrid structure and a covalent hybrid structure. Heilweil [60] studied monomeric ZDDP using vapour pressure osmometry and light scattering, found that when metal dithiophosphate was in solution in cyclohexane or benzene there existed a equilibrium between an internal chelate I monomer

and a internal chelate oligomer II as shown below in Figure 3.3. NMR [56] and vibrational [61] spectroscopy showed equilibrium between these two forms. The results also showed that the equilibrium moved to favour the monomer with increasing temperature.
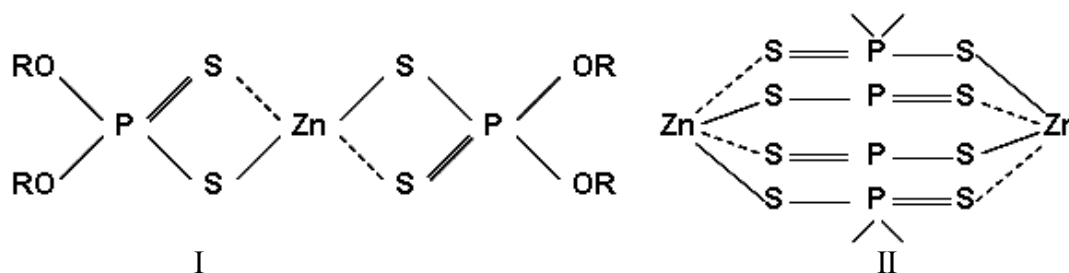


I                                                                                      II
**Figure 3.3 Possible Structures of ZDDP**

In work carried out by Fuller *et al.* [58], the researchers found that the thermal stability of neutral ZDDPs follows aryl > di-isobutyl (primary) > di-isopropyl (secondary). Rounds suggested that secondary ZDDPs are more effective in film formation but less thermally stable than primary ones; and also suggested the mechanism for the decomposition of ZDDP to be thermal for secondary, thermal plus oxidative for primary and oxidative for aryl ZDDPs. Yamaguchi [57] found that the thermal stability of aliphatic ZDDPs was determined by the number of $\beta$ hydrocarbon atoms (Figure 3.2).

### 3.1.3 The Roles of ZDDP

ZDDP is a very versatile additive in lubricating oils, acting as antioxidant, corrosion inhibitor, extreme pressure additive and antiwear additive.

Antioxidant

Oxidation of hydrocarbons occurs at high temperature when oil is heated in the presence of air, which can increase the oil viscosity and the concentration of acids in the oil. As a result, varnish and lacquer deposits may form on hot metal surfaces. The oxidation is generally recognized as proceeding by free radical chain reaction to form peroxy radicals, which then attack unoxidized oil to form new initiators and hydroperoxides. The main function of antioxidant is to interrupt the radical chain reaction by inhibition of peroxides or by radical scavenging. There are three types of antioxidants – metal deactivators, radical inhibitors and peroxide decomposers. ZDDP has the functions of both peroxide inhibition and radical scavenging. As a peroxide inhibitor, it reacts with hydroperoxide molecules, preventing

formation of the peroxy radicals. As a radical scavenger, it reacts with peroxy radicals preventing further propagation of the free radical chains [62-64].

Burn *et al.* [65] chemically modelled oxidation inhibition by ZDDP by studying the decomposition of cumene hydroperoxide in the presence of ZDDP. Three stages of breakdown of ZDDP were postulated - an initial fast stage in which disulphide was identified as an initial degradation product, a slow induction stage and a final fast stage. The reaction appeared to be catalytic, with the degradation products of ZDDP being the catalyst. Several other researchers [66-68] reported a dissociation of ZDDP to form zinc oxide which inhibits hydrolysis of ZDDP. Johnson *et al.* [69, 70] investigated the activity of ZDDP when mixed with used oil and found that the interactions between ZDDP and oxidation products decreased the activity of ZDDP.

Extreme pressure additive (EP additive)

In concentrated contacts such as cams very severe conditions (generally high load/high sliding speed), the contact temperature increases until any elastohydrodynamic film collapses. This leads to very high wear rate in the contacts, greatly increases the temperature and leads to contacts seizing or scuffing. However, when EP additives are present, this additive reacts with hot metal surface to form films which have lower shear strength and less adhesion than metal or metal oxides. This can control or prevent scuffing. ZDDP decomposes thermally at temperatures around $200\,°C$, produces a variety of sulphur- and phosphorus-containing compounds. These products react with metal surfaces and generate films on the mating surfaces. The film has been analyzed in practical systems and it was found to be containing zinc, phosphorus and sulphur [71].

Research [71] on ZDDP has shown that its EP properties rely largely on its ability to form iron sulphide. This has been proved by the study [72, 73] on the EP performances of sulphur-free phosphorus additives. A study [71] comparing the films formed under different conditions presented that the ZDDP film consists of phosphate in mild rubbing conditions but has high sulphur content in severe, heavily load/high sliding speed conditions. Tests using a four-ball test machine indicated that even a small amount of ZDDP influences the EP performance, suggesting that ZDDP has high effectiveness as an EP additive [74].

Antiwear additive

A large number of studies have been carried out on the antiwear properties of ZDDP, the antiwear film formed on the mating surfaces and the nature of the ZDDP antiwear film. Three main ways that ZDDP act as an antiwear additive have been proposed - by forming a mechanically protective film, by removing corrosive peroxides or peroxy-radicals and by digesting hard and thus abrasive iron oxide particles. Protective film formation by ZDDP is the most widely accepted mechanism of ZDDP antiwear action. Reaction between ZDDP and peroxides in the lubricant is capable of preventing metal surfaces from corrosively wearing by peroxides [75, 76]. The third suggestion is proposed by Martin and colleagues [77, 78], in which it assumed the iron oxide particles, which would abrasive wear, are 'digested' to form relatively soft iron phosphate. This theory is more controversial because of lacking direct evidence of the process that harmful iron wear particles are digested.

Corrosion inhibitor

The first patents for ZDDP were concerned with its use as a corrosion inhibitor, particularly for copper-based bearings. This aspect of ZDDP has been little explored in published research but the inhibition probably results from the formation of thermal phosphate films similar to those that form on ferrous surfaces at high temperature [210].

### 3.1.4 ZDDP Antiwear Film
#### *3.1.4.1 Mechanisms of the formation of ZDDP film*

In the literature, several different mechanisms and processes have been proposed for the formation of ZDDP tribofilms. Possible mechanisms are thermal degradation [79-84], surface adsorption [85, 86], oxidation by hydroperoxide [62, 65, 87-90], radical reaction [91], hydrolysis [92], chemical reaction with FeO and oxygen in the air [93, 94], or a combination of the above.

In 1982, Spedding and Watkins [92] investigate the antiwear action mode of ZDDP using various analytical techniques. They suggested that ZDDP predominantly decomposes in oil solutions by a hydrolytic mechanism to zinc polyphosphate and a mixture of alkyl sulphides, which are the precursors of the antiwear action of ZDDP. Meanwhile, Dacre and Bovington [95] studied the antiwear mechanism of ZDDP in terms of the adsorption of ZDDP. They found the adsorption was stronger on iron than on bearing steel, and the adsorption was physical and reversible below 40℃ but chemical at 60℃ and above. Furthermore, the

absorbed ZDDP film formed a monolayer at low temperature and when temperature increased a rapid loss of zinc content occurred from the film.

Willermet *et al.* [96] reviewed the mechanisms of ZDDP film formation in detail and suggested a four-step process under mild wear conditions:

- Adsorption of ZDDP on metallic surfaces.
- Reaction of ZDDP with the metallic surface to form phosphates and phosphothionic moieties bound to the metal surface.
- Formation of phosphate film precursors from antioxidant reactions of ZDDP.
- Condensation of the phosphates/phosphothionates species.

Yin *et al.* [97] postulated a three-step mechanism of ZDDP film formation based on results using XANES:

- ZDDP is physisorbed on steel.
- Thermal-oxidative process with oxygen or organic peroxides results in the decomposition of ZDDP producing zinc metaphosphate, $Zn(PO_3)_2$, and small amounts of zinc sulphides.
- The formation of $FeZnP_2O_7/Fe_2Zn(PO_4)_2$.

However, Yin *et al.* suggested that long-chain polyphosphates form first, and, with extended rubbing, these polyphosphates interact with the metal ions to form short-chain polyphosphates, while Willermet suggested short-chain polyphosphates form first, followed by polymerization to long-chain polyphosphates.

Using XANES, Fuller *et al.* [85] identified the presence of an intermediate species which they ascribed a linkage isomer of ZDDP formed during the thermal-oxidative decomposition of ZDDP. They suggested a five-step process of ZDDP film formation:

- ZDDP is adsorbed onto the metal surface.
- ZDDP in solution is converted to linkage isomer.
- Linkage isomer is adsorbed to the metal surface.
- Thermal-oxidation of linkage isomer and ZDDP form long-chain polyphosphates $Zn(PO_3)_2$.

- Hydrolysis of polyphosphates occurs with continued rubbing and the presence of water from the base oil to create short-chain polyphosphates.

Ferrari *et al.* [98] suggested a further step in which zinc polyphosphate is oxidized leading to the formation of Zn-O and Fe-O bonding and finally to the formation of a glass network. A simple two-step pathway of ZDDP decomposition is also suggested in this study, the removal of iron oxide and the reaction of ZDDP with nascent iron substrate.

Pearson [99] described an acid-base reaction between phosphates and iron oxides which illustrates the digestion of iron oxides to the formation of a mixed iron/zinc polyphosphate glass.

Spikes [28] summarized the activity of ZDDP in solution and identified four different types of chemical process. Firstly, ligand exchange [100, 101] takes place between Zn and other metal cations because the dithiophosphate ligands are labile. Secondly, as a highly effective oxidation inhibitor, ZDDP decomposes hydroperoxides [62] and peroxy-radicals [65, 87, 88]; but as a consequence of this decomposition, ZDDP is no longer able to form zinc phosphate antiwear film on the metal surfaces [89, 90]. Thirdly, thermal degradation [79-84] is activated at high temperature with a low level of hydroperoxides or peroxy-radicals, which leads to zinc phosphate solid deposit, alkyl sulphides, mercaptans, hydrogen sulphide and olefins. Fourthly, adsorption of ZDDP molecule on iron surfaces [85, 86] occurs. This happens *via* the sulphur atom of the P=S bond and becomes irreversible when the temperature is above 60 ℃. The behaviour of ZDDP in solution is presented as shown in Figure 3.4.
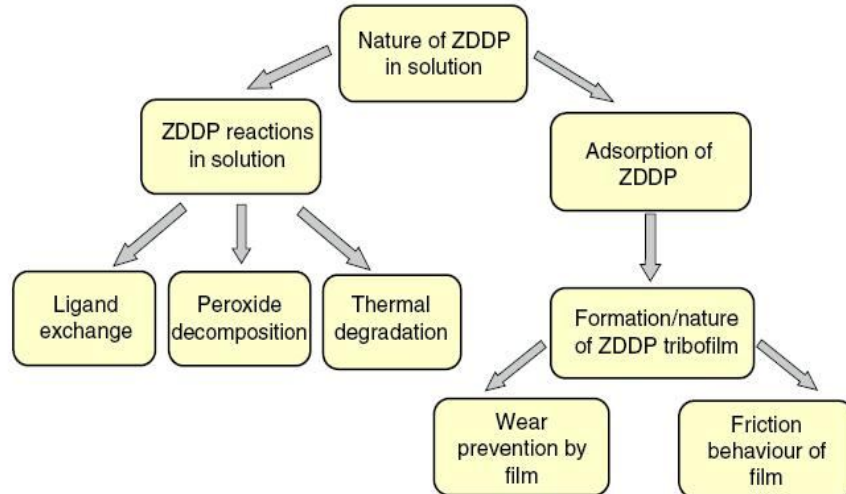
**Figure 3.4 Nature of ZDDP in Solution [28]**

There is considerable agreement concerning the overall process of the formation of ZDDP tribofilm. The widely accepted theory is that ZDDP adsorbs chemically or physically to the metal/oxide surface, as well as the ZDDP decomposition products, followed by an oxidation and degradation of ZDDP. However, there is still debate and uncertainty as to the precise chemical reactions that lead to the eventual formation of polyphosphate film under different conditions, *e.g.* whether short-chain or long-chain polyphosphate forms first, whether through a condensation, possible dependence on the amount of cations in solution, the significance of hydrolysis *etc.*

*3.1.4.2 Chemical characterization and morphology of ZDDP film*

Many different surface analysis techniques have been applied to study the chemical nature of ZDDP films. Molina [102] in 1987 used XRD to analyze the precipitates collected from a ZDDP solution and found that the precipitates consisted of 86% mass percentage of Zn pyrophosphate and 11% mass percentage of orthophosphate and were in an amorphous or microcrystalline form.

Willermet *et al.* [103] using internal reflectance IR, found that the ZDDP antiwear film contained of phosphate. Bancroft *et al.* [104] found ZDDP films were composed of a mixture of long and short chain of polyphosphate, which were chemically inter-grown with the metal oxide surface. Yin *et al.* [97] found that the film has a layered structure with short-chain polyphosphates in the bulk, and longer-chain polyphosphates at the surface. Yamaguchi and Ryason [86] observed that the tribofilms formed by aryl ZDDP contained long-chain

polyphosphates throughout the film while the alkyl ZDDP film were composed of layers containing long chains at the topmost surface and short-chain layers underneath. The aryl films also contained more unchanged ZDDP.

In 1991, Cann and Spikes [105] used in-contact IR spectroscopy to study the film generated by ZDDP. They found the ZDDP reaction films are primarily amorphous ortho- and pyrophosphates rather than polyphosphate glasses. Sheasby [21] used an optical in-contact technique to enable the direct visual observation through the transparent surface of a sapphire or glass disc. His work presented a 'friction-polymer' -like material in the contact inlet and the structure of this material was pad-like, varying dynamically .during rubbing.

The study [97] of the composition of ZDDP tribofilms using XANES provided more detailed information. The pads in the antiwear films were found to consist of a thin layer rich in quite long chain polyphosphate on top of shorter chain poly- or orthophosphate glass material. The tribofilms formed by rubbing also confirmed to be similar to thermal films generated by ZDDP in XANES study.

Another feature of interest in ZDDP films is their morphology. AFM [106] has been widely used in recent years to investigate the morphological and physical properties of ZDDP tribofilms in presence of supernatant oil. The results confirmed that these films are microscopically rough, with a structure consisting very smooth and flat, plateau-like pads separated by deep valleys, as shown below.
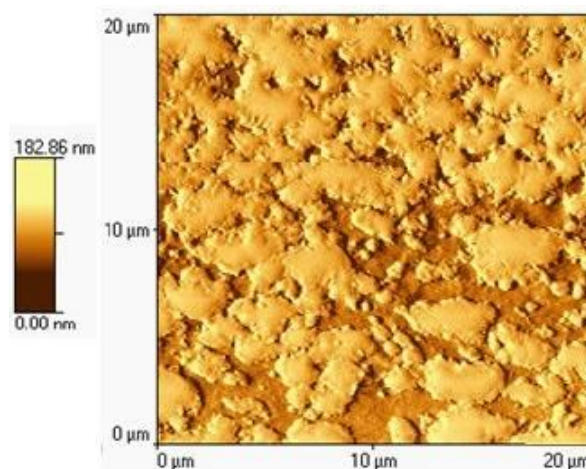


**Figure 3.5 AFM Analysis of ZDDP Film [106]**

In 1999, Smith *et al.* [107] carried out a multi-technique study on ZDDP derived films and found that the films have a thin inorganic mixed sulphide/oxide layer immediately above the Fe substrate, which formed the base for a thicker zinc-containing polyphosphate-like overlayer.

Bec *et al.* [108] in 1999 used a sliding nanoindentor, which was converted by a surface forces apparatus, to study the ZDDP tribofilms covered with supernatant test fluid. The two main findings of their work are the solid-like ZDDP film was covered with a micron-thickness, viscous liquid layer (oligomeric, phosphate-rich material); and the nanoindentation increased the hardness and elastic modulus of the film.

Martin *et al.* [109] in 2004 investigated the tribofilm of ZDDP in its depth and the interface tribofilm/substrate by using a multi-technique approach. They confirmed that the tribofilm is composed of a short chain mixed iron and zinc orthophosphate layer covered by a thin zinc pyrophosphate one.

More recently, Spikes [28] summarized the research carried out on the study of the morphology of ZDDP films and gave a common schematic diagram of the ZDDP tribofilm pad structure.
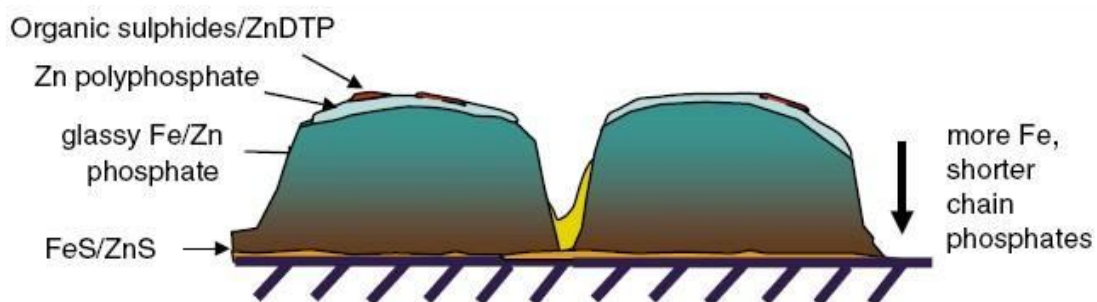


**Figure 3.6 Schematic Diagram of Pad Structure and Composition of ZDDP Tribofilm [28]**

### *3.1.4.3 Properties of ZDDP film*

To obtain extensive understanding of ZDDP antiwear mechanism, the properties of ZDDP tribofilms, such as friction performance, film thickness and hardness have been investigated using various techniques. Kennedy and Moore [110] in 1987 found that some ZDDP formulations can produce an undesirable increase in friction in thin film lubrication conditions. More recent work by Tripaldi *et al.* [111] has shown that ZDDP increases friction

in intermediate speed, mixed lubrication conditions. This has been clarified by Taylor *et al.* [112] as being due to the ZDDP-derived tribofilm being quite uneven and rough.
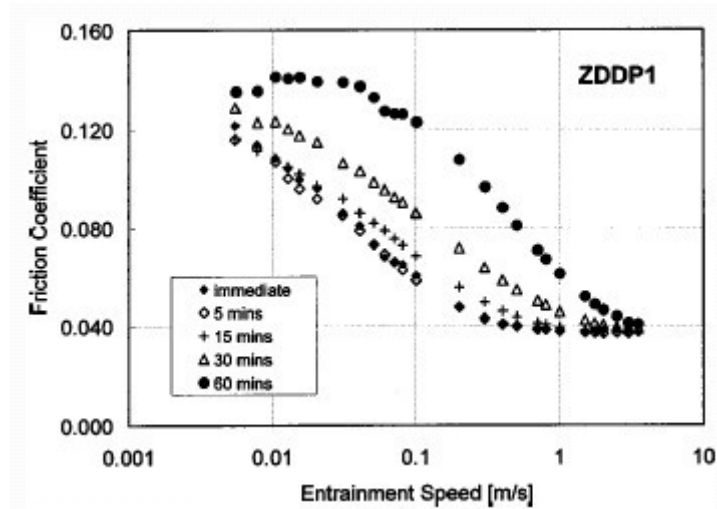


**Figure 3.7 Friction Coefficient Behaviour with Rubbing Time of ZDDP-containing Oil [112]**

Palacios [113] used EDAX in 1986 to measure the thickness of the ZDDP film varying with load, rubbing time and ZDDP concentration. He found that the full antiwear protection was provided by a ZDDP reaction film thickness of only 15 µg/cm$^2$ ($\approx$ 50 nm) although it can form films up to 40 µg/cm$^2$ ($\approx$ 140 nm). Gunsel *et al.* [40] and Tripaldi *et al.* using interferometry found the film to have thickness between 10 and 110 nm at 100℃. Taylor *et al.* [112] using MTM-SLIM to measure film thickness under sliding-rolling conditions with varying rubbing time and temperature found that at typical engine operating temperatures (between 100℃ and 150℃), the film was the thickest, at 120-160 nm. Further study on the stability of this film showed no appreciable change after extended rubbing in base oil for up to 24 hours.
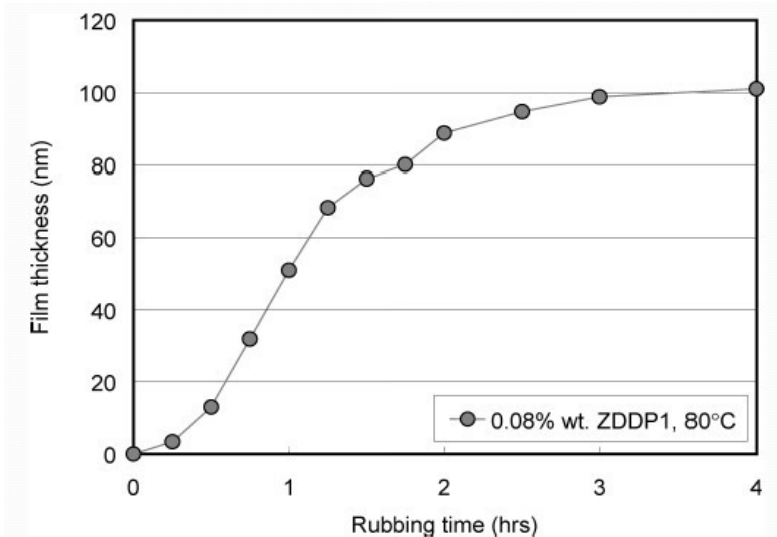
**Figure 3.8 Film Thickness Measured by SLIM [112]**

Only static measurements have been applied for mechanical characterization of the tribofilm formed by ZDDP. Bec *et al.* [108] studied films formed in a cam/follower simulation wear tester and found the moduli were in the range of 15-90 GPa by using a modified surface force apparatus. Graham *et al.* [114] studied tribofilms derived from alkyl ZDDP and aryl ZDDP using AFM and IFM and found that the streaks within aryl films have moduli much lower (≈50 GPa) than that of the large antiwear pads in the alkyl film (>70 GPa). Warren *et al.* [115] also observed the elasticity of the ZDDP films and found that the centre of the large antiwear pads were more stiff and elastic than the small pads and the valleys of the off pad regions.

It is evident from the above that the study on the functions of ZDDP in lubricating oils, the way it forms film on metallic surfaces and the antiwear performance of its films has given us a good understanding. However, the work referenced in the review above was mainly focussed on simple solutions, consisting of only ZDDP in base oil. A great deal of research has also studied the behaviour of ZDDP in the presence of other additives. Previous research on dispersants and the interaction between ZDDPs and dispersants is described below.

## 3.2 Review of Dispersants

### 3.2.1 Introduction

Dispersants are used in all engine oils to disperse and suspend undesirable materials such as soot particles to prevent them from aggregating.

Dispersants are used as lubricant additives to keep two types of solid material suspended and dispersed in engine oils and thus prevent agglomeration, blocking of oil ways and sludge deposition. One is engine soot particles from incomplete combustion of fuel. Soot is produced mainly in diesel engines but, with direct injection gasoline engines, is also found now in gasoline engines. In addition to soot, the oxidative degradation of various components of engine lubricants leads to the formation of carbonaceous particles known as sludge and surface deposits such as varnishes and this material is maintained in suspension by the dispersant.

The various ways that dispersant additives suspend soot particles and other deposit precursors include suspending aggregates in the bulk lubricant when they form, modifying soot particles so as to prevent their aggregation and lowering the surface and interfacial energy of the polar species in order to prevent their adherence to metal surfaces [116, 117].

### 3.2.2 Function of Dispersant

Dispersants are generally molecules designed to have a large hydrocarbon 'tail' and a polar hydrophilic head group, usually oxygen- or nitrogen-based, as shown below. There is generally another 'connecting group' or a link between these hydrocarbon tails and the polar heads, most often a succinimide, phenol and phosphonate. The tail section serves as a solubilizer in the base fluid while the polar group is attracted to contaminants in the lubricant [118]. Most dispersants prevent agglomeration by adsorbing onto and surrounding the solid contaminants and forming micelles in which the long-chain hydrocarbon tail prevents other soot particles from getting close enough to stick together. The suspended micelles also prevent the adhesion of polar soot particles on metallic surfaces. Research has shown that particles with associated dispersant molecules are unable to coalesce because of either steric factors or electrostatic factors [119].
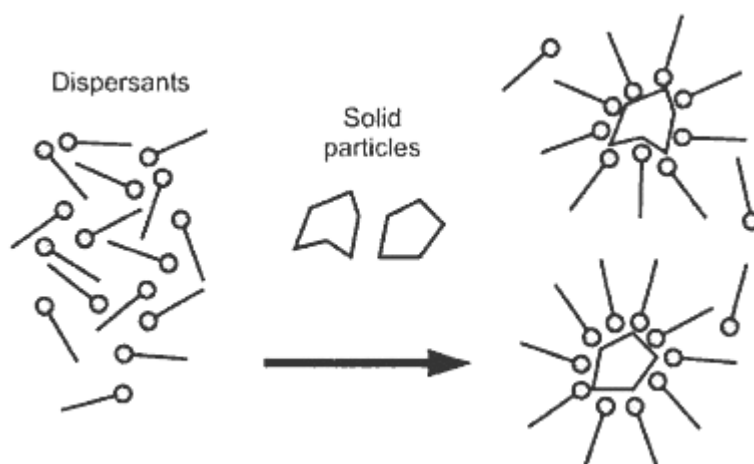
**Figure 3.9 Function of Dispersant [118, 119]**

### 3.2.3 Structure and Synthesis of Dispersants

Structure

The hydrocarbon group in dispersant molecules is polymeric and, depending on its molecular weight, dispersants can be classified into polymeric dispersants and dispersant polymers [120]. Polymeric dispersants have lower molecular weight than dispersant polymers, with values between 3000 and 7000, and >25000 respectively. Different types of olefins are used to make polymeric dispersants, including polyisobutylene, polypropylene, polyalphaolefins and mixture of thereof. Among these, polyisobutylene-derived dispersants with molecular weights of 1000-2000 are most widely used. Dispersant properties and effectiveness are not only determined by their molecular weight but also by the molecular-weight distribution and the length and degree of branching.

The main type of dispersant currently used in engine oils is polyisobutylene succinic anhydride/polyamine (PIBSA-PAM), which can be mono-, bis- or tris-. Structures of them are shown below [118]. The dispersants applied in this research are mainly PIBSA-PAM.
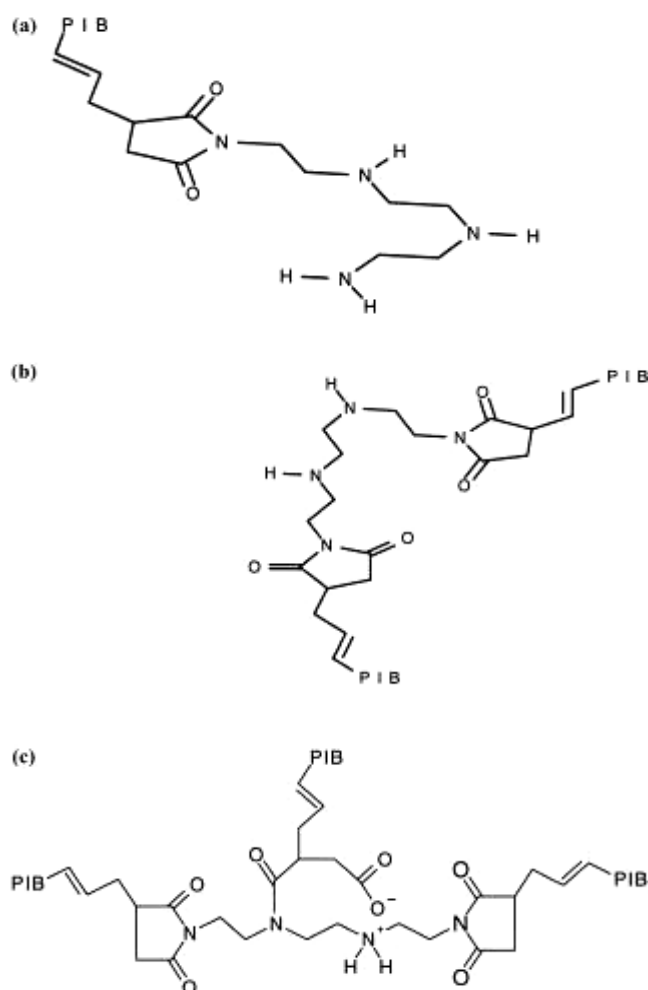
**Figure 3.10 Different Types of Succinimide Molecule: (a) Mono-, (b) Bis-, (c) Tris- succinimide [118]**

The polar group is usually nitrogen- or oxygen- based. Nitrogen- based groups are derived from amines and they are usually basic and are the main type used.

Synthesis of PIBSA-PAM dispersants:

Hydrocarbon group

Polyisobutylene is the most frequently used source of the hydrocarbon groups in dispersants, and can be produced through an acid-catalyzed polymerization of isobutylene. This polymerization is shown below in Figure 3.11. Generally, the reactivity of dispersant depends on the substituted olefins in its molecule because of steric factors - the more substituted the olefin, the lower the reactivity. The chain length of these hydrocarbon groups determines the oil solubility of these dispersants – the longer chain-length hydrocarbon derived dispersants have higher oil solubility.
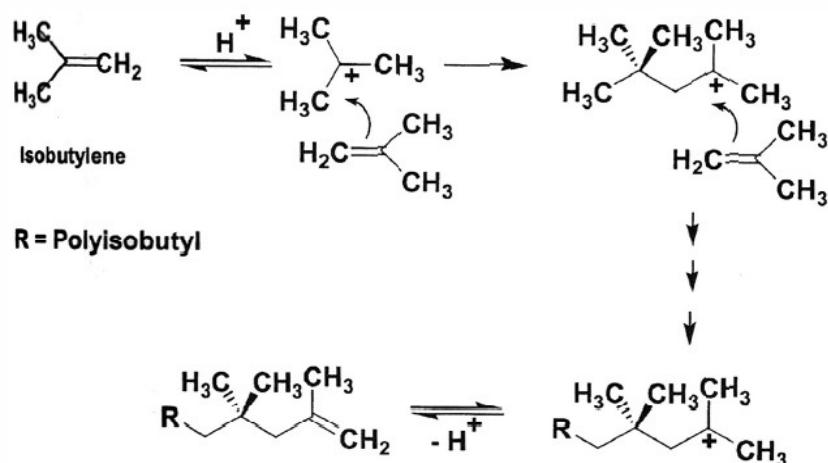
**Figure 3.11 Acid-catalyzed Polymerization of Isobutylene [121, 122]**

Connecting group

Succinimide is mostly used as a connecting group, which is formed by the reaction between a cyclic carboxylic acid anhydride. Alkenylsuccinic anhydride is the precursor for introducing the succinimide connecting group in dispersants. The reaction mechanism can be described as below:
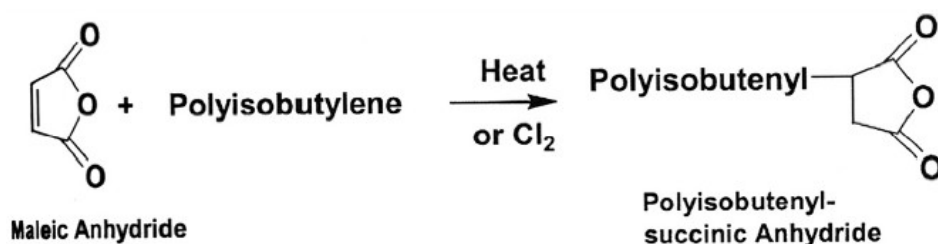


**Figure 3.12 Polyisobutenyl-succinic Anhydride Formation [123]**

The polar group

Polyamines are the most commonly used polar groups in dispersants. These are produced by chlorination of ethylene followed by a reaction with ammonia as shown below. Amines are classified into primary amino groups, secondary amino groups and tertiary amino groups, as shown in Figure 3.14. Their reactivities differ, resulting in different reaction products when mixed with anhydride. The primary amino group reacts with anhydride to form a cyclic imide, the secondary amino group reacts and forms an amide/carboxylic acid, but the tertiary amino group does not react with anhydride at all [124].
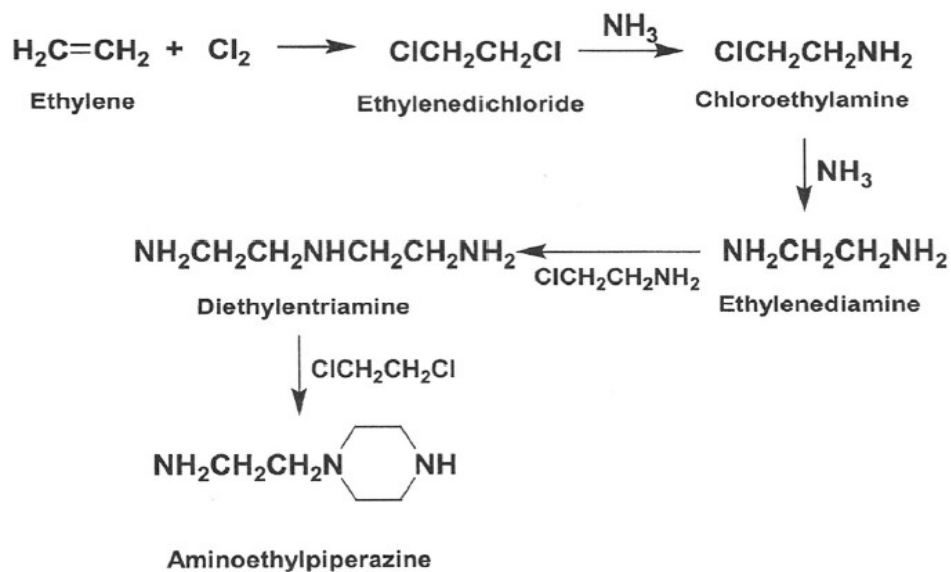
**Figure 3.13 Synthesis of Polyamine [120]**

—NH₂        Primary amino group

$>$NH        Secondary amino group

$>$N—        Tertiary amino group
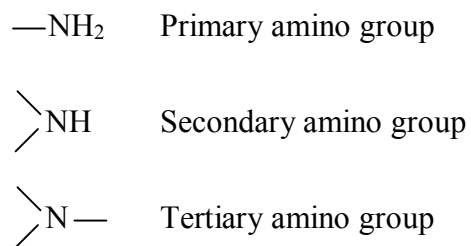
**Figure 3.14 Amine Structures [120]**

The overall synthesis of mono/bis-PIBSA-PAM dispersants is summarised below in Figure 3.15.
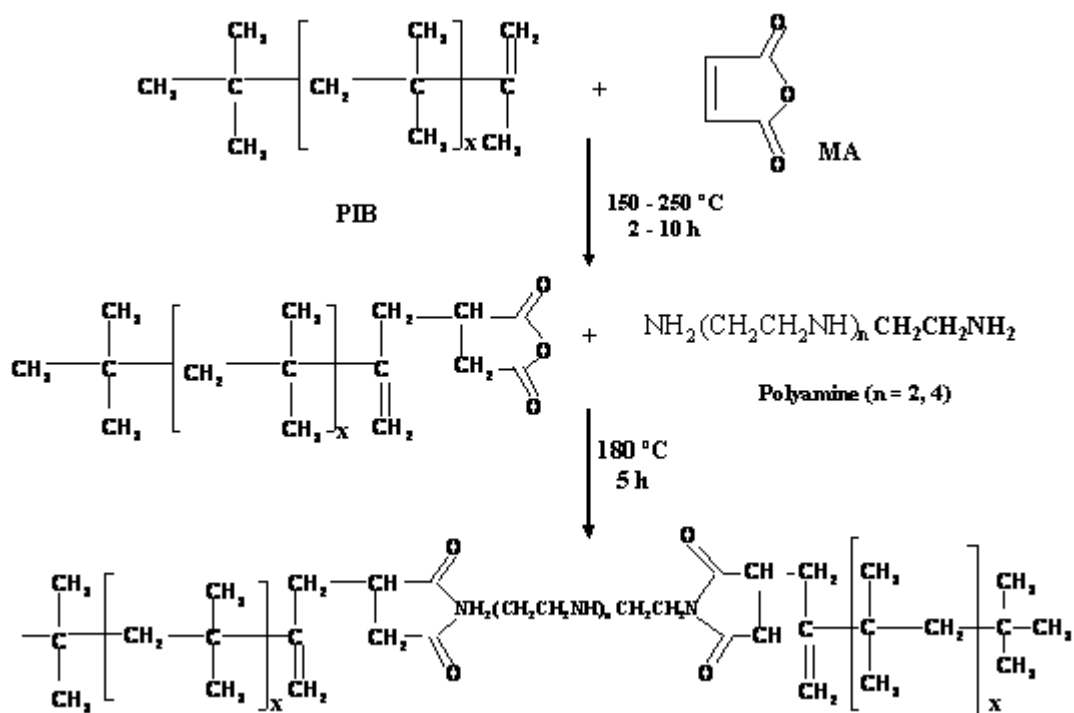
**Figure 3.15 Reaction Scheme for the Synthesis of Bis-PIBSA-PAM [118]**

### 3.2.4 Dispersant Properties

The properties of dispersants depend on all the three parts in dispersants molecules, the hydrocarbon group, the connecting group and the polar group. These properties include dispersancy, thermal and oxidative stability, viscosity characteristics. This review focuses on dispersancy.

Generally, for dispersants having the same connecting group and the polar group, lower molecular weight dispersants have higher ability to associate with polar particles but lower ability to suspend them. Branched chains also show improved dispersancy. So in practice, to obtain good dispersancy, dispersant designers have to select both the molecular weight and branching carefully. Experience has demonstrated that for most PIBSA-PAMs, optimal performance originates when the hydrocarbon group contains 70-200 carbon atoms and also extensive branching. Dispersants containing larger hydrocarbon groups but similar branching, have lower affinity to polar particles.

The connecting group and the polar group together determine the overall polarity of a dispersant, which implies the ability of suspending contaminants in the bulk lubricant. However, it is not easy to predict the overall polarity of dispersants since dispersants have many bonds with various combinations of atoms and the contaminants can be acidic or basic.

Basic nitrogen-containing dispersants are more extensively used in gasoline engines because some of the particles derived from lubricant oxidation are acidic.

For the oxidative and thermal stability of dispersants, research [125, 126] has shown that the rate of oxidation of the paraffinic group (polyisobutyl group) is slower than that of groups containing multiple bonds (polyisobutenyl and benzylic groups), which implies that highly branched alkyl group have a higher susceptibility towards oxidation than linear or unbranched alkyl groups. However, the polar groups in an amine-derived dispersants are oxidized at a higher rate than oxygen-derived groups. For thermal stability, dispersants based on 1000-2000 molecular-weight polyisobutylenes are relatively stable, except at very high temperature [127, 128].

## 3.3 Interaction between ZDDP and Dispersant

The interactions between ZDDP and dispersant have been studied extensively. The effect of this interaction on the multifunction properties of ZDDP and the dispersancy of dispersant can be either synergistic or antagonistic.

A few papers [129, 130] suggest that there is a synergistic interaction between ZDDP and dispersant, which results in a package containing of both ZDDP and dispersant showing greater dispersancy than the additives separately.

However, antagonistic interactions between ZDDP and dispersant have been more widely reported. It has been suggested that dispersants can reduce the activity of ZDDP (antiwear and antioxidative properties) [131, 132], lower the adsorption capability of ZDDP on metallic surfaces [133] and increase the ZDDP decomposition temperature [131, 134]. Complexation is thought to be the main mechanism of the interaction between ZDDP and dispersant. However, the nature of this complexation is controversial. Some researchers have stated the complexation is between the decomposition products of ZDDP and dispersant through P-N bonding [131, 135] while others suggested a Zn-N bonding [136-139]. The interaction may take place both in the bulk lubricant (complexation) and on the metallic surfaces (adsorption

competition). The ability of dispersant to solubilise the ZDDP antiwear film will also be suggested in the current research.

A competing reaction of succinimide-type dispersant with ZDDP was found under thermo-oxidative conditions by Bancroft and Park [140], which led to a slower rate of reaction/deposition onto the metal surface.

Work on the interaction between ZDDP and succinimide molecules [141] suggests that monosuccinimides have a much stronger interaction with ZDDP than bis-succinimides due to steric effects.

Ramakumar *et al.* [142] also found that low N-content dispersants form weak complexes in solution while higher N-content dispersants form more tightly-bound complexes.

Martin *et al.* [143] found that succinimides only slightly impede the antiwear performance of ZDDP in mild wear conditions, and the wear of a ZDDP and dispersant mixture is similar to that of ZDDP alone.

ZDDP-amine systems have been studied and it has been found that the tendency to form complexes is influenced by the structure of the amine. The structure of several amines is represented as shown below [136]. The effects of structure of amines on the interaction between it and ZDDP are interpreted later in this chapter.
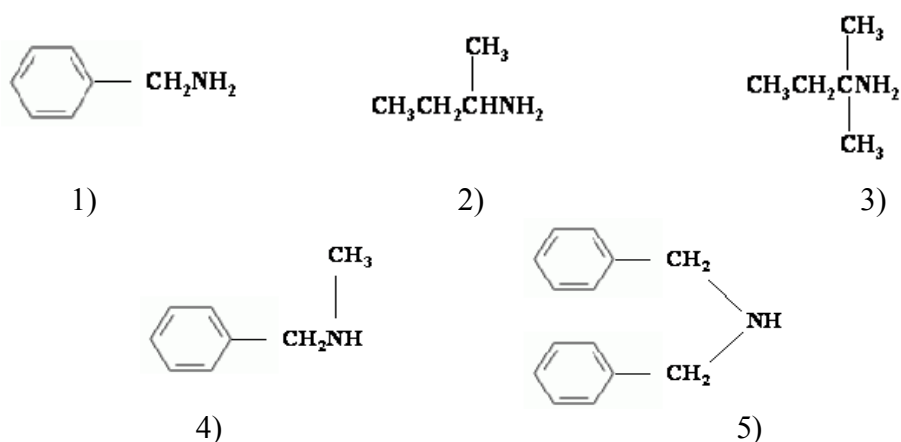


**Figure 3.16 Molecular Structures of Some Amines Used to Study ZDDP Interactions, 1) Benzylamine, 2) S-butylamine, 3) T-butylamine, 4) Benzyl-methylamine, 5) Dibenzylamine [136]**

Shiomi *et al* [136] found that a complex is formed between ZDDP and succinimides and proposed a reaction mechanism (Figure 3.17) of the interaction. They postulated an attack by the nitrogen atom(s) on the zinc cation of the ZDDP molecule. They also proposed that the tendency to form complexes with ZDDP is influenced by the structure of the amine. Amines with little steric hindrance around the nitrogen, such as s-butylamine or benzylamine form complexes with ZDDP in a ratio 2:1 whilst amines of medium steric hindrance such as t-butylamine or benzylamine form complexes with ZDDP in the ratio 1:1. In the case of amines such as tribenzylamine, complexes were not isolated. However, it has also been suggested [131, 142] that the interaction between dispersant and ZDDP may be through N bonding to P in ZDDP molecule in addition to the zinc atom.
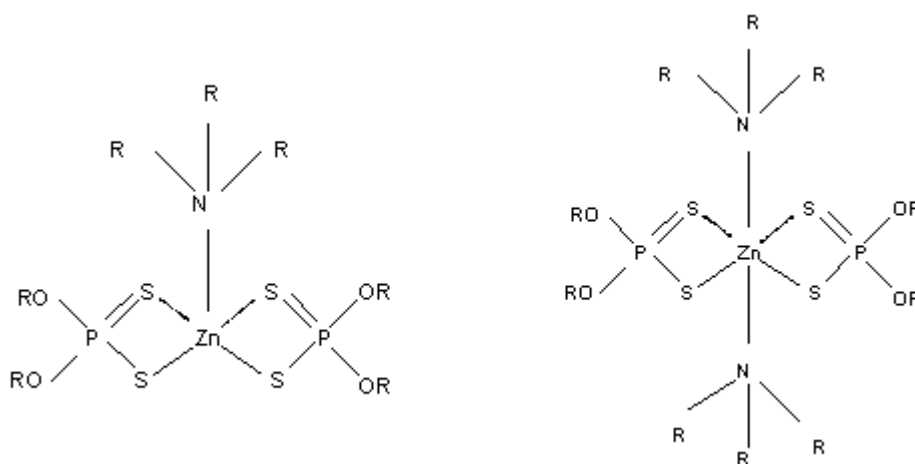


**Figure 3.17 Structures of Complex of ZDDP and Amine 1:1, complex of ZDDP and Amine 2:1 [136]**
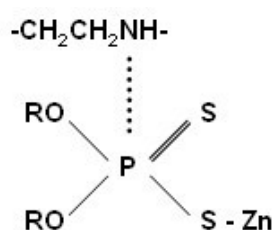


**Figure 3.18 Complexation between ZDDP and dispersant through N-P bonding [131]**

Recently, using XANES analysis, Yamaguchi, Zhang, *et al.* [144, 145] found an organic phosphate complex formed between ZDDP and dispersant which resisted precipitation. They suggested that this resulted in an enhancement and facilitation of the decomposition of ZDDP to short chain polyphosphates, in contrast to dispersant-free ZDDP solutions which formed

long-chain polyphosphates. The chemical composition of the tribofilm was mainly ammonium/zinc polyphosphate. The authors also stated that dispersants do not alter the reactions by which polyphosphates are formed, but simply decrease the polyphosphate chain length.

In other research carried out by Yamaguchi *et al.* [146], the authors showed that dispersant slowed the rate at which ZDDP forms antiwear films on metallic surfaces of passenger car engine.

To protect the nitrogen in dispersant molecule from N-P bonding or N-Zn bonding with the ZDDP molecule, two approaches have been used, both based on post-treating the PIBSA-PAM dispersant, *i.e.* ethylene carbonate (EC) treatment and borated dispersants.

Ashless succinimide dispersant do not have particularly good antioxidant, antifriction, antiwear or acid neutralization properties [147, 148], but borated dispersants possess antioxidation, antiwear, and friction-reducing properties [149]. The molecule structure of a borated dispersant is shown in Figure 3.19 below:
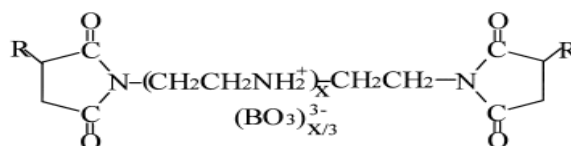


**R=Polyisobutylene X≥3 [149]**
**Figure 3.19 Borated Polyisobutylene Succinic Anhydride/Polyamine (Borated dispersant)**

# Chapter 4 Literature Review - Wear Testing

Since many machine failures are initiated by wear, understanding and prediction of wear has long been an important preoccupation of industry and academic research. This chapter briefly introduces the main types of wear mechanism and then the methods of producing and measuring wear in laboratory bench tests are reviewed. Finally the way to characterize wear using Archard's equation and the use of wear maps are demonstrated.

## 4.1 Introduction

Wear is recognized as the progressive damage and removal of material from a surface during sliding or rolling contact against a mating surface. It leads to reduced durability and reliability of machines, as well as the cost of the replacement of these machine components. Therefore, research on characterizing and reducing wear is of great interest to both academia and industry.

Factors influencing wear include load, relative sliding speed, contact geometry, temperature, local environment and properties of the rubbing surfaces [150]. Under lubricated conditions, these parameters may depend and vary with the nature of the lubricant. Reciprocating sliding is also thought to provide different wear behaviour from continuous, single direction sliding since it provides different fluid film response and wear particle flow [151]. This makes the measurement and study of wear quite complicated and problematic.

It is generally recognised that there are four primary types of wear: abrasive wear, adhesive wear, fatigue wear and corrosive wear [152]. These wear mechanisms rarely act independently in practical systems and frequently more than one mechanism will be involved in realistic rubbing conditions. They can also act in a synergistic manner, to produce faster wear than the sum of the individual wear mechanisms.

A large number of test methods to produce and quantify wear are described in the literature. Zum Gahr [153] has classified five levels of simple tests, in addition to the field test of the entire system. These are bench tests, sub-system tests, component tests, simplified component tests and model tests. This review mainly focuses on laboratory bench wear tests. These are the lowest level in the hierarchy above and slide (and in some cases also roll) two specimens against each other in a simple manner to produce wear. The specimens are generally selected to be low cost, easily reproduced or available pieces of the materials of interest. Standard bench tests, such as the four-ball, block on ring, ball/pin on disc and V-block tests are commonly used to simulate wear under different conditions. Furthermore, wear tests are

performed in countless number of ways to relate the properties of rubbing materials, mechanical system and environment to reality.

There are several ways of measuring and analysing wear. Methods of measuring wear can be categorised into mass loss, linear, area and volume measurements, thin layer activation (TLA) and inductively-coupled plasma emission spectroscopy (ICP-AES) [154]. Wear debris, worn surface and subsurface microstructure are also often examined to identify the main type of wear mechanisms involved [155].

Based upon a large number of wear tests, Archard derived a predictive wear equation that has become widely used to characterize wear in a given system [156]. At the outset it must be emphasised that this equation is not universally obeyed and is always an approximation. Archard's wear equation relates the wear volume $V$ to the hardness of wearing materials, load $W$ and sliding distance $L$ by an equation of the form:

$$V = \frac{K_A WL}{H} \qquad (4.1)$$

In this equation, the non-dimensional proportionality constant $K_A$ is termed the Archard wear coefficient and can be to characterize the wear resistance of a material and lubricant combination.

In the context of the wear of lubricated systems, it should be noted that Archard's wear equation takes no account of any hydrodynamic film formation. It should be applied only when there is negligible such film or the extent of separation by a film is invariant.

## 4.2 Wear Mechanisms

As mentioned above, wear is classified into four main types depending on the material removal mechanism. These are shown schematically below.
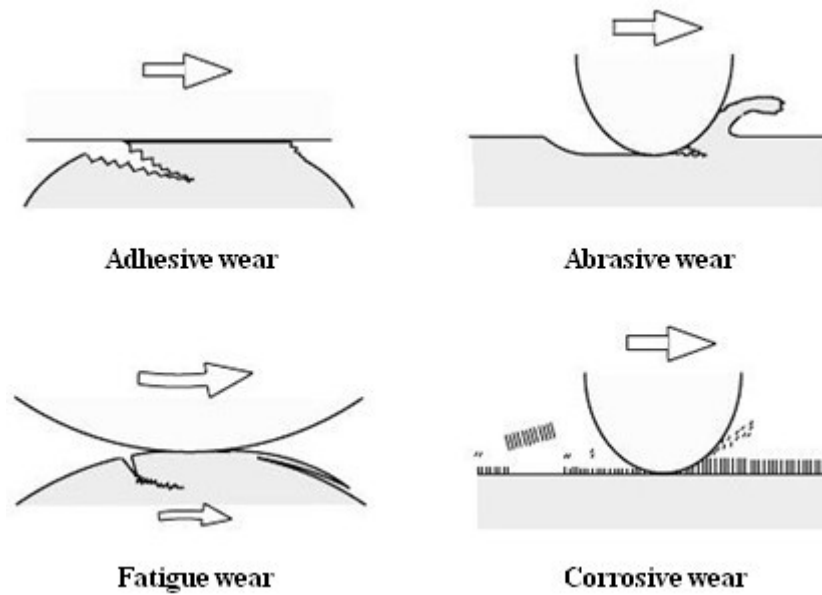
**Figure 4.1 Wear Mechanism Models [157]**

Adhesive wear

Adhesive wear is generated when there is adhesion followed by permanent removal of the adhered material from one or both of the two surfaces. Adhesive wear happens when there is adhesive bonding between the asperities of two relatively-moving surfaces; plastic deformation occurs and a crack initiates and propagates in the contact region under compression and shearing. When the crack reaches the contact interface, material transfer and resultant adhesive wear will be promoted. The result of adhesive wear is characteristically a matted, torn surface, grooved in the direction of sliding, and often with transferred ridges of material [158]. Adhesive wear tends to be more prevalent when identical materials are rubbed together since bonding and adhesion occurs more readily in this condition. Adhesive wear is prevented or reduced in systems where active chemicals are present that can react rapidly with clean surfaces to form films and prevent adhesion. This means that rates of adhesive wear are normally much smaller in lubricated systems with oils containing additives than in unreactive base oils and dry systems. Severe adhesive wear occurs where an unreactive lubricant is used in high loading with high sliding, when the rate of removal of a reaction film is faster than its rate of formation, or when the yield strength of rubbing surfaces is exceeded, which breaks up any protective chemical film formed on the surfaces.

Abrasive wear

In the case of plastic contact between different metallic surfaces, the asperities of the relatively harder surface penetrate to the softer one and remove particles from the latter

surface; the resultant wear is called abrasive wear. After penetration, ploughing takes place in sliding, and this ploughing can cause removal of surface material and the formation of an abrasive groove on the softer surface. For ductile materials, wear particles are generated by the mechanism of microcutting; while the particles are generated by crack propagation for brittle material. According to material properties at the contact region and the contact environment, abrasive wear is commonly classified to two-body and three-body wear modes. Two-body wear occurs when the rough and harder surface is abrading the softer surface, while the more common three-body wear mode occurs when the hard wear particles are free to roll and slide between the two rubbing surfaces. Clearly one strategy for reducing two body abrasive wear is to have two surfaces of similar hardness, while reduction of three body abrasive wear can be obtained by using very hard surfaces.

Corrosive wear

Corrosive wear refers to the removal of chemically-reacted layers of material which are being continually formed on rubbing surfaces. When surfaces are rubbing together in a corrosive liquid or gas lubricated system, chemical or electrochemical interactions take place to form a reaction product on the surfaces. These reaction products usually prevent or reduce adhesive wear. However they are generally softer than the substrate and are thus more easily abraded. If abrasion takes place, fresh surfaces will be exposed and react. This process results in removal of reacted substrate material and thus wear. If abrasive removal of the film is rapid, the actual wear rate depends on the rate of the corrosive reaction.

Fatigue wear

Fatigue wear is surface failure caused by the development of cracks initiated and propagated in rubbing surfaces by repeated stress cycles resulting from asperity contact. When these cracks reach a critical size, the material above them is removed. Fatigue wear usually happens when the sliding is not severe enough to produce adhesive and abrasive wear, such as in low slide to roll ratio contact conditions.

During rubbing, the dominant wear mode may change from one to another. This may be because wear changes contact geometry and properties of the rubbing surfaces, and also because additives in lubricant may react to form surface films over time.

Adhesive/Corrosive balance

An adhesive/corrosive balance is often seen in formulated oil lubricated systems, where chemical reactivity of rubbing materials and additives in lubricant varies with the operating conditions or additive concentration. Under some conditions, such as using unreactive oil, unreactive surface, low temperature or high load, the reactivity of rubbing materials or additives in lubricant is low, which results in a slower rate of protective film formation and thus high adhesive wear. As the conditions (typically temperature or additive concentration) are changed, more surface reaction can occur, which reduced adhesive wear and thus overall wear. However under more extreme changes of condition, surface reaction may become so fast that corrosive and thus overall wear is excessive. There is thus an intermediate range of conditions which gives lower wear than either extreme.

Studies [159] on antiwear mechanism of ZDDP have shown evidence of this adhesive/corrosive balance. As shown in Figure 4.2, wear rate is large when the ZDDP is at a low concentration. According to the research on the antiwear mechanisms of ZDDP [28], a certain amount of ZDDP needs to be present since ZDDP to react with iron oxide on the steel surface to form an antiwear film. Small amounts of ZDDP may not enough to form a protective film.
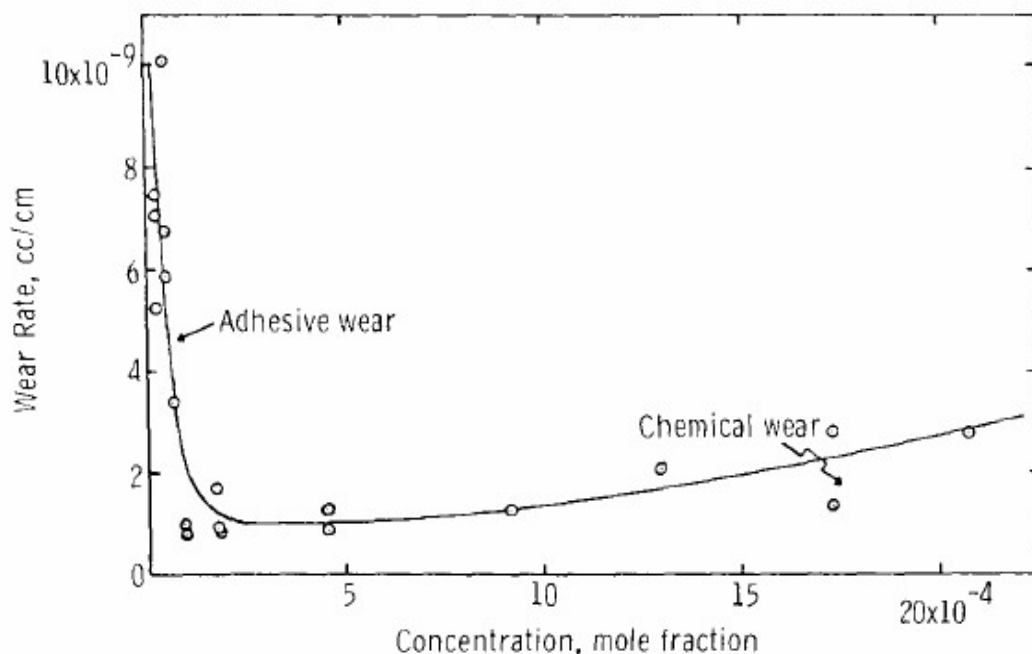


**Figure 4.2 Effect of Concentration of ZDDP on Wear Rate [160]**

## 4.3 Types and Conditions of Contact

Type of relative movements

In terms of the relative movements of two rubbing surface, wear tests can be classified into pure sliding and mixed rolling-sliding. Wear caused by both these two types of movements needs to be investigated since they are separately related to different realistic tribological contacts, for example the movement of piston rings and cams in engines respectively. Standard test such as four-ball, block on ring, ball/pin on disc operate in pure sliding, rubbing one surface against a stationary counterpart, while tests such as the mini traction machine (MTM) with a ball-on-disc configuration move both surfaces with respect to the contact and thus can produce mixed rolling-sliding. A key difference between pure sliding and rolling-sliding is that in pure sliding, the contacting region of one of the surfaces remains buried in contact all the time, whereas in rolling-sliding fresh regions of both surfaces enter the contact continually. Wear tests can also be divided into continuous, unidirectional sliding and reciprocating sliding. In the former the entrainment speed and thus lubricant film thickness are constant while in the latter they vary and the entrainment speed falls to zero during reversal. Also reciprocation can result in very different wear particle behaviour in the reversal zones.

Types of contact geometry

Wear is also influenced by the contact geometry and contact pressure distribution, which vary with the specimens used in different types of wear tests. Point contact can be seen in four-ball, ball on disc and MTM; while line contact and area contact is seen in block on ring and pin on disc tests separately. Often sliding point contact is preferred in bench tests, even though it is quite uncommon in practical engineering devices, simply because such contacts pose no alignment problems to ensure repeatable loading. In both point and line contacts, as wear progresses it changes the contact geometry, contact pressure and other parameters, which subsequently leads to difficulties in studying and predicting wear. Therefore tests that produce appropriate wear without changing the contact geometry too much are valuable when quantifying wear.

Most standard bench tests are based on pure sliding, partly because this localises wear on one surface, thus making it easier to measure but also because it is simpler to drive one surface than two. Most tests also operate under severe conditions of load so as to generate measurable wear in a reasonably short time. However in reality, most machine components are lubricated by formulated oils and operate in non-severe conditions where only slow rates of wear, *i.e.* 'mild wear' occurs. Such wear requires long test times before sufficient material has been removed to be measured accurately. For the study and prediction of lubricated wear we need ways of measuring mild wear in realistic conditions, which must involve reasonably short test time and measure very small amounts of wear which do not change contact geometry too much.

## 4.4 Measuring Wear

A number of ways have been developed to measure wear, as wear quantification is the only way to characterize and subsequently predict wear. Brown [155] and Ruff [161] have reviewed test methods for measuring wear.

Mass loss

This method is a widely used wear quantification technique because it is convenient and straightforward, in which it calculate the wear by weighing the sample before and after the test. However, it is only suitable for the tests in which the mass loss is high relative to the total mass of the specimen, so this method requires large wear rate and relatively small specimens. Further, mass loss gives very little information on the distribution of wear over the rubbing surface and great care must be taken to clean the specimens in case of deposit of oxidized oil and debris.

Dimensional changes

Another way of quantifying wear is to measure the dimensional changes of specimens, which includes linear, area and volume measurements after the wear tests.

Linear measurement is generally used in pin-on-disc wear tests where it quantifies wear by measuring the pin length reduction continuously during the test. However it is also applied to measure the change in diameter of cylindrical shafts, discs or bushes after wear tests. In this measurement, a high resolution displacement transducer and relatively high rate of wear are required to determine wear rates accurately.

Area measurement is commonly used in the 4-ball, high frequency reciprocating rig (HFRR), 4-ball and block on ring to measure the change in contact geometry and scar on the stationary surface. Then volume of removed material can be estimated by multiplying the measured area by depth of the wear scar, calculated from its diameter. However, this calculated value is always an approximation since it presumes a consistent wear depth distribution across the scar.

Volume measurement techniques include AFM [162], light interferometry [163] and other 3-D surface profilometers. These techniques allow very precise measurements of small amount of material removed from specimens and thus are suitable for the measurements of very mild wear under both pure sliding and mixed rolling-sliding conditions. Gahlin [164] used AFM to measure the local wear volume and to map the distribution of wear based on comparing the topography of the same surface region before and after testing, which has the sensitivity to measure 30 nm wear depths. Recently, commercial scanning white light interferometry microscopy (SWLI) [165] has been applied to map the rubbed the surface topography to study the antiwear performance of ZDDP-containing lubricants and it has been shown that antiwear films must be removed from the wear scar prior to measurement to obtain accurate measurements of mild wear volume.

Thin Layer Activation (TLA)

TLA has been used to measure wear and corrosion in industrial and engine components. It uses high-energy charged particles beam to produce a radioactive surface layer and then detecting the quantities of metallic radioisotopes removed from the surface during wear. The radioisotopes decay with the emission of gamma radiation. Therefore the wear can be monitored by measuring the radioactivity of either the lubricant or the surface using a gamma detector. Although very small amounts of radiation are involved this method is complicated by the need to address health and safety implications of the use of radioactive materials.

Inductively Coupled Plasma- Atomic Emission Spectroscopy (ICP-AES)

In ICP-AES, a plasma source is used to dissociate the metal-containing sample in a solution into atoms or ions, exciting them to a higher energy level. The excited metal atoms or ions then emit photons of a characteristic wavelength, which can be recorded by a spectrometer and compared to standards to quantify the metal present. Fan and Spikes [166] developed a mild wear test method by employing the ICP-AES to monitor the concentration of iron in lubricant solution from which wear rates in mild lubricated wear in rolling-sliding contact could be determined. ICP-AES was suited to this because of it is able to measure very low concentrations of a wide range of metals simultaneously. It proved to be reliable and repeatable in their study.

The current research will adopt volume measurement technique using a white light interferometry microscopy to study the wear properties of ZDDP- and/or dispersant-containing lubricants.

## 4.5 Archard's Wear Equation and Wear Maps

The most widely-accepted, quantitative relationship between wear rate and operating conditions is Archard's wear equation:

$$V = K_A WL/H \qquad (4.1)$$

in which the non-dimensional constant $K_A$ is termed Archard Wear Coefficient. The coefficient $K_A$ is commonly used to characterize the wear resistance of both material and lubricant. By rearranging Equation 4.1 it can be seen that

$$K_A = VH/WL \qquad (4.2)$$

and dimensional analysis indicates that $K_A$ is thus non-dimensional. In practice a simpler form of the wear equation is often used which does not include the hardness:

$$V = KWL \qquad (4.3)$$

Here $K$ is another coefficient, which has dimensions and is often simply called the "wear coefficient" [152]. It is generally quoted in units of mm$^3$/N·m.

This coefficient can vary enormously; wear in very mild conditions has wear coefficient values of less than K = 10$^{-9}$ mm$^3$/N m while severe wear can have values of 10$^{-4}$ mm$^3$/N m or more. The table below classifies wear dominated by the various types of wear mechanism. Archard [156] explained that *'K may be described as the coefficients of wear and, in a series of experiments with the same combination of materials, changes in K denote changes in surface conditions.'* The wear coefficient is therefore of great importance so that enormous research has been carried out to study wear resistance of materials and lubricants in terms of *K*.

Though Archard's wear equation is the most commonly-used wear equation, it makes no assumption about the rubbing surface topography or its variation with time.

| Classification | Wear Mechanisms (dry sliding conditions) | Wear coefficient range |
|---|---|---|
| Wear dominated by mechanical behaviour of materials | 1. Asperity deformation and removal | 10$^{-4}$ |
| | 2. Wear caused by plowing | 10$^{-4}$ |
| | 3. Delamination wear | 10$^{-4}$ |
| | 4. Adhesive wear | 10$^{-4}$ |
| | 5. Abrasive wear | 10$^{-2}$ - 10$^{-1}$ |
| | 6. Fretting wear | 10$^{-6}$ - 10$^{-4}$ |
| | 7. Wear by solid particle impingement | 10$^{-6}$ - 10$^{-4}$ |

**Table 4.1 Classification of Wear Mechanisms and Wear Coefficient Range [167, 168]**

Based upon a large body of literature data, Lim and Ashby [169, 170] have produced wear maps. These maps present wear data in a graphical manner to show the dominant wear mechanisms under different conditions and their relationship, as well as the anticipated wear rates. In this model, the asperity temperature at the contact is assumed to dominate the dry sliding of steels on pin-on-disc wear testers under most conditions. As shown below, wear rate values are presented on normalised load and sliding speed axes and divided into regimes where different wear mechanisms are dominant. Wear severity levels and correlated mechanisms under certain conditions can be predicted and presented by using this type of

wear map. However, Lim and Ashby's map only presents the relations between these variables for two steel surfaces under dry, pure sliding condition.
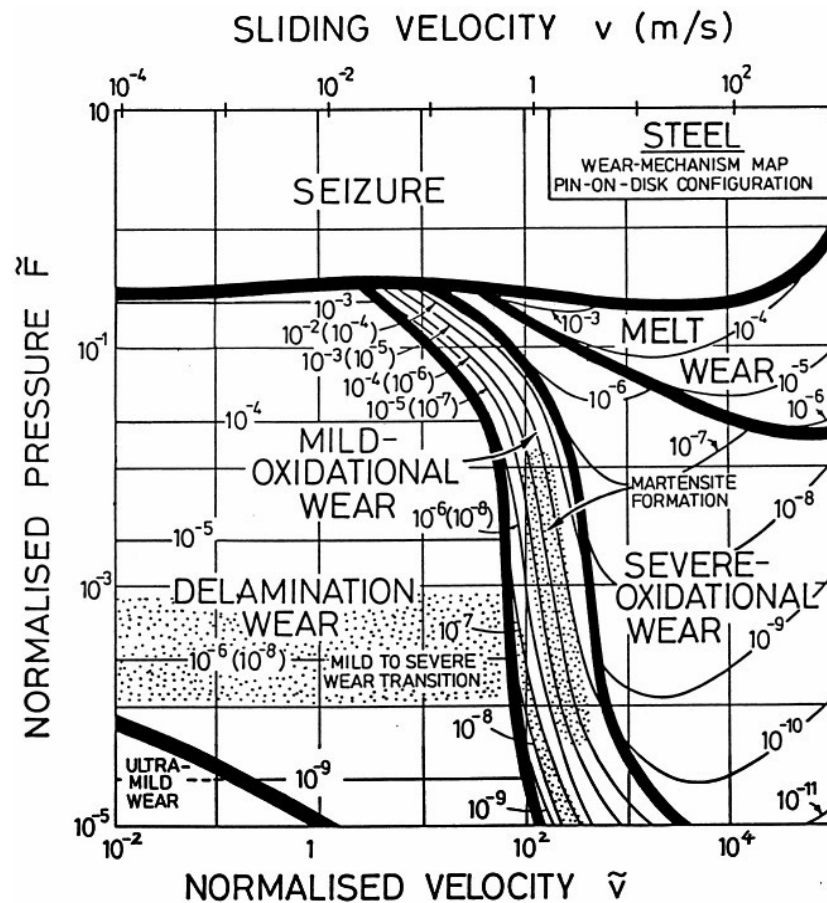


**Figure 4.3 Wear Mechanisms Map for Steel [169]**

For steel under lubricated conditions, Beerbower [171] presented a wear map providing the relation between wear rate and the specific oil film thickness as shown in Figure 4.4. In his map, specific wear rate is plotted against specific oil film thickness of a given system in which the hardness of rubbing pair and the load at the contact point are constant. The specific film thickness in this wear map is the elastohydrodynamic film thickness derived from Dowson and Higginson [172] divided by the effective roughness of the two surfaces, thus it involves several key operating conditions - load, viscosity, velocity and roughness.
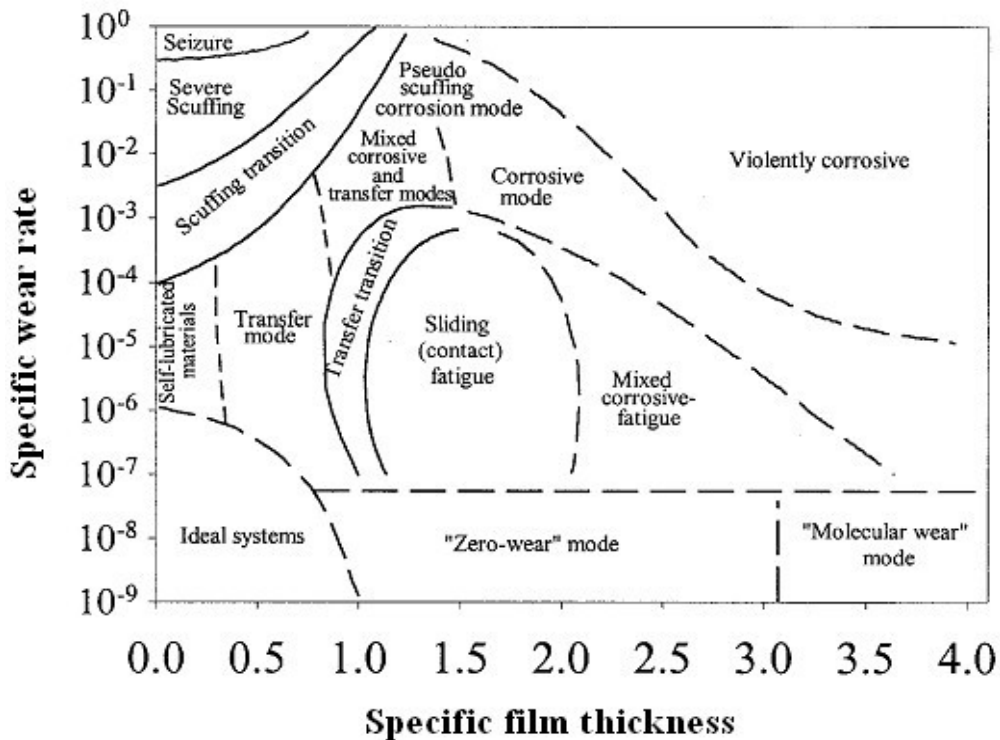
**Figure 4.4 Wear Mechanisms Map for Steel under Lubricated Conditions [171]**

Wear maps have gone through extensive development since Beerbower, Lim and Ashby. Researchers have extended the concept of wear mapping to include steel [169, 170], ceramics [173], metal-matrix composites [174], polymers [175], coatings [176], cutting tools [177] and so on. These wear maps provide an enormous database for wear under different conditions through a direct graphical presenting way, which should benefit both academia and industry in wear prediction and machine design.

In the current study, wear coefficients for different lubricants will be calculated to investigate the effect of concentration and type of additives on the antiwear properties of ZDDP-containing oils.

# Chapter 5 Experimental Techniques and Materials

Several different test methods were used in this study including methods for measuring lubricant film thickness on or between surfaces, and different ways for obtaining and measuring wear methods. This chapter describes these methods, the test protocols used and shows examples of typical results. At the end the chapter the lubricants and specimens materials employed in this study are listed.

## 5.1 Introduction

The tribological properties of lubricant additives can be investigated by measuring friction and wear performances in rubbing contacts and comparing this performance with lubricants containing no additives or alternative additives. Since lubricant additives must influence friction and wear by forming films of some sort on rubbing surfaces, it is also important to measure and monitor the presence and the properties of these films and correlate these to friction and wear performance.

In current study, several test rigs were selected to study the film formation, friction and wear properties of the additives of interest. The Mini Traction Machine-Spacer Layer Interferometry Method (MTM-SLIM) was chosen to monitor the film thicknesses developed on rubbed surfaces and also to measure Stribeck friction curves. The MTM-reciprocating rig under both pure sliding and mixed rolling sliding conditions was used to study the wear resistance of antiwear additive-containing oils, as well as another pure sliding method, the High Frequency Reciprocating Rig (HFRR). Scanning White Light Interferometry (SWLI) and Atomic Force Microscopy (AFM) were used to characterize the rubbing surface and the wear track, both to examine the boundary films present and also to quantify wear volumes.

In this chapter, these test methods are introduced separately, followed by information of the lubricants and rubbing materials employed.

## 5.2 MTM-SLIM

### 5.2.1 MTM
The mini traction machine (MTM; PCS Instruments, Acton, UK) consists of a steel ball loaded against the flat surface of a steel disc. The ball and disc are driven by independent motors and rotating separately, so that any desired combination of rolling and sliding can be obtained. This tribometer collects friction data by using a load cell located on the ball driver.

The steel disc is fully submerged in lubricant in a bath with a temperature controller to heat and maintain the lubricant temperature. When a test is in process, the lateral force on the ball generated from friction is detected by a load cell and recorded. The lubricant bath is covered by a metal lid and surrounded by an insulated container so that the temperature of the lubricant can be controlled and maintained within the range from ambient (or lower with optional cooler) to 150ºC. All the parameters of the MTM tests, such as speed of ball and disc, temperature, load and duration, can be controlled by a programmable series of commands in a computer. Curves of entrainment speed *versus* friction coefficient can be obtained as the test progresses.

### 5.2.2 MTM-SLIM

In MTM-SLIM, an optical attachment is used with the normal MTM to enable additive film formation on the ball track to be monitored using optical interferometry during a test.

Optical interferometry has been successfully employed to study elastohydrodynamic (EHD) lubricants for many years [163]. One variant of optical interferometry is 'SLIM' (spacer layer image mapping). This is based on optical interferometry. The principle of spacer layer image mapping is shown in Figure 5.1. One of the flat surfaces of a glass disc is coated with a thin chromium layer on top of which is a silica layer. This surface is loaded against a reflective steel ball. White light is employed as the light source. When shone into the contact through the uncoated face of the disc, one beam is reflected directly back from the semi-reflective chromium layer of the glass while another goes through the silica spacer layer and lubricant film before being reflected back from the steel ball surface. The latter beam thus travels two spacer layer and oil film thicknesses further than the former, so that the two beams have a phase difference. Therefore, upon recombination they interfere, constructively or destructively. The thickness of the lubricant film can be determined from the difference in distance travelled between the two beams. The interference image is captured by a digital colour camera, and then the red, green and blue colour of each pixel in the image is converted, *via* a calibration chart, to a film thickness map over the contact. Clearly the thickness directly calculated from the image contains the thickness of the silica spacer layer coating, so that obtaining the absolute lubricant film thickness necessitates the subtraction of the spacer layer thickness, which can be calculated at the beginning of a test with a direct contact of the glass disc and the steel ball.
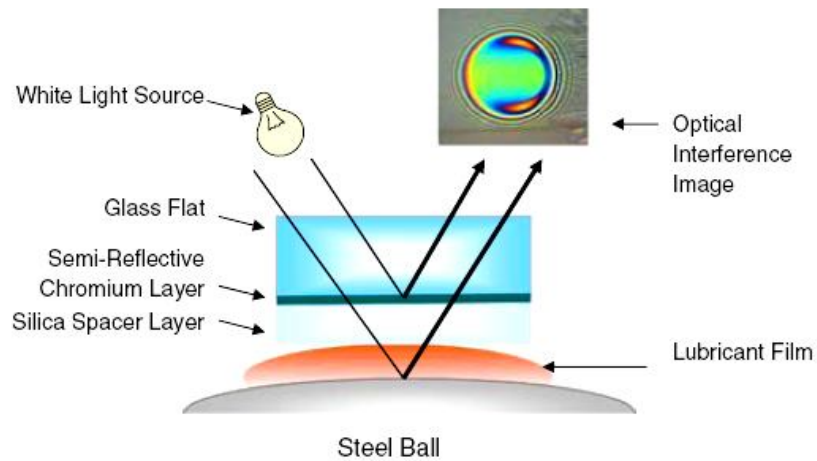
**Figure 5.1 Principle of Spacer Layer Image Mapping**

Normally, one limitation of the spacer layer method is that it cannot be used to measure the thickness of films formed on rubbing surfaces where there is both sliding and direct solid-solid contact occur, as are required for ZDDP film formation. If such sliding contact is present, the silica and chromium layer coated on the glass surface necessary for interference are abraded rapidly. However, a technique has been developed by Taylor and Spikes [178-180] in which the SLIM approach can be used to measure the thickness of ZDDP antiwear films. This is done by periodically halting motion in the MTM and capturing interference images from the stationary ball surface in situ, *i.e.* without moving the ball from the lubricant bath. The arrangement of the MTM-SLIM rig is shown schematically in Figure 5.2.
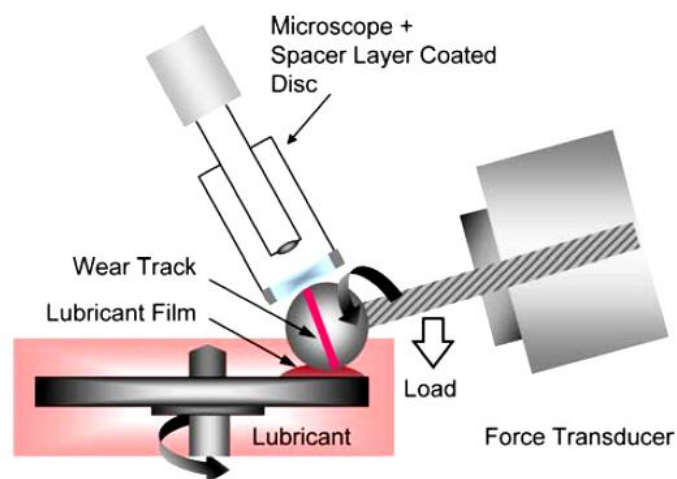


**Figure 5.2 Schematic Diagram of In-situ Spacer Layer Interferometry Setup on the MTM**

The spacer layer image mapping setup is attached to the mini traction machine *via* a three-way moveable stage. Normally, an MTM-SLIM test consists of several steps as listed below [106]:

(a) The lubricant bath is heated with the steel ball and disc rotating without contact until the required test temperature is reached.

(b) Motion is then halted and the stationary steel ball is loaded upward against the coated glass window. An interference image of the glass disc/ball contact is captured for subsequent analysis to determine the spacer layer thickness.

(c) The steel ball is then unloaded from the glass window and a rubbing test is carried out for a set duration at the set temperature. In this, the steel ball is loaded against the steel disk and the two rubbed together in mixed rolling/sliding condition at low entrainment speed and thus in mixed or boundary regime. If suitable additives are present this generates a tribofilm on the rubbed track on both the steel ball and steel disk.

(d) Motion is then halted again, the rubbed track on the stationary steel ball is loaded against the glass window, and an interference image of the window/ball contact is captured. By comparison with the initial image, the interference colours present can be used to determine the thickness of any transparent, solid-like tribofilm formed on the track.

(e) Procedures (c) and (d) are then repeated over a total test time of several hours to obtain a series of interference images and thus maps of the variation of tribofilm thickness on the ball with rubbing time.

In this way, the films formed on rubbing tracks can be visualized and measured. By plotting the measured film thicknesses against rubbing time, the rate of film formation (and removal) can be obtained. Clearly friction can also be measured periodically as described in the previous section. Typical SLIM images and friction curves are as shown below:
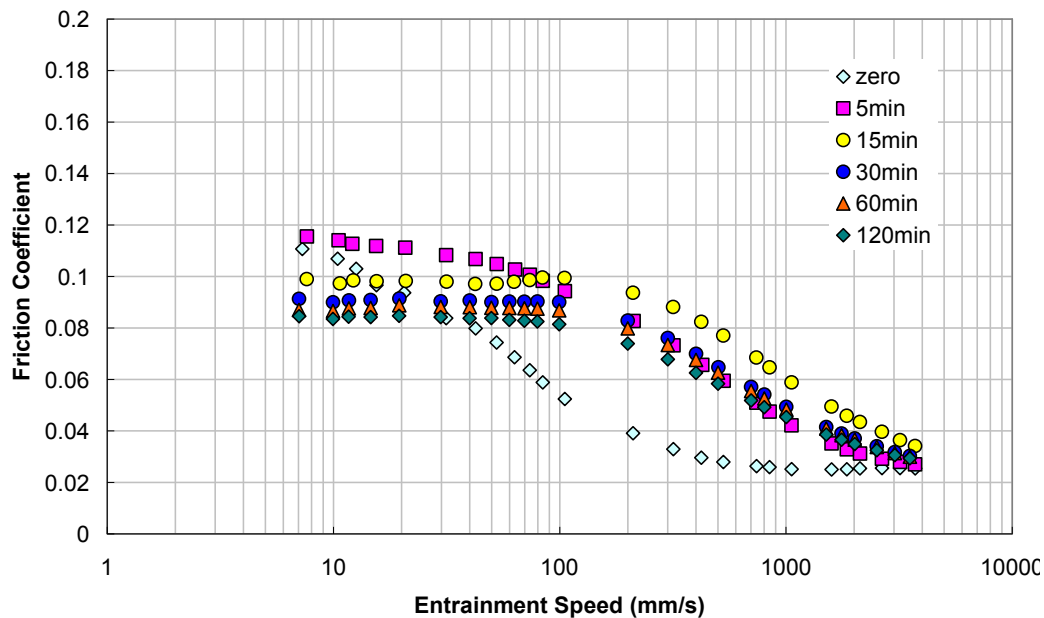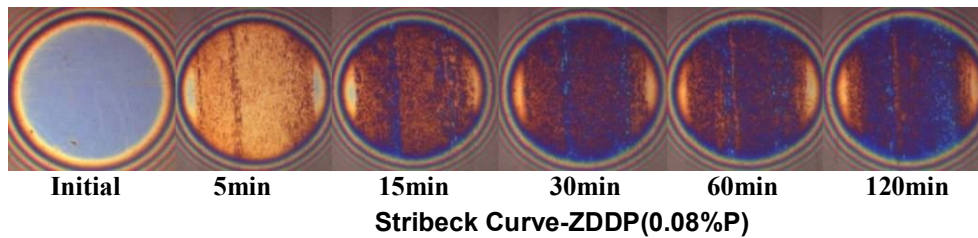
**Figure 5.3 Typical MTM-SLIM Results**

## 5.3 MTM-Reciprocating and HFRR Wear Tests

### 5.3.1 MTM-Reciprocating

In normal MTM or MTM-SLIM tests, the wear tracks on the ball and disc are both circumferential tracks (that on the ball is not central since the ball is tilted as shown in Figure 5.2). This means that wear is distributed over a long track so that when wear is very small (mild wear) it is difficult to measure accurately. A way is needed to localize the wear so that it can be measured from, ideally, a single SWLI image.

There is also another issue that needs to be considered in studying wear; whether motion should be pure sliding or rolling/sliding and, indeed, whether pure sliding gives different wear rates from mixed rolling/sliding conditions.

To help localize wear and thus make it easier to measure, a reciprocating mechanism can be added to the standard MTM system. This mechanism replaces the existing belt-driven system for the disc and allows the disc to be driven in continuously oscillating motion. The mechanism allows the disc to oscillate over different stroke length with frequency of disc oscillation set by programming using the same computer as used to set the other testing parameters of load, ball speed, test duration and temperature. In the current work a preset stroke length of 4 mm was used to localize the wear on the disc over this length.

The normal MTM motion is mixed rolling/sliding, which means the ball rotates against to the oscillating disc, as shown in Figure 5.4 a). However the ball speed can be set to zero in the reciprocating MTM programme, which converts the contact conditions to pure sliding, as shown in Figure 5.4 b). To prevent frictional torque from driving the ball moving, a small pin is employed to prevent the ball shaft rotating.
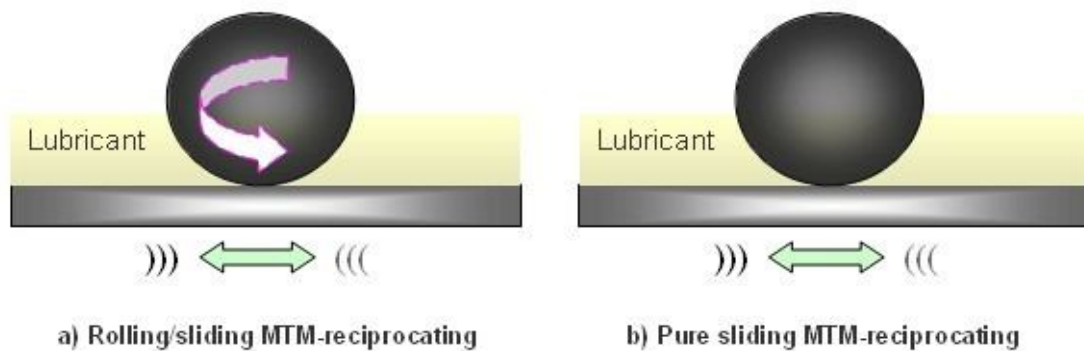


**Figure 5.4 Schematic Diagrams of MTM-reciprocating Motions**

The speed of the ball can be preset when mixed rolling/sliding condition is required, while the disc speed for both pure sliding and mixed rolling/sliding is sinusoidal. Average disc speed is proportional to the given frequency, $f$, and stroke length, $l$, in the form of:

$$u_d = 2fl \tag{5.1}$$

In this equation, the average disc speed is in mm/s when the frequency is in Hz and the stroke length is in mm.

The specimens are collected and cleaned after each test (the way of cleaning is described at the end of this chapter), and they are then measured by Wyko and/or AFM. Photographs of

the disc specimen are shown in Figure 5.5, one of which illustrates the wear track produced by during reciprocation. The wear scar is small enough to be captured with a single SWLI image and thus the wear can be quantified easily.
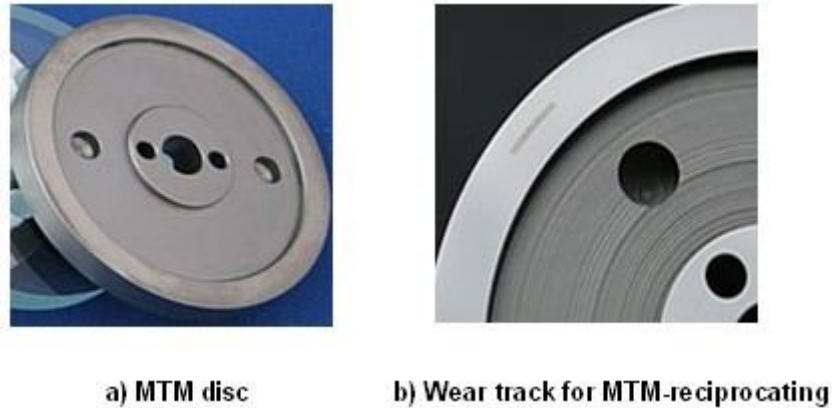


a) MTM disc          b) Wear track for MTM-reciprocating
**Figure 5.5 MTM Disc Specimens and Wear Track**

Probably the only drawback of this MTM-reciprocating system is that the wear track is an approximately circular segment which makes the wear depth distribution along this track quite difficult to calculate. However, this can be addressed by using a commercial analysis program with the data file created by the SWLI instrument. The SWLI captures the topography of the small region which contains the wear track and simultaneously creates a data file of the height distribution of this whole region. A functional program is then coded to pick up the height distribution data along the wear track centre and plot it in a graph. Results have proved to be reliable by comparing them with direct mathematic analysis calculations, as shown in Chapter 8.

**5.3.2 HFRR**

The High Frequency Reciprocating Rig (HFRR) has been used for many years as a wear characterizing test rig and is the industry standard test for diesel fuel lubricity described in ASTM D6079, CEC F-06-A, ISO 12156, EN 590, JPI-5S-50 and IP 450 [PCS Instrument, Acton, UK]. This mature technique was applied in the current study as a reference wear test to compare with the pure sliding MTM-reciprocating tests. Furthermore, the high frequency in the HFRR shortens the test duration compared to the MTM-reciprocating system whose frequency has a maximum of 20Hz, which is limited depending on the stroke length.

**Figure 5.6 HFRR Specimens**

A schematic diagram of HFRR is shown in Figure 5.7. It can be seen that in an operating HFRR, the disc specimen is stationary while the ball is oscillating, which is opposite to the pure sliding MTM-reciprocating test.
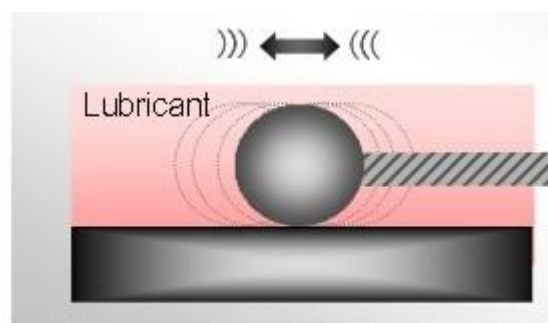

HFRR
**Figure 5.7 Schematic Diagram of HFRR**

When the contacts are lubricated, the above three methods all localize the wear to be easily quantified by surface analysis apparatus and together they provide a series of linked tests which should illustrate the effects of rolling-sliding and stroke length.
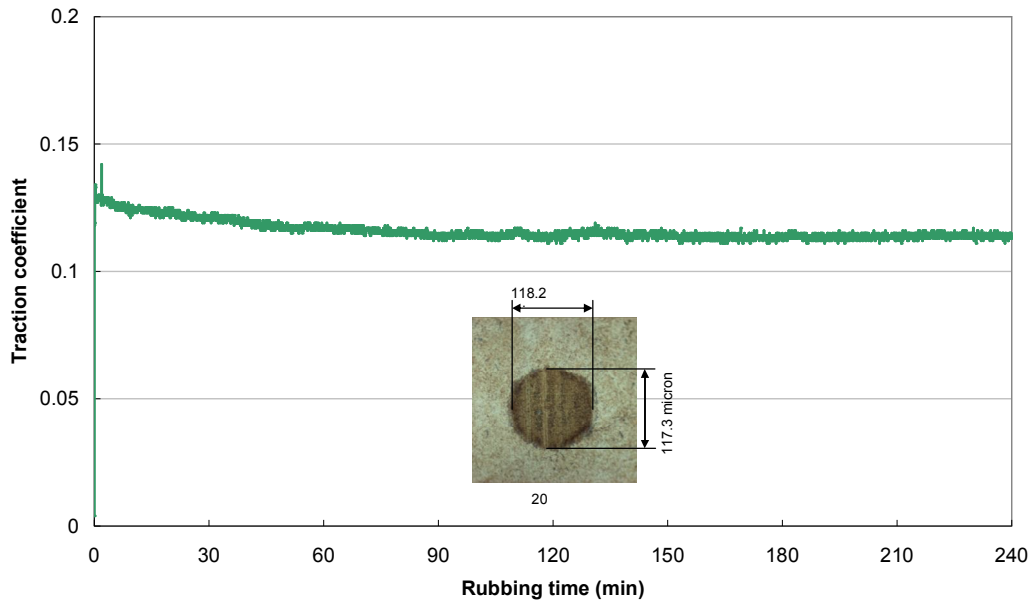
**Figure 5.8 Typical HFRR Results**

## 5.4 Wyko and AFM

Accurate wear measurement has been of great interest for years both for use in mild wear tests and also to help understand the origins of mild wear. Running-in, mild and severe wear are three typical regimes of a wear system, of which two of them - running-in and mild wear produce too small amount of wear to be measured easily. However too much wear can change the contact geometry greatly and result in variations of wear mechanism. Therefore, techniques are needed which are able to accurately measure very small amount of wear. Wyko and AFM are capable of mapping surface topography at the nano-scale and thus quantify tiny amounts wear. In this study, specimens were analyzed by Wyko and/or AFM after each test.

### 5.4.1 Wyko SWLI

The Wyko SWLI uses scanning white light interferometry to map the surface topography to very high resolution. It is based on a similar principle to the SLIM introduced previously. In the current study, a commercial scanning white light interferometry microscopy, a Wyko NT9100 Optical Profiler shown in Figure 5.9 was used to capture visual images of the rubbed specimens.
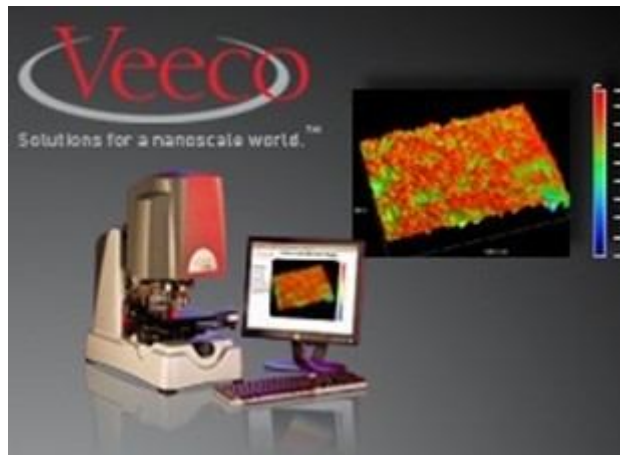
**Figure 5.9 SWLI Wyko NT9100**

This Wyko is very easy and quick to use compared to other surface analysis methods, and it can map surfaces without contacting them, which avoids specimen damage and contamination. The main function of this is to obtain 2D and 3D height distributions of the surface of specimen, as shown in Figure 5.10. Volume analysis can be achieved by operating software available with this Wyko profiler. This software firstly sets a reference plane as the average height of the unworn region outside the wear track; the wear volume is then calculated as the worn volume under this reference plane. One drawback of is technique is that the use of light interferometry may cause confusion if the light travels through transparent or translucent objects.
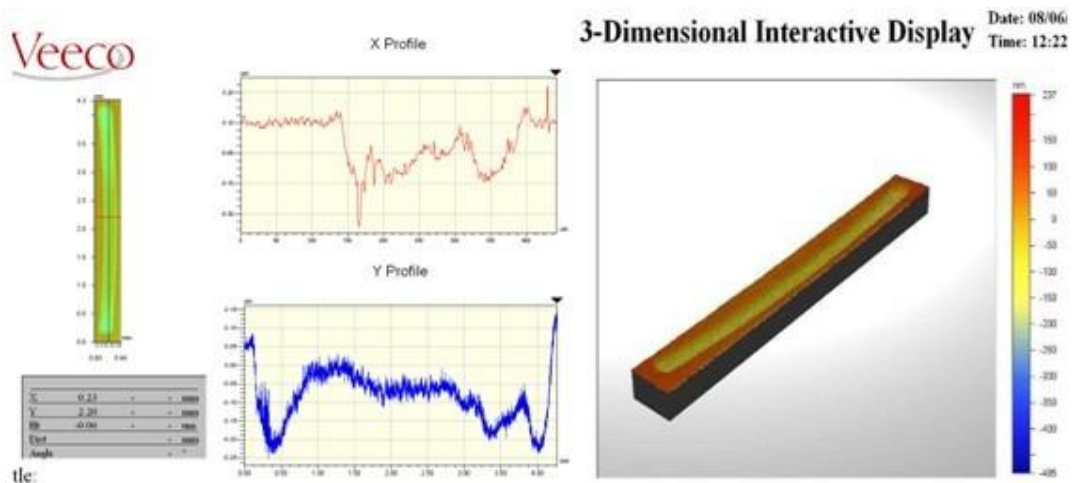

a) 2D analysis of the wear track    b) 3D image of the wear track
**Figure 5.10 Wyko Surface Analyses**

In current study, Wyko was used routinely to profile the height distribution along the wear tracks and calculate the wear volume of many specimens. Figure 5.10 a) shows a Wyko interference image from a reciprocating MTM disc after a test and illustrates the crescent-shaped wear scar formed on the disc surface. Also shown are profiles across the wear scar in the x-direction (across the crescent) and y-direction (along the crescent). Figure 5.10 b) shows a 3-D topography map from which the wear volume is calculated.

### 5.4.2 AFM

The scanning tunnelling microscopy was invented by Binnig in 1986 and was described in chapter 2. AFM is a similar technique in which the tip is attached to the free end of a cantilever and is then brought proximity of a sample surface. The mechanical interaction between the tip and sample surface leads to bending of the cantilever. During scanning, the tip is moved up and down to maintain a constant repulsive force between the tip and the surface, to draw the height map. The technique was later developed by Mate [181] to measure also the lateral force between the tip and sample surface (LFM). This force is considered to represent the friction force at the microscale. Subsequently AFM has been extensively developed to study various materials (metal semiconductors, soft biological samples, conductive or non-conductive materials) and environments (air, liquid, vacuum) [182]. The disadvantage of AFM compared with some other surface analysis techniques like scanning electron microscopy (SEM) is that the single scan size of AFM is limited, a maximum height on the order of 10-20 micrometers and a maximum scanning area of about 150×150 micrometers.
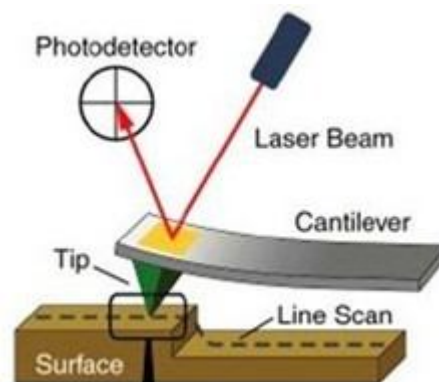


**Figure 5.11 Schematic of AFM Main Components**

At the end of MTM tests, the discs can be analyzed using AFM in contact mode in order to investigate the morphology and the physical properties of ZDDP antiwear film. After a ZDDP film has been formed on a disc specimen, AFM is employed to scan the regions of interest to obtain surface topography. Traditionally, in order to obtain the thickness of ZDDP film formed on the rubbed track, AFM needs to scan the rubbed track and the adjacent non-rubbed region to determine the film thickness by subtracting these two heights. This approach makes two assumptions. The first is that there is no wear of the metal surface below the ZDDP film; the second is that ZDDP does not form film outside the wear track.
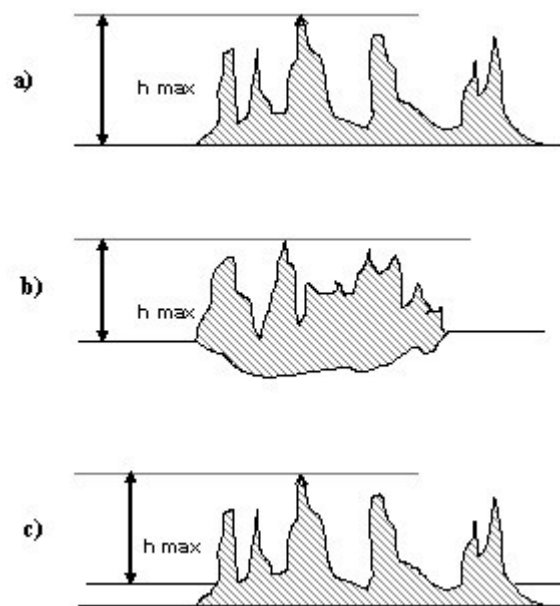
**Figure 5.12 Representation of the Principle of the AFM Antiwear Film Thickness Determination: (a) not assuming wear and film outside the wear track, (b) estimated film appearing thin because of wear, (c) estimated film appearing thinner because of lubricant film outside the wear track.**

### 5.4.3 EDTA Method

According to the principles of the SWLI and AFM methods, their theoretical maps of the wear track covered by ZDDP film can be presented as shown in Figure 5.13. In AFM, the tip travels on top of the solid surface to obtain the real surface topography; while for SWLI, in principle the white light is reflected from the metal surface below any transparent film. However it has been shown that the presence of a transparent film, such as a ZDDP film, may produce additional internal reflections which appear as spurious amounts of wear [165]. This means that neither method is able to measure wear accurately when a ZDDP film is present.

However, this problem has been solved by employing an aqueous solution of ethylenediaminetetraacetic acid (EDTA) to remove the ZDDP film before the measurements [106].
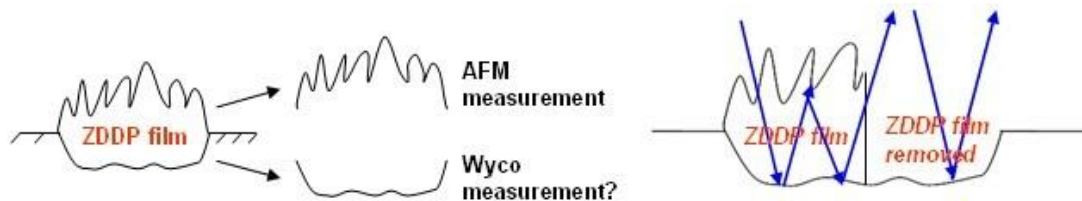


**Figure 5.13 Theoretical Surface Measurements by Wyko and AFM**

It is widely accepted that the ZDDP film formed on steel surfaces composes of metallic phosphate compounds based on Zn (II) and Fe (III) cations. EDTA is a chelating agent which can complex with most divalent and trivalent metal ions so that it can extract the Zn and Fe cations from ZDDP film. The chemical structure of EDTA and its complexation with zinc cation is shown in Figure 5.14.
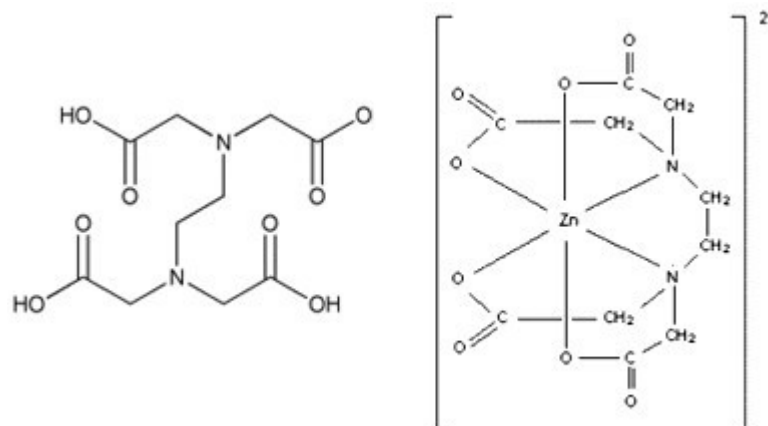


**Figure 5.14 EDTA Structure and Its Complexation with Zinc Cation.**

Therefore, an AFM-EDTA method [106] has been developed to remove ZDDP film to obtain more accurate results. The method is described as:

*'After ZDDP antiwear films had been analysed using AFM, a droplet of 0.05 M EDTA sodium salt solution in distilled water was deposited on the disc wear track using a micropipette and wiped off with the paper tissue after a set time. After some experimentation, a time of 1 min was found to be suitable.'*

After the film removal, the wear track is scanned by AFM again and its depth obtained. Then the film thickness is easily calculated by subtracting the height values of the film top and the wear track bottom. This method can also be applied to remove the ZDDP film before a wear volume measurement by Wyko. If the film is removed the white light goes straight to the bottom of the wear track before being reflected back, eliminating the possibility of internal reflections.
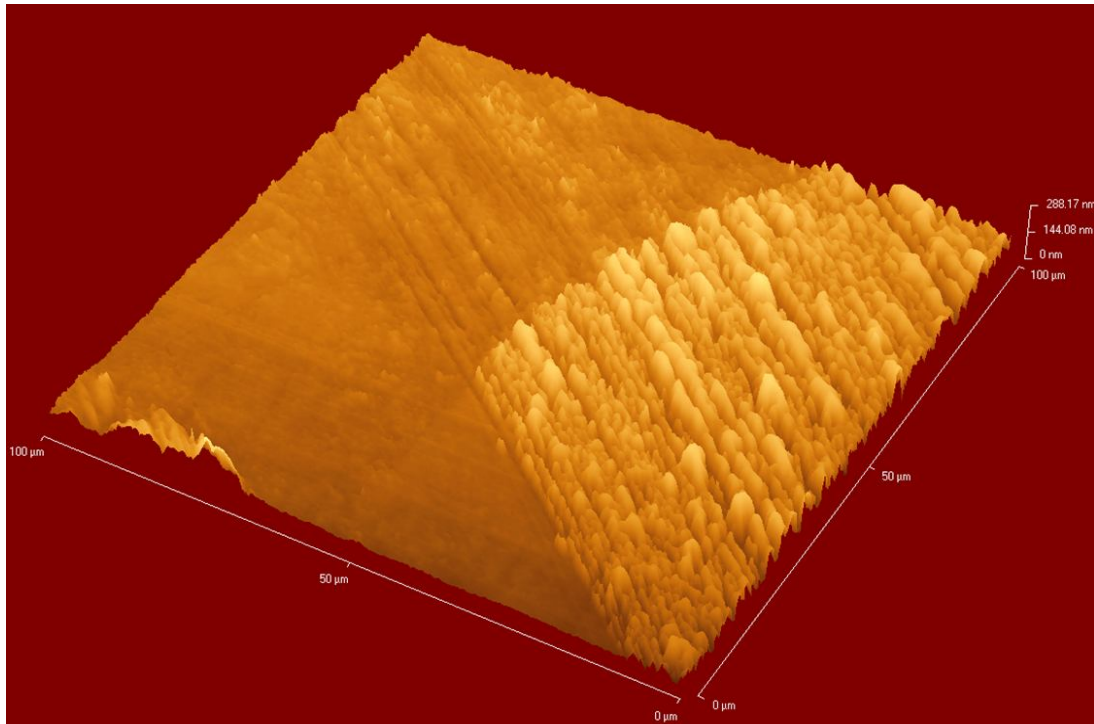

**Figure 5.15 Typical AFM-EDTA Method Results**

## 5.5 Lubricants, test conditions and specimens

### 5.5.1 Lubricants

All the lubricants used in this study were provided by Chevron Oronite Company LLC., Richmond, CA, USA, and are based on a group II base oil (100N). The measured viscometric properties of this base oil are listed in Table 5.1. Three different concentrations; (0.02 P wt%, 0.05 P wt% and 0.08 P wt%) of a secondary ZDDP in base oil and three different types of dispersant; (non-post treated dispersant, ethylene carbonate (EC) treated dispersant and borated dispersant) were employed. Details of the additives employed are shown in Table 5.2:

| Code | Description | Viscosity at 40 ℃ (m Pa s) | Viscosity at 100 ℃ (m Pa s) | Viscosity Index |
|------|-------------|-----------------------------|------------------------------|------------------|
| 100N | Group II base oil | 20.124 | 4.0922 | 102.1 |

**Table 5.1 Details of Base Oil Used**

| Code | Additives |
|------|-----------|
| ZDDP | Zinc dialkyldithiophosphate (secondary) |
| NPT | Non-post treated dispersant |
| BOR | Borated dispersant |
| ECT | Ethylene carbonate treated dispersant |
| Sulf | Overbased calcium sulfonate detergent |
| B-Sulf | Borated calcium sulfonate detergent |
| Sali | Overbased calcium sulfonate detergent |
| MoDTC | Molybdenum dithiocarbamate |

**Table 5.2 Details of Additives**

### 5.5.2 Test Conditions

In this study, most MTM-SLIM tests were carried out under one set of conditions. The test temperature was 100°C and the load applied was 31 N, which corresponds to an initial mean Hertz pressure of 0.95 GPa and a Hertz contact diameter of 250 μm. The slide-roll ratio employed was 0.5, where this is defined as the ratio of sliding speed $V_s = (V_b - V_d)$ to the entrainment speed $V = (V_b + V_d)/2$, where $V_b$ and $V_d$ are respectively the speed of the ball and disc with respect to the contact. The entrainment speed used during slow speed "film-forming" conditions was 0.050 m/s which corresponds, for the lubricant viscosity used, to a theoretical EHD film thickness of 8 nm and thus a lambda ratio, defined as the ratio of theoretical EHL film thickness to the composite surface roughness, of 0.5. The test duration was 120 minutes for a single test, but for ZDDP film removal tests, it was 120 minutes for the ZDDP film formation stage plus 120 minutes for the film removal stage.

For the wear tests, to maintain consistency, MTM-reciprocating tests were carried out under similar conditions of temperature and load to the MTM-SLIM tests *i.e.* temperature = 100°C, load = 31 N. The frequency applied was 10 Hz and stroke length was 4 mm, which gave an average disc speed over a stroke of 0.08 m/s. For pure sliding MTM the ball was held stationary, so the average entrainment speed was 0.08 m/s. In mixed sliding-rolling the ball speed was set to 0.02 m/s, so the average entrainment speed was respectively 0.05 m/s and 0.03 m/s for the forward and reverse disc directions. To decide the test duration, several trial tests were carried out, as will be discussed in next chapter.

HFRR test conditions were chosen to match reasonably closely the pure sliding MTM conditions. The test temperature was 100°C. The load was 3.92 N to provide a maximum Hertz pressure of 1.04 GPa (the MTM maximum Hertz pressure was 0.95 GPa). The stroke length and frequency were 1 mm and 50 Hz to give an average ball speed of 0.01 mm/s. The duration of the HFRR test is discussed in the next chapter.

### 5.5.3 Test Specimens

Specimens used for MTM and MTM-related tests were made of AISI 52100 steel with hardness 750-770 VPN. They were provided by PCS Instruments. The disc and ball diameters were 46 mm and 19.05 mm respectively. The root mean square roughness, $R_q$, of both balls and discs was $11 \pm 3$ nm, giving a composite surface roughness of $\approx 16$ nm. These specimens were meticulously cleaned prior to testing. The ball and disc were both immersed in toluene overnight to dissolve anticorrosive oil from the specimens and they were successively immersed in toluene and isopropanol in an ultrasonic bath for 15-30 minutes. Both upper and lower specimens for use in the HFRR are made of AISI 52100 steel, manufactured to comply with CEC and ASTM standards. They were also provided by PCS Instruments. The upper specimens were 6 mm diameter balls with hardness 800 HV and surface finish of less than 0.05 µm $R_a$. Lower, disc specimens had hardness 800 HV and a surface finish of less than 0.05 µm $R_a$. They were cleaned before use in a similar fashion to the MTM test specimens

Before each test, all components of the test rigs which might come into contact with the test lubricants were cleaned successively by toluene and isopropanol and dried with a hair dryer.

# Chapter 6 New mild wear test method development

This chapter describes three different mild wear tests and their use to measure wear for a standard ZDDP/dispersant-based lubricant. Methods of processing wear measurements to obtain wear coefficients are described and discussed. The repeatability and reliability of the test methods are analysed. It is noted that in pure sliding tests, for the lubricant studied higher wear rates are observed on the stationary surface, which is always in contact, than on the surface which is moving with respect to the contact. It is found that a rolling/sliding, reciprocating MTM test method gives measurable wear in a test in which the contact area and the mean contact pressure do not vary significantly during the test. This test method is thus preferred for further work. At the end of the chapter, a protocol of this mild wear test method is listed.

## 6.1 Introduction

There are many wear test rigs described in the literature, but in this study the reciprocating MTM and HFRR rigs were selected to investigate mild wear. This was based primarily on their availability and their widespread use in industry to measure lubricated wear. However they also had the advantage of spanning sliding and rolling-sliding test conditions. The mild wear test method protocols were developed by carrying out preliminary tests and analysis as described below.

At the beginning of this chapter, ways to calculate wear coefficients from wear data using Archard's wear equation are described. The method of calculating wear coefficient depends on the type of test rig and whether the ball or disc specimen is being measured.

Wear localization, in order to produce easily measurable wear with one image using optical methods, was achieved by using the two reciprocating rigs, the reciprocating MTM and the HFRR. The main issue that needed to be decided was the test duration, which had to be designed to produce measurable amount of wear but not so much as to greatly change the contact geometry and thus contact pressure. Initially, the HFRR as a standard wear test rig was used to run tentative tests and the test results from this were used to deduce the appropriate test duration for both HFRR and reciprocating MTM tests. Several tests with different durations were carried out to see if the wear rate was constant for a given lubricant and test conditions, as expected from the Archard equation.

Wear tests were then carried out using two types of reciprocating MTM condition to investigate their repeatability and reliability. Results were compared with those from HFRR tests. Both types of reciprocating MTM test were found to be reliable in producing measurable wear amount and suitable for mild wear characterization. Results from tests to explore the relation between film formation and antiwear properties of ZDDP and dispersant-containing lubricants are discussed in Chapter 8 and 9.

Wear volume measurements were made by both SWLI Wyko and AFM after film removal by an EDTA solution, to determine the most convenient way to measure wear. It was found that a combination of SWLI Wyko with EDTA treatment was most suitable.

From the images taken by SWLI Wyko, more information than just the wear volume can be obtained, such as the wear depth distribution along the wear track on the disc specimens, the relation between wear depth and entrainment speed, *etc.*

At the end of this chapter, the protocols of the overall mild wear test methods determined from preliminary work are described.

## 6.2 Wear Coefficient Calculation

Archard's equation is employed in the current study to calculate wear coefficients. Because of differences in the relative movements of the specimens in the different test methods, Archard's equation has been deduced into two forms, which are suitable to calculate the wear coefficients of ball and disc specimens respectively.

### 6.2.1 Ball Wear

In the case of HFRR and pure sliding, reciprocating MTM, no matter whether the ball or the disc is oscillating, one region of the ball stays in contact throughout the whole test. This means that the wear coefficient can be calculated simply by using the volume loss of the ball specimen. As shown below in Equation 6.2, the wear coefficient is deduced to be proportional to the ball wear volume $V_{ball}$, divided by applied load $W$, test time $T$, frequency $f$ and stroke length $l$. In this equation, $L$ is the total sliding distance and $N$ refers to the total number of cycles.

Assuming constant hardness, the Archard wear equation is:

$$V_{ball} = KWL \qquad\qquad (6.1)$$

where $K$ is the wear coefficient. Rearrangement and substitution for sliding distance gives:

$$K = \frac{V_{ball}}{WL} = \frac{V_{ball}}{W \times N \times 2l} = \frac{V_{ball}}{2WTfl} \tag{6.2}$$

In the case of mixed rolling/sliding reciprocating MTM, the ball is rotating, which means that wear on the ball is distributed along a circle. This wear cannot be easily or conveniently measured by SWLI Wyko, so the main interest is in the wear on the disc.

### 6.2.2 Average Disc Wear

In reciprocating MTM contact, the rubbing motion produces a crescent-shaped wear scar on the disc. The average wear rate coefficient over this whole crescent was calculated in a similar fashion to the HFRR ball, by dividing the total wear volume measured using the Wyko by the load multiplied by the sliding distance. This results in a similar equation to Equation 6.2.

$$K = \frac{V_{disc}}{2WTfl} \tag{6.3}$$

### 6.2.3 Local Disc Wear

In the reciprocating MTM, the sliding conditions vary considerably at different positions in the stroke. This means that the wear rate may vary along the stroke, so it is of interest to analyse and calculate wear rate at each stroke location.

For pure sliding reciprocating MTM rigs, the stationary ball and oscillating disc produce a sinusoidal variation in sliding speed and thus also in entrainment speed. Both of these may lead to a variation of the wear depth along the wear track.

If we consider a strip of breadth $2a'$ at some location across the wear track, the Archard wear equation at this location will be given by:

$$v_{ball\ strip} = KwL \tag{6.4}$$

where $v$ is the wear volume of this strip, $w$ is the load on this strip and $L$ is the sliding distance it experiences. The latter is given by $2Nu_st_s$ where $N$ is the number of cycles, $u_s$ is the average local sliding speed and $t_s$ is the time the strip is in contact on each pass. For pure sliding contact this time $t_s$ is equal to $2a'/u_s$ so the total sliding distance is $4a'N$. This should be obvious for a pure sliding contact since it is simply the contact breadth times $2N$. However it is introduced formally here in terms of sliding speed since it is less obvious for a rolling-sliding contact, as will be discussed below. For pure sliding contact we thus have:

$$v_{disc\ strip} = Kw2Nu_st_s = KwN4a'$$

(6.5)

The wear volume of the strip is the wear cross sectional area across the scar at the location of interest, $A_{disc\ strip}$, multiplied by the breadth of the strip $2a'$. The former can be measured directly using the Wyko as described in appendix A. If the value of $2a'$ used is taken to be equal to the wear scar diameter on the ball then we know that the load $w$ on the strip is equal to the total applied load even though the value of $a'$ cancels. We thus have:

$$K = \frac{v_{ball\ strip}}{wN4a'} = \frac{A_{ball\ strip}2a'}{WN4a'} = \frac{A_{ball\ strip}}{2WfT}$$

(6.6)

where $f$ is the stroke frequency and $T$ the total test time.
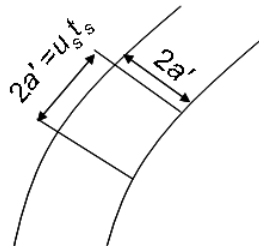


**Figure 6.1 Diagram of Disc Wear Strip**

For the reciprocating MTM operating in mixed sliding-rolling conditions where the ball rotates at constant speed, the analysis is slightly different from the pure sliding case. The diagram of the disc wear strip is as shown in Figure 6.1. The wear volume of the disc strip is still

$$v_{disc\ strip} = Kw2Nu_st_s$$

(6.7)

However the sliding speed depends on both the ball and disc speed and is thus not directly related to $t_s$, which depends only on the disc speed, $u_d$. For wear of a strip breadth $2a'$ we thus have:

$$v_{disc\ strip} = Kw2Nu_st_s = Kw2Nu_s\frac{2a'}{u_d}$$

(6.8)

$$K = \frac{v_{disc\ strip}}{wN4a'}\frac{u_d}{u_s}$$

(6.9)

As for the stationary ball, the wear volume of the disc strip can be equated to the wear cross sectional area multiplied by the strip width and the load on the strip of width $2a'$ to $W$, so:

$$K = \frac{A_{disc\ strip}}{2WN}\frac{u_d}{u_s} = \frac{A_{disc\ strip}}{2WfT}\frac{u_d}{u_s}$$

(6.10)
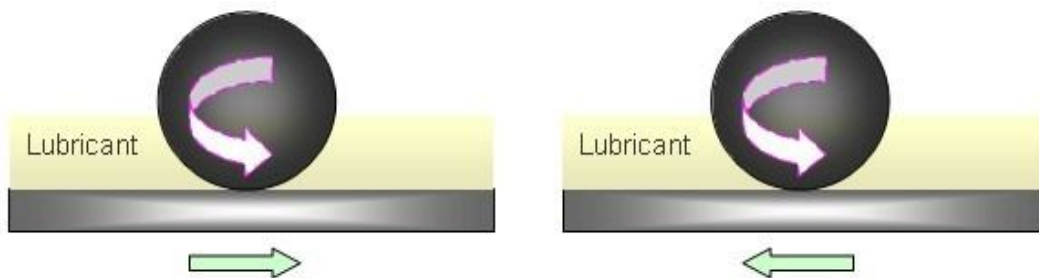


**Figure 6.2 Ball and Disc Movements for Mixed Rolling/Sliding Reciprocating MTM**
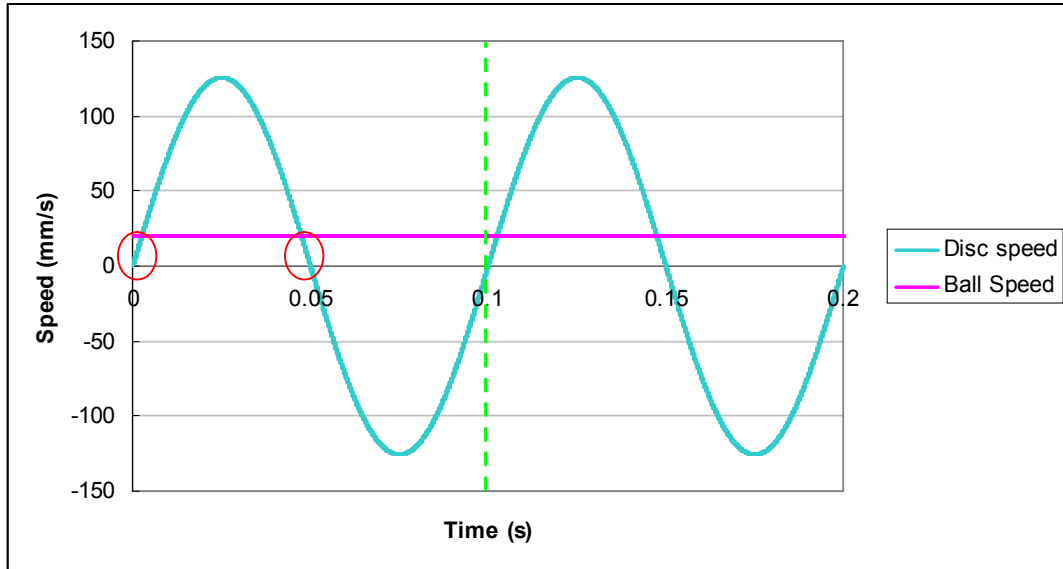
**Figure 6.3 Speed _versus_ Time over 2 Cycles for Mixed Rolling/Sliding, Reciprocating MTM**

For mixed rolling/sliding, the ball moves continuously in one direction while the disc reciprocates as shown in Figure 6.2. Thus the sliding speed at a given location is actually $|u_{d(t)} \pm u_{b(t)}|$ where the $\pm$ refers to the two different directions of the disc within each cycle.

Thus the wear volume is given by:

$$v_{disc\ strip} = Kw2a'N\frac{\|\,|u_d|-|u_b|\,\| + \|\,|u_d|+|u_b|\,\|}{|u_d|}$$
(6.11)

$$A_{disc\ strip} = KwN\frac{\|\,|u_d|-|u_b|\,\| + \|\,|u_d|+|u_b|\,\|}{|u_d|}$$
(6.12)

so the wear coefficient is

$$K = \frac{A_{disc\ strip}}{WfT}\left(\frac{|u_d|}{\|\,|u_d|-|u_b|\,\| + (|u_d|+|u_b|)}\right)$$
(6.13)

where $u_d$ is the local value of the disc surface speed and $u_b$ the ball surface speed.

When $|u_b| = 0$ and $|u_d| > |u_b|$, this equation becomes the same as Equation 6.6.

When $|u_d|<|u_b|$, this equation becomes

$$K = \frac{A_{disc\ strip}}{WfT}\left(\frac{|u_d|}{|u_b|-|u_d|+|u_d|+|u_b|}\right) = \frac{A_{disc\ strip}}{2WfT}\left|\frac{u_d}{u_b}\right| \qquad (6.14)$$

Equation 6.13 implies that for constant wear coefficient, the wear depth should vary along the crescent-shaped disc track in the rolling-sliding conditions, while it should be constant in pure sliding. In practice however, for both rolling-sliding and sliding conditions the entrainment speed varies along the track, so the lambda ratio and thus the wear coefficient may also vary. In current study, the wear coefficients used were generally calculated from the cross sectional scar area in the middle of the wear track on the disc where $u_d = \pm 125.7$mm/s.

## 6.3 Measuring Wear

The specimens were collected after each test and lightly rinsed several times in cyclohexane to dissolve the remained lubricant. Wear tracks of these specimens were then treated by the EDTA method introduced in Chapter 5 before they were measured by the SWLI Wyko.

As described in Chapter 5, the maximum single scanning area of AFM is about $150\times150$ μm$^2$. Therefore it could not be applied to quantify the wear volumes of HFRR and reciprocating MTM tests since the worn area for these two tests are around $100\times1000$ μm$^2$ and $300\times4000$ μm$^2$ respectively. Though AFM can also measure the wear depth and map the surface topography in limited areas it is still not as convenient as SWLI Wyko. In this study the wear area and volume measurements were carried out by the SWLI Wyko. Details of the way that wear was evaluated on the balls and discs using the Wyko software are presented in Appendix A.

## 6.4 Test Duration

HFRR wear tests were carried out initially, to produce wear with a lubricant containing a specific concentration of ZDDP and dispersant. In this study, the lubricant used was ZDDP

(0.05 P wt%) and dispersant (0.1 N wt%) blended in base oil. The applied load was 3.92 N, the stroke length was 1 mm, the stroke frequency was 50Hz and the test temperature was 100 ℃. After this 4 hour test, the specimens were treated with the EDTA solution and wear measured by the SWLI Wyko. Typical wear tracks on both ball and disc are shown below in Figure 6.4 and 6.5.
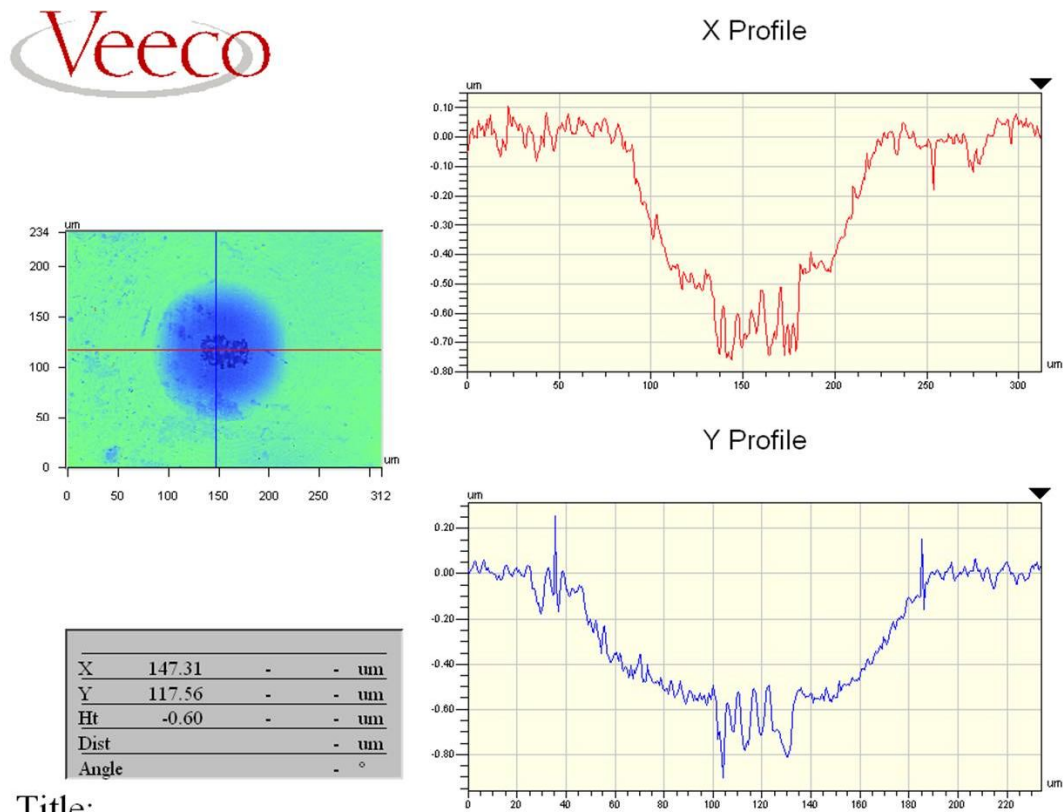


**Figure 6.4 Wyko Image of the Wear Scar on the HFRR Ball**
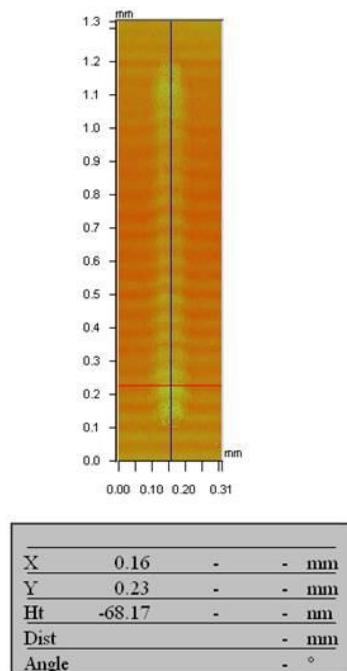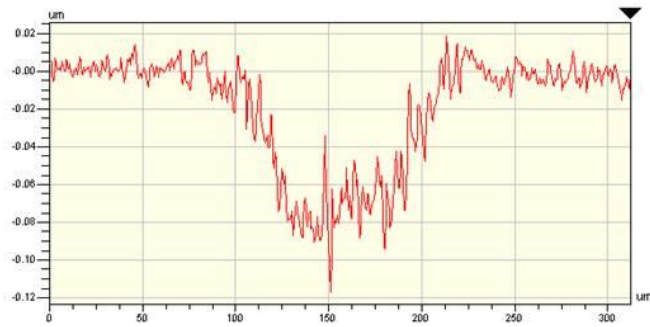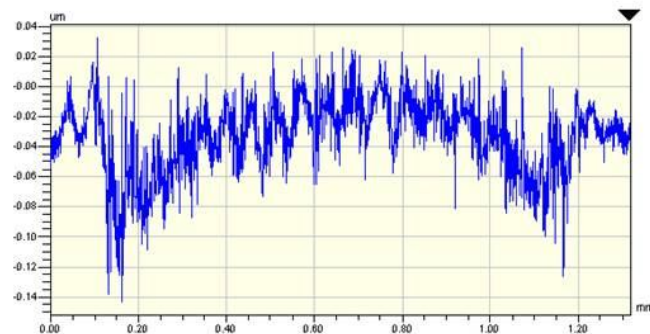
**Figure 6.5 Wyko Image of the Wear Scar on the HFRR Disc**

The wear volume $V_{ball}$ on the ball was then measured by SWLI Wyko. It was found to be 6431 $\mu m^3$ for the above test. From Equation 6.2, using the conditions of this HFRR test, the wear coefficient $K$ was calculated to be $1.14 \times 10^{-9}$ mm$^3$/N·m. Theoretically, the wear coefficient of HFRR tests should be similar to the pure sliding reciprocating MTM tests because of the similarity in contact conditions of these two tests. Therefore, the wear coefficient $K$ from HFRR test could be used to estimate appropriate test duration for pure sliding reciprocating MTM tests lubricated by the same fluid. Based on this calculation, the test duration for pure sliding reciprocating MTM tests was set to 4 hours, while the duration of the mixed rolling/sliding reciprocating MTM tests was set to 16 hours.

## 6.5 Reciprocating MTM Repeatability and Reliability

To investigate the repeatability and reliability of reciprocating MTM tests, several tests were carried out using the above lubricant.

### 6.5.1 Repeatability

Firstly, five mixed rolling/sliding reciprocating MTM tests were carried out on the solution (0.05 P wt% + 0.1 N wt%) for 16 hours each. The test conditions were: the applied load was 31 N, the stroke length was 4 mm, the stroke frequency was 10Hz and the test temperature was 100℃. At the end of each test, the disc specimen was taken out and treated with EDTA solution. Wear coefficients were calculated from Wyko measurements using Equation 6.10, and these are shown in Table 6.1.

| | 1 | 2 | 3 | 4 | 5 | average |
|---|---|---|---|---|---|---|
| Wear coefficients ($mm^3$/N·m) | $0.85 * 10^{-9}$ | $0.74 * 10^{-9}$ | $0.62 * 10^{-9}$ | $0.76 * 10^{-9}$ | $0.72 * 10^{-9}$ | $0.74 * 10^{-9}$ |

**Table 6.1 Wear Coefficients of Mixed Rolling/Sliding, Reciprocating MTM Tests**

Standard deviation was employed to describe the repeatability of this wear test. The equation for calculating standard deviation is:

$$\sigma = \sqrt{\frac{1}{n}} \sqrt{\sum_{i=1}^{n} (Xi - \overline{X})^2} \qquad (6.15)$$

In this equation, $\sigma$ is the standard deviation, $n$ is the number of values, $Xi$ refers to the wear coefficient of each test, and $\overline{X}$ is the mean wear coefficient ($0.74 * 10^{-9}$ $mm^3$/N·m). For these five tests, the standard deviation is $0.07 * 10^{-9}$ $mm^3$/N·m, which is relatively low compared to the mean wear coefficient. It indicates that the data points tend to be close to the mean value, which means high repeatability of such tests. Similar results were obtained from pure sliding, reciprocating MTM tests. In this study, nevertheless, all the wear tests have been repeated at least once and the values averaged to obtain more accurate results.

### 6.5.2 Reliability

According to the above Equation 6.2, 6.3, 6.9 and 6.14, the wear coefficient should depend on the applied load but not on the contact area and thus not on the contact pressure. This implies that the wear rate, expressed as wear volume per unit time, will not vary with the change in mean contact pressure that occurs in ball on flat contacts as wear takes place. This seems quite unlikely, since contact pressure will influence the severity of the contact condition, while the change in contact geometry will increase the extent of lubricant

entrainment. The lack of an apparent pressure dependence probably reflects the fact that the Archard wear equation was derived by studying the wear of flat, conforming contact where wear does not result in a significant change of mean pressure [168]. To produce useful and transferable wear coefficients the author for use in non-conforming contacts it is desirable that the mean contact pressure does not vary significantly during a test and that that this pressure can be specified.

In the HFRR tests described above the contact radius was initially 0.04 mm, corresponding to a mean pressure of 0.7 GPa, but at the end of the test it was 0.07 mm (as shown in Figure 6.5), corresponding to a mean pressure of 0.23 GPa. This indicates that wear coefficient values determined from these HFRR tests represent values averaged over a very wide pressure range.

The tests carried out on the same lubricant by the two types of reciprocating MTM tests show much smaller pressure variations. Wear scars are shown in Figure 6.6, 6.7 and 6.8.
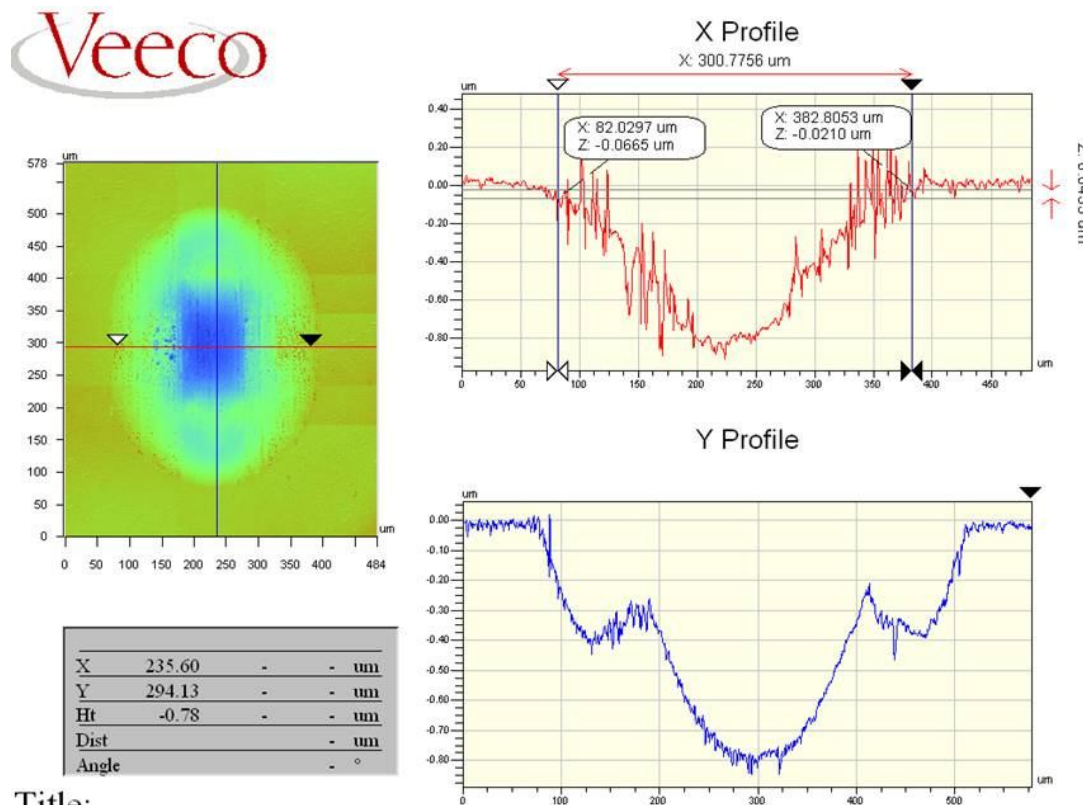


**Figure 6.6 Wyko Illustration of the Wear Scar on the Pure Sliding Reciprocating MTM Ball**
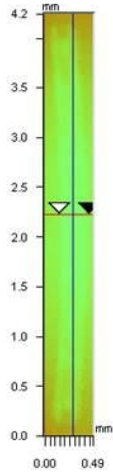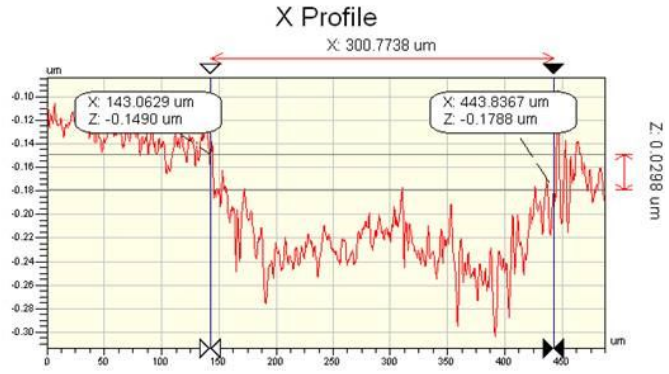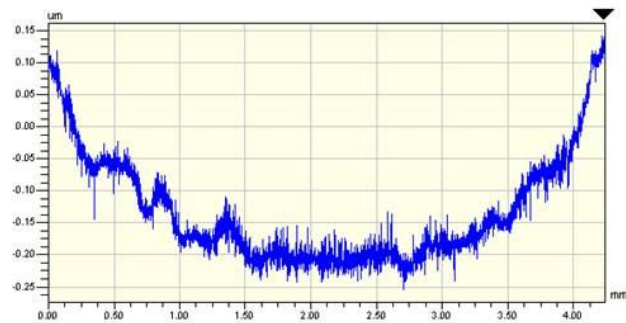
**Figure 6.7 Wyko Illustration of the Wear Scar on the Pure Sliding Reciprocating MTM Disc**
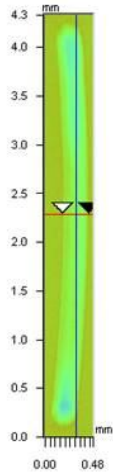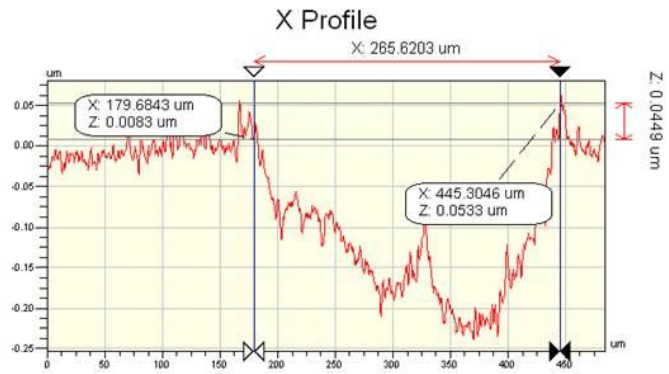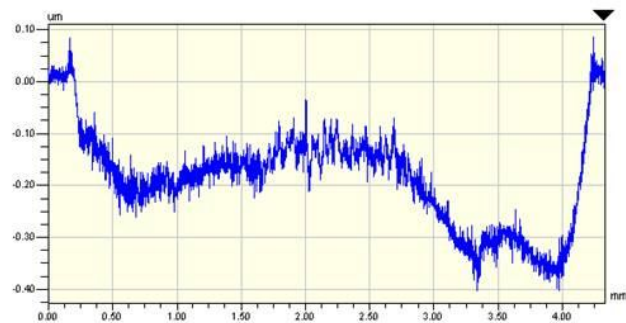


**Figure 6.8 Wyko Illustration of the Wear Scar on the Mixed Rolling/Sliding Reciprocating MTM Disc**

The wear scar on the ball and disc for pure sliding reciprocating MTM test (Figure 6.6 and 6.7) both show semi contact widths of about 0.15 mm, which is slightly bigger than the initial value of 0.12 mm. However, the wear scar on the MTM ball was not perfectly round, since the length along the rubbing direction (vertical) is bigger than the one along the horizontal direction. This results in larger contact area and lower mean pressure. The mean contact pressures at the beginning and end of the test are 0.64 GPa and 0.36 GPa respectively. The variation is much less than in the HFRR.

The wear track on the disc after mixed rolling/sliding reciprocating MTM test is shown in Figure 6.8. The width of this track was almost constant even though the test lasted 16 hours and was the same as the ball scar diameter. The final semi contact widths were 0.133mm compared to starting values of 0.12mm, corresponding to mean pressured of 0.64 and 0.57 GPa respectively. Therefore the wear coefficient for this mixed rolling/sliding reciprocating MTM test can be considered to originate at an almost unchanging contact geometry and pressure, and consequently this mild wear test method should be accurate and useful to quantify mild wear under specified conditions.

### 6.5.3   Running-in

Another important point needs to be considered is the running-in wear period, in which the wear rate of the rubbing components is much greater than during steady-state wear. Typical wear behaviour of rubbing components over their life span is shown in Figure 6.9. It can be seen that during the running-in period, the wear volume increases rapidly with time. This is followed by an extended steady-wear rate period during which wear volume removal is linear with rubbing time.
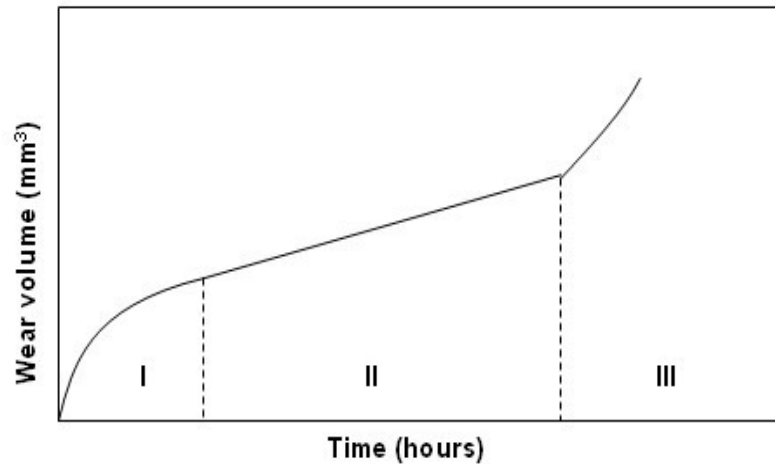
**Figure 6.9 Wear Behaviour: (I) Running-in; (II) Steady-state Wear; (III) Wear out [183]**

The transition from running-in to steady-state wear can be characterized by monitoring the changing of several criteria such as surface roughness, friction and wear. In the running-in wear process, as a consequence of changes in surface composition, microstructure and third-body distribution, the surface roughness varies and this results in increased conformity of the rubbing surfaces [184]. Once the steady-state wear regime is reached, the surface topography, the friction and wear rate stabilize. Therefore, friction/time and wear rate/time curves are commonly employed to characterize the completion of running-in. In this study, HFRR tests and two types of reciprocating MTM test were carried out with different test durations to estimate the time of completion of running-in. Friction was monitored during the tests. Results are shown in Figures 6.10, 6.11 and 6.12. All these tests were carried out with the ZDDP (0.05 P wt%) and dispersant (0.1 N wt%) in base oil solution.
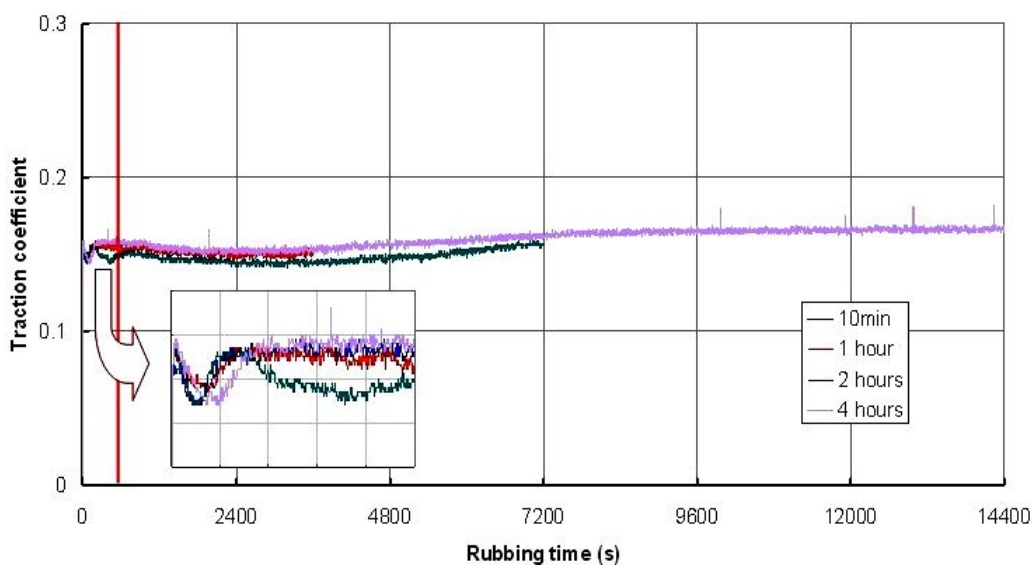


**Figure 6.10 Friction/Time Curves of HFRR Tests**
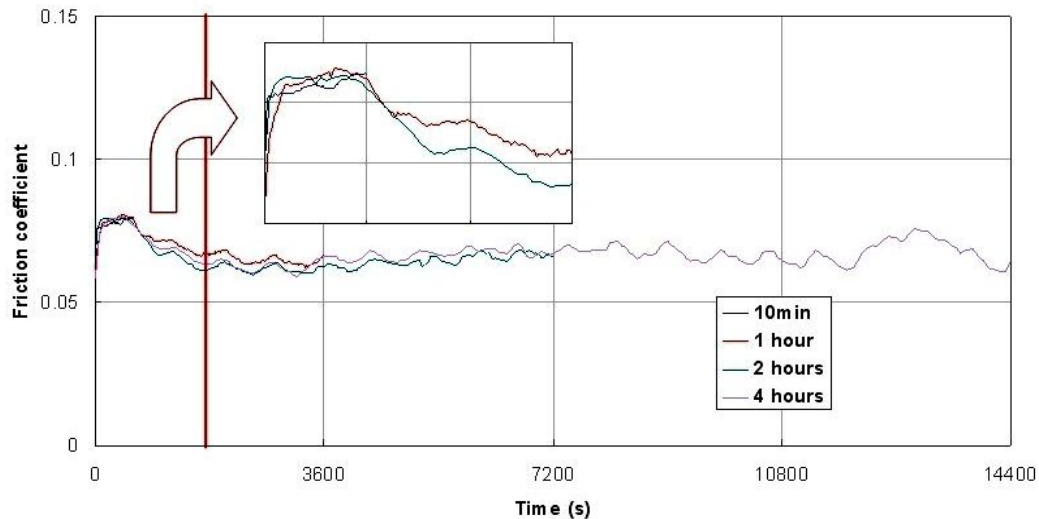
**Figure 6.11 Friction/Time Curves of Pure Sliding Reciprocating MTM Tests**
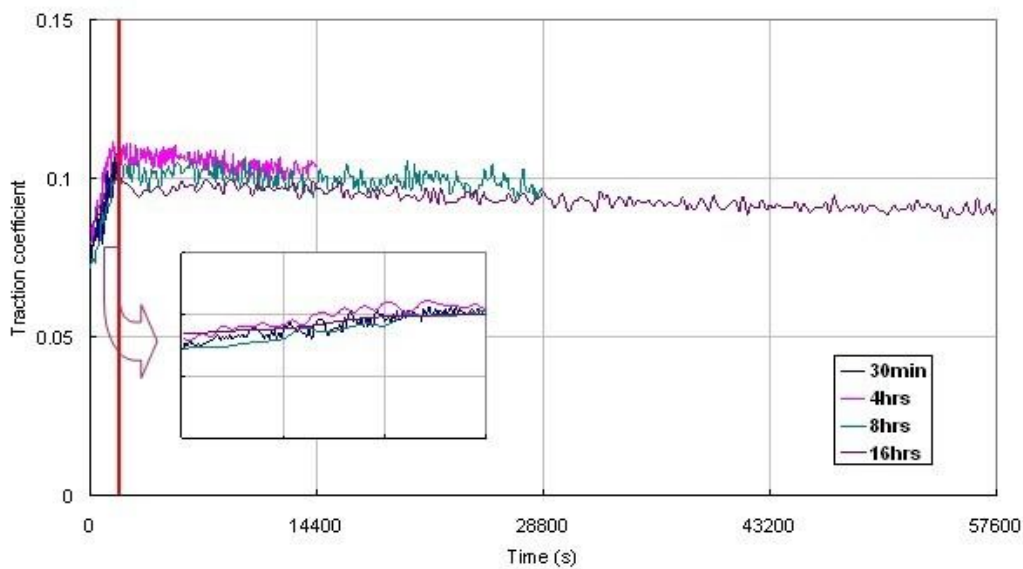


**Figure 6.12 Friction/Time Curves from Mixed Rolling/Sliding, Reciprocating MTM Tests**

As mentioned above, friction was observed during each test to obtain the time within which friction stabilizes. This time was then assumed to be the running-in period for each type of wear tests. After comparing friction variation of all these tests, for the two pure sliding wear tests, running-in wear was recognized to be completed in 10 minutes, while for mixed rolling/sliding, reciprocating MTM it was recognized to be completed in 30 minutes.

The wear coefficients after different test durations were calculated as shown in Table 6.2 and 6.3 by using the wear volumes on the balls for pure sliding wear tests and worn areas in the middle of the wear track for mixed rolling/sliding reciprocating MTM tests.

| Durations (hrs) | Wear coefficient $K$ (mm³/N·m) | |
| :---: | :---: | :---: |
| | HFRR | Pure sliding Reciprocating MTM |
| 0.17 | $9.79*10^{-9}$ | $8.15*10^{-9}$ |
| 1 | $3.15*10^{-9}$ | $3.45*10^{-9}$ |
| 2 | $2.03*10^{-9}$ | $2.56*10^{-9}$ |
| 4 | $1.91*10^{-9}$ | $1.65*10^{-9}$ |

**Table 6.2 Wear Coefficients from HFRR and Pure Sliding Reciprocating MTM Tests**

| Durations (hrs) | Wear coefficient $K$ (mm³/N·m) | |
| :---: | :---: | :---: |
| | Original | Running-in subtracted |
| 0.5 | $1.81*10^{-9}$ | |
| 4 | $1.24*10^{-9}$ | $1.16*10^{-9}$ |
| 8 | $1.29*10^{-9}$ | $1.26*10^{-9}$ |
| 16 | $1.02*10^{-9}$ | $0.99*10^{-9}$ |

**Table 6.3 Wear Coefficients from Mixed Rolling/Sliding Reciprocating MTM Tests**

For the two pure sliding wear tests, the wear rate during running-in is much higher than that during steady-state wear, and furthermore in steady-state wear process the wear rate varies with test time. The latter is probably due to the change in contact geometry and thus mean contact pressure. It is therefore difficult to extract a value which can be used to relate to practical wear. However, for the mixed rolling/sliding Reciprocating MTM wear test, the wear rate did not change much, especially after four hours.

The wear rate at different test durations was calculated using the wear coefficient equations described above, but with the running-in wear volume and running-in time (0.5 hours) subtracted. Wear rates for mixed rolling/sliding, reciprocating MTM wear tests are quite consistent, whether or not the running-in wear is subtracted, especially for long duration tests such as 8 hrs and 16 hrs. Therefore, in current study, wear coefficients were simply calculated using Equation 6.6 by measuring wear track areas across the middle of wear tracks after 16 hrs rubbing.

## 6.6 Wear Variation along Disc Track

As can be seen in Figure 6.8, for rolling/sliding reciprocating MTM, the wear depth and thus wear volume varies along the wear track, with more wear at the ends than in the centre. Two main factors are believed to influence this wear distribution.

### 6.6.1 Sliding Distance Factor

According to Equation 6.10, for rolling/sliding reciprocating MTM the wear is proportional to the value of sliding speed divided by disc speed. This ratio varies with speed within each cycle of the wear test and as shown as the sliding distance ratio in Figure 6.13.
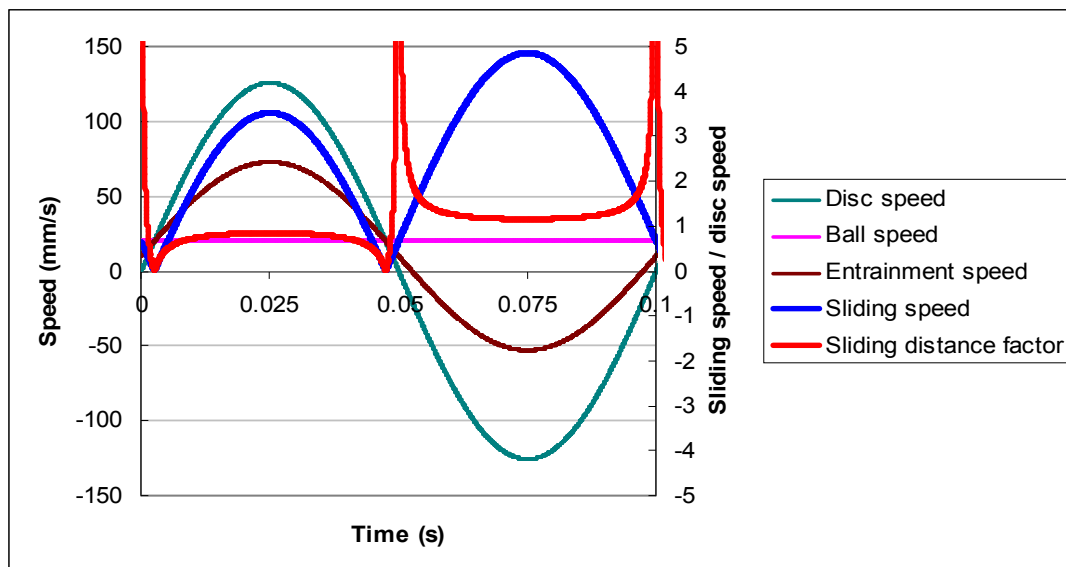


**Figure 6.13 Speeds and Sliding Distance Factor in One Cycle**

In practice wear occurs during both halves of the reciprocating cycle and the total wear at any location should depend on the sum of the sliding distance ratios of the two half cycles. This combined value, the sliding distance factor value, varies along the wear track as shown in Figure 6.14; it is equivalent to the bracketed term in Equation 6.14. It can be seen that this factor is extremely high when the disc speed is lower than the ball speed, which means that, if the wear coefficient is constant, the wear depth should be much greater at the two ends than in the middle of the disc wear track. This is shown in Figure 6.8 and was evident in all the mixed rolling/sliding reciprocating MTM test results.

106
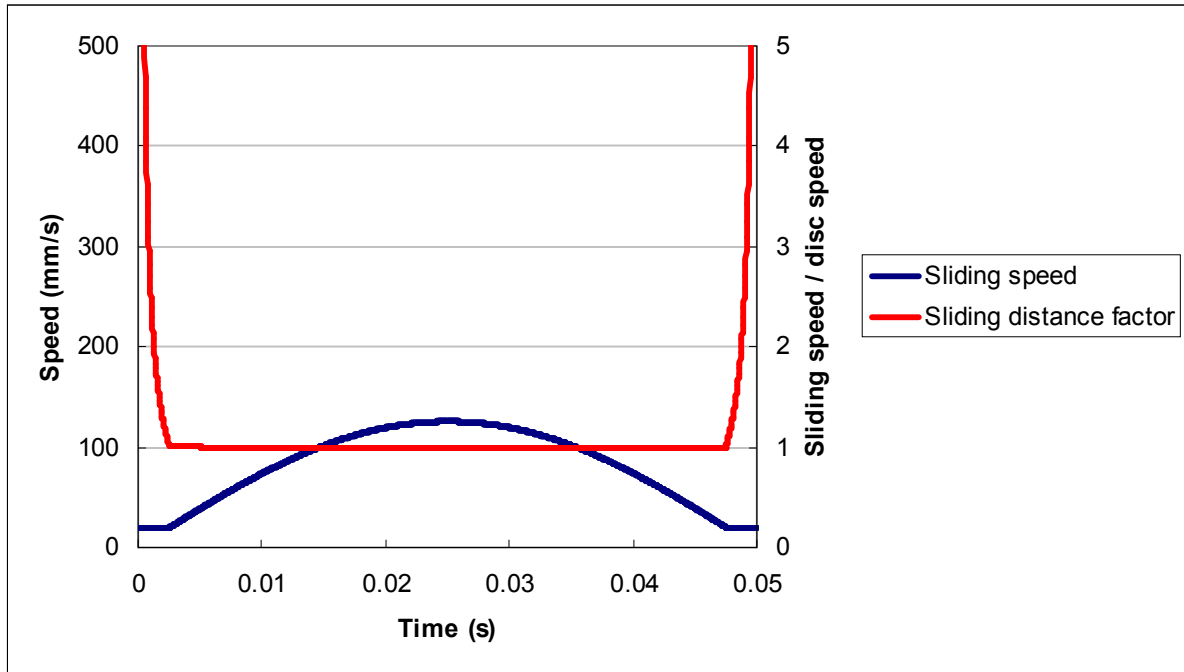
**Figure 6.14 Simplified Sliding Speed and Sliding Distance Factor in One Cycle**

### 6.6.2 Wear Depth and Entrainment Speed

According to elastohydrodynamic (EHD) theory the film thickness within a ball on flat contact increases with entrainment speed [172]. As shown in Figure 6.13, the entrainment speed reaches a maximum when the contact is in the middle of the wear track, and thus greatest lambda ratio will be presented at this point. This means that there may be less wear in the middle of the wear track, since the thickest fluid film is formed to protect surfaces from wear.

To test this possibility the variation along the wear track of wear depth with entrainment speed was measured. The scar is crescent-shaped due to the rotation of the disc. As a result of the crescent shape the longitudinal profile does not follow the centre line of the scar exactly. Additional analysis was carried out using the raw interferometer data to obtain profiles along the centre line and then the wear depth distribution along the centre of the wear track is drawn. The entrainment speed variation along the wear track was the calculated, as shown in Figure 6.13. Wear depth was then plotted against entrainment speed as shown in Figure 6.15. The wear depths at the extreme ends of the track are very high and are not shown.
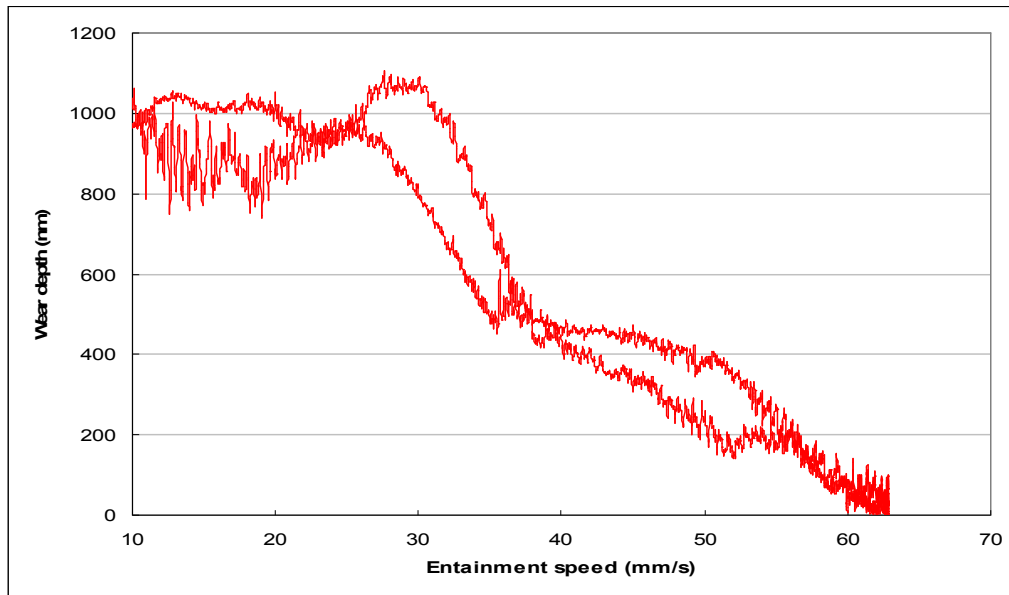
**Figure 6.15 Wear Depth Plotted against Entrainment Speed**

According to Equation 6.13 and Figure 6.14, the wear depth of the middle section of the wear track should be constant. But in fact the wear depth reduces with increasing entrainment speed over most of the track, suggesting that mixed lubrication influences wear.

## 6.7 Comparison of Ball and Disc Wear

For both the HFRR and sliding reciprocating MTM it was found that, for the ZDDP/dispersant solution studied in this chapter, that the total wear volume and thus average wear rate was considerably higher on the ball than on the disc. In the case of the HFRR, the ball and disc wear rates were $1.14 \times 10^{-9}$ and $0.37 \times 10^{-9}$ mm$^3$/N·m respectively. This needs further investigation.

## 6.8 Standard Protocol of Mild Wear Test Method

After the above trial tests and calculations, the protocol of a standard mild wear test method was developed for use in most further work. This is as follows.

(a) The ball and disc specimens are successively cleaned by toluene and Analar acetone and assembled in the MTM to run in a mixed rolling/sliding reciprocating MTM test for 16 hours. This test operates at a load of 31N, a stroke length of 4 mm, a stroke frequency of 10Hz and a test temperature of 100℃.

(b) After the test is complete, the specimens are taken out and lightly rinsed in cyclohexane several times. To remove the film formed on the disc wear track, a droplet of 0.05 M EDTA sodium solution in distilled water is then deposited on the wear track using a micropipette and wiped off with a paper tissue after 1 minute.

(c) The whole wear track area on the disc is measured using a SWLI Wyko. The wear area is measured 3 times across the central region of the track using Wyko software as described in Appendix A.

(d) The wear coefficient is calculated by applying Equation 6.12 in this Chapter.

## Chapter 7 Film Formation and Friction Results – ZDDP and Dispersants

This chapter presents film formation and friction properties of ZDDP- and/or dispersant-containing baseline solutions measured using various techniques. It is found that a film build-up and smoothing process occurs during the formation of ZDDP antiwear film, which corresponds directly to friction performance. Solutions containing different types of dispersants in base oil show different adsorption ability on metal surface and various friction behaviours. Dispersants are found to be antagonistic to the film forming action of ZDDP, in terms of both the rate of antiwear film formation and the ultimate film thickness.

## 7.1 Introduction

To explore the mechanisms of the antagonism between ZDDP and dispersant, as described in the literature review in Chapter 3, the performance of ZDDP alone and dispersant alone in baseline solutions need to compared with that the tribological performance of mixtures of ZDDP and dispersant in solution. In this chapter, firstly the film formation and friction properties of ZDDP and dispersant alone in base oil solutions are investigated. Secondly the effect of dispersant on the film formation and friction properties of ZDDP are tested and discussed. Finally the impact of dispersant on ZDDP films is studied. Several possible mechanisms of the antagonism between ZDDP and dispersant are suggested at the end of this chapter.

## 7.2 Film Formation and Friction Properties of ZDDP-containing Solution

### 7.2.1 ZDDP Film Formation
The study of the film formation of ZDDP-containing baseline solutions was carried out by running MTM-SLIM tests with different concentrations of ZDDP in base oil solutions. For the ZDDP-containing solutions, several preliminary tests were run with different concentrations of ZDDP to explore how ZDDP forms film on rubbing surfaces. Additionally, later in the study, tests were run on the ZDDP baseline solutions followed by an additional standard test run with dispersant solutions (which will be described later in this chapter). These tests also yielded further data of the film formation by ZDDP solutions. Therefore results from many repeat tests on the film forming properties of ZDDP solutions were accumulated.
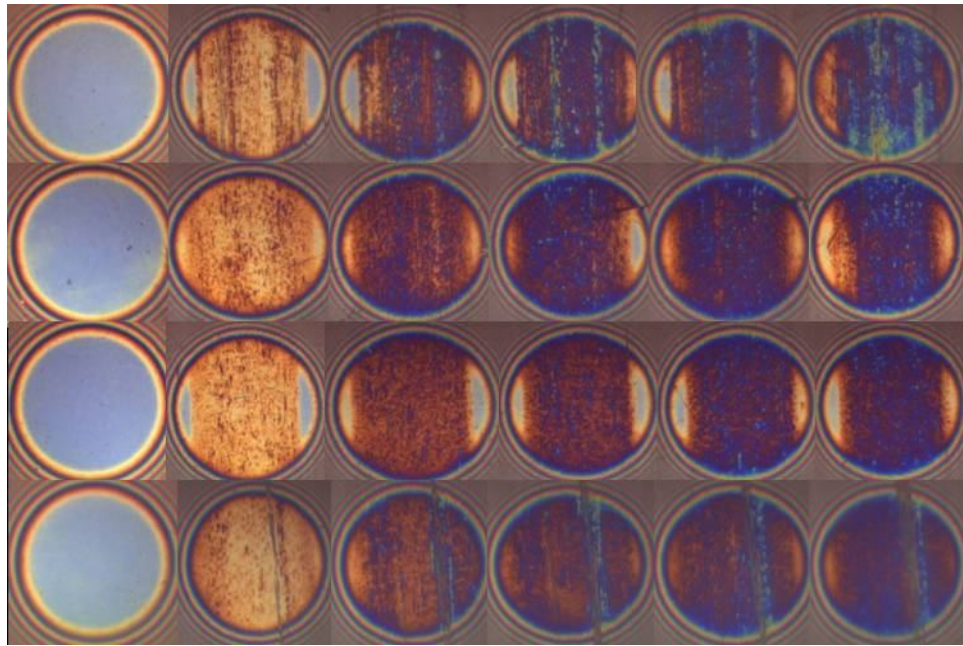
**Figure 7.1 Repeatable SLIM Images of ZDDP (0.05 P wt%)**

Figure 7.1 shows MTM-SLIM images from four repeat tests using 0.05 P wt% solution. It can be seen that the film build up behaviour is very similar in each test.

Figure 7.2 below shows a series of images taken at each interval of the tests, randomly picked out from all the test results of ZDDP-containing solutions. The corresponding average film thicknesses on the wear track were obtained by analysing the images, and are shown below in Figure 7.3 plotted against rubbing time.
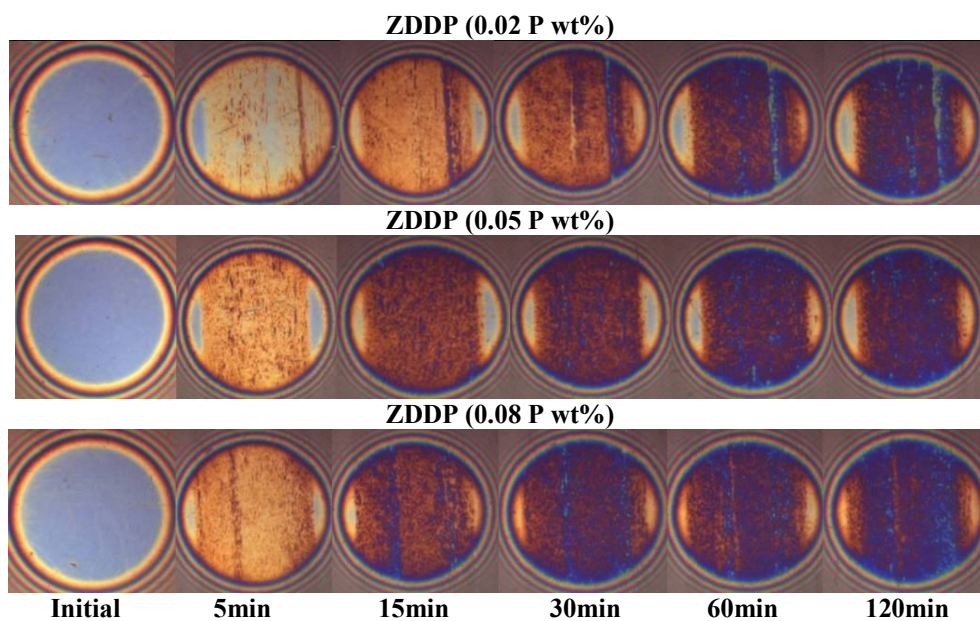


**Figure 7.2 SLIM Images of Different Concentrations of ZDDP**

**Film Thickness-ZDDP**
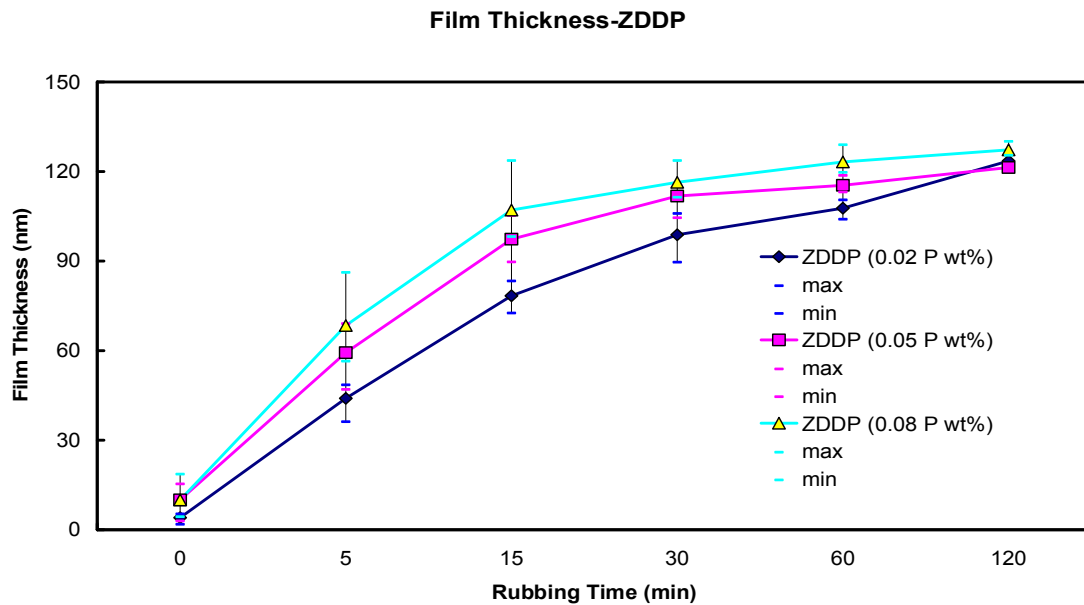


**Figure 7.3 Average Film Thicknesses of Different Concentrations of ZDDP**

From the interferometry images, it can be seen that the trends of ZDDP film formation are more or less the same regardless of the ZDDP concentration. The evolution of the ZDDP film can be recognized as a rapid stage followed by a stabilizing step. As shown in the graph, the rate of film-forming is much higher in the first 30 minutes than in the last hour. Under these test conditions, 0.02 P wt% and 0.08 P wt% ZDDP form antiwear films of 60 to 110 nm thickness respectively after 30 minutes, while after 2 hours rubbing the film stabilizes at a thickness of around 120 nm. It seems that these films of a thickness of around 120 nm prevent bulk steel surfaces from the continual attack by ZDDP in solutions to react with surfaces and increase film thickness since the results of several longer trial tests with various concentrations of ZDDP solutions showed that the films did not grow any thicker. Additionally, further tests which are described later in this study showed that the previously-formed films on specimens at a thickness of around 120 nm cannot be removed by rubbing them in a base oil solution. On the other hand, the rate of ZDDP film formation does slightly depend on the concentration (when between 0.02 P wt% and 0.08 P wt%). It can be seen that the higher concentration of the ZDDP shows slightly faster film formation.

At first sight, the results would suggest that a constant film thickness reached after prolonged rubbing due to a balance between formation and removal of the film as suggested by some authors [211]. However other work has studied this possibility by replacing the ZDDP solution by base oil at the end of the film formation stage and then continuing rubbing under

the same condition [185, 186]. This showed negligible removal of the film by rubbing. Thus it seems that the stabilised film thickness is an inherent property of the ZDDP and test conditions and that some factor stops film growth once this has reached a critical value. The reason why ZDDP film does not grow any thicker after reached a critical value will be discussed later in this chapter.

AFM was also applied to measure the thickness of ZDDP antiwear film; the results can be seen in Figure 7.4. In the upper part of the figure, the areas 1 and 2 are parts of the wear track, while area 3 is outside of the wear track. The ZDDP film formed on area 2 has been removed by EDTA solution (method is described in chapter 6). The graph shown under the image is the height distribution along the black line in the top left image. By comparing the height different between inside and outside of the wear track, it can be seen that the film thickness is around 120 nm, which is consistent with the results obtained from MTM-SLIM tests.
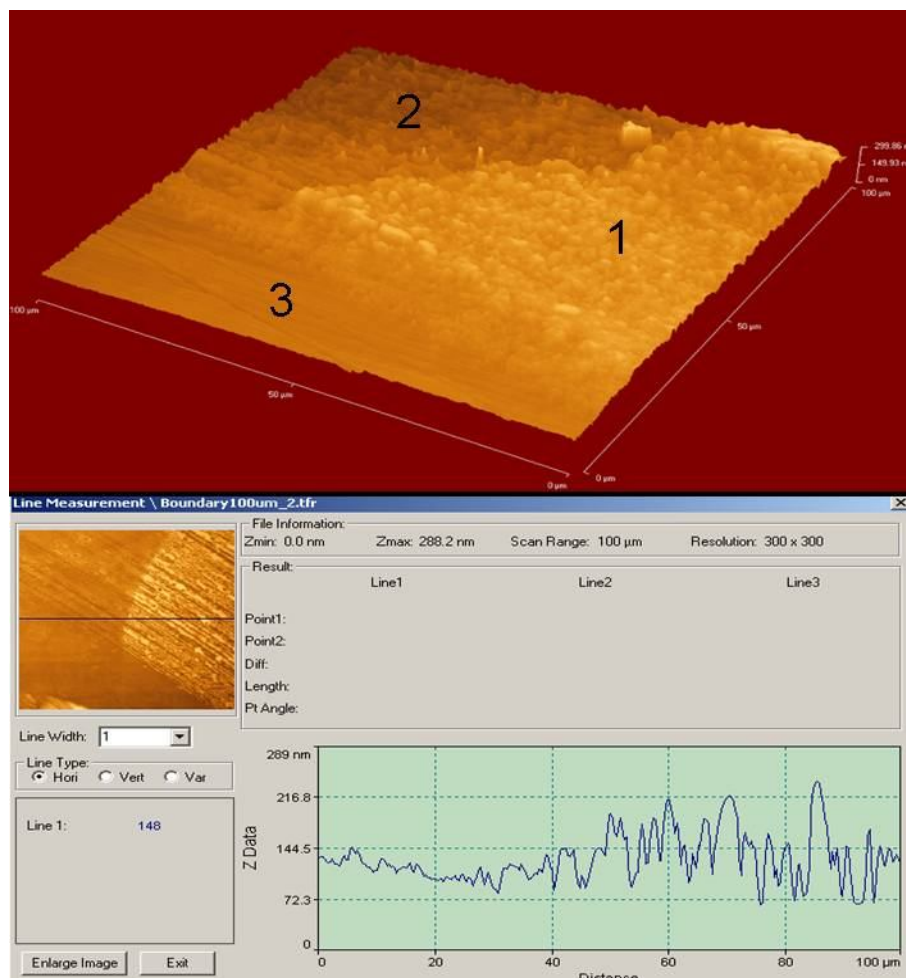


**Figure 7.4 AFM Results on ZDDP Film: 1. ZDDP Film; 2. Inside the Wear Track; 3. Outside the Wear Track**

## 7.2.2 Friction of ZDDP-containing Solutions

At each time interval during the tests, friction coefficient is measured over a range of entrainment speeds at a fixed slide-roll ratio in order to obtain Stribeck curves, which can be related the performance of the film formed. Only two series of Stribeck curves are shown below, since for ZDDP solutions of different concentrations (0.02 and 0.08 P wt%) the friction behaviours are similar to each other and the friction behaviour of the solution with 0.05 P wt% ZDDP lies between these two. The curves show how friction coefficient varies from negligible EHD film at low entrainment speed to thick EHD film at high entrainment speed, *i.e.* from the boundary lubrication regime at low speed to the fluid lubrication regime at high speed. It can be seen from the graph that the progressively growing film causes a rapid increase in friction coefficient in the first 15 to 30 minutes, especially in the mixed lubrication regime at intermediate speeds but also at low speeds. At higher rubbing times, friction coefficient starts to fall slowly at both low speed and intermediate speeds. Difference between the Stribeck curves at different concentration of ZDDP-containing solutions can be recognized in the 15 minute and 30 minute Stribeck curves. It seems that higher concentration (0.08 P wt%) of ZDDP-containing solution reaches highest friction faster than the lower concentration one (0.02 P wt%).
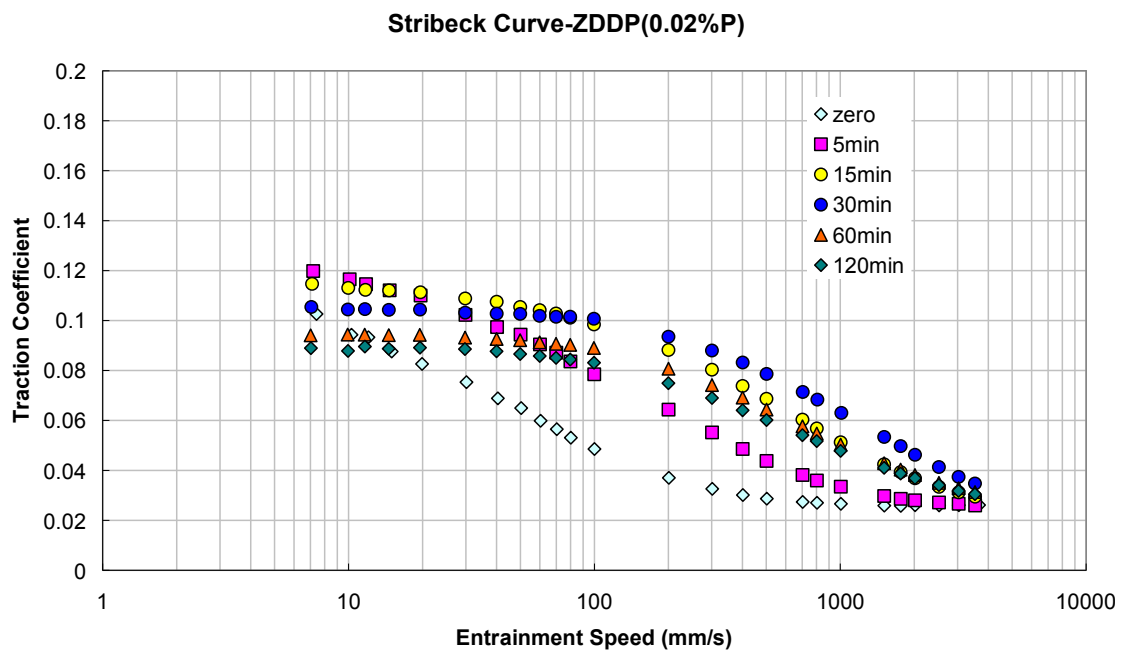


**Figure 7.5 Stribeck Curves of ZDDP (0.02 P wt%) in Base Oil Solution**

## Stribeck Curve-ZDDP(0.08%P)
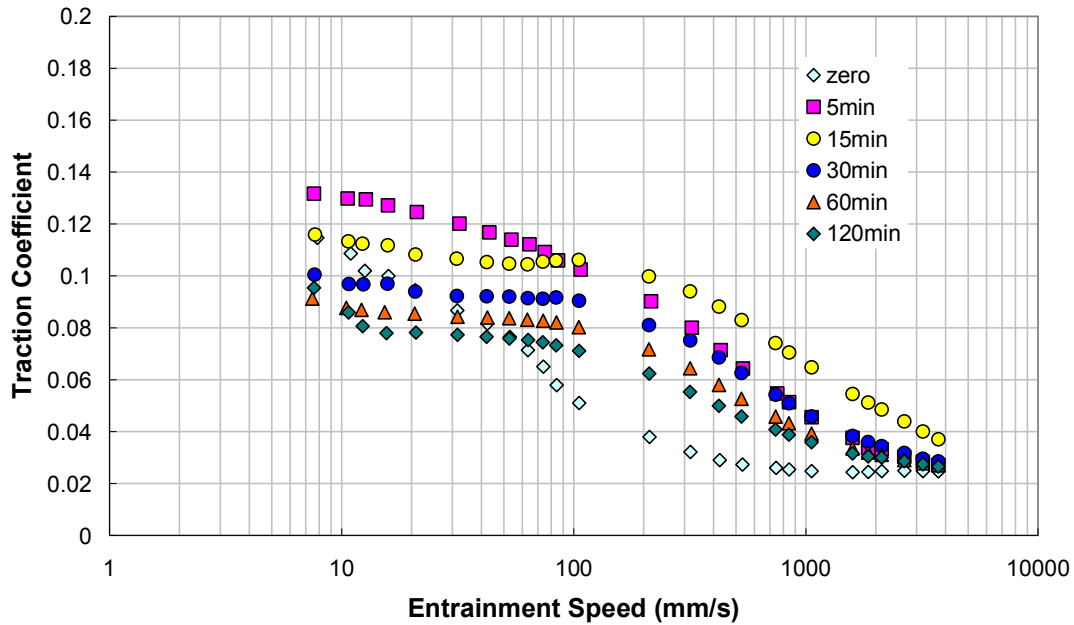


**Figure 7.6 Stribeck Curves of ZDDP (0.08 P wt%) in Base Oil Solution**

### 7.2.3 Discussion

The friction behaviour of different concentrations of ZDDP in base oil solutions relates to its film formation properties. Initially, the friction coefficient is measured before rubbing, so the friction behaviour is essentially that of the base oil (containing ZDDP) and the properties of the steel surface instead of the properties of the ZDDP antiwear film. Thereafter, a ZDDP film forms and the friction originates from the properties of this film. Two different friction responses of ZDDP films can be distinguished. One is at low speeds in the boundary lubrication regime where friction can increase, decrease or maintain the same and is believed to depend on the lubricity of the film and to be related to the nature of the ZDDP alkyl chains. Thus straight and long alkyl chains gives lower friction than branched, short ones [111, 187]. The other response is a shifting of the Stribeck curves to the right during rubbing so that friction starts to fall below its low speed value at higher and higher entrainment speed. This is believed to occur because the ZDDP film is very rough, and thus roughness allows lubricant to leak out of the inlet, so postponing the onset of fluid entrainment into the contact to higher speed.

The friction behaviour of the ZDDP tested above is interesting in that both low speed boundary friction and intermediate speed friction increase and then decrease during rubbing.

The intermediate speed behaviour can be ascribed to the formation of a rough film which then becomes smoother. However the behaviour at low speed is less easy to explain. Friction initially rises above the base oil value and then falls below it. This means that the outer surface of the ZDDP film, which presumably determines the boundary friction, changes in composition, from an initially high friction form to a lower friction one.

To summarize the overall behaviour of ZDDP-containing baseline solutions, several features are noted:

- ZDDP forms film rapidly in the first 15 to 30 minutes which then stabilizes at the thickness of around 120 nm under the test conditions.

- The rate of ZDDP film formation depends only very slightly on the concentration of ZDDP. Higher concentrations of ZDDP forms films faster between 0.02 P wt% and 0.08 P wt%. However, almost the same film thickness forms after 2 hours rubbing regardless of the content of ZDDP.

- Friction of the ZDDP-containing oil increases at the beginning, especially in mixed lubrication regime, and then gradually reduces over the rest of the test. This suggests that the original ZDDP film gives higher friction than the subsequent, smoothened one.

## 7.3 Film Formation and Friction Properties of Dispersant-containing Solution

Three types of dispersants solutions have been tested using MTM-SLIM, at the same nitrogen concentration (0.1 N wt%). The interferometry images are shown as in Figure 7.7.
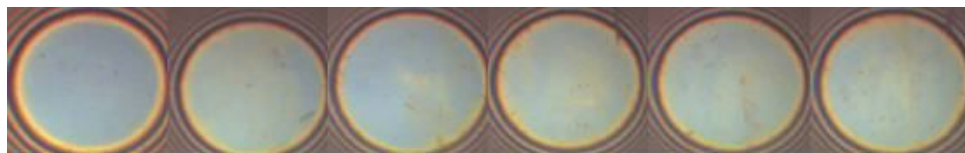

**SLIM images of EC treated dispersant in base oil**
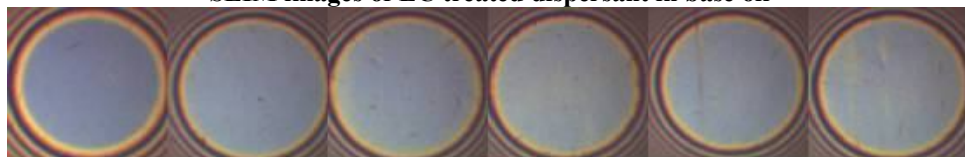

**SLIM images of borated dispersant in base Oil**

**SLIM images of non-post treated dispersant in base Oil**

| Initial | 5min | 15min | 30min | 60min | 120min |

**Figure 7.7 SLIM Images of Dispersants-containing Solutions**
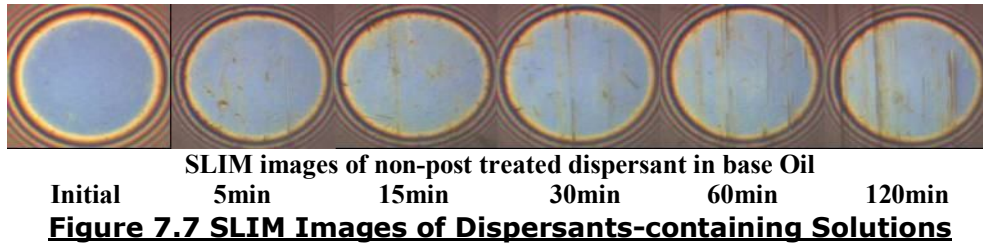
It can be seen from these images that no measurable film is formed on the surfaces. However, from the literature it is known that dispersants are able to adsorb on metal surfaces by attaching their polar 'head' to the metal surfaces. Therefore, any adsorbed layer is probably squashed in the static contact to a film thickness less than that measureable by SLIM (*ca* 5 nm). EHD tests were therefore carried out to investigate the thickness of the adsorbed layers on steel surface since this method can measure the layer thickness in rolling and rolling-sliding contact conditions. The results are shown in Figure 7.8. It can be seen that, compared to the oil film formed by base oil, dispersants are all able to form adsorbed layers with different thickness on steel surfaces. EC-treated and Borated dispersants form 5 to 10 nm thick layers on steel surfaces under these conditions, while the non-post treated dispersant forms a thinner and possibly variable layer.



**Figure 7.8 EHL Tests on Dispersant-containing Solutions**
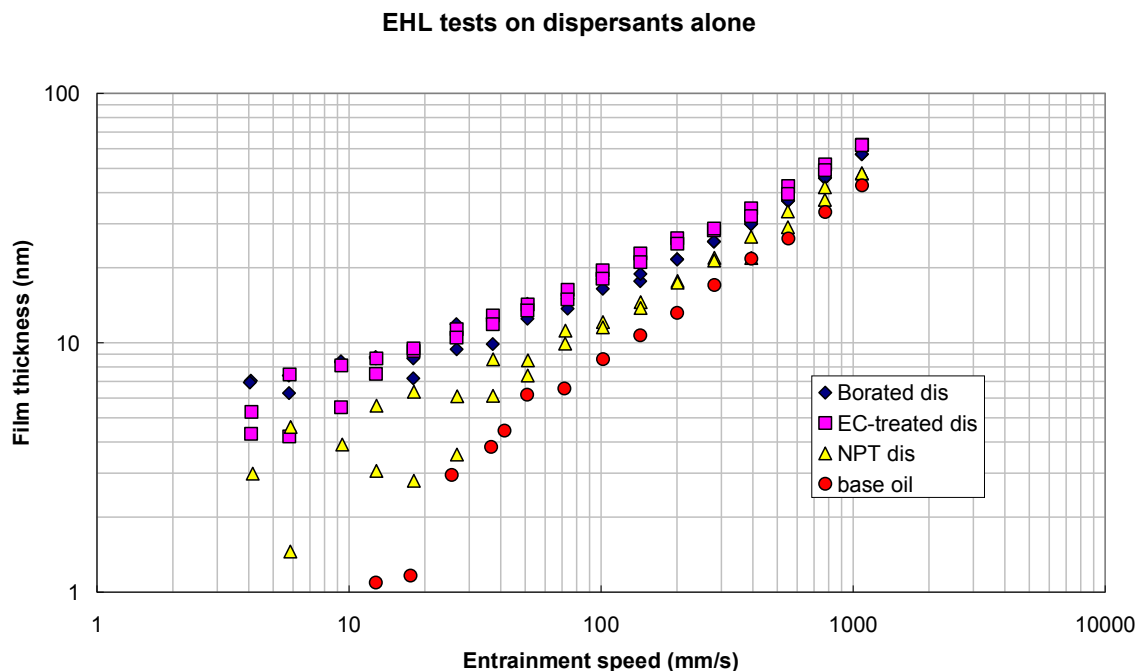
The MTM friction behaviour of these dispersant solutions is presented in Figure 7.9. Compared to base oil and ZDDP-containing solutions, significant reductions in friction

118

coefficient are seen for the borated and EC-treated dispersant, but not for the non-post treated one. For the non-post treated dispersant the friction at low speeds is similar to the base oil but the friction at intermediate speeds is slightly increased. The reason for this is not clear.

**Stribeck Curve - EC-Treated dispersant**



**Stribeck Curves of EC-treated Dispersant in Base Oil**
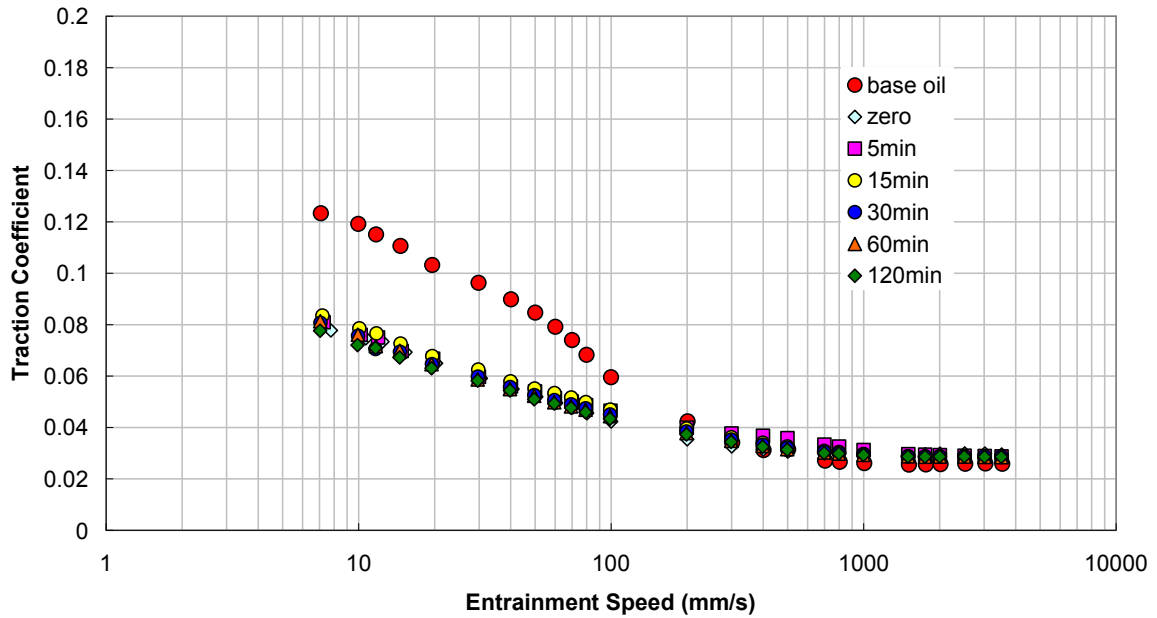
**Stribeck Curve-Borated dispersant**



**Stribeck Curves of Borated Dispersant in Base Oil**
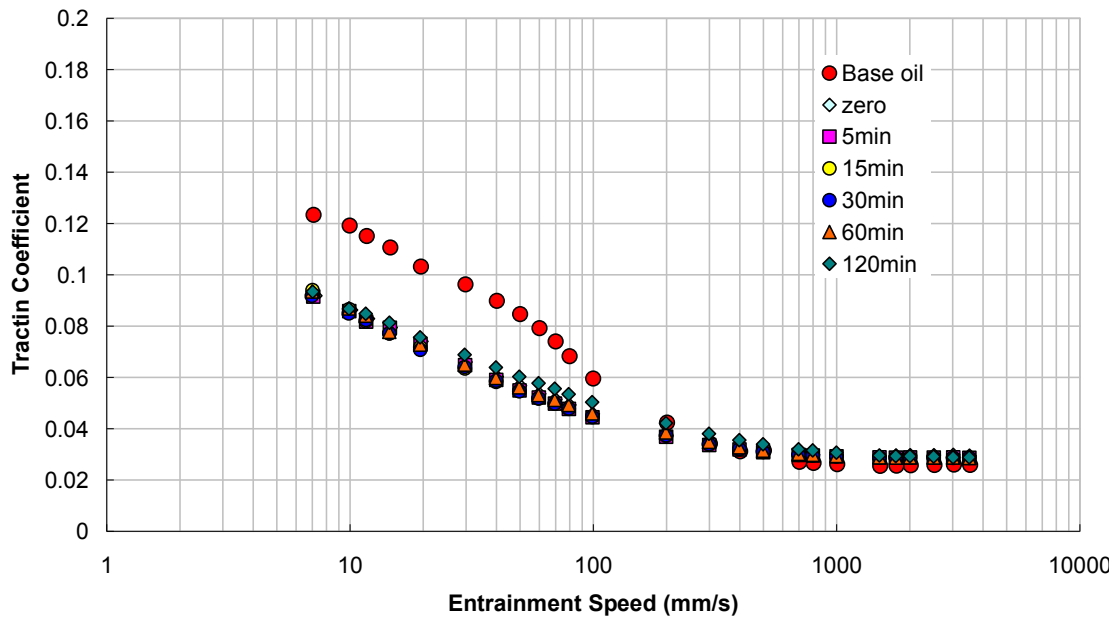
**Stribeck Curve-NPT dispersant**
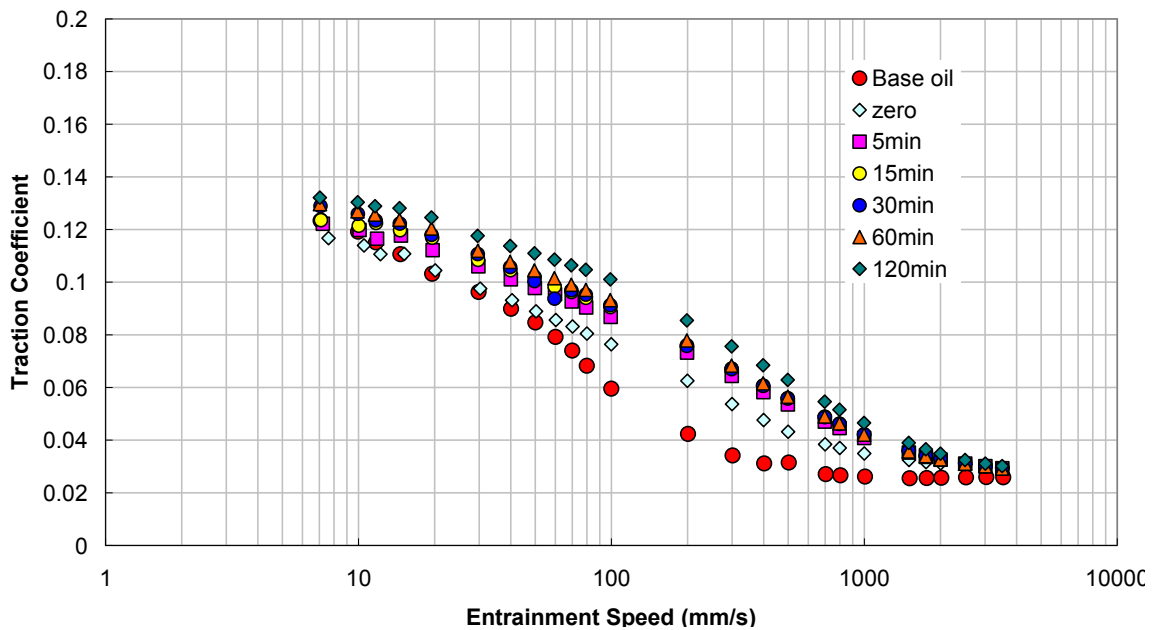


Stribeck Curves of Non-post Treated Dispersant in Base Oil
**Figure 7.9 Stribeck Curves of Dispersants-containing Solutions**

## 7.4 Film Formation and Friction Properties of the Solution Containing both Dispersant and ZDDP

The effect of dispersants on the film formation and friction properties of ZDDP-containing solutions is firstly investigated by using MTM-SLIM to test solutions containing both ZDDP and dispersant.

### 7.4.1 Film Formation and Friction Properties of the Solutions Containing EC-treated Dispersant and ZDDP

Firstly, several trial tests were carried out to monitor the film forming of the solutions with various ZDDP and EC-treated dispersant concentrations. Results are shown in Figure 7.10. It can be seen that, when EC-treated dispersants are added to ZDDP-containing solutions, they slow down the rate at which ZDDP forms a film on the rubbing surfaces. The decrease depends on the concentration of both ZDDP and dispersant. The rapid film forming step in the first 15 to 30 minutes of each tests running on ZDDP is slowed down to different extent by added dispersant, and with higher N/P ratio, this slow-down is more obvious.
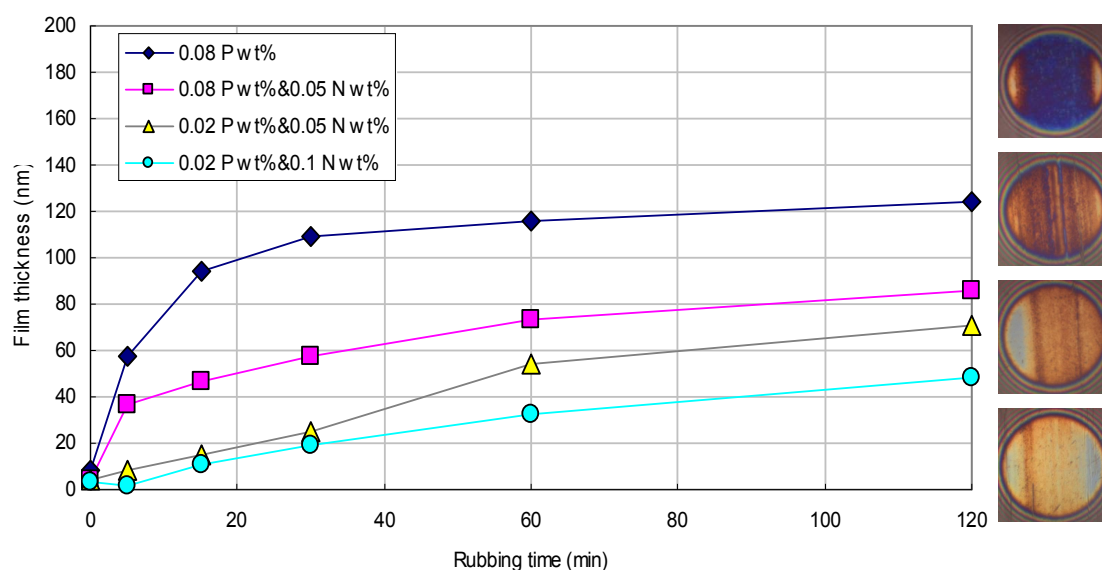
**Figure 7.10 Impact of Dispersant on ZDDP Film-forming**

To study the effect of N/P ratios on ZDDP antiwear film formation and friction, blends of ZDDP with EC-treated dispersant were tested with systematically varying concentrations of both. Film thicknesses after 2 hours rubbing and typical friction behaviour are shown in Figure 7.11, 7.12 and 7.13. It is obvious that, in general, the film thickness increases when either N content is decreased or P content is increased. Figure 7.12 shows the relation between N/P ratios and film thickness. Basically, the overall trend shows that the film thickness grows as the N/P ratio is decreased. As shown in Figure 7.13, the friction increases gradually and slowly in all lubrication regimes. The low boundary friction of the EC-treated dispersant is gradually lost as the low speed friction approaches that of ZDDP alone. The friction curves shift to higher speed but more slowly than for ZDDP alone, probably because of bound the slow-down effect on ZDDP film forming by dispersant.
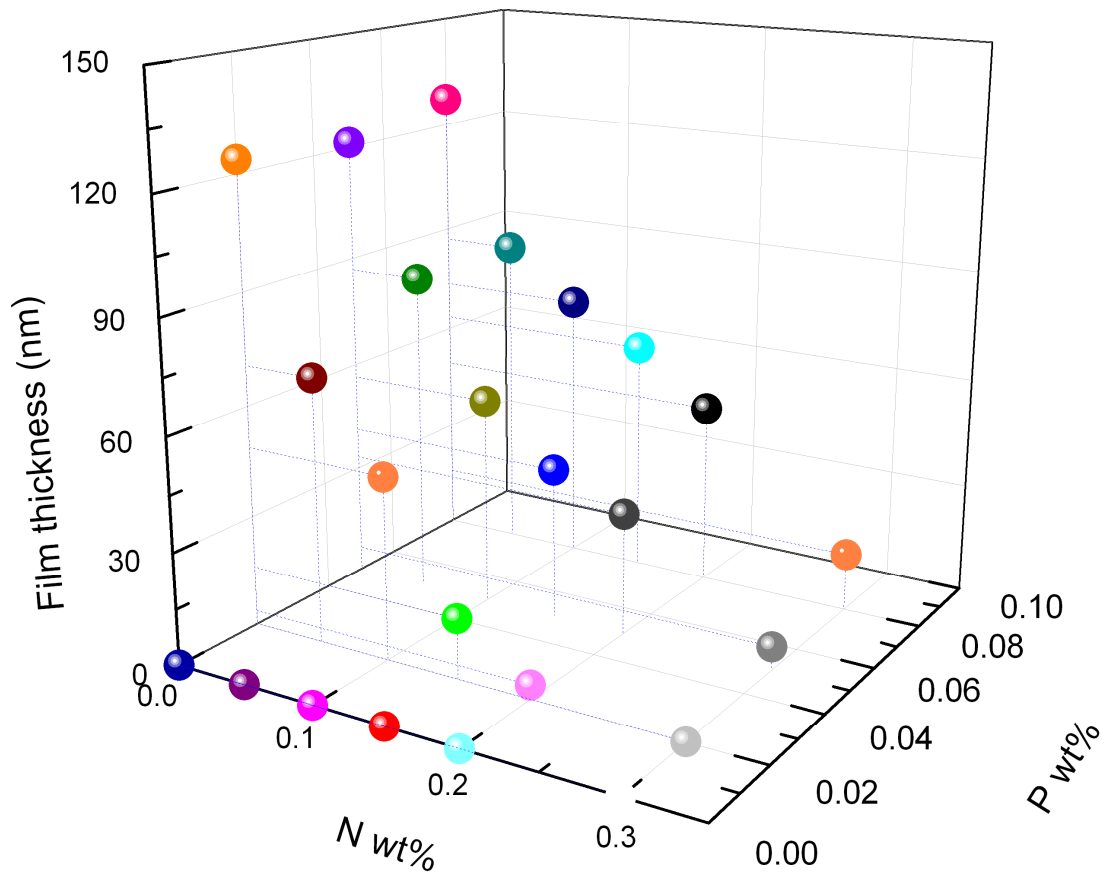
**Figure 7.11 Film Thicknesses of Solutions Containing Different Concentrations of EC-treated Dispersant and ZDDP after 2h Rubbing**
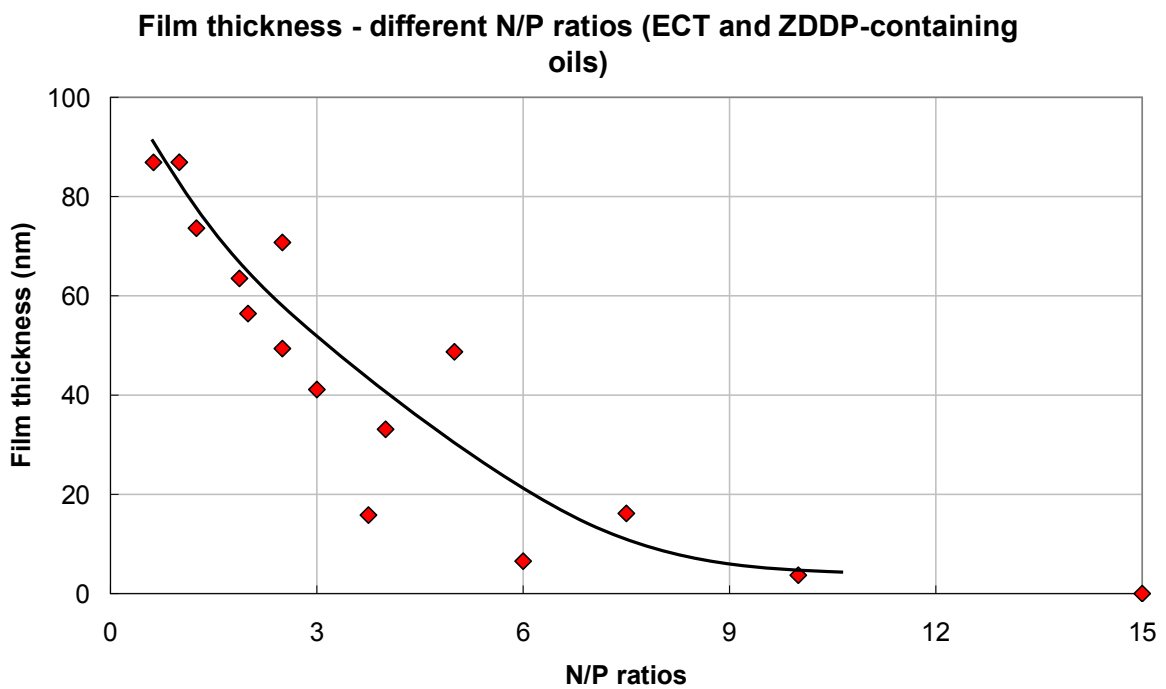


**Figure 7.12 Film Thicknesses of Solutions with Various N/P Ratios after 2h Rubbing**

**Stribeck Curve-ZDDP (0.05%P)+ECT**



Figure showing Traction Coefficient (y-axis, 0 to 0.2) versus Entrainment Speed (mm/s) (x-axis, 1 to 10000, log scale). Legend: zero (open diamond), 5min (magenta square), 15min (yellow circle), 30min (blue circle), 60min (orange triangle), 120min (green diamond).
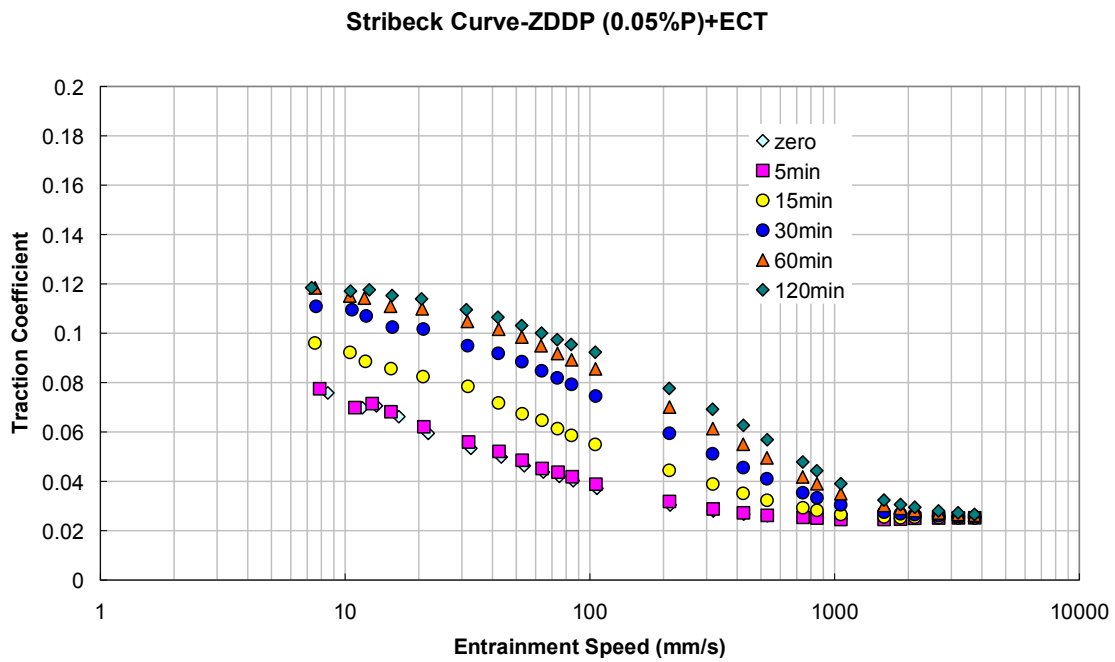
**Figure 7.13 Typical Stribeck Curves of Solution Containing both ZDDP and EC-Treated Dispersant**

For extreme conditions, such as when the concentration of EC-treated dispersant is relatively high and the N/P ratio is large, the ZDDP antiwear film formation seems to be entirely stopped by dispersant, as shown in Figure 7.14. The friction behaviour of these two solutions is shown in Figure 7.15. The solution with ZDDP (0.05 P wt%) and dispersant (0.15 N wt%) takes a long time to form a film, but the Stribeck curves show that once a film forms, it increases the friction. However, for the solution with ZDDP (0.05 P wt%) and dispersant (0.3 N wt%), no ZDDP film occurs and the friction is more or less the same as for the EC-treated dispersant alone in base oil solution. This blend was also tested for a longer duration (4 hours), but there was still no film formed.
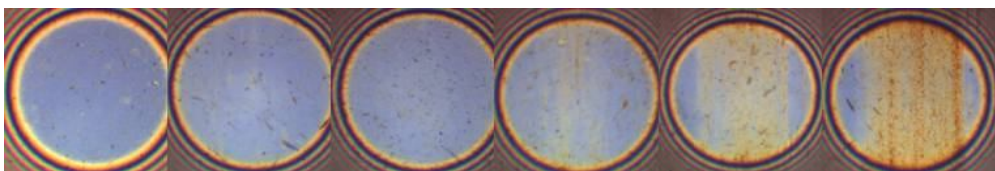


**a) SLIM images of solution containing ZDDP (0.05 P wt%) and dispersant (0.15 N wt%)**
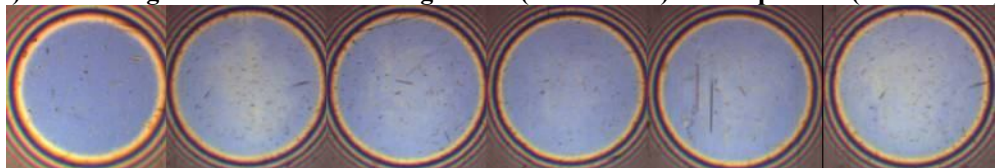
**b) SLIM images of solution containing ZDDP (0.05 P wt%) and dispersant (0.3 N wt%)**

**Figure 7.14 SLIM Images of High Dispersant Content Solutions**

**Stribeck curve-ECT dis (0.15%N) + ZDDP (0.05%P)**
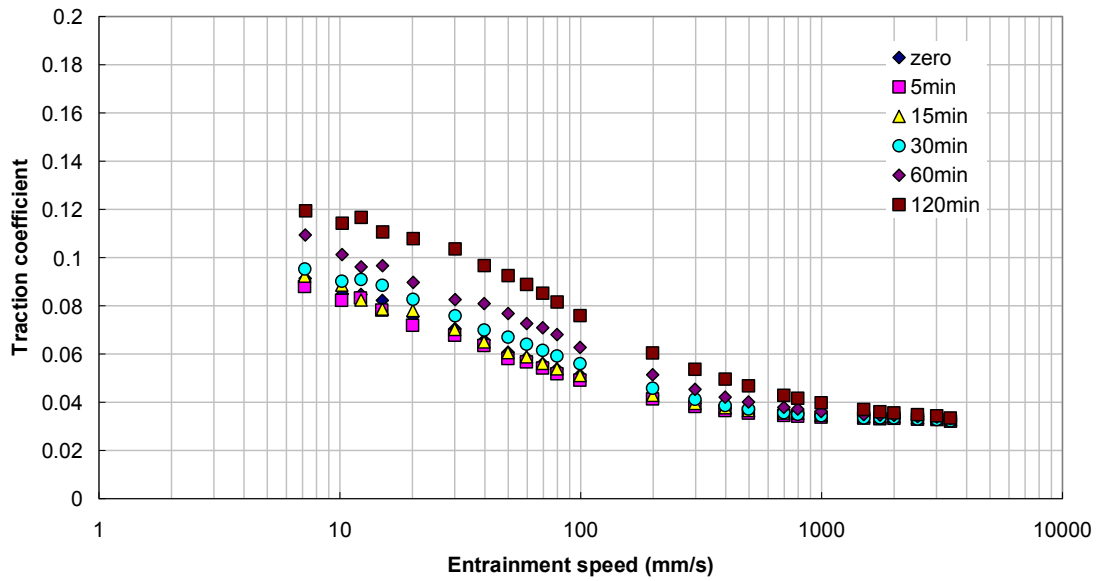


a)  **Stribeck Curves of Solution Containing ZDDP (0.05 P wt%) and Dispersant (0.15 N wt%)**

**Stribeck curve-ECT dis (0.3%N) + ZDDP (0.05%P)**
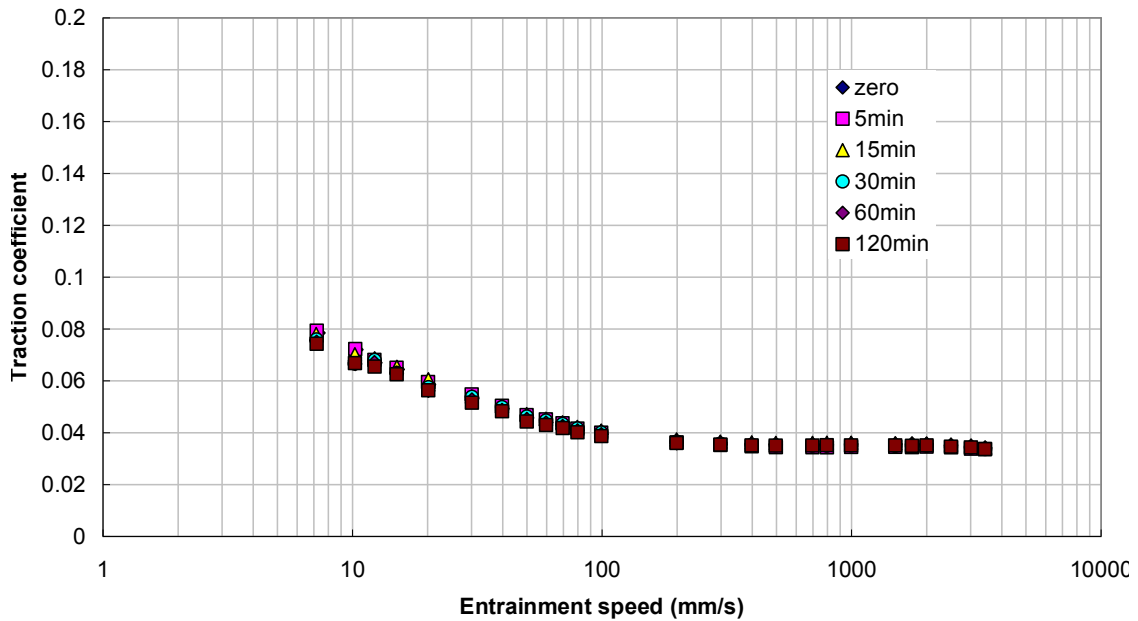


b) **Stribeck Curves of Solution Containing ZDDP (0.05 P wt%) and Dispersant (0.3 N wt%)**
**Figure 7.15 Stribeck Curves of High Dispersant Content Solutions**

## 7.4.2 Film Formation and Friction Properties of the Solutions Containing ZDDP and other Dispersants

Tests have been also carried out on solutions containing ZDDP with borated dispersant and with non-post treated dispersant. The film forming and friction properties are shown below in a few representative graphs, since the way dispersants affected the ZDDP film forming and friction were similar to each other.

The effect of borated dispersant on ZDDP film formation and friction is quite similar to that of EC-treated dispersant, as well as the extent of this effect. The film thickness after 2 hours rubbing is also determined by the N/P ratio, and the friction increase is thought to be caused by the formation of ZDDP film. Non-post treated dispersant also shows the same tendency.

However, non-post treated dispersant shows slight differences from the two treated ones. For the non-post treated dispersant and ZDDP-containing blends, the film thickness is generally 5 nm thicker than those formed by ZDDP and EC-treated or borated dispersant with the exactly same N and P content. The friction increase is also slightly faster and larger than that caused by ZDDP with treated dispersants.

**Film Thickness (Borated dispersant + ZDDP)**
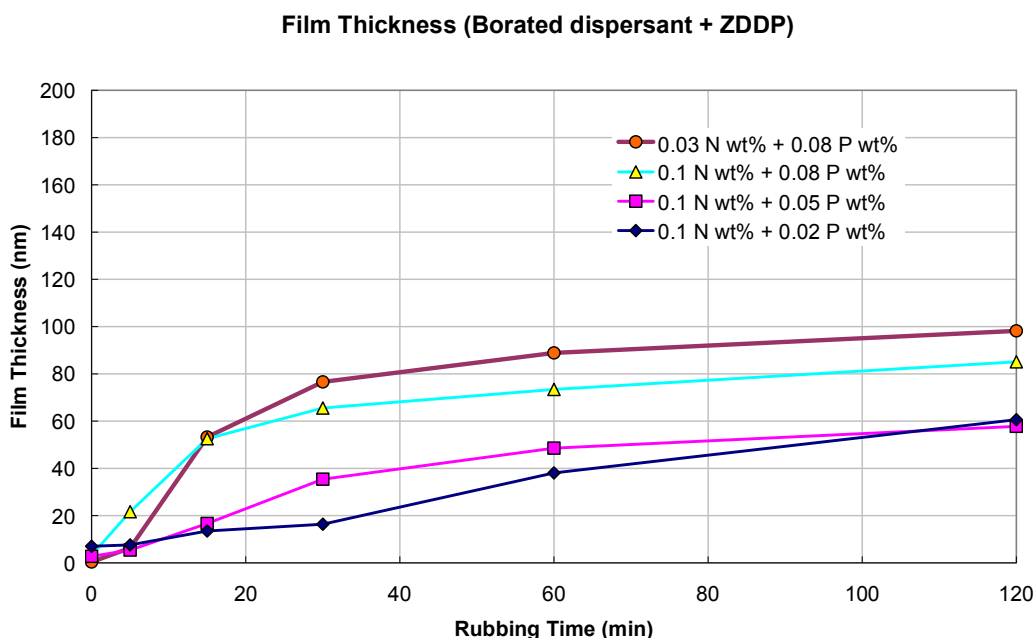


**Figure 7.16 Film Thickness of ZDDP and Borated Dispersant in Base Oil**

**Stribeck Curve-ZDDP (0.05 P wt%) + Borated dispersant (0.1 N wt%)**
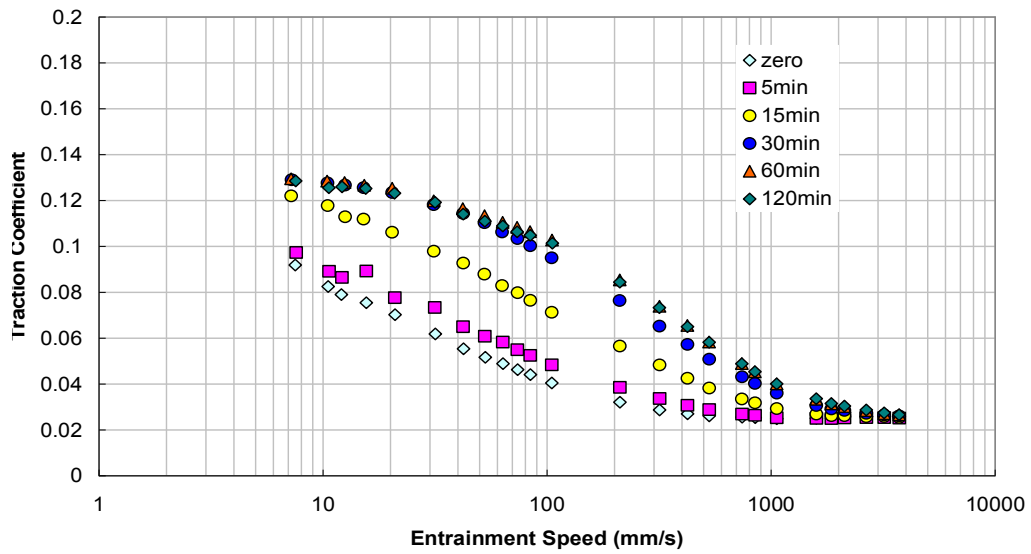


**Figure 7.17 Typical Stribeck Curves of ZDDP and Borated Dispersant in Base Oil**

**Film Thickness - non-post treated dispersant + ZDDP**
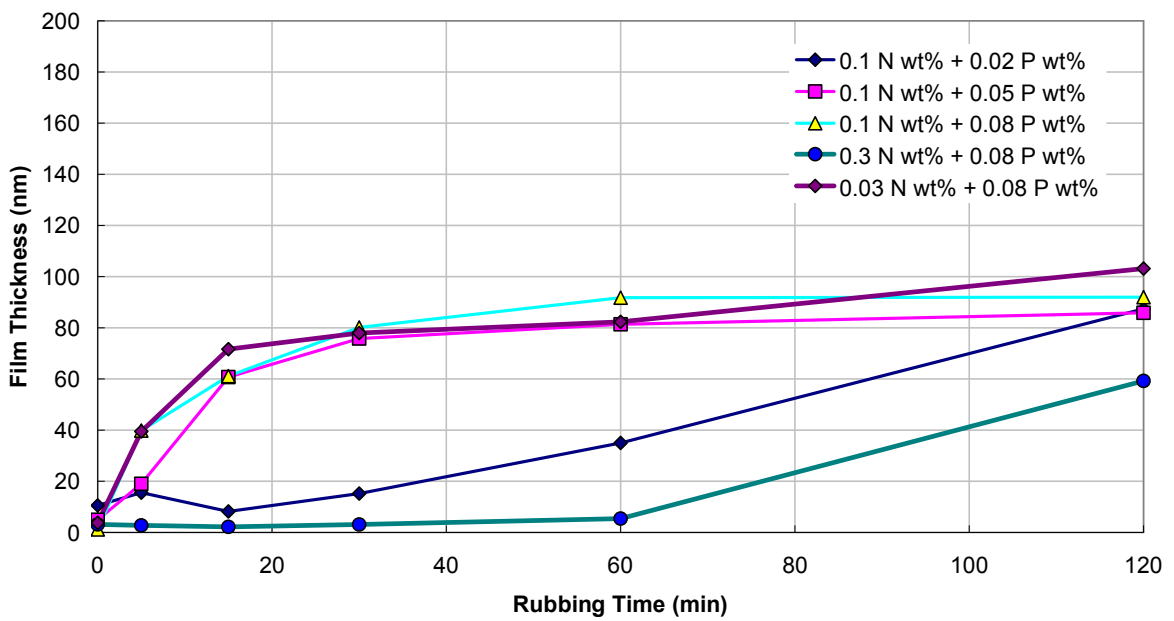


**Figure 7.18 Film Thickness of ZDDP and Non-post Treated Dispersant in Base Oil**

**Stribeck Curve-ZDDP (0.05 P wt%) + NPT dispersant (0.1 N wt%)**
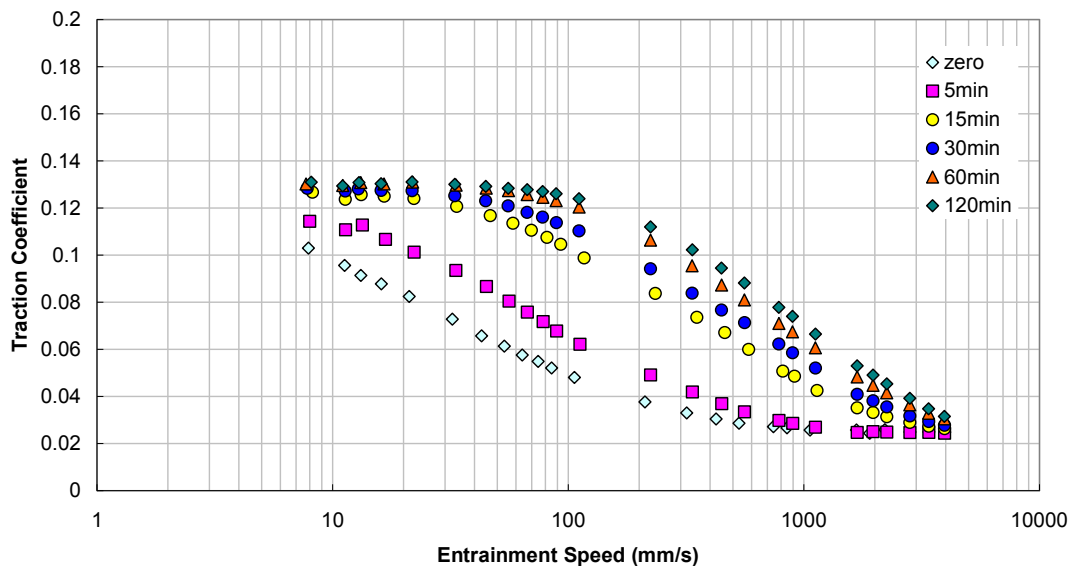


**Figure 7.19 Typical Stribeck Curves of ZDDP and Non-post Treated Dispersant in Base Oil**

### 7.4.3 Summary

The performance of dispersant and ZDDP-containing solutions can be summarized as follows:

- When dispersant is added to ZDDP-containing baseline solutions, it decreases the rate of ZDDP antiwear film formation. This decrease is determined by the concentration of both ZDDP and dispersant, with the N/P ratio and the overall N content both influencing the film thickness. When the concentration of dispersant is extremely high, the ZDDP film is stopped from forming.

- Compared to the friction behaviour of ZDDP alone in base oil solutions, the friction of solutions containing both ZDDP and dispersant increases more slowly and gradually. The friction behaviour is the almost the same as the same dispersant-containing solutions before a ZDDP film forms, but once a ZDDP film is formed, friction behaviour approaches that of other ZDDP-containing solutions (but more slowly).

- The two post treated dispersants show almost the same effect on the ZDDP film forming and friction. When mixed with ZDDP with same N and P content, non-post treated dispersant shows the same trend as the two other post treated ones, but forms slightly thicker film and gives faster friction increase.

127

## 7.5 Film Formation and Friction Properties of Dispersant on ZDDP Film

To investigate the influence of different types of dispersants on ZDDP antiwear film removal, tests were conducted in which a film is formed by a ZDDP-containing oil in an initial 2 hour rubbing test, then the test rig is halted and the oil is drained and replaced by a ZDDP-free, dispersant-containing lubricant before another two hours rubbing under the same conditions. Results are shown below. The study on dispersant and ZDDP-containing solutions showed that the film thickness and friction behaviour depend on the relative concentration (or N/P ratio) of both dispersant and ZDDP. The influence of dispersant on ZDDP film removal is investigated by applying different concentrations of different types of dispersants on the formed ZDDP film. Since the films formed by different concentrations of ZDDP are almost the same after 2 hours rubbing, only one ZDDP concentration was used, 0.05 P wt.%.

Figure 7.20 shows a typical ZDDP film built up and removal (by EC-treated dispersant) process. It can be seen that the ZDDP film formed on the rubbing track is rapidly, but only partially, removed by a dispersant-containing lubricant. Removal occurs in the first 5 minutes of the test, but the film thickness decreases little in the rest of the test. Figure 7.21 shows how the calculated film thickness varied during the tests in which different concentrations of EC-treated dispersants were used to remove ZDDP film under rubbing. The content of EC-treated dispersant seems to have little affect on the rate or extent of ZDDP film removal, since all the lubricants with different contents of dispersant removed the ZDDP film to around 70 nm after 2 hours rubbing. Another key phenomenon found in all these tests is that the film thickness decreases by around 20-40 nm immediately after the replacement of ZDDP-containing lubricant by dispersant-containing lubricant and reheating, which suggests that the dispersant-containing oil dissolves part of the ZDDP film without rubbing, probably by complexation of components of ZDDP film and dispersant.

Similar tests have been carried out using borated and non-post treated dispersants and the same tendency (Figure 7.22 and 7.23) of ZDDP film removal was found. The only difference between these results is the thickness of the remaining film. In Figure 7.24, average film thicknesses measured at each interval of the tests are plotted against rubbing time. This shows

the rates at which these dispersants remove ZDDP film, and that non-post treated dispersant removes ZDDP film faster that the other two. For EC-treated, borated and non-post treated dispersants, the thicknesses of the remaining film are about 60, 70 and 50 nm.

A test was carried out using base oil to replace the ZDDP-containing oil, and applying the same procedures as the above. The thickness of ZDDP film decreased a little then increased to its original value during the 2 hours of rubbing in base oil, which is thought to result from the film transferring from the ball to the disc and back. Therefore ZDDP film is strong enough to resist the rubbing in base oil and its removal by dispersants is thought to be chemical.

The ZDDP film does not grow thicker in prolonged tests even though it is strong enough to resist the rubbing in base oil. This suggests a possibility that some chemical substance in the solution stops the film growing beyond a certain thickness, possibly ZDDP itself or its decomposition products. Therefore it is crucial to verify whether ZDDP (or its decomposition products) is detrimental to the film. Study of ZDDP film formation carried out by Fujita and Spikes [185] showed that the eventual thickness of a secondary ZDDP film increases with temperature. Therefore, a test was carried out in the current study in which a pre-formed ZDDP film was immersed in a solution containing the same ZDDP but at a lower temperature of 40 ℃, to see whether ZDDP in solution removed part of the film. The group III base oil was replaced by a less viscous one to maintain the solution viscosity at the same value as that during film formation at higher temperature. The remaining test conditions were maintained the same as that of the ZDDP film formation stage. Results are shown in Figure 7.26. The film thickness maintained the same when rubbing at a lower temperature, which thus suggests that ZDDP is not active in film removal.

Typical friction behaviour is presented in Figure 7.25. Friction coefficient transitions smoothly from the fluid lubrication regime to the mixed and boundary lubrication regime as the entrainment speed is reduced, which is similar to the dispersant alone in base oil solutions. However, the friction is slightly higher than the corresponding dispersant-containing oil, which may due to the remained ZDDP film. Therefore, the overall friction behaviour is believed to be the combination effect of both ZDDP film and dispersant-containing oil.

For this study on the effect of dispersant on pre-formed ZDDP film, it can be summarized:

- The three types of dispersants all remove the ZDDP film partially and apparently chemically, regardless of their concentration. Different dispersants removes ZDDP film to slightly different extents. Between 50 and 70 nm of the 120 nm ZDDP film is removed, depending on the dispersant.

- A reduction on the thickness of ZDDP film thickness was found when dispersant-containing oil replaced the ZDDP-containing oil and then it was simply heated, which indicates complexation of the components of ZDDP film and dispersant to form soluble species.

- Neither base oil not ZDDP solution tested at a lower temperature remove the pre-formed ZDDP film.

- The overall friction behaviour of the dispersant-containing oil on ZDDP film is influenced by both the dispersant and ZDDP.
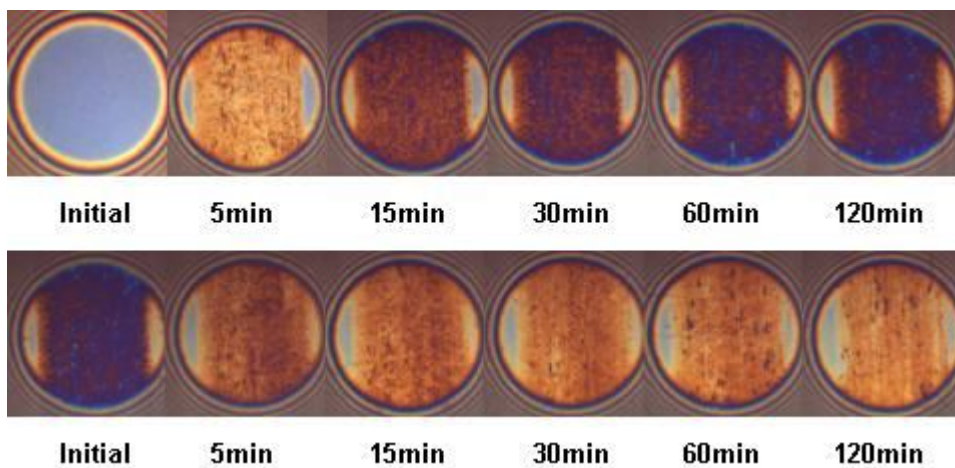


**Figure 7.20 Typical ZDDP Film Removal by Dispersant**

**Film Thickness-ECT dis on ZDDP film**
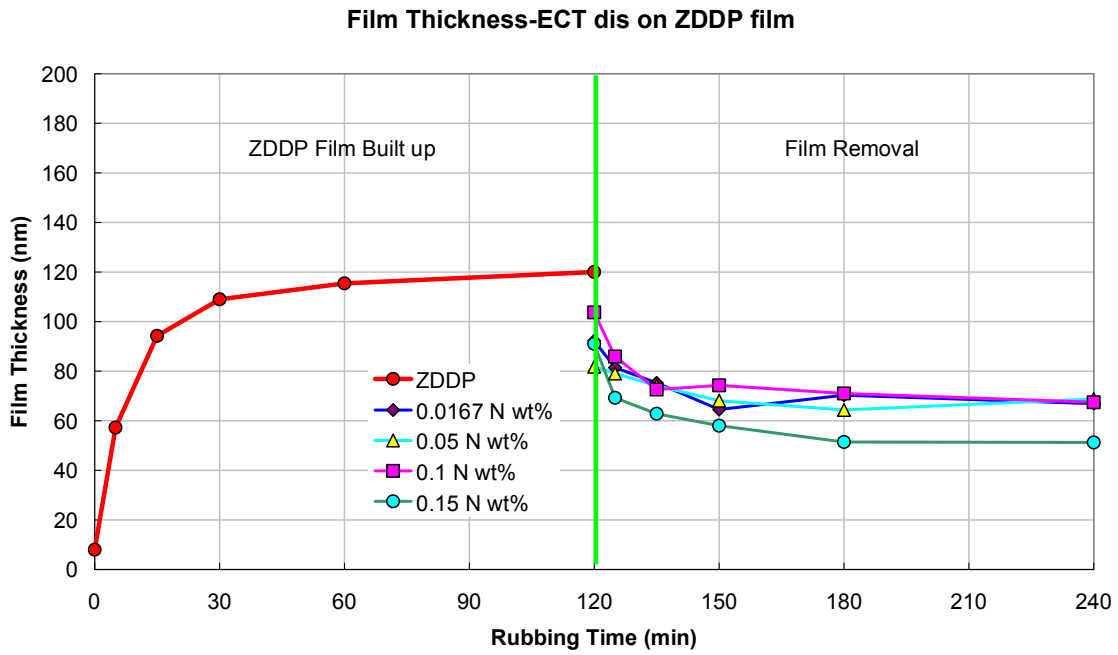


**Figure 7.21 Effect of EC-treated Dispersant on Pre-formed ZDDP Film**

**Film Thickness-Borated dis on ZDDP film**
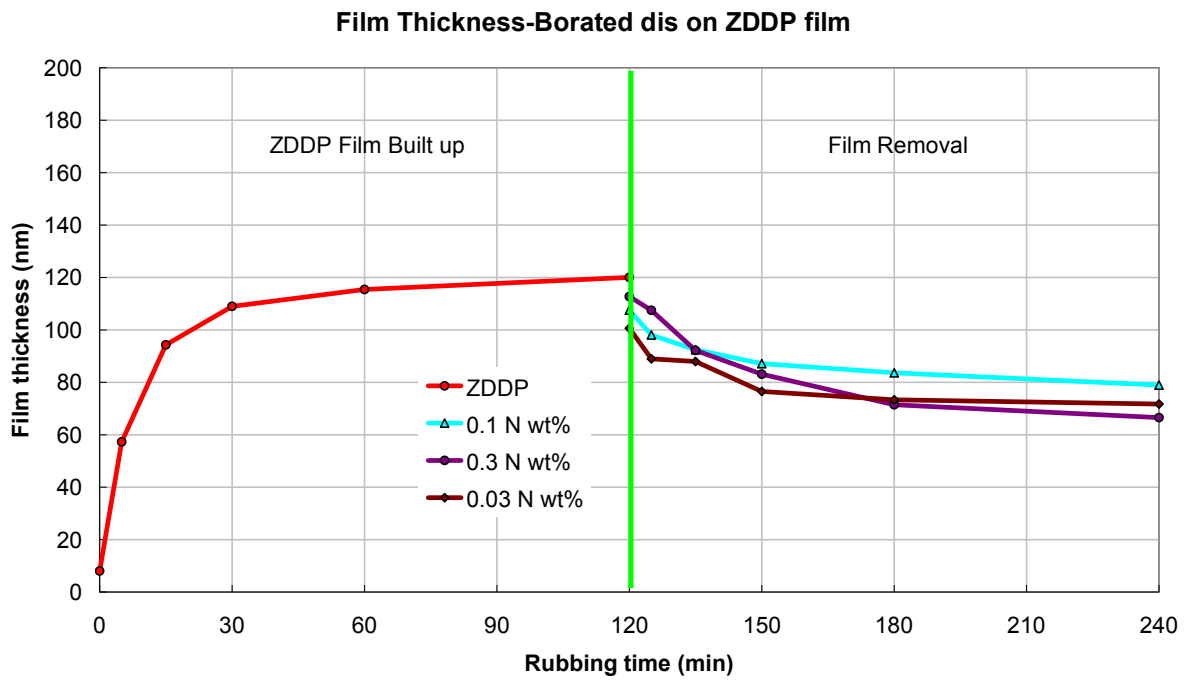


**Figure 7.22 Effect of Borated Dispersant on Pre-formed ZDDP Film**

**Film thickness-NPTdispersant on ZDDP film**
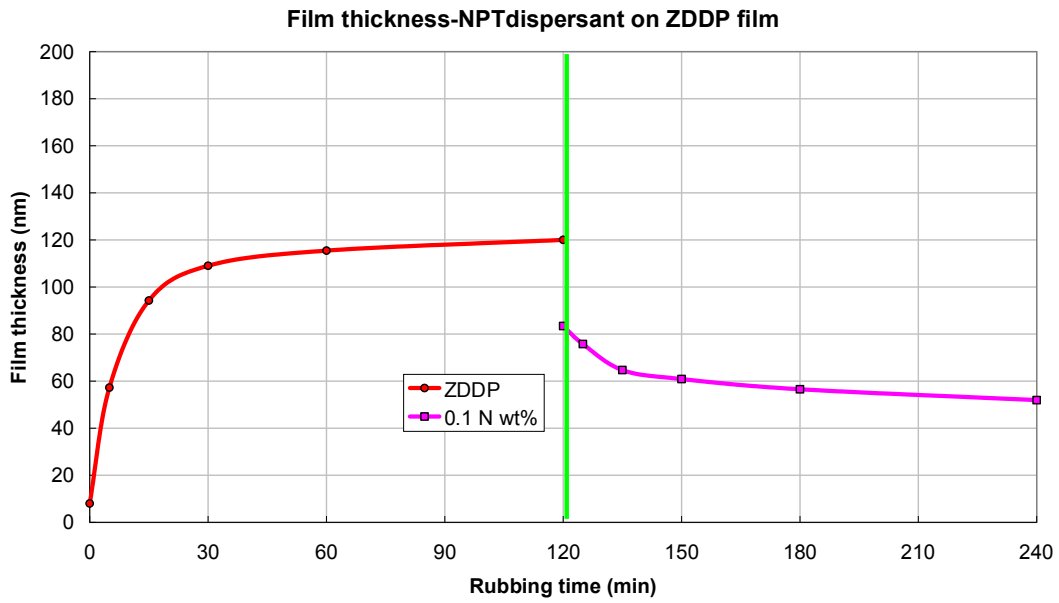


**Figure 7.23 Effect of Non-post Treated Dispersant on Pre-formed ZDDP Film**

**Film thickness - ZDDP film removal**
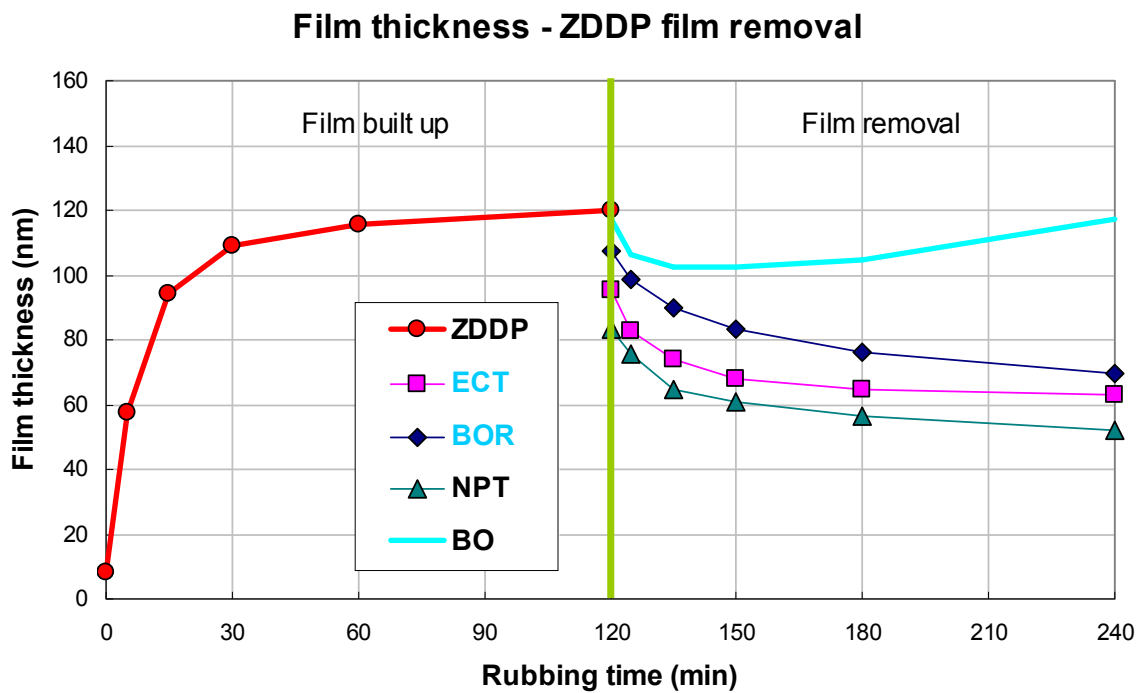


**Figure 7.24 Summary of ZDDP Film Removal by Dispersants**

**Stribeck Curve-ECT dis on ZDDP (0.05%P)**
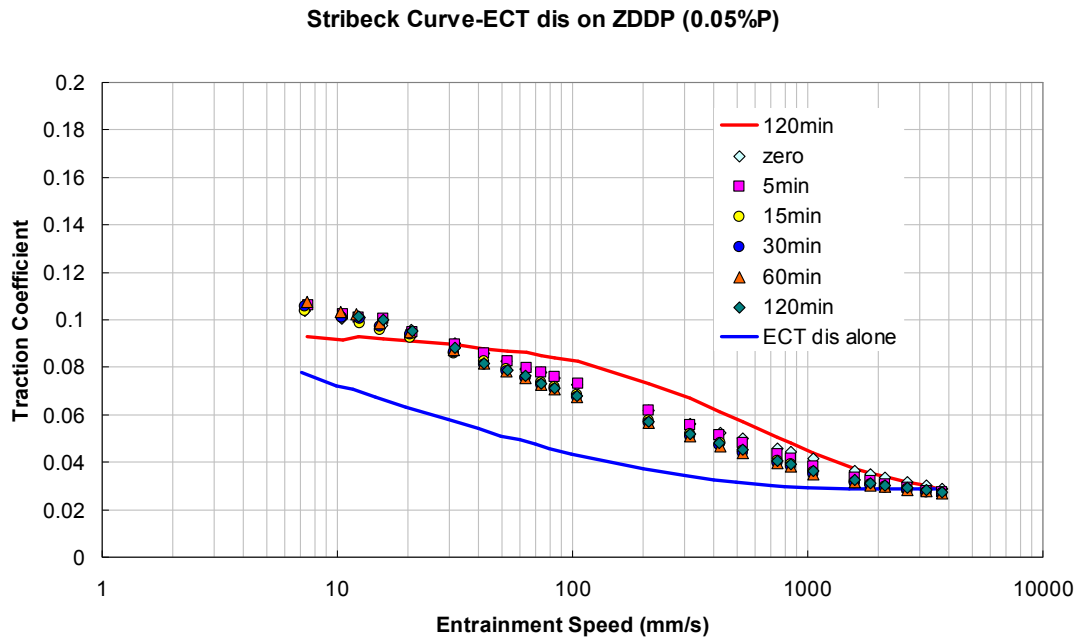
**Figure 7.25 Stribeck Curves Showing Impact of Dispersant-containing Lubricant on Friction of Pre-formed ZDDP Film**

Note: Red curve - the friction behaviour of stabilized ZDDP film; Blue curve – the friction behaviour of ECT dispersant solution
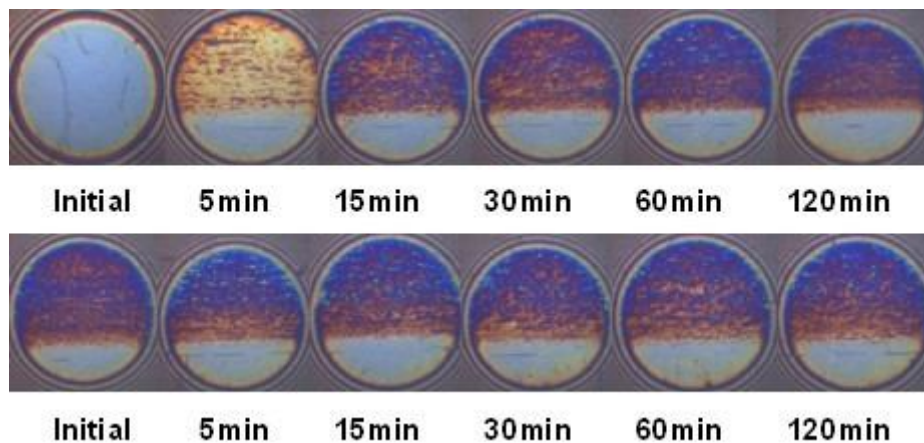


**Figure 7.26 Effect of ZDDP solution at 40 ℃ on Pre-formed ZDDP Film**

## 7.6 Discussion

The tribological behaviour of ZDDP- and dispersant-containing baseline lubricants and the effect of three types of dispersants on ZDDP film formation have been investigated. The study has shown the effectiveness of ZDDP film-forming and the antagonistic interaction between ZDDP and dispersants.

For ZDDP-containing oil, the antiwear film forms rapidly at the beginning of each test, regardless of the ZDDP concentration between 0.02 and 0.08 P wt%, which means that this secondary ZDDP is very active in reacting with the rubbing surfaces and presumably also effective in protecting rubbing surfaces from wear. A rapid increase in friction (especially in the intermediate speed region) occurs once the ZDDP film starts to form, which indicates that the original ZDDP film gives high friction. In the rest of each test, the film is getting smoother and as a result, friction decreases in all three lubrication regimes. It could be postulated that during the rubbing, the original film goes through a slow reconstruction process or some further formation of ZDDP film happens in the valleys of a rough ZDDP film. Further surface analysis needs to be carried out to compare the roughness and structure of the films formed at different time intervals.

Dispersants adsorb on rubbing surfaces and can give low friction behaviour. These thin layers cannot be detected by MTM-SLIM, which may be due to their being squashed flat in a stationary high pressure contact and thus becoming too thin to measure using SLIM. Their adsorbed films can, however, be detected in rolling conditions using ultrathin film interferometry and are between 5 and 10 nm thick. The two post treated dispersants give lower boundary friction than the non-post treated one and these two also form thicker and more regular boundary films as measured by ultrathin film interferometry.

Dispersants when added to ZDDP-containing oils slow down the rate at which ZDDP forms film on rubbing surfaces. The extent of this slow-down depends on the relatively concentration of both ZDDP and dispersant. Generally, the film thickness increases when either dispersant content is reduced or ZDDP content is increased. Thus film thickness is related to N/P ratio in the lubricant although it also seems also to be affected by the overall N level regardless of P concentration. This suggests that there may be complexation of dispersant and ZDDP (or its decomposition products) in solution. Furthermore, when the dispersant content is very high (0.3 N wt%), no measureable ZDDP film is formed on the rubbing surfaces. It is possible that ZDDP is blocked from the surface by the adsorption of excess dispersant. When the N/P ratio (0.05 P wt% + 0.15 N wt%) is not too extreme, it takes a longer time for ZDDP to form film on the rubbing surfaces and this formation immediately causes the boundary friction to increase for the two post treated dispersants. Considering the performance of ZDDP alone in base oil solution, the ZDDP studied is effective in forming a

film on rubbing surfaces, thus protecting them from wear, but not in reducing friction. Nevertheless, the effect of three types of dispersants on ZDDP film formation differs. EC-treated and borated dispersant are gentle in this effect, which may indicate that the bonding between N atom in dispersant and ethylene carbon or boron reduces the negative effect of dispersant on ZDDP film forming.

Dispersants partially remove pre-formed ZDDP films from surfaces during rubbing regardless of concentration. However, they remove the films to different extents, which implies that different extents of protection of the N atom by different post treatments (or no post treatment) influence removal. The overall level of removal ranged from 50 nm for the borated dispersant to 70 nm for the non-post treated one. Another type of removal found in all these tests was that the film thickness decreased by around 20-40 nm immediately after replacement of ZDDP-containing lubricant by dispersant-containing lubricant and reheating, which may infer that the dispersant-containing oil dissolves part of the ZDDP film, probably by complexation of the components of ZDDP film and dispersant. In the literature, it has been shown, under different conditions and with different ZDDPs, that dispersant can remove most of a ZDDP film leaving only about 20 nm, (as compared to 50 to 70 nm in this study) [185]. This may be due to the different structure of film formed by different ZDDPs and/or different dispersants have different film removal ability. Since the ZDDP film has been proved to consisting long chain polyphosphates in the outer layer and short chain polyphosphates in the bulk, it may be possible that the removed part of ZDDP film is mostly long chain polyphosphate. Further surface analysis work needs to be carried out to study the differences in chemical composition between the original ZDDP film and the one remaining after immersion and rubbing with dispersant.

The ZDDP film does not grow any thicker than a critical value. This does not appear to be due to a balance between film formation and removal since a pre-formed film is not removed by rubbing in base oil or in ZDDP solution at lower temperature. It can postulate that the diffusion of Fe through the film or within the channels separating the pads might be the way it reaches and reacts with ZDDP to form thicker film on pre-formed film. Once the film is thick enough to separate the surfaces fully, the diffusion of iron to the outer surface ceases and the ZDDP film thickness stabilizes at this critical value.

Based upon the results and discussion above, four main possible mechanisms of the antagonism between ZDDP and dispersant can be suggested.

- Complexation of dispersant and ZDDP or its decomposition products takes place in the lubricant to reduce the activity of ZDDP.

- Similar complexation happens at the rubbing surfaces, presumably to a greater extent since dispersant adsorbs on the surfaces.

- Adsorption of dispersant blocks ZDDP from forming films rapidly on the surfaces.

- Dispersant chemically removes ZDDP film from surface by solubilisation.

Tests using different concentrations of ZDDP without dispersant show that ZDDP concentration has little effect on eventual film thickness but does influence the rate of film formation for the ZDDP studied. This would imply that complexation is more likely to affect rate of film formation than eventual thickness. Based on the results, the author believes that three effects probably occur.

- Dispersant removes the outer layer of ZDDP film, probably that consisting largely of polyphosphate and/or having high alkyl content. This occurs with pre-formed ZDDP film and presumably also occurs with solutions containing both ZDDP and dispersant.

- Dispersant also slows the formation of ZDDP film, probably mainly by complexation at the surfaces, where the concentration of dispersant will be much higher than in the bulk.

- At very high dispersant concentrations, adsorbed dispersant blocks the surfaces and thus suppresses any significant ZDDP film formation.

# Chapter 8 Wear Results – ZDDP and dispersants

This chapter presents wear measurements and thus wear coefficients on solutions of ZDDP, of dispersant and of blends of the two additives in base oil. It is found that ZDDP itself is highly effective in reducing wear rate but that the dispersant alone increased wear rate compared to the base oil. The influence of ZDDP concentration, dispersant concentration and N/P ratio on wear rate is explored. It is found that for blends of the two additives, wear rate increases with increase of dispersant content but is largely independent of ZDDP content over the range of concentrations studied. These wear results are compared with ZDDP film thickness results described in Chapter 7 and a simple wear model based on the two sets of results is proposed.

## 8.1 Introduction

To explore the antagonism between ZDDP and dispersant, the wear resistance of solutions containing blends of ZDDP and dispersant were compared to investigate the influence of dispersant and ZDDP ratio on antiwear ability.

In this chapter, firstly the wear resistance of solutions containing just ZDDP or EC-treated dispersant is investigated. Then the effect of N:P ratio on the antiwear properties of blends of ZDDP and dispersant is studied. Finally the antiwear and film formation properties of the same lubricants are correlated in order to study the effect of dispersant on ZDDP.

## 8.2 ZDDP or Dispersant alone

Initially, several HFRR tests were carried out to investigate the effectiveness of ZDDP in reducing wear.

The base oil was firstly tested using the HFRR to obtain a comparison reference and the typical resulting wear scar on the HFRR ball is shown in Figure 8.1. After a standard 4 hours HFRR test, the diameter of the wear scar on the ball was 178.6 μm, and the maximum wear depth approximately 1.4 μm. The wear volume was measured and wear coefficient was calculated. For the base oil in the current study, the HFRR wear coefficient is $3.53*10^{-9}$ $mm^3/N \cdot m$.
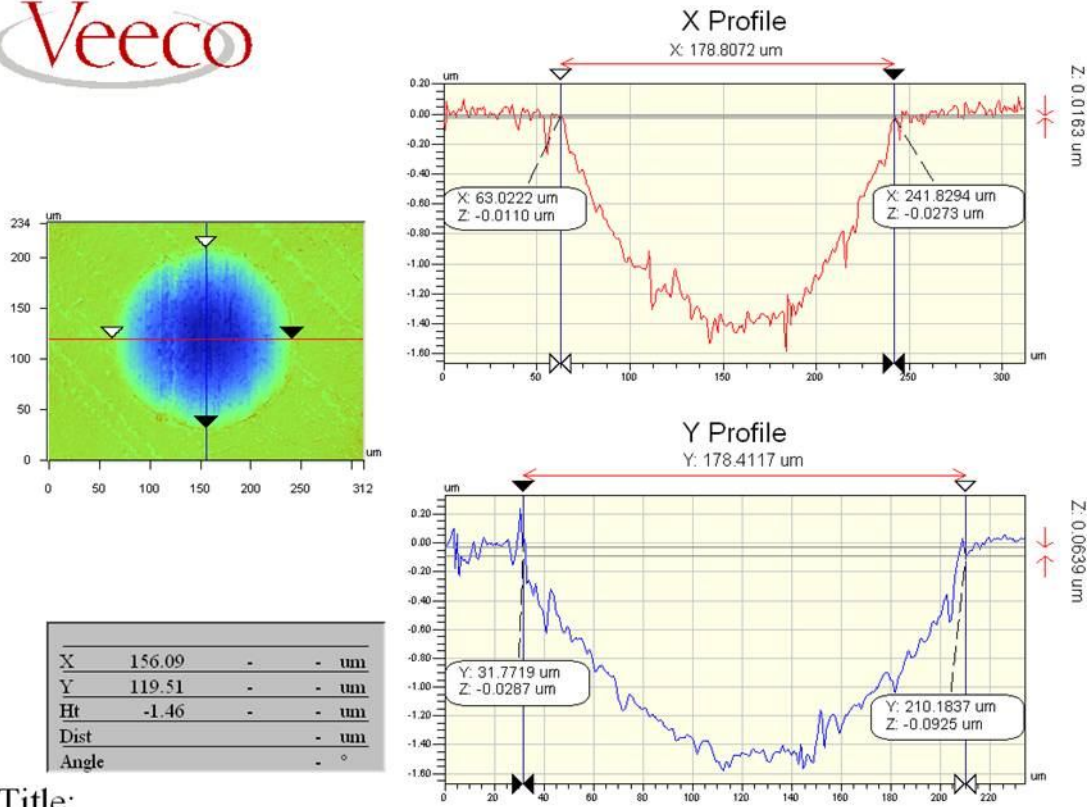
**Figure 8.1 Wear Scar on the HFRR Ball Tested with Base Oil**

A solution with very low content of ZDDP (0.005 P wt%) was then tested and the result is shown in Figure 8.2 below. Compared to the results of base oil, even very small amount of ZDDP proved to be very effective in wear resistance. The wear scar diameter is 86.1 μm and the maximum wear depth 0.11 μm. Wear volume on the ball is 1582.5 μm$^3$, corresponding to a wear coefficient of $0.28*10^{-9}$ mm$^3$/N·m.

EC-treated dispersant alone in base oil was also tested in the HFRR at a concentration of 0.1% wt. N. A typical result is shown in Figure 8.3. The wear rate of this dispersant-containing solution is much higher than the one with ZDDP and higher even than the base oil alone. Dispersant is not known as an antiwear additive but it reduces friction, as shown in the MTM-SLIM results in Chapter 7. However these HFRR results showed that dispersant increases wear when added to base oil. There is rarely any wear testing work carried out on dispersant alone in base oil solutions and the reason why dispersant increases wear is not obvious.

Results on these three baseline solutions are listed in Table 8.1.
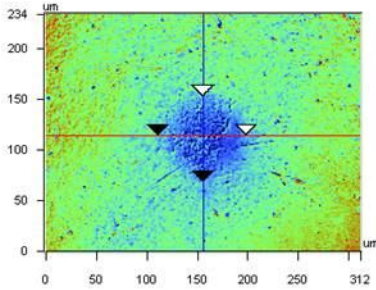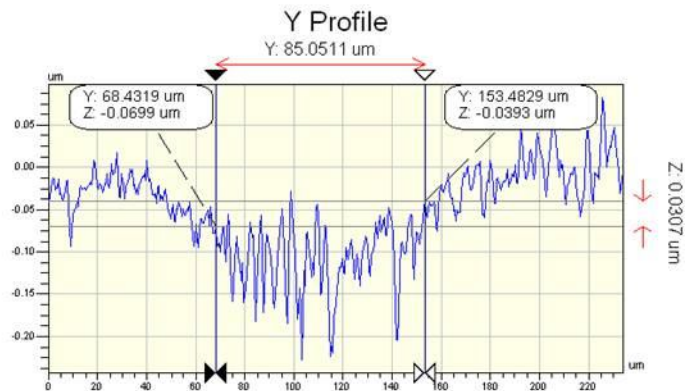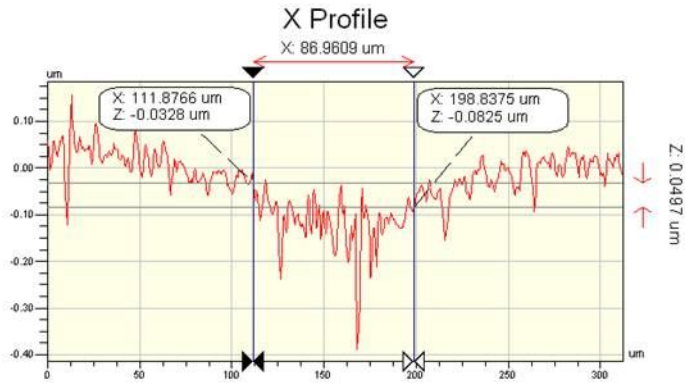
**Figure 8.2 Wear Scar on the HFRR Ball Tested with ZDDP (0.005 P wt%)**
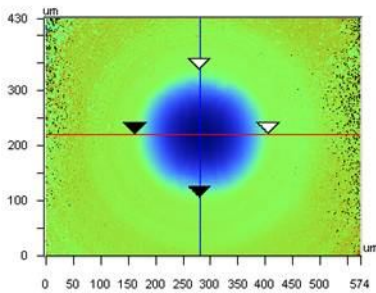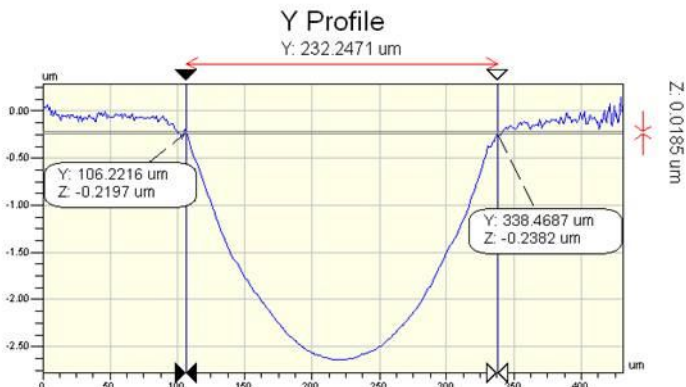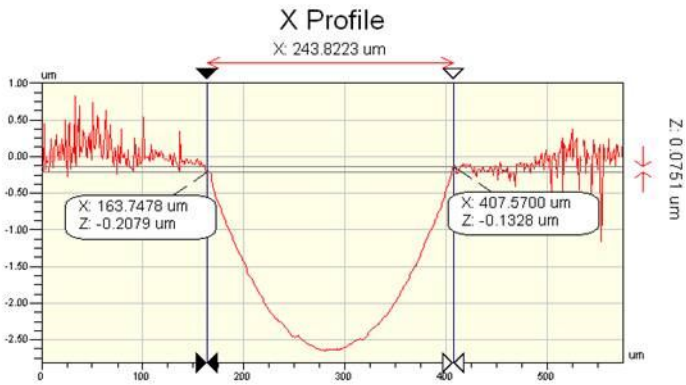


**Figure 8.3 Wear Scar on the HFRR Ball Tested with ECT Dispersant (0.1 N wt%)**

| Lubricants | Wear scar diameter on the ball (μm) | Wear volume (μm³) | Wear coefficient $K$ (mm³/N·m) |
|---|---|---|---|
| Base oil | 178.6 | 19914 | $3.53*10^{-9}$ |
| ZDDP (0.005 P wt%) | 86.1 | 1582.5 | $0.28*10^{-9}$ |
| Dispersant (0.1 N wt%) | 243 | 76540 | $13.6*10^{-9}$ |

**Table 8.1 Comparison of Behaviour of Base oil, ZDDP (0.005 P wt%) and EC-treated Dispersant (0.1 N wt%) Solution**

To investigate the influence of concentration of ZDDP on antiwear properties, solutions with different contents of ZDDP were tested by the newly developed sliding/rolling, reciprocating MTM mild wear test method. Example results are shown in Table 8.2. Each of these three solutions was tested three times. One wear track image of each test was randomly selected and shown in Table 8.2. The wear depths of the wear track on the disc specimens were measured and averaged and the wear coefficients were then calculated for each lubricant.
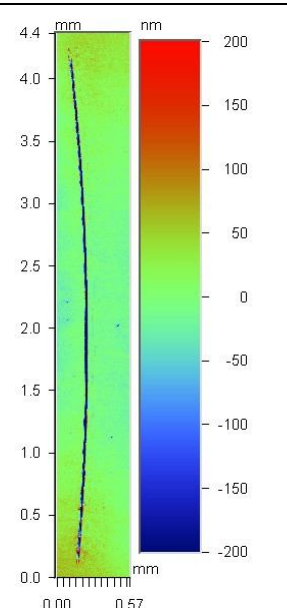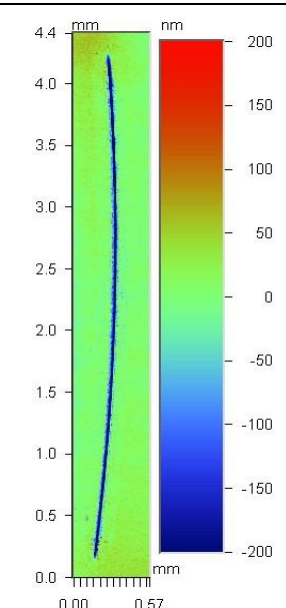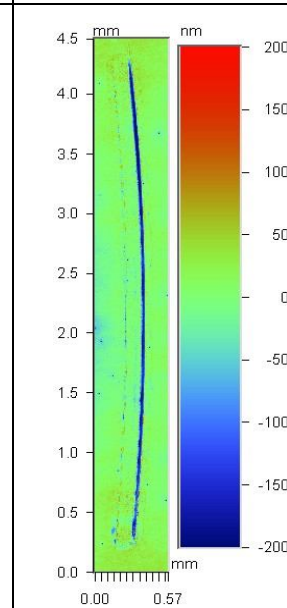
| Lubricants | ZDDP (0.02 P wt%) | ZDDP (0.05 P wt%) | ZDDP (0.08 P wt%) |
|---|---|---|---|
| Wear track on disc |  |  |  |
| Wear depth (nm) | 35 | 40 | 40 |
| $K$ (mm³/N·m) | $0.20*10^{-9}$ | $0.23*10^{-9}$ | $0.23*10^{-9}$ |

**Table 8.2 Mixed Rolling/Sliding, Reciprocating MTM Tests Results on Different Concentrations of ZDDP**

It can be seen that the wear track shape, the wear depths and wear coefficients for these lubricants with different contents of ZDDP are similar to each other, which indicates that this

ZDDP is a very effective antiwear additive and that a very small amount of ZDDP is capable of protecting rubbing surface from wear.

The effect of concentration of ZDDP on wear rate has been studied previously [160], as was shown in Figure 4.2 in Chapter 4. This study illustrated an adhesive/corrosive wear balance when different concentrations of ZDDP were applied. Nevertheless, it also indicated that the wear rate maintained approximately consistent regardless of the concentration of ZDDP when the latter was higher than a certain value (about $2*10^{-4}$ mole fractions in the study).

## 8.3 Wear Resistance of ZDDP- and Dispersant-containing Lubricants

A series of rolling/sliding, reciprocating MTM wear tests were carried out in which the concentrations of ZDDP and EC-treated dispersant were systematically varied to provide a wide range of N/P ratios. Results are shown in a 3D representation in Figure 8.4.
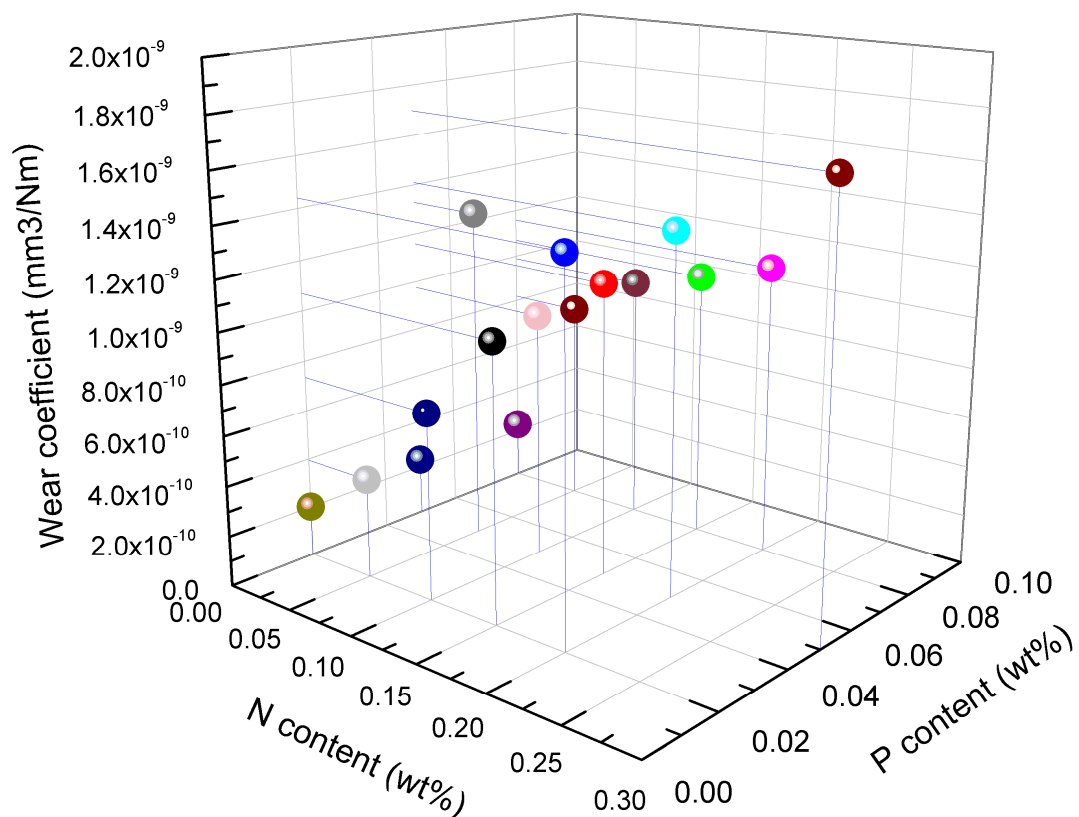


**Figure 8.4 Wear Coefficients of Solutions Containing Different Concentrations of EC-treated Dispersant and ZDDP**

Unfortunately the tendency of how the N and P content of these solutions impact wear rate is unclear in this 3D graph. Figure 8.5 and 8.6 show the impact of P and N content separately at a fixed concentration of the other component. These show that increase of N content tends to increase wear rate regardless of the P content. The level of P has little effect on wear rate except at very low N content when wear rate increases and then decreases with increasing P content.
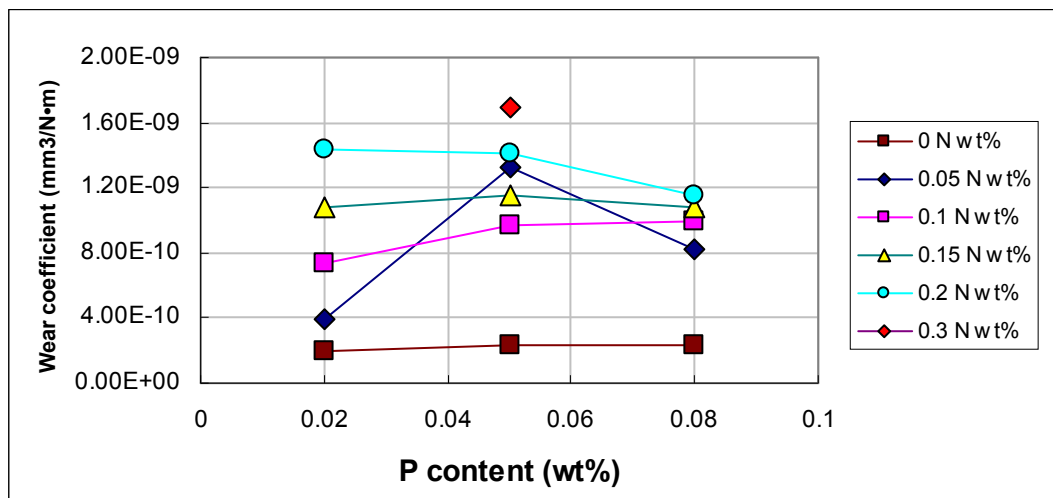


**Figure 8.5 Effect of P Content on Wear Rate**
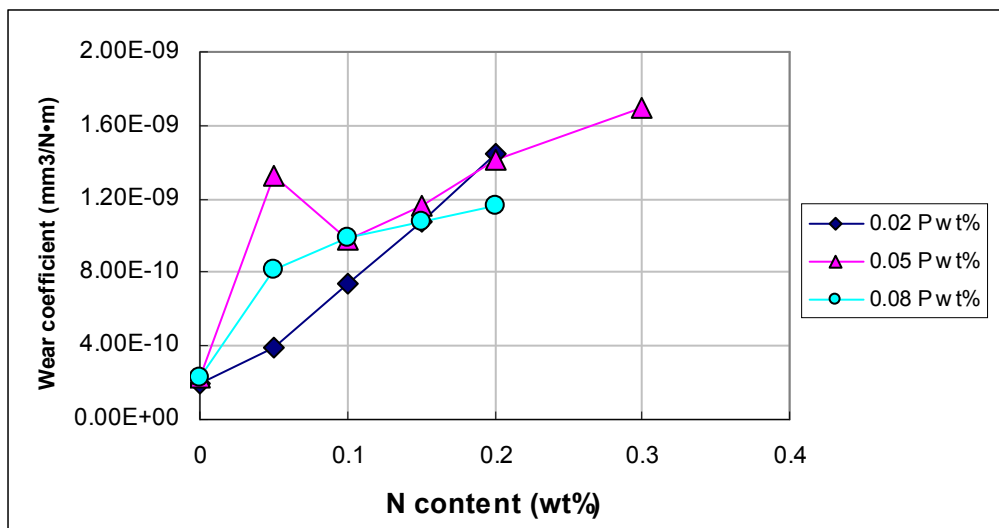


**Figure 8.6 Effect of N Content on Wear Rate**

## 8.4 Relation between Wear Resistance and Film Thickness

Comparing the influence of N/P content on ZDDP film thickness and wear results, Figure 7.11 is reproduced here as Figure 8.7. Comparing this with the wear coefficient results in Figure 8.4, it can be seen that the two are not linearly related to each other. However, it cannot be concluded that the wear resistance is wholly independent of the thicknesses of ZDDP film. The dependence of film thickness on P and N contents are illustrated more clearly in Figure 8.8 and 8.9. Film thicknesses depend on both P and N content in the solutions, increasing with P content but decreasing with N content. The wear coefficient data is affected to larger extent by the N content than the P content. This implies that the N content might be the key factor which relates the film thickness and wear coefficient to each other.
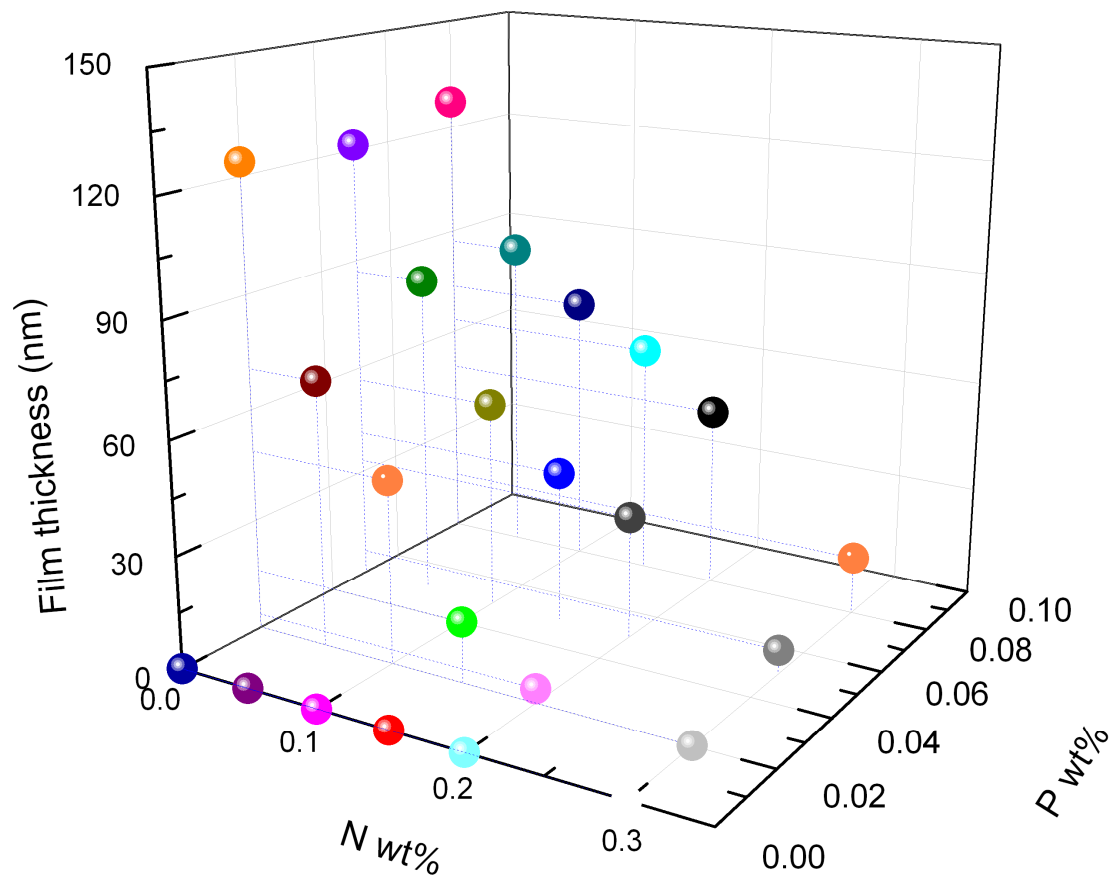


**Figure 8.7 Film Thicknesses of Solutions Containing Different Concentrations of EC-treated Dispersant and ZDDP after 2h Rubbing**
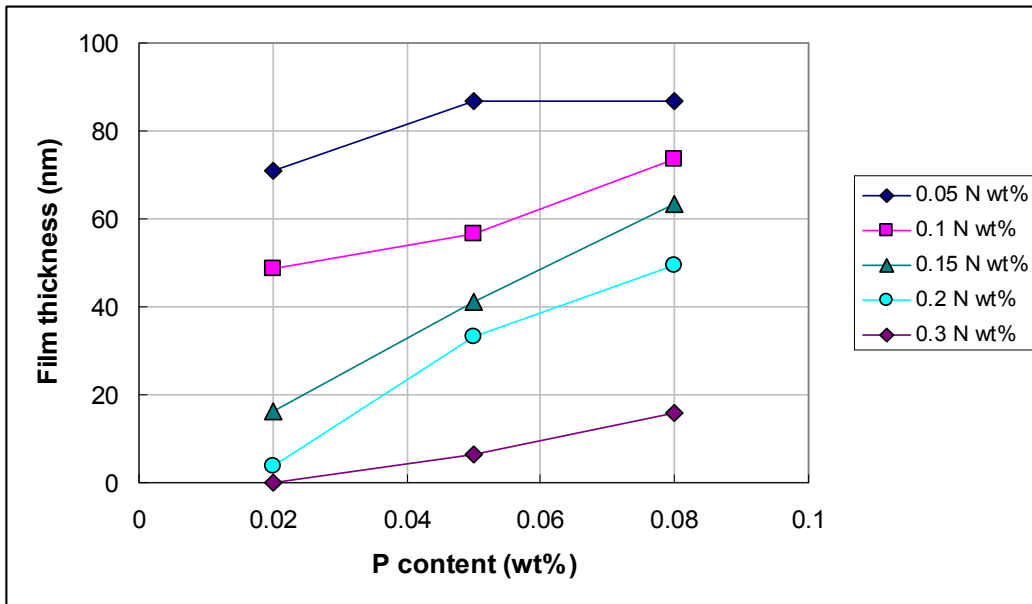
**Figure 8.8 Effect of P Content on Film Thickness**
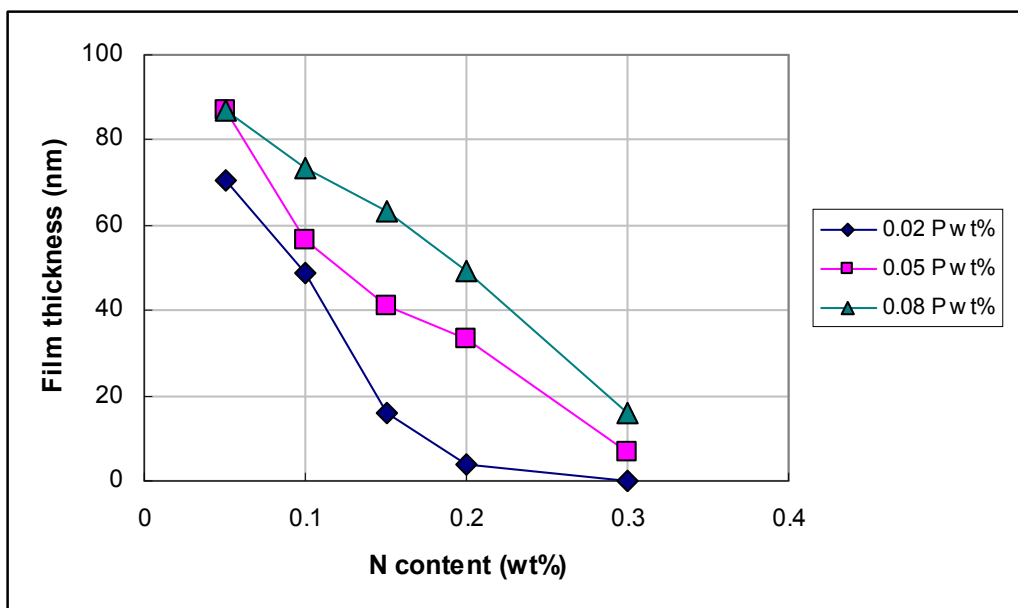


**Figure 8.9 Effect of N Content on Film Thickness**

## 8.5 Summary

Solutions of ZDDP in base oil have been tested by the HFRR and the newly-developed rolling/sliding, reciprocating MTM mild wear test. Compared to the results obtained from the HFRR test on base oil it showed that even a small amount of ZDDP can provide high antiwear performance. Tests on different concentrations of ZDDP-containing solutions show

that once a low concentration of ZDDP is present (corresponding to 0.02 P wt%) the wear rate remains approximately constant as P content is increased up to 0.08 P wt%. It was also shown in Chapter 7 that base oil cannot remove ZDDP film under similar rubbing conditions, which indicates that ZDDP film is strong enough to be resistant to wear by base oil once it is formed on rubbing surface.

HFRR tests on EC-treated dispersant alone in base oil solution showed that dispersant increased wear when added to base oil. The reason for this is not understood.

For the blends containing both ZDDP and EC-treated dispersant, wear rate varied with the P and N content. N:P ratios were plotted against wear coefficients but this did not give a clear trend. When wear coefficient was plotted against N and P ratio separately the trends were more clear. When N content was fixed, increasing P content resulted in a film thickness increase but had little effect on wear rate. This implies that a higher content of ZDDP forms a thicker film but that a thicker film does not lead to lower wear; *i.e.* even a thin ZDDP film provides effective wear protection. On the other hand, an increase in N content led to the film thickness decreasing and the wear coefficient increasing, even though there was no direct correlation between film thickness and wear coefficient.

The results can be best explained by a model in which ZDDP reduces wear by forming a protective film on the rubbing surfaces. However this film needs only to be very thin to control wear. Dispersant increases wear by promoting the local and transient removal of parts of the ZDDP film, which results in loss of iron from the surface and thus wear. The rate of this removal and thus the wear rate increases with dispersant concentration and thus the rate of film removal. The fact that ZDDP concentration has little effect on wear rate suggests that, once a region of film is removed by dispersant, the subsequent initial formation of a thin protective film is very rapid and largely independent of P concentration. However the subsequent growth in thickness of the film does depend on concentration, as indicated by the film thickness results, although this is largely irrelevant in terms of wear protection.

# Chapter 9 Effect of other Additives on the Tribological Properties of ZDDP

In this chapter, the effect of several other key additives commonly applied in engine lubricants on the film formation, friction and wear properties of ZDDP are studied. MTM-SLIM and the new mild wear test method are carried out on these additives to evaluate their intrinsic film forming and wear behaviour. Detergents are found to form quite thick films, depending on the detergent structure. These films show significant differences in wear resistance. MoDTC and ZDDP act in a synergistic manner both in friction and antiwear performances. Film formation and antiwear properties of solutions containing both dispersant and a sulfonate detergent are investigated by the addition of ZDDP; while friction and wear behave dissimilarly.

## 9.1 Introduction

So far this thesis has focussed primarily on two additives, one ZDDP antiwear additive and three dispersants. In practice, of course, many different types of additive are used in engine oils. In this chapter the film-forming, friction and wear properties of some other important engine oil additives are investigated. Of particular interest was to determine the extent to which these additives interfere with the action of ZDDP and to apply the newly-developed mild wear tests to such additives. Three different three-component additive systems, comprising combinations of sulfonate and a post-treated dispersant with different concentrations of ZDDP, were also investigated regarding film forming, friction and wear properties. A list of additives tested in this part of the study is shown below in Table 9.1.

| Code | Additives | | | | | | | |
|---|---|---|---|---|---|---|---|---|
| | Sulf | B-Sulf | Sali | MoDTC | ECT | BOR | 2Z | 8Z |
| 1 | √ | | | | | | | |
| 2 | | √ | | | | | | |
| 3 | | | √ | | | | | |
| 4 | √ | | | | | | √ | |
| 5 | √ | | | | | | | √ |
| 6 | | √ | | | | | √ | |
| 7 | | √ | | | | | | √ |
| 8 | | | √ | | | | √ | |
| 9 | | | √ | | | | | √ |
| 10 | | | | √ | | | | |
| 11 | | | | √ | | | √ | |
| 12 | | | | √ | | | | √ |
| 13 | √ | | | | √ | | | |
| 14 | √ | | | | √ | | √ | |
| 15 | √ | | | | √ | | | √ |
| 16 | √ | | | | | √ | | |
| 17 | √ | | | | | √ | √ | |
| 18 | √ | | | | | √ | | √ |

**Table 9.1 Additives Tested in Current Study**

**Note: Sulf – overbased calcium sulfonate detergent (55mM CA/Kg); B-Sul – borated calcium sulfonate detergent (55mM CA/Kg); Sali – overbased calcium salicylate detergent (55mM CA/Kg); MoDTC – Molybdenum dithiocarbamate (1.17 wt%); ECT – EC-treated dispersant (0.1 N wt%); Bor – borated dispersant (0.1 N wt%); 2Z – ZDDP (0.02 P wt%); 8Z – ZDDP (0.08 P wt%)**

## 9.2 Detergents

Detergents are very important additives in engine oils, with two main roles; (i) to maintain the cleanliness of high temperature engine parts around the combustion chamber and (ii) to neutralize acids in engine oils so as to maintain the basicity of the oil during its drain interval despite its incorporation of acidic combustion gases. However it has been found that the tribological properties of ZDDP are affected by the presence of detergents, as described below.

### 9.2.1 Effect of Detergents on the Film Formation and Friction Properties of ZDDP

When overbased detergents are used in oils in the absence of ZDDP, most research has identified the formation of a quite thick (100+ nm), solid-like film of calcium carbonate in the form of calcite on the rubbing surfaces [188-192]. It has been suggested that this film can impart antiwear or EP behaviour [193]. The behaviour of overbased detergents in the presence of ZDDP is less clear, with reports of both improved and diminished antiwear performance [194, 195]. There are three suggested possibilities in terms of the interference between detergents and ZDDP [195]: 1) additive interaction in bulk oil reduces the ability of the additives to reach surfaces; 2) competition in adsorption of additives on surfaces results in either ZDDP or detergent forming a film in preference to the other; 3) a bifilm forms, incorporating components from both additives, leading to different antiwear performance.

A study using electrical contact resistance (ECR) has found that the detergent retards the film formation of ZDDPs [196, 197], while preferential adsorption [198] of a phenate detergent on steel surface in comparison to a secondary ZDDP has also been reported. Taylor *et al.* [178] have employed MTM-SLIM to study the tribological behaviour of a secondary ZDDP in the presence of a sulphonate detergent and found that the rate of film formation by ZDDP is slowed down by the sulphonate detergent and the film formed is thinner than that without detergent. However, whether the interaction is synergistic or antagonistic, the interference between detergent and ZDDP is highly complex and depends strongly on the nature of the detergent.

To characterize the chemical composition of the film formed by a solution which contains both ZDDP and detergent, surface analysis techniques such as XPS [189], TOF-SIMS [190, 191] and XANES [192] have been carried out and results showed that zinc, calcium, phosphorus and sulphur were present.

Regarding the effect of detergent on friction performance of ZDDP-containing oils, Falex pin-V block [194] and block-on-ring [199] tests have shown friction reduction in boundary lubrication. In the Falex wear test [194], the addition of detergent reduced the friction for oils containing ZDDP and this was explained in terms of the formation of mixed films on the surface. The reason for this reduction has been explored by Kubo *et al.* [191] where it was found that the content of calcium is inversely related to friction. However, an MTM test [178] under mixed rolling/sliding conditions has shown that a blend of sulfonate detergent and ZDDP gave higher boundary friction than ZDDP alone.

### 9.2.2 Test Results on Film Formation and Friction Properties of Detergents- (and ZDDP-) Containing Oils

Standard MTM-SLIM tests were firstly carried out on three different types of detergent to explore the film formation and friction properties of the detergents alone. Results are shown in Figure 9.1. An overbased borated sulfonate in base oil solution is the most effective in film formation among these three detergents. The steady state thicknesses of these films formed by sulfonate, borated sulfonate and salicylate solutions are 80, 118 and 42 nm respectively.
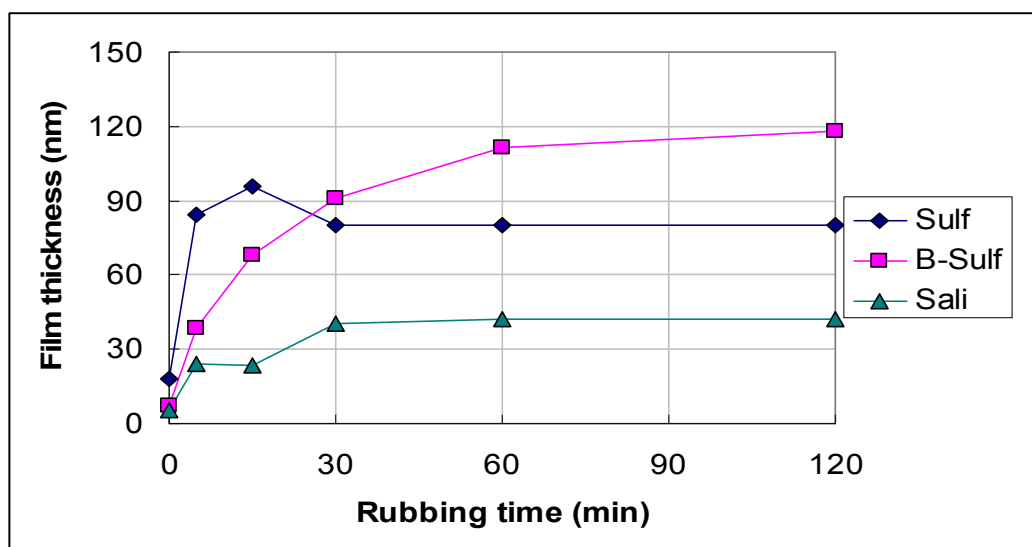


**Figure 9.1 Film Formation Curves of Different Types of Detergents**

**Note: Sulf – overbased calcium sulfonate; B-Sul – overbased borated calcium sulfonate; Sali – overbased calcium salicylate**

To investigate the interference between detergents and ZDDP, standard MTM-SLIM tests were carried out on the blends of these two additives in base oil solutions. SLIM images and film formation curves are shown below:



ZDDP (0.02 P wt%)

ZDDP (0.08 P wt%)

Sulfonate

Sulfonate + ZDDP (0.02 P wt%)

Sulfonate + ZDDP (0.08 P wt%)
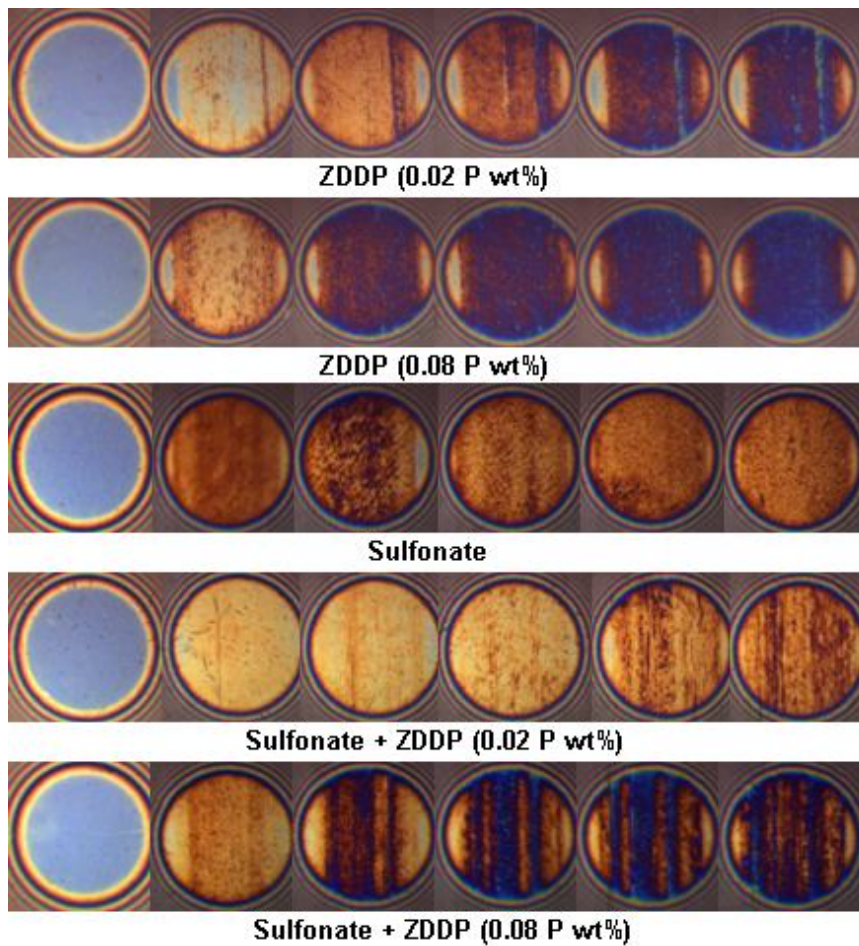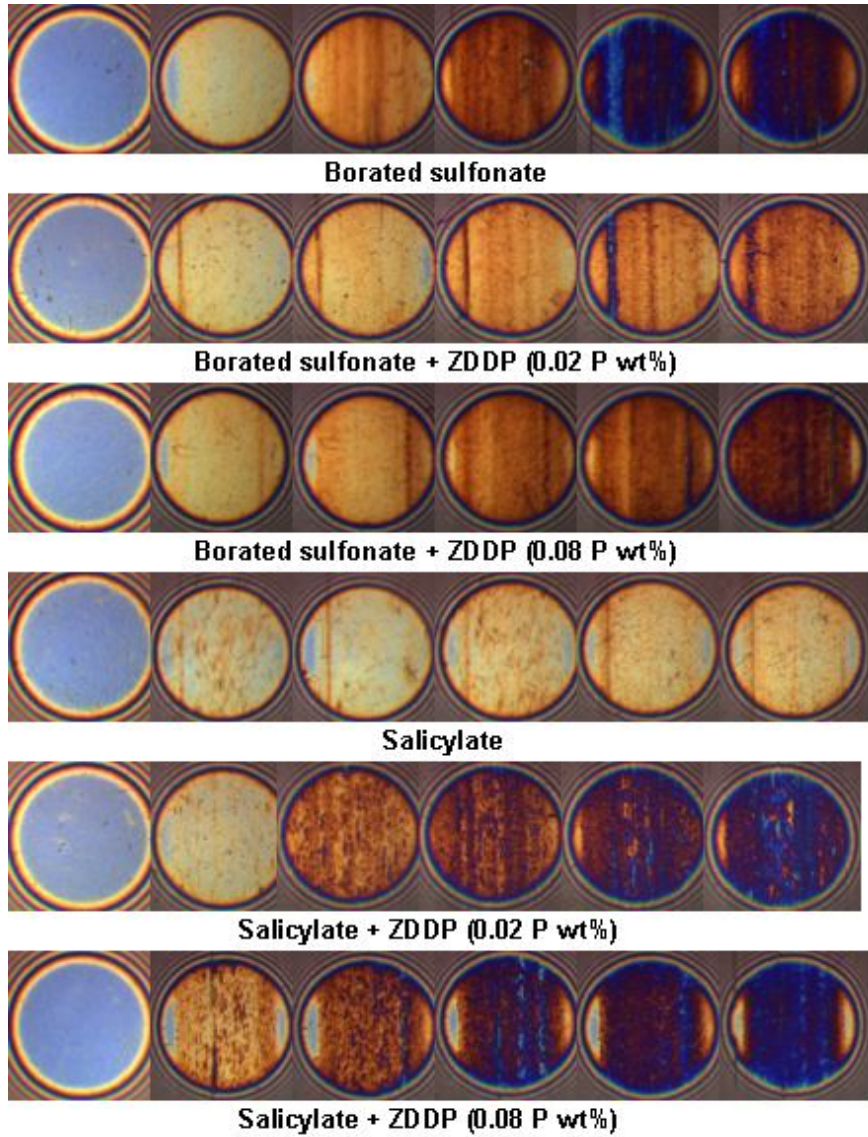
**Figure 9.2 SLIM Images of Detergent- and ZDDP-containing Solutions**
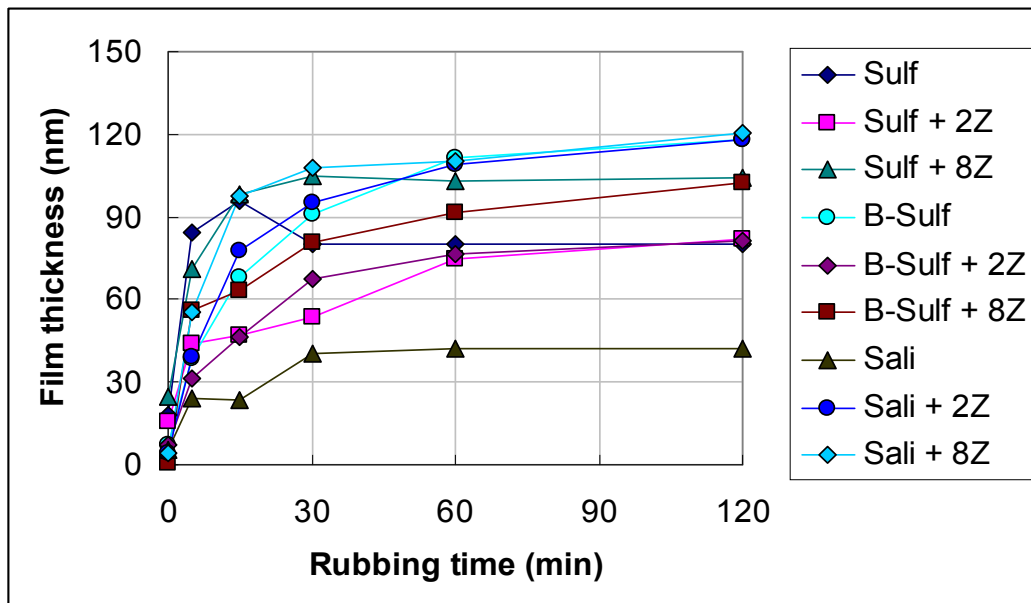
**Figure 9.3 Film Thicknesses of Detergent- and ZDDP-containing Solutions**

**Note: Sulf – overbased calcium sulfonate detergent; B-Sul – overbased borated calcium sulfonate detergent; Sali – overbased calcium salicylate; 2Z – ZDDP (0.02 P wt%); 8Z – ZDDP (0.08 P wt%)**

*9.2.2.1 Sulfonate*

It can be seen that when ZDDP at a concentration of 0.02 P wt% was added to sulfonate detergent solution, the rate of film formation was lower than either with ZDDP or sulfonate alone. However, eventually the film thickness reached was almost the same as that formed by sulfonate solution. A higher concentration of ZDDP (0.08 P wt%) showed relatively rapid film formation behaviour to reach a steady state film thickness which was greater than that formed by sulfonate or sulfonate + ZDDP (0.02 P wt%). These results may imply that, at a low concentration of ZDDP, competition in adsorption of sulfonate and ZDDP on steel surfaces occurs. In this case, both additives struggle in reaching the surfaces in high concentration, which results in a slower film formation process. For the higher ZDDP concentration it seems that ZDDP dominates in the competition, to give a trend of film forming quite similar to that of ZDDP alone. However, the performance of the solutions containing both additives may result from the bi-film formed by both additives, so friction measurements are still needed on these solutions to provide more evidence.

The friction behaviour of ZDDP solutions and sulfonate (+ ZDDP) solutions is shown below in Figure 9.4 to 9.8. The film formed by sulfonate alone shows an initial slope characteristic of a good organic friction modifier, with low friction that increases with speed in the boundary lubrication regime. As rubbing occurs, the friction at low speeds increases slightly

but there is a marked shift in the friction curve, with the mixed lubrication region moving to higher speed, similar to the behaviour seen with ZDDP. This has been ascribed to the formation of a thick, rough film of calcium carbonate [193]. When ZDDP (0.02 P wt%) is added, there is a slight increase in low speed friction. For the solution containing sulfonate and a higher concentration of ZDDP (0.08 P wt%), the low speed friction increases markedly during rubbing. It is also seen that the overall friction increases. Additionally, compared to the friction behaviour of ZDDP baseline solution (represented in Figure 9.4), the friction performance of solutions containing both ZDDP and sulfonate is different from either, which suggests a combinational effect.
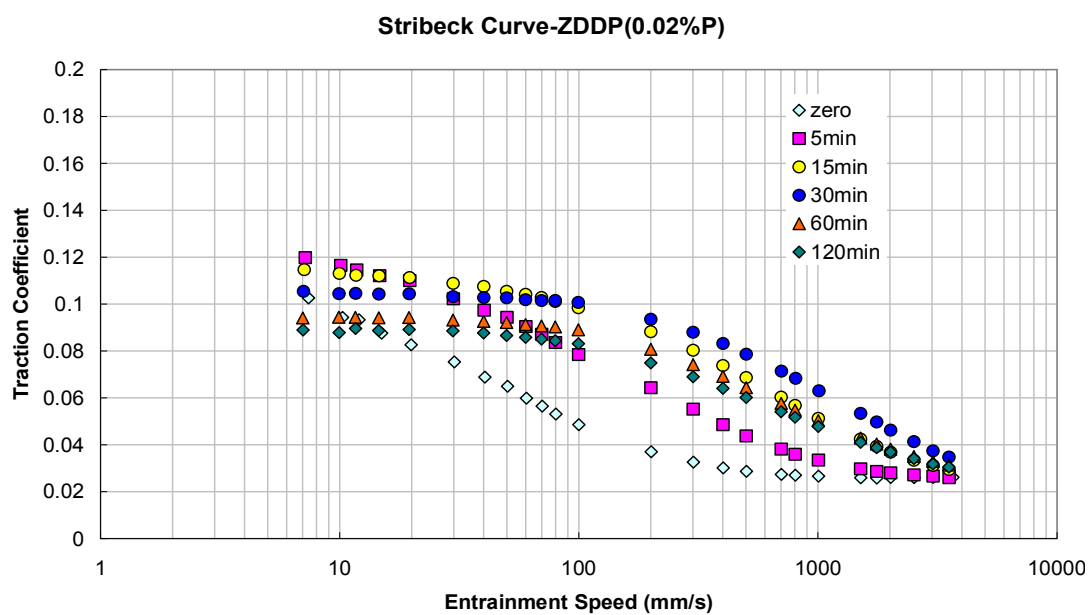


**Figure 9.4 Stribeck Curves of ZDDP (0.02 P wt%) in Base Oil Solution**
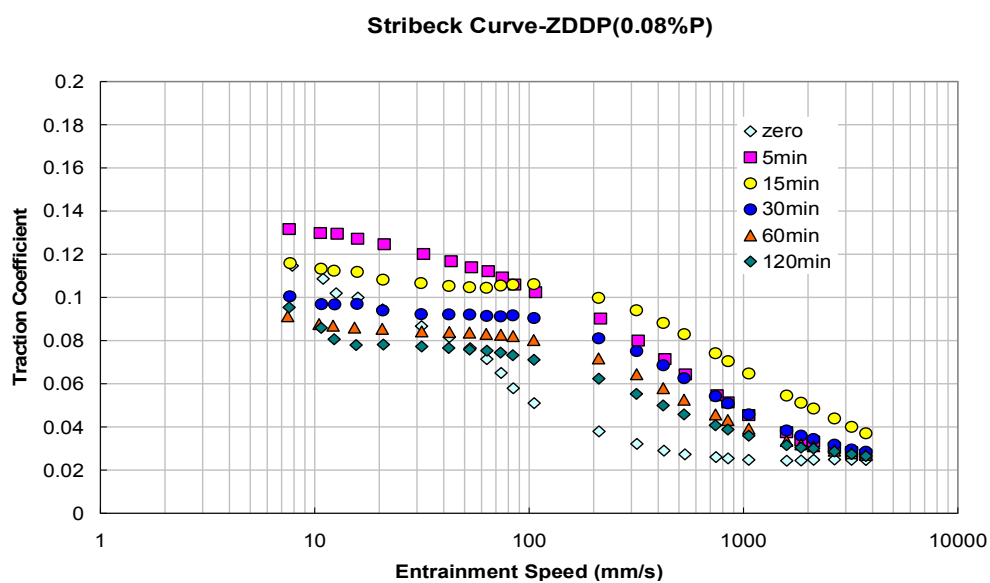


**Figure 9.5 Stribeck Curves of ZDDP (0.08 P wt%) in Base Oil Solution**

154

**Stribeck curve-Sulfonate**
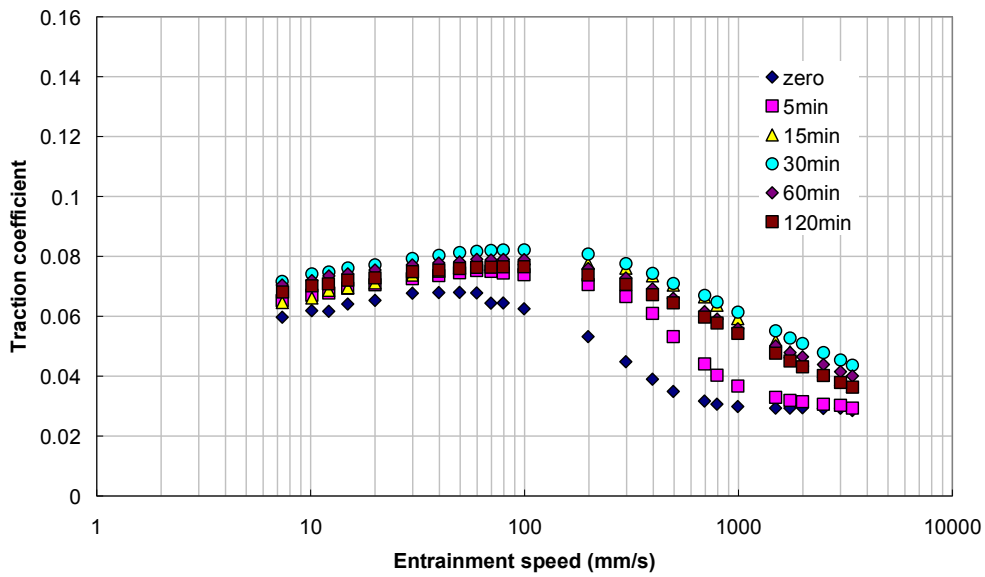


**Figure 9.6 Stribeck Curves of Sulfonate in Base Oil Solution**

**Stribeck curve-Sulfonate + ZDDP (0.02%P)**
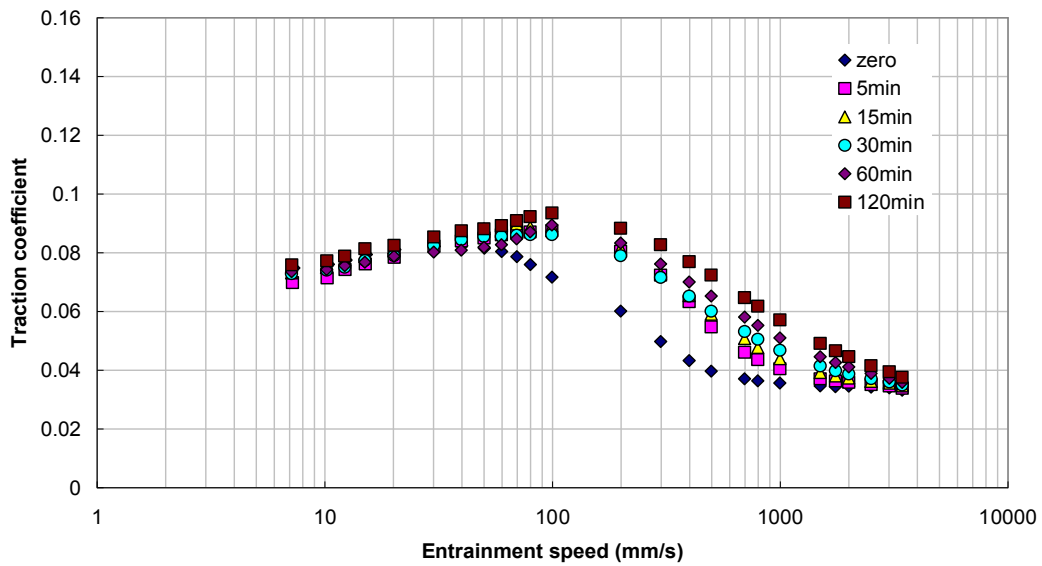


**Figure 9.7 Stribeck Curves of Sulfonate + ZDDP (0.02 P wt%) Solution**

**Stribeck curve-Sulfonate + ZDDP (0.08%P)**
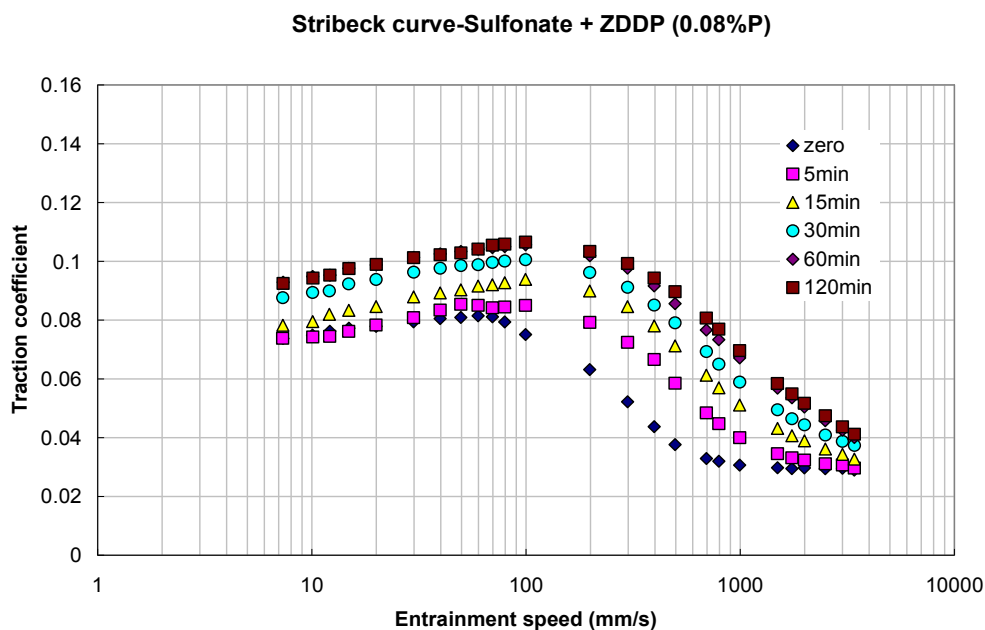


**Figure 9.8 Stribeck Curves of Sulfonate + ZDDP (0.08 P wt%) Solution**

*9.2.2.2 Borated sulfonate*

Both ZDDP and borated sulfonate detergent can form films with a thickness of about 120 nm on their own, but blends of the two additives give thinner films. This indicates an antagonistic response between borated sulfonate and ZDDP. The trends of film forming of these solutions are similar to the detergent and ZDDP baseline solutions. The friction behaviour of these borated sulfonate solutions is quite consistent, and a typical one is shown in Figure 9.9. The borated sulphonate shows classical organic friction modifier behaviour at low speed, although friction is higher than for the non-borated sulphonate. This behaviour is retained on addition of ZDDP. Relating film formation and friction performance of solutions containing ZDDP and/or borated sulfonate, it is still unclear how these two additives interfere in solution or on the steel surfaces.

**Stribeck curve - B-Sulf**



Figure 9.9 Stribeck Curves of Borated Sulfonate in Base Oil Solution

**Stribeck curve - B-sulf + 8Z**
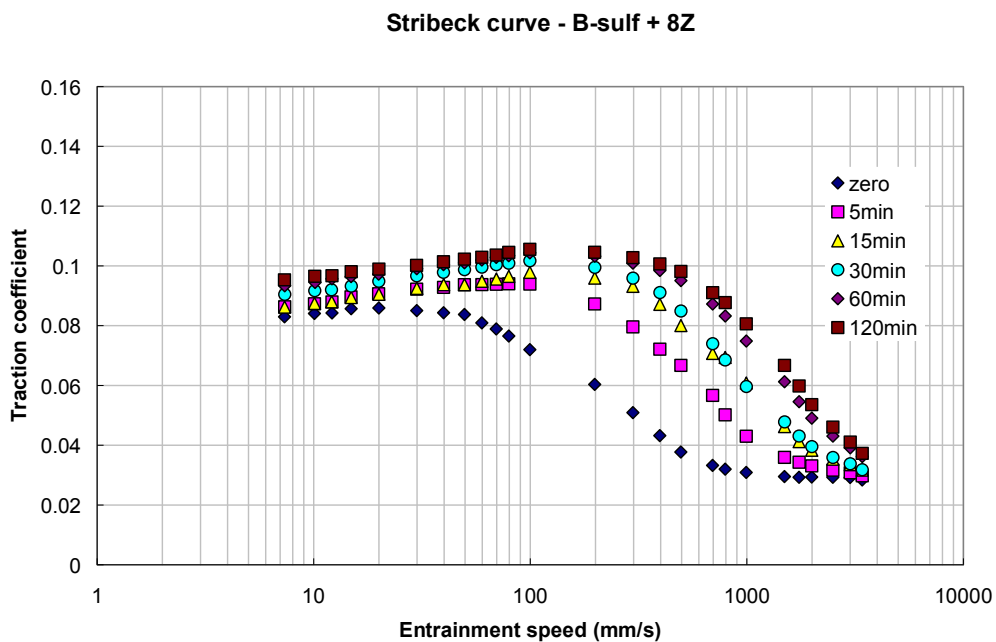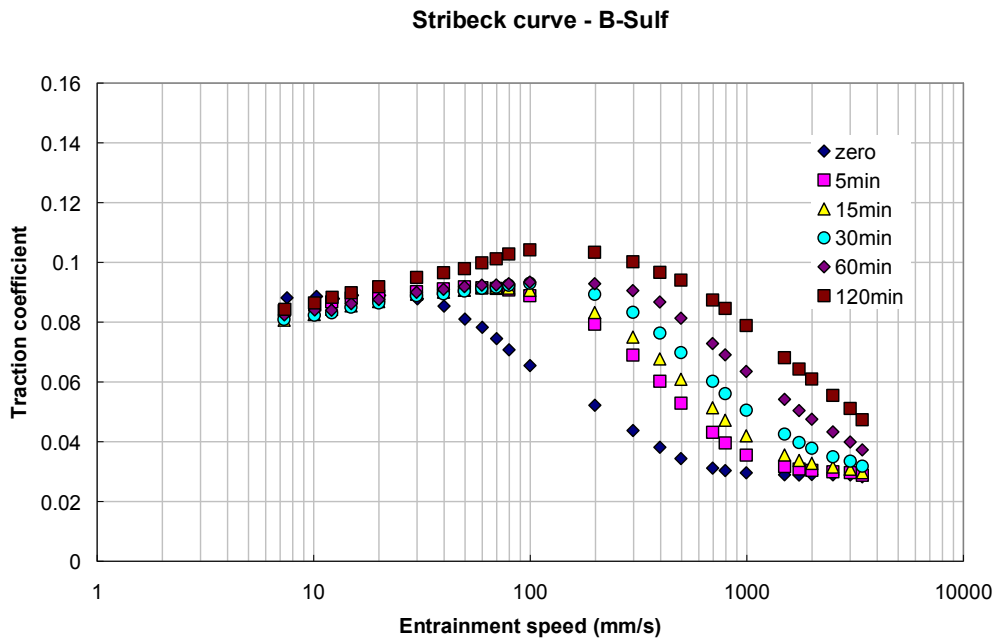


Figure 9.10 Stribeck Curves of Borated Sulfonate + ZDDP (0.08 P wt%) in Base Oil Solution

### 9.2.2.3 Salicylate

Salicylate forms thinner films than the other two detergents. However when ZDDP is added, the solution containing salicylate becomes effective in film formation. The film forming behaviour of a solution containing salicylate and ZDDP (0.08 P wt%) was almost the same as that of a ZDDP baseline solution. As shown in Figure 9.11, 9.12 and 9.13, the addition of

ZDDP greatly affects the friction of salicylate and addition of the higher content of ZDDP (0.08 P wt%) results in essentially the same friction behaviour as a typical ZDDP baseline solution. The domination of ZDDP is more obviously seen with salicylate than with the other two types of detergent.

**Stribeck curve-Salicylate**



**Figure 9.11 Stribeck Curves of Salicylate in Base Oil Solution**

**Stribeck curve-Salicylate + ZDDP (0.02%P)**



**Figure 9.12 Stribeck Curves of Salicylate + ZDDP (0.02 P wt%) Solution**

**Stribeck curve-Salicylate + ZDDP (0.08%P)**
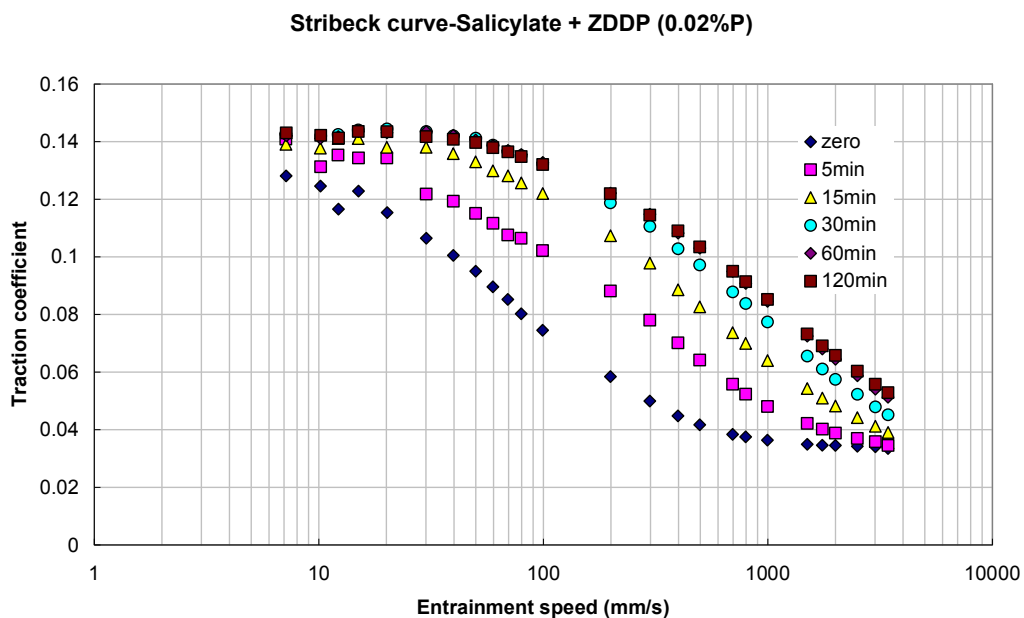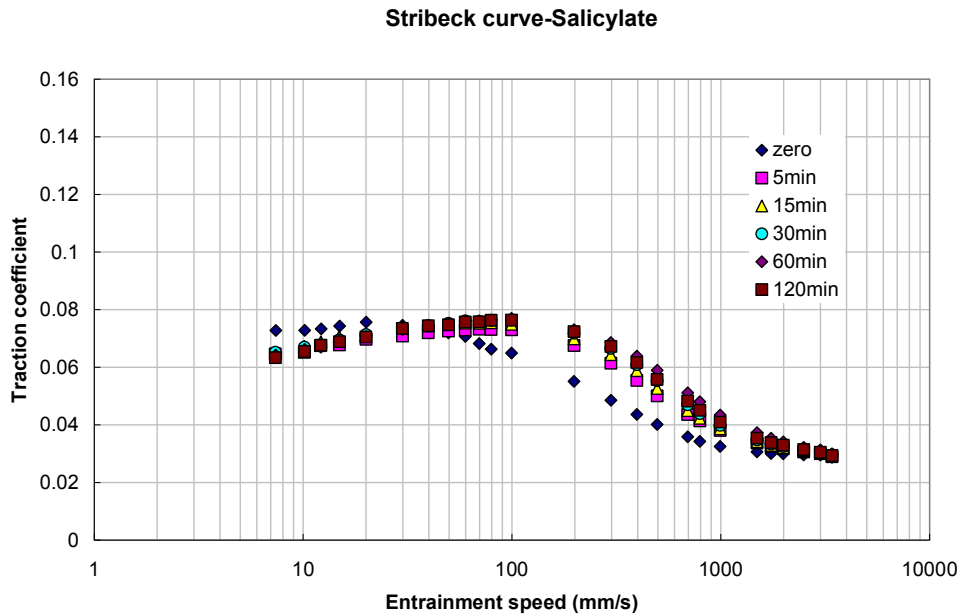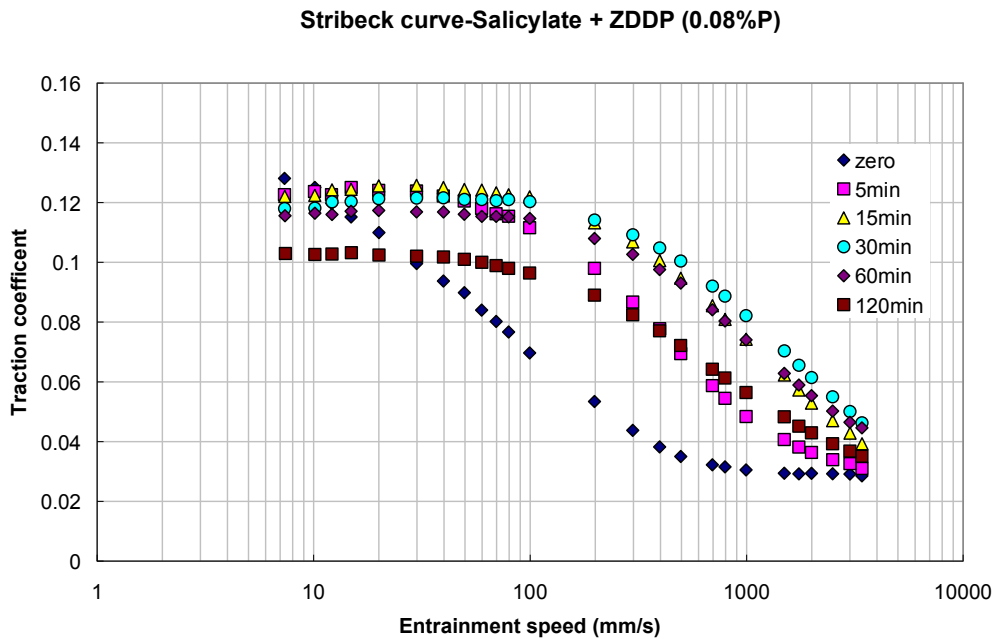
**Figure 9.13 Stribeck Curves of Salicylate + ZDDP (0.08 P wt%) Solution**

### 9.2.3 Effect of Detergents on Antiwear Properties of ZDDP

A considerable amount of research has been carried out to evaluate the effect of detergents on the antiwear properties of ZDDP, and results show that the effect can be in either synergistic or antagonistic depending on the type of detergent and the test conditions. A four-ball wear tester was employed by Rounds [195] to study the effect of detergents on ZDDP antiwear performance. The study showed that at low load, all detergents studied reduced the ZDDP antiwear effectiveness but several overbased sulfonates synergistically maintained low wear with ZDDP at higher load; TBN, type and test conditions determined whether the detergent is detrimental to ZDDP antiwear properties. Yamada *et al.* [194] found that the addition of detergent deteriorated the antiwear performance of ZDDP in a four-ball test, probably due to competitive adsorption. In his further valve train study on an overbased detergent this deterioration was even worse. However, other researchers have reported synergistic effect of detergents on ZDDP antiwear performance. Najman *et al.* [200] found the addition of a detergent resulted in substantial decrease in wear of a ZDDP solution. Shirahama *et al.* [134] also showed a beneficial effect of detergent on ZDDP antiwear performance using Falex wear and four-ball seizure tests. Cleary it needs a realistic wear test to investigate the effect of particular types of detergent on ZDDP antiwear property.

**9.2.4 Wear Tests Results of Detergents (+ZDDP) Solutions**

Exploratory HFRR tests were firstly carried out to investigate the wear properties of sulfonate solution. A resulting wear scar on the ball is shown in Figure 9.14 below. After a standard 4 hour, standard HFRR test the wear on the ball was negligible. Insignificant wear was also presented on the disc. Therefore, compared to the wear results obtained on base oil and ZDDP (presented in Chapter 8), this sulfonate proved to be very effective in wear resistance.

MTM rolling/sliding wear tests were carried out on the detergent solutions with/without the addition of ZDDP (0.08 P wt%). Some of the results are illustrated in Figure 9.15 to 9.17 and listed in Table 9.2. Results showing negligible wear produced by several additives are not presented graphically. Sulfonate solutions were also found to be highly resistant to wear under mixed rolling/sliding condition. The wear scars on the disc specimens tested in both sulfonate solutions in the presence and absence of ZDDP were too small to be measured. Nevertheless, regardless of the similarity in film formation between sulfonate and borated sulfonate, the latter showed different antiwear ability. The maximum wear depth on the MTM disc lubricated in borated sulfonate solution is 0.54 μm and the area $A_{disc\ strip}$ is 164.7 μm$^2$, corresponding to a wear coefficient of 3.05*10$^{-9}$ mm$^3$/N·m, while the maximum wear depth on the MTM disc lubricated in borated sulfonate + ZDDP (0.08 P wt%) solution is 0.74 μm and the area $A_{disc\ strip}$ is 249.7 μm$^2$, corresponding to a wear coefficient of 4.18*10$^{-9}$ mm$^3$/N·m. Unlike the above two types of detergents, salicylate itself was found to be weaker in film-forming but the film formed is still strong in protecting surfaces from wear.

Blend of salicylate and ZDDP (0.08 P wt%) presented an antagonistic response in wear resistance, since wear on the rubbing specimens lubricated by this blend was greater than the one lubricated by either of these two additives alone in base oil solution. The maximum wear depth on the MTM disc lubricated by the salicylate and ZDDP (0.08 P wt%) solution is 0.13 μm and the area $A_{disc\ strip}$ is 21.4 μm$^2$, corresponding to a wear coefficient of 7.35*10$^{-10}$ mm$^3$/N·m.

| Lubricants | $A_{disc\ strip}$ ($\mu m^2$) | Wear coefficient ($mm^3/N \cdot m$) |
|---|---|---|
| 8Z | negligible | negligible |
| Sulf | negligible | negligible |
| B-Sulf | 164.7 | $3.05 \times 10^{-9}$ |
| Sali | negligible | negligible |
| Sulf + 8Z | negligible | negligible |
| B-Sulf + 8Z | 249.7 | $4.18 \times 10^{-9}$ |
| Sali + 8Z | 21.4 | $0.74 \times 10^{-9}$ |

**<u>Table 9.2 Wear Behaviour of Different Detergent Solutions</u>**

**Note: Sulf – overbased calcium sulfonate detergent; B-Sul – borated calcium sulfonate detergent; Sali – overbased calcium salicylate detergent; 8Z – ZDDP (0.08 P wt%)**
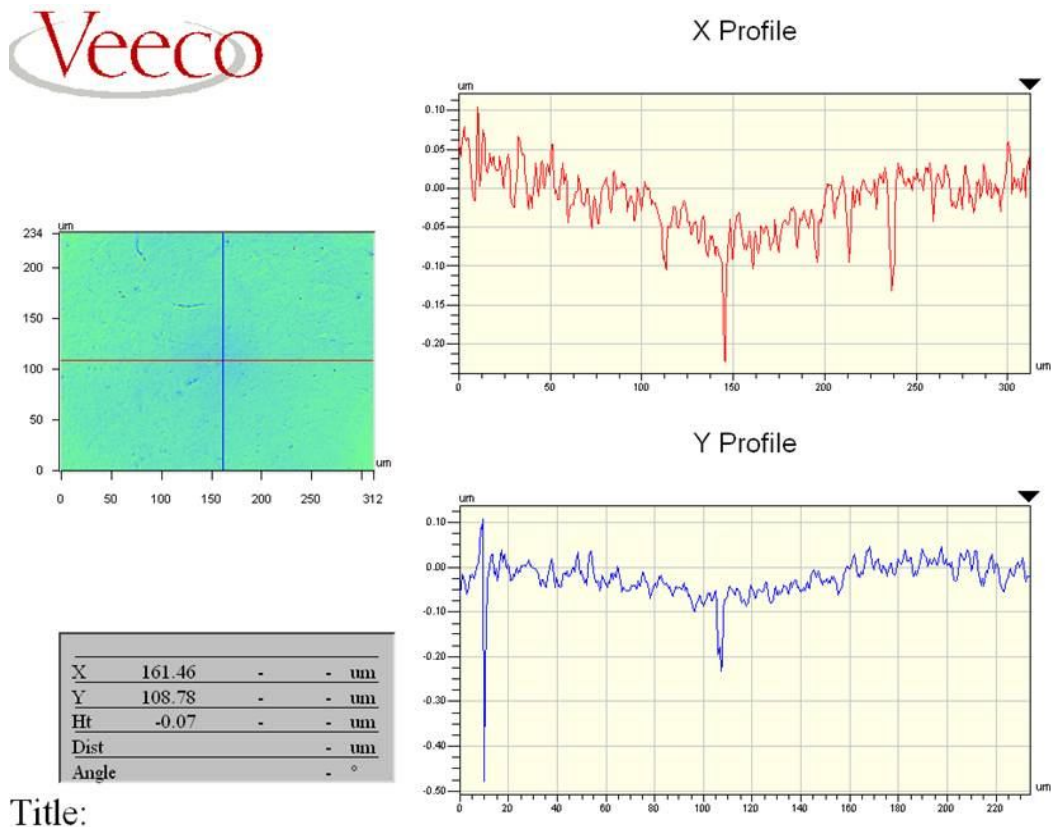


**<u>Figure 9.14 Wear Scar on the HFRR Ball Tested with Sulfonate</u>**
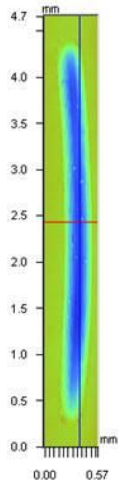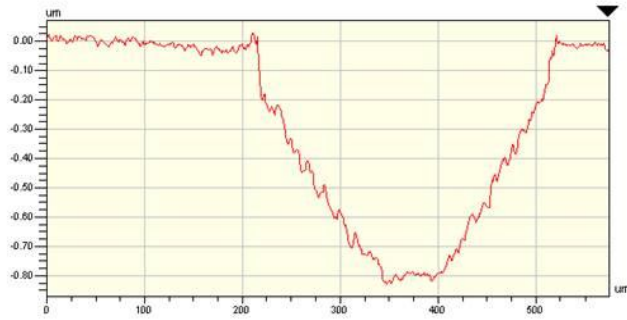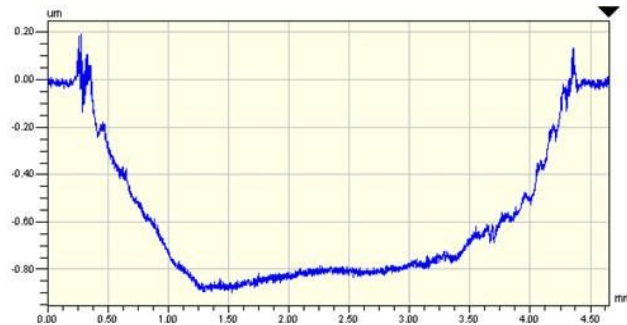
**Figure 9.15 Wear Scar on the MTM Disc Tested with Borated Sulfonate**
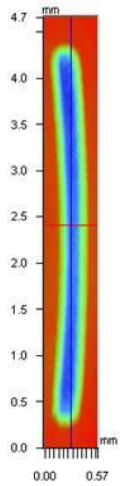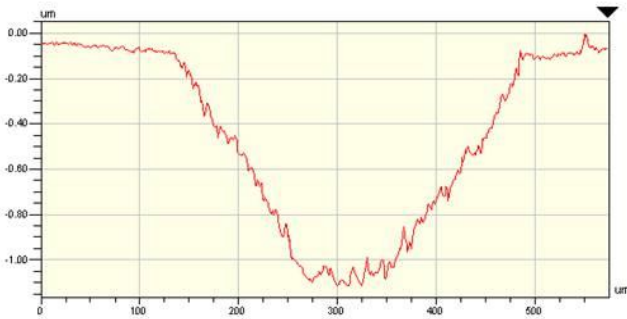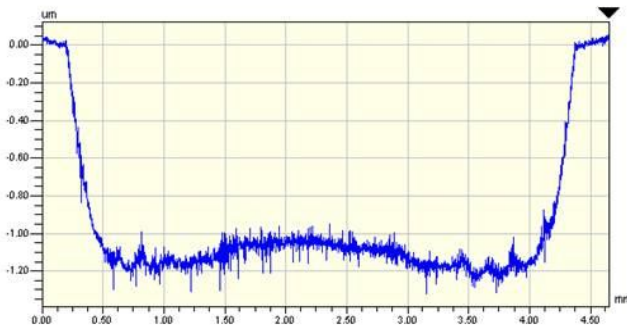


**Figure 9.16 Wear scar on the MTM disc tested with borated sulfonate + ZDDP**
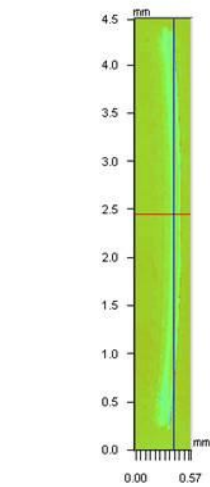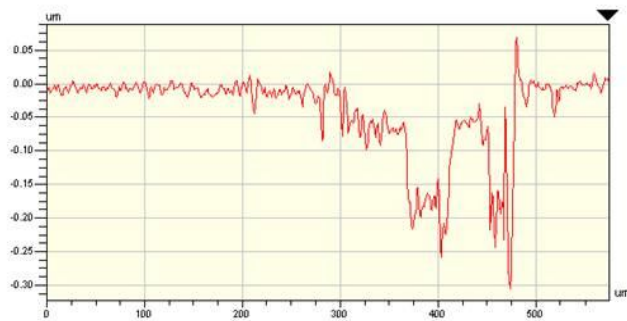
**(0.08 P wt%)**

**Figure 9.17 Wear Scar on the MTM Disc Tested with Salicylate + ZDDP (0.08 P wt%)**

### 9.2.5 Summary of Detergent Behaviour

The study shows that the tested sulfonate detergent forms thick films on rubbing surfaces as reported in previous work [193]. The film is believed to consist of calcite. The formation of the thick film corresponds to relatively high friction at intermediate speeds, similar the effect seen when ZDDP antiwear film is formed. The most likely reason for this, as suggested in previous work, is that, as the thick, rough film grows, higher entrainment speed is required to generate a fluid film thick enough to separate the contacting surfaces and thus enter EHD lubrication regime; this means that the friction curve is shifted right with the increasing test time. Meanwhile, the initial friction curve at the beginning of the test shows lower friction than that of base oil (as the initial friction curve shown in Figure 9.4 and 9.5), which indicates that this sulfonate adsorbs to reduce friction. Furthermore, it is noteworthy that this sulfonate gives lower boundary friction than mixed friction. This implies that at higher speed, the film asperities have higher shear strength than they do at low speed. This might be due to thermal effects [193] or be an intrinsic property of monolayer-thick, saturated surfactant films [201, 202].

When this sulfonate is blended with increasing concentrations of ZDDP, the rate of film formation is affected to different extents. A competition in reaching the surfaces is thought to be the reason, which is also supported by the comparison of friction behaviour of these solutions. A low speed friction increase is also observed when ZDDP is added to sulfonate solution. This low speed friction increase may result from the competition between these two additives in interacting the rubbing surface; higher concentration of ZDDP (0.08 P wt%) more likely dominates in the competition since the ZDDP antiwear film gives higher friction than that of sulfonate.

Antiwear studies show that the sulfonate is also highly resistant to wear, no matter whether it is blended with ZDDP. However, whether the film formed by sulfonate acts in the same way as ZDDP film needs to be investigated in future work.

Though borated sulfonate and salicylate are less commonly used as detergents than sulfonate, they still show noteworthy performance in film formation, friction and wear. Borated sulfonate forms similar thick films to the antiwear additive ZDDP, but blends of the two additives gives thinner films. This indicates that ZDDP acts antagonistically when added to the borated sulfonate solution; this action thus should cause more reduction in film thickness when the concentration of ZDDP is increased but in fact it does not. Otherwise there is an alternative possibility, that at higher concentration of ZDDP (0.08 P wt%), the ZDDP takes the place of initially dominant borated sulfonate on the surfaces since the film thickness firstly decreases and then increases with an increased ZDDP content. The friction behaviour of borated sulfonate solution is similar to that of the sulfonate solution, but, by contrast, it does not change much by the addition of ZDDP. Therefore, it can be assumed that the addition of ZDDP reduces the activity of borated sulfonate in film formation but does not change the outer layer of the film which is mainly formed by borated sulfonate and gives typical friction behaviour of a borated sulfonate film. Surface analysis using XPS and micro-reflectance infrared spectrometry by Willermet *et al.* [64] has observed a partial replacement of zinc in antiwear film by calcium from detergents. Wear test shows that the thick film formed by borated sulfonate is not strong in wear resistance. Based on the assumption that this layer is present in the outer layer of the film formed by the blends of ZDDP and borated sulfonate and the layer underneath partially consists of calcium polyphosphate, the reason

why the addition of ZDDP reduces its antiwear ability can be explained. However, this still needs to be further studied.

Salicylate forms thinner film than the other two detergents. The addition of ZDDP greatly affects the film formation and friction behaviour of salicylate, which indicates an obvious domination of ZDDP when blended with salicylate. This domination of ZDDP is probably due to the relatively higher activity of ZDDP than that of salicylate in interacting with rubbing surfaces. However, the thin film formed by salicylate still shows high wear resistance. The solution containing both salicylate and ZDDP (0.08 P wt%) causes more wear than either of the two additives in base oil solutions. The reason of this antagonistic response needs to be investigated in future work.

## 9.3 Friction Modifier (MoDTC)

### 9.3.1 Effect of MoDTC on Film Formation, Friction and Wear Properties of ZDDP

Friction modifiers, such as molybdenum dialkyldithiocarbamates (MoDTC), are another important type of additive commonly used in engine oils to improve efficiency. Thorough research on the mechanism by which MoDTCs reduce friction has been carried out since their initial addition to engine oils in the 1980s. The formation of tiny $MoS_2$ sheets on rubbing surfaces has been suggested by researchers [203] and is believed to be the main principle of friction reduction by MoDTCs.

The effects of MoDTC on the film formation of ZDDP have been studied through various approaches. ECR study [204] has shown that MoDTC slows down the formation of ZDDP films. This slow-down was also evident in an MTM-SLIM study [205]. Most work has suggested that the competitive adsorption of both additives towards surfaces leads to a lower rate of film formation. The study using MTM-SLIM also showed that the addition of MoDTC did not change the ZDDP film thickness much but reduced the roughness [205]. Contradictorily, using XPS measurement, Morina *et al.* stated that the film formed by a ZDDP and MoDTC solution was thinner than the one formed by a ZDDP solution. Substantial surface analyses carried out using diverse types of techniques has confirmed that the film composition changes when MoDTC is added to ZDDP-containing oils. XANES has

been applied by Kasrai *et al.* to characterize the composition of the films and has shown that the addition of MoDTC shortens the polyphosphate chains. Morina *et al.* [206, 207] employed EDX and XPS to study the films formed by blends of ZDDP and MoDTC and detected the presence of $MoS_2$. Most researchers have concurred that MoDTC reduces friction, especially in the boundary lubrication regime, when added to a ZDDP solution. The reason has been suggested to be the formation of $MoS_2$ sheets on ZDDP antiwear films.

The effect of MoDTC on the antiwear ability of ZDDP has been estimated by HFRR [205], pin-on-plate rig [207], ball-on-plane rig [208] *et al.* HFRR results have shown that wear resistance of ZDDP is reduced by the addition of MoDTC, which is in agreement with the pin-on-plate test. On the other hand, a synergistic response in antiwear performance has been found when testing an MoDTC and ZDDP solution using a ball-on-plane rig.

### 9.3.2 Test Results on Film Formation, Friction and Wear Properties of MoDTC- (and ZDDP-) Containing Oils

Film formation and friction behaviour of MoDTC solutions were tested using MTM-SLIM to explore their film forming and friction properties. As shown in Figure 9.18, film thicknesses were plotted against rubbing time. SLIM images are shown in Figure 9.19. MoDTC forms only a very thin film on the surface (thinner than 20 nm). The addition of ZDDP significantly affects the film formation behaviour, though the resulting film is still thinner than the one formed by a ZDDP solution alone (around 120 nm). This film thickness increases slightly when the concentration of ZDDP is increased. For the two solutions containing different amount of ZDDP (0.02 and 0.08 P wt%), film thicknesses after two hours rubbing were 83 and 101 nm respectively. Friction curves of the MoDTC solution are shown in Figure 9.20, in which relatively low friction was present at all speeds. Stribeck curves of the solution containing MoDTC and ZDDP (0.08 P wt%) are shown in Figure 9.21. The friction behaviour of MoDTC and ZDDP (0.02 P wt%) solution lies in between the previous two solutions. At intermediate speeds, when ZDDP is present there is still a shift to the right of the Stribeck curve during rubbing but this is mitigated by the low boundary friction. Compared to the Stribeck curves of ZDDP solutions, when MoDTC is added the boundary friction is significantly reduced, from 0.09 to 0.06. Therefore, the addition of MoDTC slightly reduces the ZDDP film thickness but, simultaneously, considerably reduces the high boundary friction of ZDDP.
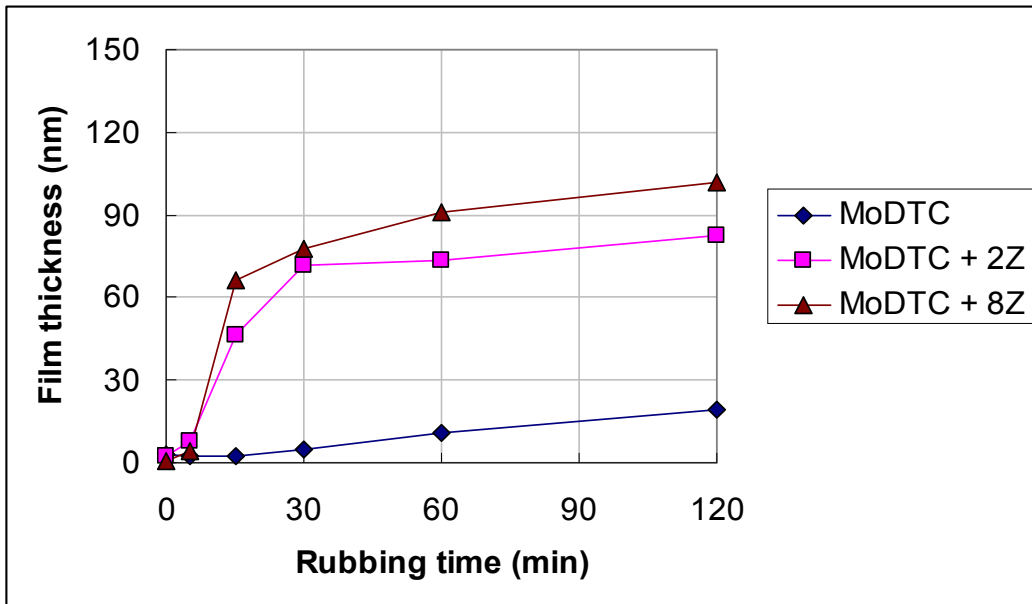
**Figure 9.18 Film Thickness of MoDTC- (and ZDDP-) Containing Solutions**



MoDTC

MoDTC + ZDDP (0.02 P wt%)
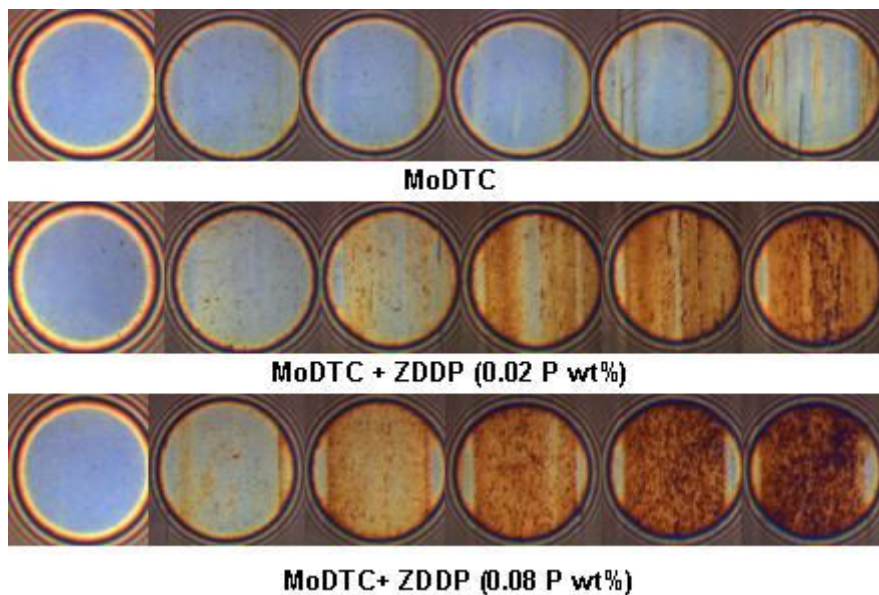
MoDTC+ ZDDP (0.08 P wt%)

**Figure 9.19 SLIM Images of MoDTC- (and ZDDP-) Containing Solutions**

**Stribeck curve-MoDTC**
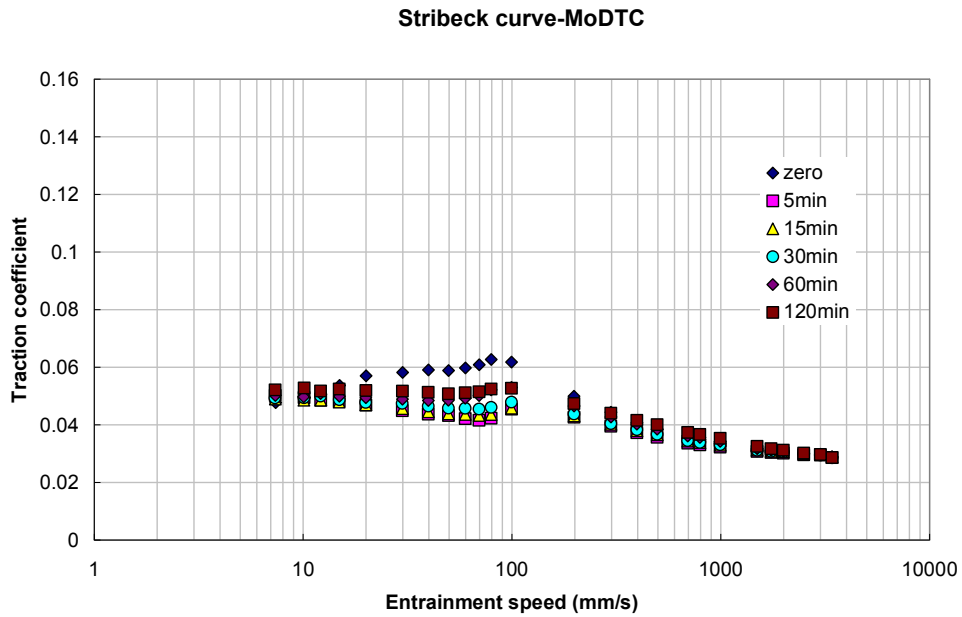


**Figure 9.20 Stribeck Curves of MoDTC Solution**

**Stribeck curve-MoDTC + ZDDP (0.08%P)**
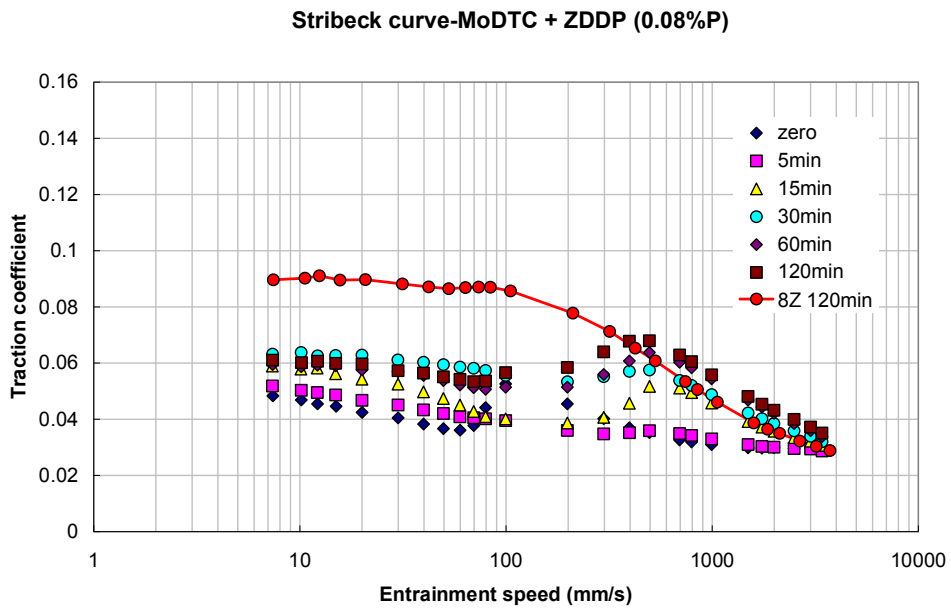


**Figure 9.21 Stribeck Curves of MoDTC + ZDDP (0.08 P wt%) Solution**

### 9.3.3 Wear properties

The MTM rolling/sliding mild wear test method was employed to investigate the wear performance of MoDTC-containing solutions in the presence and absence of ZDDP. For the MoDTC solution, mild wear was shown on the disc specimen. The area of the strip was 19.7 $\mu m^2$, corresponding to a wear coefficient of $3.96*10^{-10}$ $mm^3/N \cdot m$. Wear was further reduced

by the addition of ZDDP and the resulted area of disc strip is 10.8 $\mu m^2$, corresponding to a wear coefficient of $2.83*10^{-10}$ $mm^3/N{\cdot}m$.

To summarize, in current study, in the absence of ZDDP, MoDTC has been found to be capable of forming very thin films with significantly reducing boundary friction. The addition of ZDDP results in essentially the same film forming behaviour as a typical ZDDP baseline solution, but the friction remains very low. Wear resistance of MoDTC is reasonable and this is improved by the addition of ZDDP. Thus obvious synergistic responses are observed in film formation, friction and wear properties when ZDDP is added to MoDTC solution. According to previous studies on the interactions between ZDDP and MoDTC, this might be due to tiny $MoS_2$ sheets formed on the ZDDP antiwear films, which is also favoured by current study.

## 9.4 Dispersant + Sulfonate (+ ZDDP)

Substantial research has been carried out to study the additive-additive interactions in lubrication. Spikes [209] has reviewed these interactions and summarized several main types. However, the recent increasing use of multifunctionalized additives makes the process and mechanisms involved in these interactions more complicated to investigate.

In current study, different combinations of additives have been tested to explore the effect of ZDDP on film formation, friction and wear behaviour. MTM film thickness growths and film thicknesses formed by these blends after 2 hours rubbing are shown in Figure 9.22 and Table 9.3. As described in Chapter 7, dispersants do adsorb on rubbing surfaces but the thin layer of adsorption was not measurable with the SLIM method, so the films formed in Fig 9.22 cannot be ascribed to the dispersant component. It can be seen that EC-treated dispersant greatly reduces the ability of sulphonate detergent to form a film whereas borate dispersant has less effect.
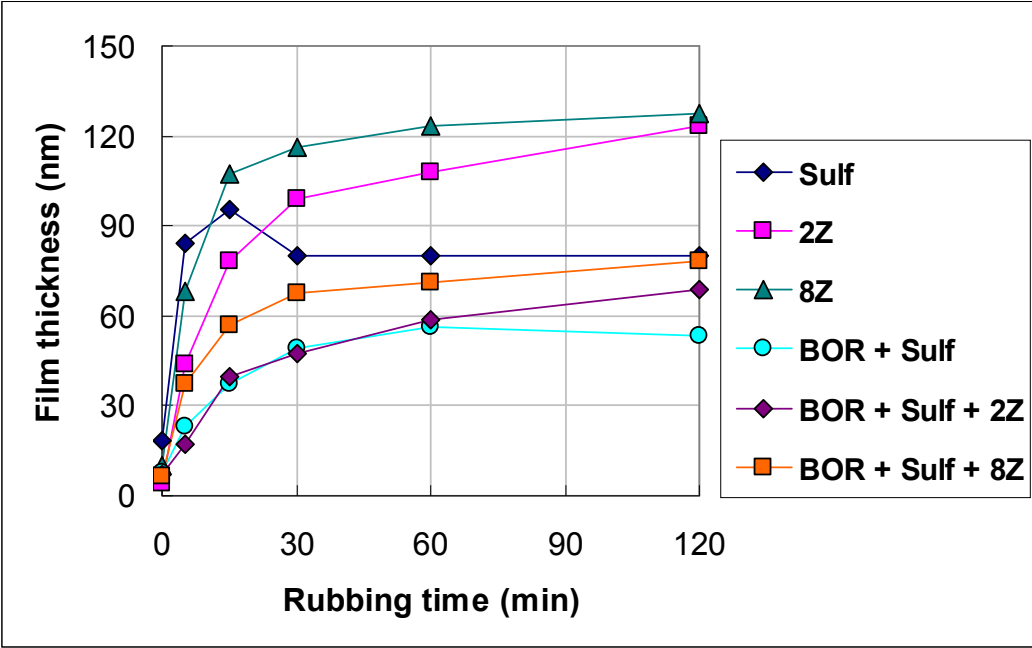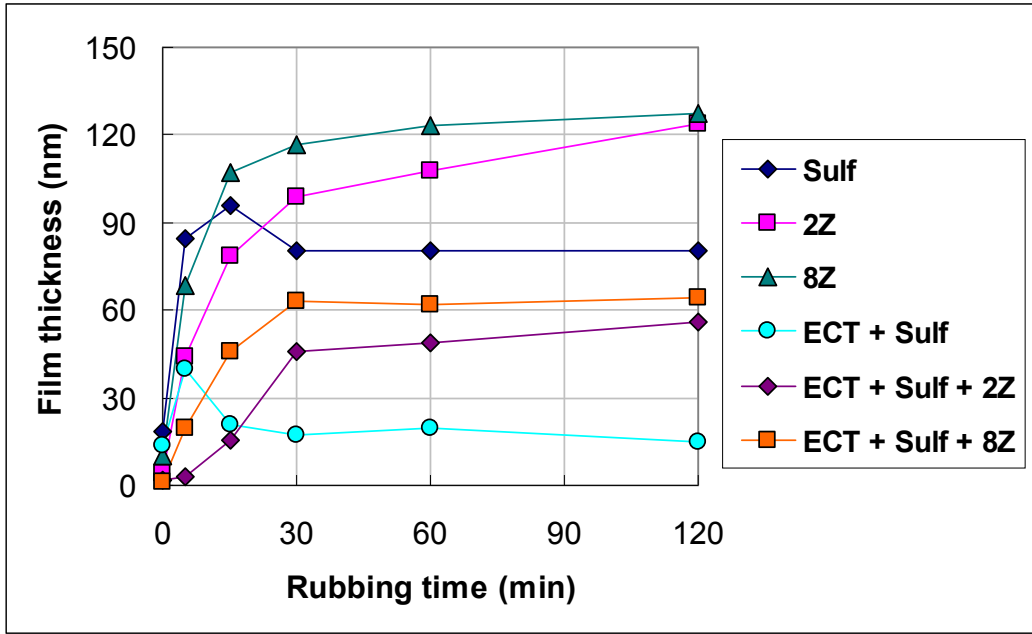
**Figure 9.22 Film Thicknesses of Dispersants + Detergents- and ZDDP-Containing Solutions**

| Additives | | Film thickness (nm) |
|---|---|---|
| ECT dispersant + Sulfonate | - | 15.0 |
| | + ZDDP (0.02 P wt%) | 55.7 |
| | + ZDDP (0.08 P wt%) | 64.5 |
| Borated dispersant + Sulfonate | - | 53.5 |
| | + ZDDP (0.02 P wt%) | 68.5 |
| | + ZDDP (0.08 P wt%) | 78.2 |

**Table 9.3 Film Thicknesses of Different Additives Combinations**

Stribeck curves are drawn to demonstrate the friction performance of these additives blended together in base oil solutions. The addition of dispersant decreased the friction of ZDDP-containing oil, as presented in Chapter 7; however, this addition contrarily increased the friction of sulfonate-containing oil compared to the latter alone in base oil. When the two additives were blended with ZDDP, friction changed a little, possibly due to the competition in film formation between sulfonate and ZDDP and the similarity of the friction behaviour of the films formed by these two additives. On the addition of ZDDP, borated dispersant presented relatively stable friction when blended with sulfonate, compared to EC-treated dispersant.
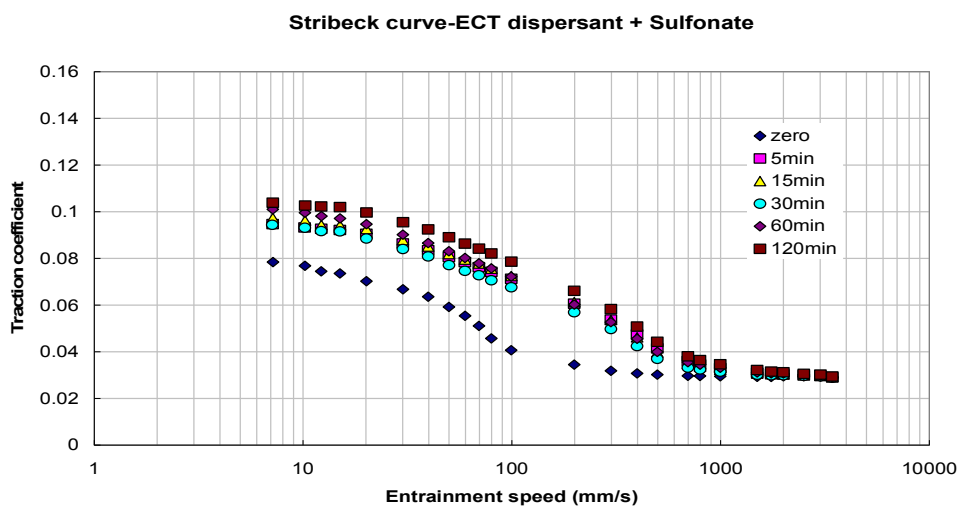


**Figure 9.23 Stribeck Curves of ECT Dispersant + Sulfonate Solution**
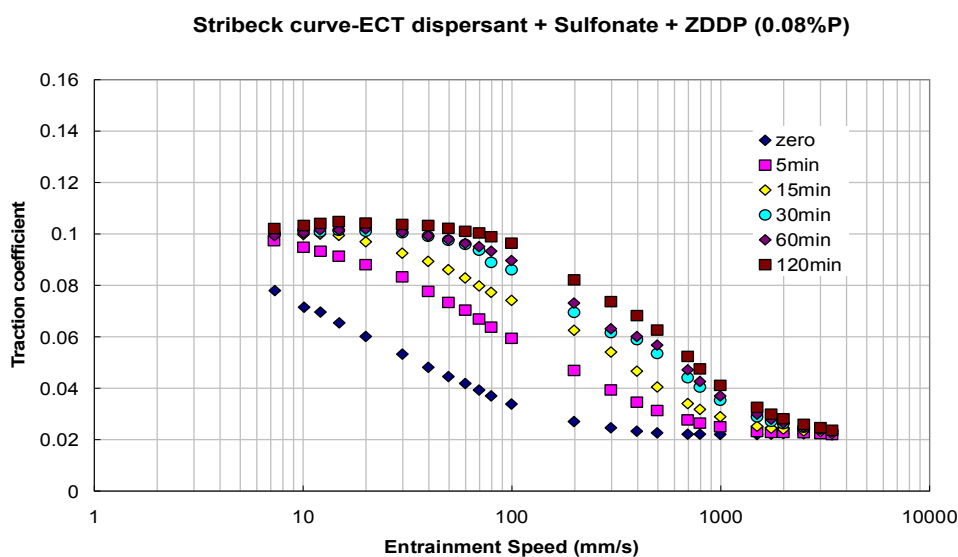


**Figure 9.24 Stribeck Curves of ECT Dispersant + Sulfonate +ZDDP (0.08 P wt%) Solution**
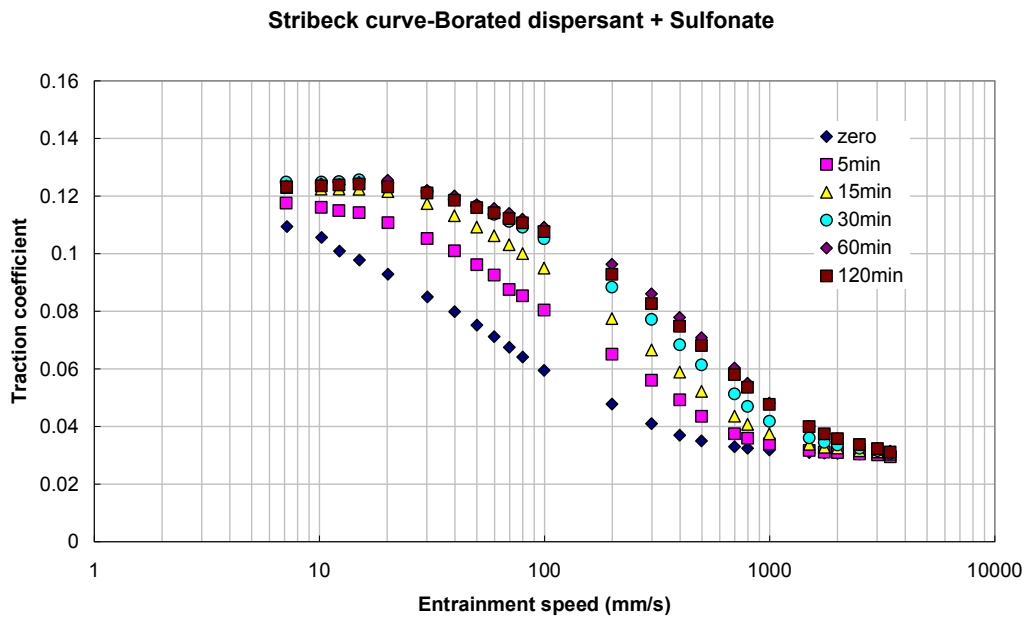
**Figure 9.25 Stribeck Curves of Borated Dispersant + Sulfonate Solution**
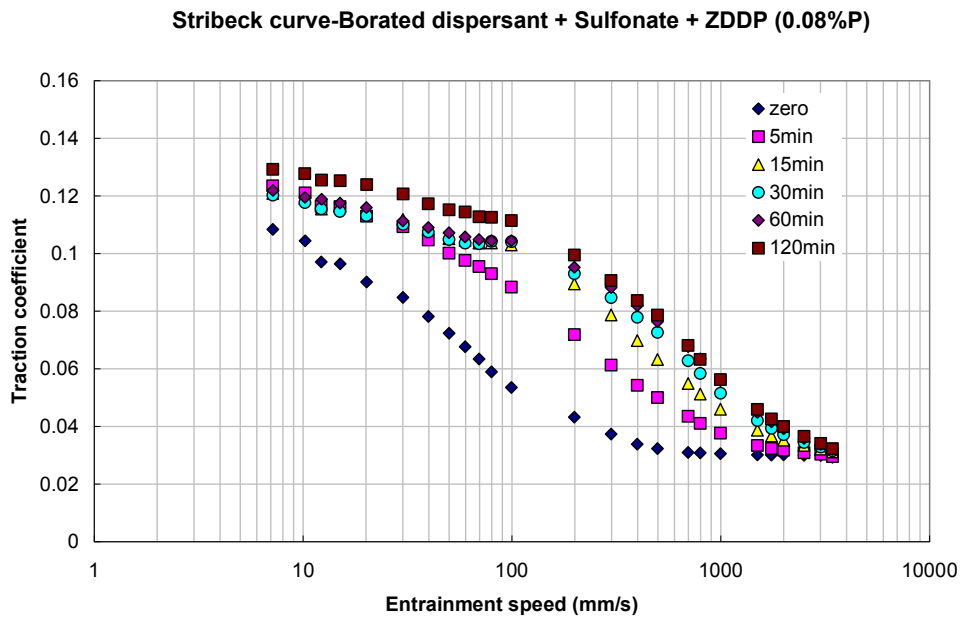


**Figure 9.26 Stribeck Curves of Borated Dispersant + Sulfonate +ZDDP (0.08 P wt%) Solution**

The wear behaviour of these additive combinations has been investigated by the mixed rolling/sliding, reciprocating MTM. Results are shown below in Figure 9.27-9.28 and Table 9.4. For the two dispersant + sulfonate solutions, negligible wear was found on the discs, which may result from the protective film formed by sulfonate, even though the film formed by EC-treated dispersant and sulfonate solution was very thin. However, this remarkable

wear resistance was decreased by the addition of ZDDP (0.08 P wt%). It seemed that an antagonism was present in wear since ZDDP is well known as an effective antiwear additive. The reason of this is not clear.

| Lubricants | $A_{disc\,strip}$ (μm$^2$) | Wear coefficient (mm$^3$/N•m) |
|---|---|---|
| ECT + Sulf | negligible | negligible |
| ECT + Sulf + 8Z | 30.9 | $6.22*10^{-10}$ |
| Bor + Sulf | negligible | negligible |
| Bor + Sulf + 8Z | 139.6 | $2.32*10^{-9}$ |

**Table 9.4 Wear Behaviour of Dispersant + Detergent + ZDDP Solutions**

**Note: Sulf – overbased calcium sulfonate detergent; ECT – EC treated dispersant; Bor – borated dispersant; 8Z – ZDDP (0.08 P wt%)**
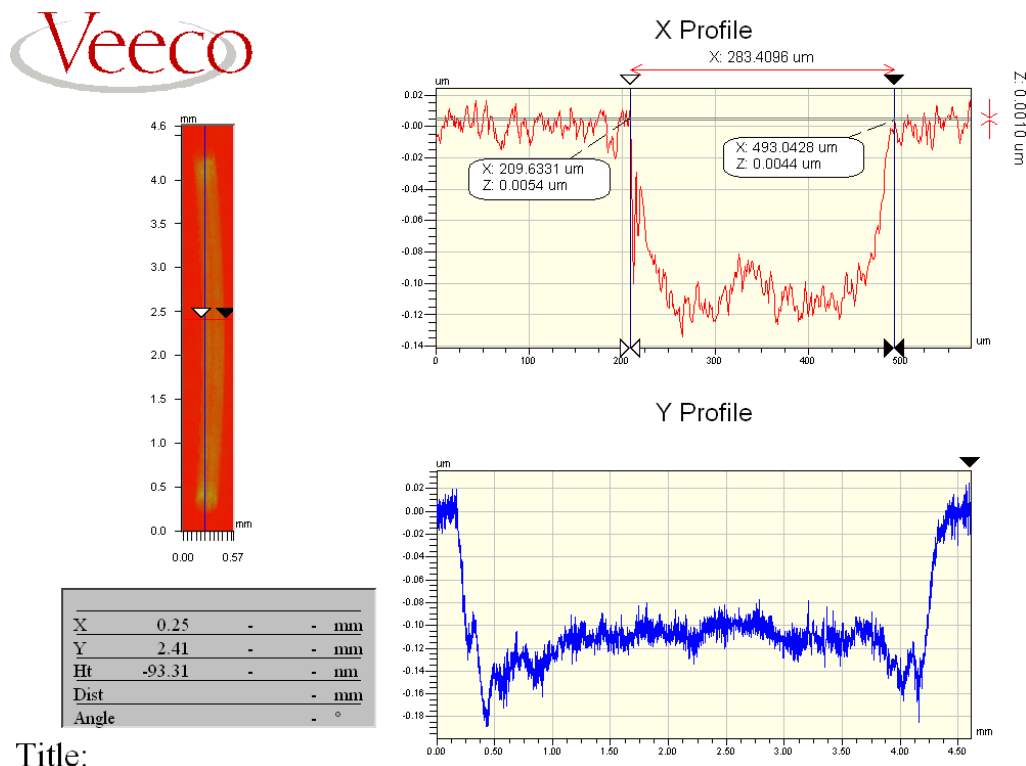


**Figure 9.27 Wear Scar on the MTM Disc Tested with ECT Dispersant + Sulfonate + ZDDP (0.08 P wt%)**
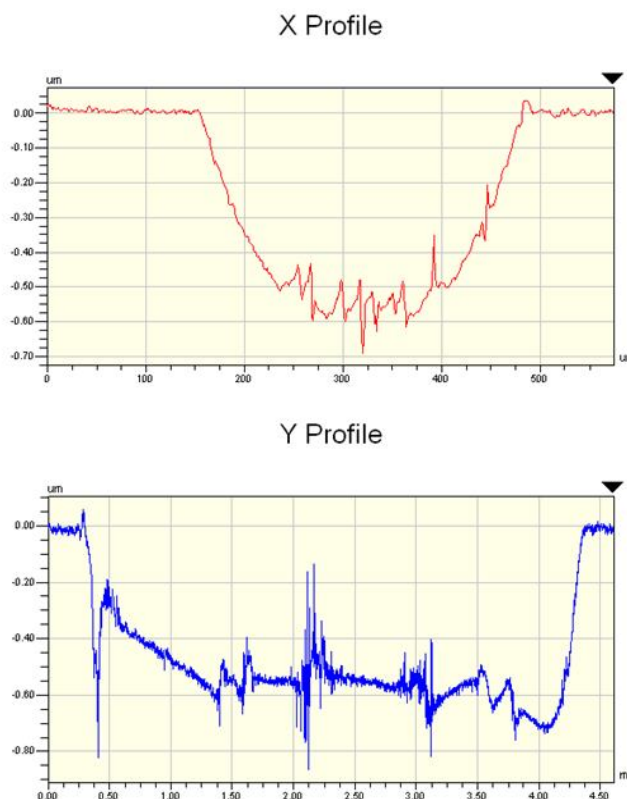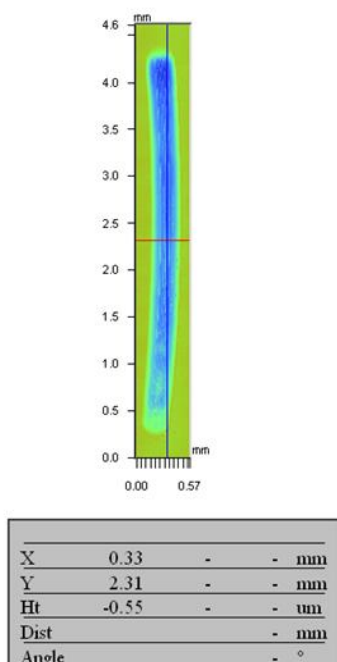
**Figure 9.28 Wear Scar on the MTM Disc Tested with Borated Dispersant + Sulfonate + ZDDP (0.08 P wt%)**

To summarize the tribological behaviour of these three additives systems requires comparison with the additives alone in solution, and combinations of any two of them. To aim at estimating the effect of other additives on the performance of ZDDP, the overall behaviour of ZDDP is employed firstly as a reference, as was described in Chapter 7 and 8. Secondly, the performance of other additives excluding ZDDP is presented. In the end, the effect of single additives or the combinations of two additives on ZDDP performance is discussed. However, the role of ZDDP in this study can be replaced by any of the other additives to investigate the interference between any two, three or more of them, which would certainly result in much more further study and this will be taken into consideration in future work.

The film thicknesses of solutions containing ZDDP, sulfonate and dispersants are plotted against rubbing time in Figure 9.29 below. The addition of sulfonate and two post treated dispersants decreases the ZDDP film thickness. Of particular interest, for a single additive the rate of ZDDP film forming and the final film thickness are more severely influenced by dispersant than sulfonate. It has been suggested that complexation and adsorption competition

174

towards steel surfaces between ZDDP and dispersants, and dispersants chemically-removing ZDDP film are the two ways by which dispersants reduce the activity of ZDDP. On the other hand, sulfonate behaves less detrimentally than dispersant in current study, though it has been reported that sulfonate diminishes the film formation properties of ZDDP. The final film thickness rather than the rate of film forming is more prominently reduced by sulfonate (though the composition of the film might also be changed). It thus seems that the effect of sulfonate on ZDDP film formation is likely to depend on their relative ability to reach surfaces. Regarding the corresponding friction behaviour, the addition of dispersant considerably increases the boundary friction, which may result from that the outer layer of ZDDP film (which is long chain polyphosphate having low friction) being chemically removed by dispersant; and short chain polyphosphate in the bulk film, which gives higher friction, being exposed. In the case of sulfonate, the bi-film formed under the interaction of ZDDP and sulfonate possesses intermediate friction between that of short chain and long chain polyphosphate layer of ZDDP film, as shown in Figure 9.30. However, the boundary friction of this ZDDP and sulfonate solution is higher than that of either of these two additives alone in base oil solution. The boundary friction is possibly dependent on the rubbing conditions, since it has been found that the friction of ZDDP solution was reduced by the addition of sulfonate in several pure sliding tests.

Interaction between dispersant and detergent is less studied. In the current study, the sulfonate film is greatly deteriorated by dispersant, not only the rate of film formation but also the film thickness, especially by EC-treated dispersant. The corresponding thinner film gives lower friction, which indicates that the thick sulfonate film gives high friction. Compared to the friction curve of sulfonate, two types of dispersants show lower high speed friction but higher boundary friction.
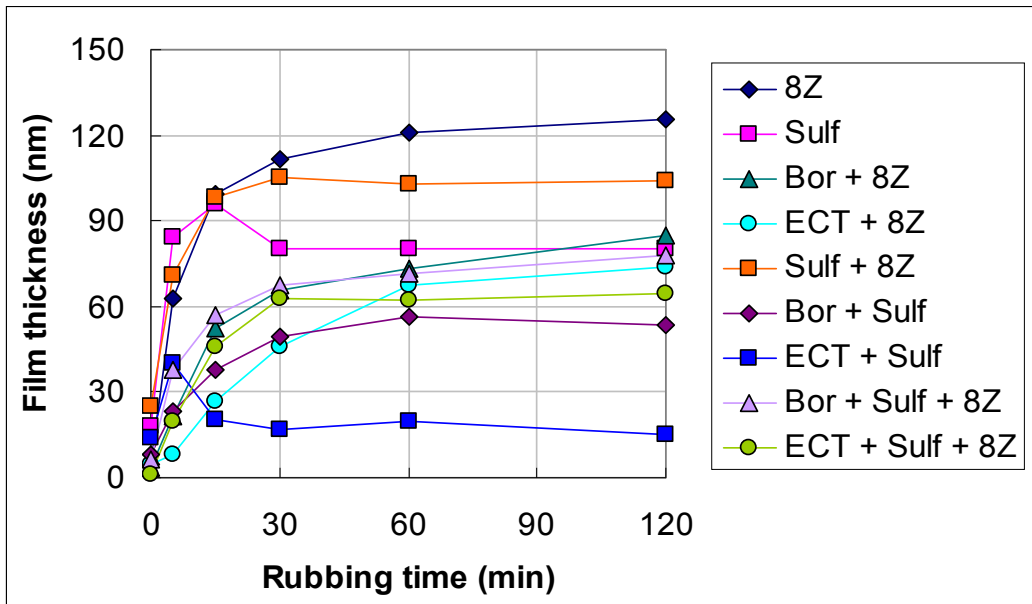
**Figure 9.29 Effect of Dispersant, Detergent on ZDDP Film Formation**
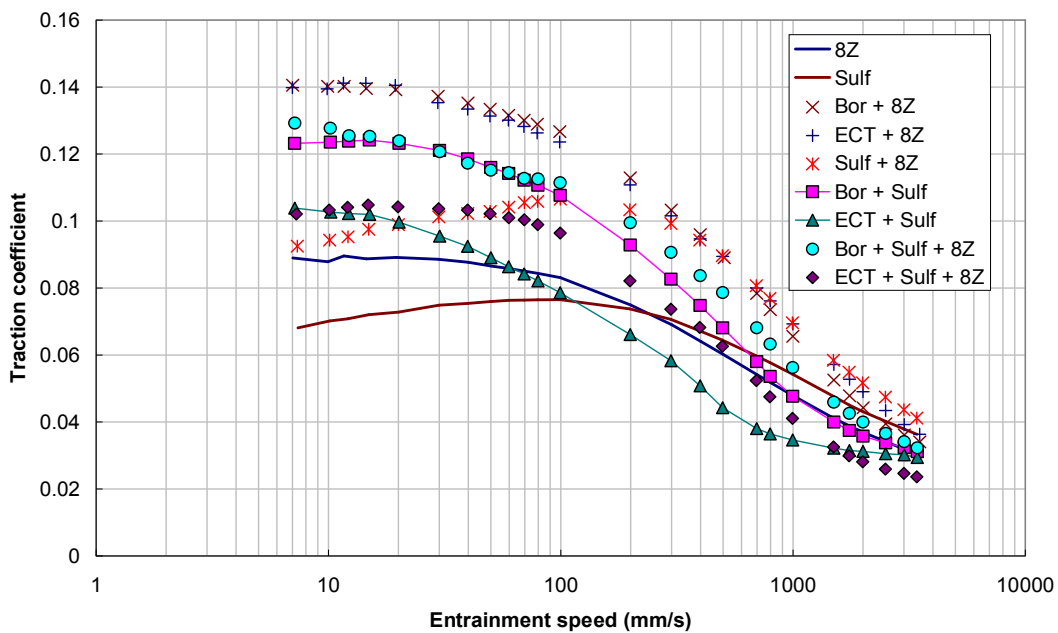


**Figure 9.30 Friction Curves of Different Additives after 2 hrs Rubbing**

To explore the effect other additives on the performance of ZDDP, friction curves of solutions containing ZDDP are selected and drawn below in Figure 9.31 and 9.32. When borated dispersant is added to ZDDP solution, it increases friction at all speeds. This might be due to the removal of outer layer of ZDDP film. Addition of sulfonate reduces ZDDP film thickness and possibly changes the composition of the film, which results in a great increase in the intermediate speed friction. The combination of borated dispersant and sulfonate seems to give combined effect on friction performance since the boundary friction is somewhere

176

between the two additives with ZDDP. This combined effect is less obvious for the EC-treated dispersant.
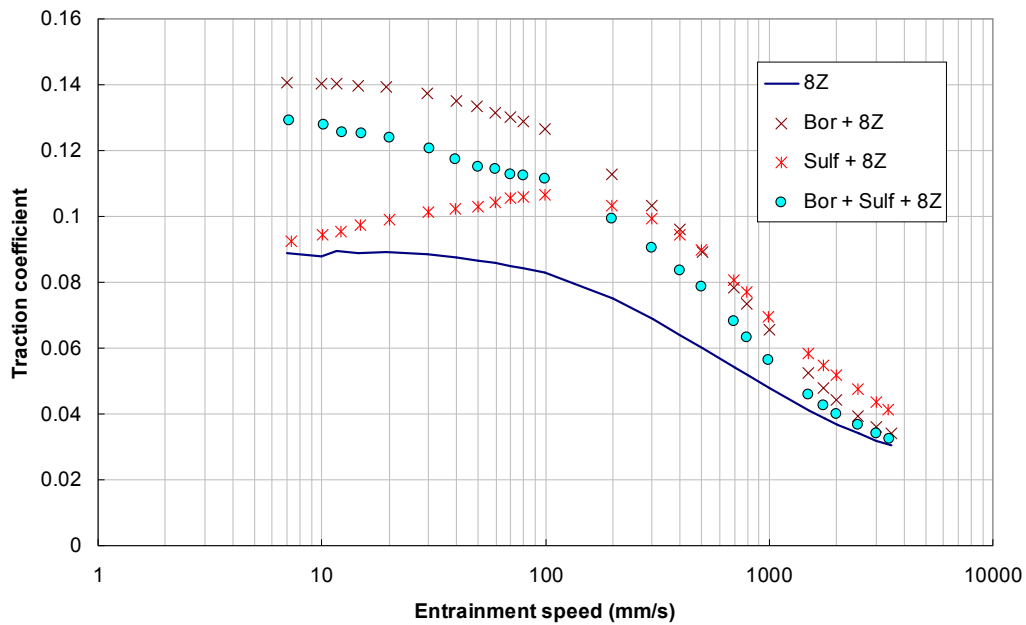


**Figure 9.31 Friction Curves of Borated Dispersant, Sulfonate and ZDDP Solutions**
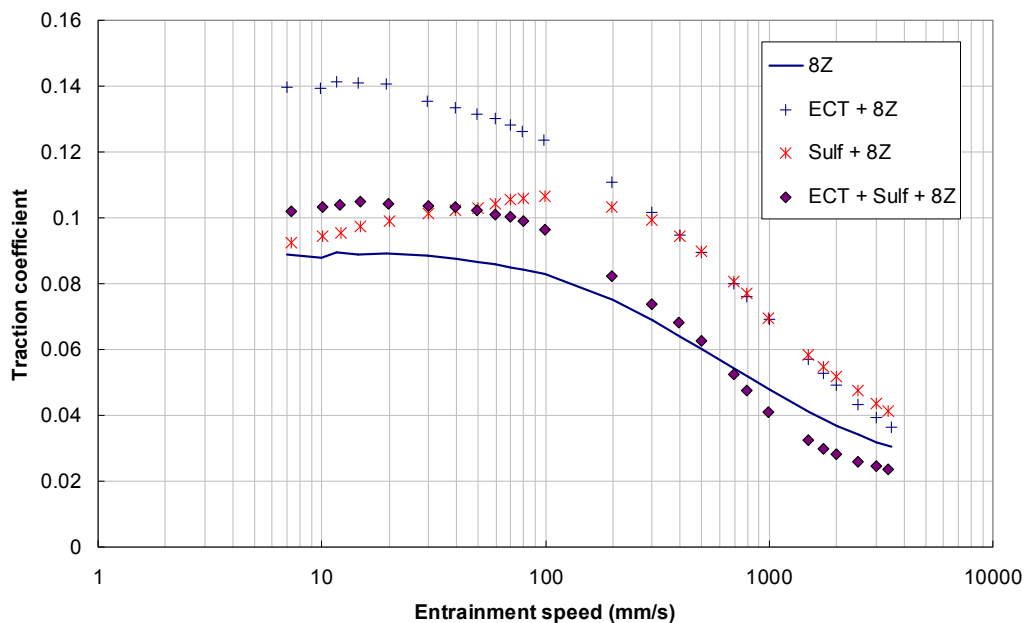


**Figure 9.32 Friction Curves of EC-treated Dispersant, Sulfonate and ZDDP Solutions**

The overall wear behaviour of these additive combinations is shown in Table 9.5. The wear caused by the solutions containing ZDDP, Sulfonate, Sulfonate + ZDDP and Sulfonate + dispersant are all negligible, which indicates that films formed by ZDDP, sulfonate and the

combinations of them are highly wear resistant. The dispersant and sulfonate solution also causes negligible wear, probably because the sulfonate film consists of calcite so its removal cannot lead to the loss of bulk material. Wear caused by solutions containing dispersant and ZDDP is believed to involve ZDDP film forming, followed by this film being chemically removed by dispersant. In this process, the chemically-removed ZDDP film consists of iron polyphosphates and possibly other components with Fe cations. Then the ZDDP film removal leads to the loss of iron from bulk material, which is another way of saying 'wear'. Therefore, considering this chemical removal, the measureable amount of wear caused by the combination of three additives is reasonable.

| Lubricants | $A_{disc\ strip}$ ($\mu m^2$) | Wear coefficient ($mm^3$/N•m) |
|---|---|---|
| Sulf | negligible | negligible |
| B-Sulf | 164.7 | $3.05*10^{-9}$ |
| Sali | negligible | negligible |
| Sulf + 8Z | negligible | negligible |
| B-Sulf + 8Z | 249.7 | $4.18*10^{-9}$ |
| Sali + 8Z | 21.4 | $7.35*10^{-10}$ |
| MoDTC | 19.7 | $3.96*10^{-10}$ |
| MoDTC + 8Z | 10.8 | $2.82*10^{-10}$ |
| ECT + Sulf | negligible | negligible |
| ECT + Sulf + 8Z | 30.9 | $6.22*10^{-10}$ |
| Bor + Sulf | negligible | negligible |
| Bor + Sulf + 8Z | 139.6 | $2.32*10^{-9}$ |

**Table 9.5 Wear Behaviour of Solutions Containing Different Additives**

**Note: Sulf – overbased calcium sulfonate detergent; B-Sulf – borated calcium sulfonate detergent; Sali – overbased calcium salicylate detergent ; ECT – EC-treated dispersant; Bor – borated dispersant; 8Z – ZDDP (0.08 P wt%)**

# Chapter 10 General Discussion

In this chapter, the film formation, friction and wear behaviour of ZDDP and dispersant solutions are discussed, the antagonistic response between these two additives is described and possible mechanisms involved are proposed. It is suggested that the antagonism occurs primarily through competition in reacting with rubbing surfaces and complexation between these two additives. Additionally, the ways that several other additives affect the performance of ZDDP-containing solutions are analyzed. Comparison of the tribological properties of these additives alone in base oil solutions, suggests that these additives act in various ways to affect film formation, friction and wear properties of ZDDP solution.

## 10.1 Discussion of the Effect of Dispersant on the Action of ZDDP

The overall behaviour of ZDDP alone in base oil solution is first discussed in this section. The relationship between the performance and the nature of ZDDP is then explored. This is followed by a similar discussion on dispersants. The effect of dispersant on ZDDP behaviour is then related to the mechanisms of antagonism between ZDDP and dispersant.

### 10.1.1 ZDDP

<u>a) Film formation</u>

ZDDP antiwear film-forming goes through a rapid stage in the first 30 minutes of each MTM-SLIM test, followed by stabilization over the remaining test time. At the end of each test, the film thickness reaches around 120 nm, even for prolonged tests. Increasing concentration of ZDDP leads to an increased rate of ZDDP film-forming but not a thicker, stabilized film. This is shown in Figure 10.1 (reproduced from Figure 7.3, Chapter 7).

**Film Thickness-ZDDP**
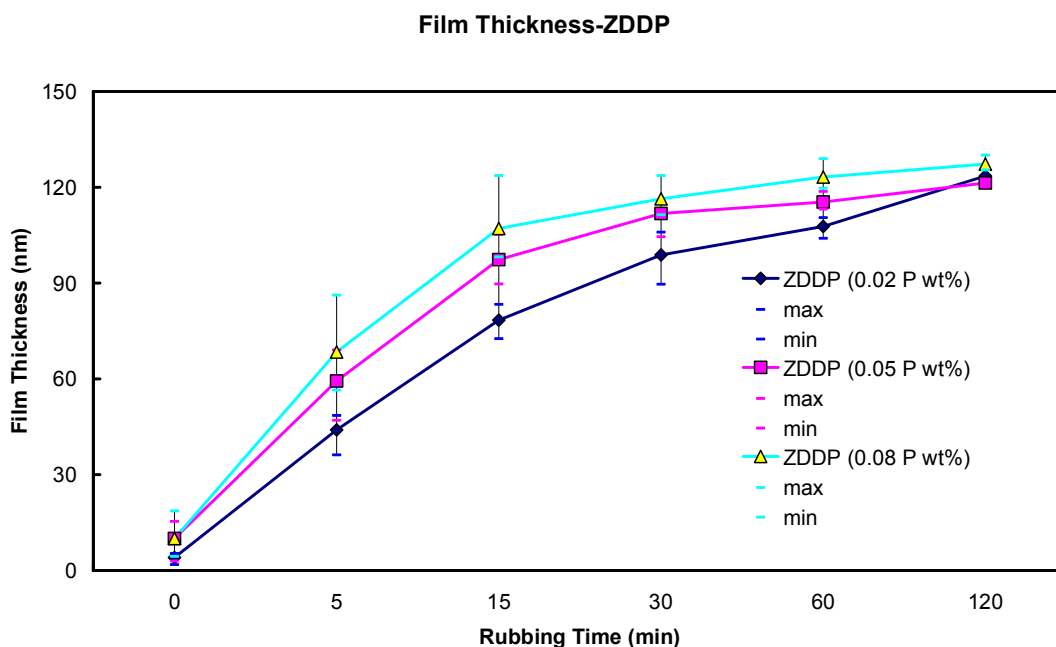


**Figure 10.1 Average Film Thicknesses of Different Concentrations of ZDDP**

Substantial literature has stated that ZDDP is very effective in adsorbing and reacting with steel surfaces to form an antiwear film [28]. This has also been confirmed by the current

study, in which the ZDDP films form rapidly. The fact that a faster film-forming rate occurs with higher ZDDP concentration suggests that higher concentration of ZDDP or its decomposition products leads either to faster adsorption on steel surfaces or faster chemical reaction as the film develops.

However, prolonged tests show that the ZDDP antiwear film does not grow any thicker than a critical value. At first sight this might result from a balance between film formation and removal. But this assumption has been eliminated by tests in which the ZDDP solution was replaced by a base oil solution after the film was formed and then rubbing resumed. This showed almost no removal of film by rubbing. Therefore the ZDDP antiwear film must possesses an inherent property under a given set of test conditions which stops the film from growing above a critical value. This has been further confirmed by rubbing the pre-formed ZDDP film in a solution containing the same ZDDP with the same solution viscosity at a lower temperature. Again the film is not removed by rubbing, indicating that ZDDP itself is not active in film removal, but only in film formation. The reason for the ZDDP film stabilising at a critical thickness may result from the diffusion of iron from the surface through the ZDDP film or within the channels separating the pads, which catalyses the film reaction. Such diffusion will depend on the thickness of film present and will become slower and eventually cease when a critical thickness is reached.

b) Friction

A rapid increase in friction coefficient was found takes place in the first 15 to 30 minutes of each test, especially in the mixed lubrication regime but also at low speed, followed by subsequent fall, at both low speeds and intermediate speeds. Higher ZDDP concentration in the range 0.02 to 0.08 P wt% leads to a shorter time to reach the maximum friction. This behaviour is illustrated in Figure 10.2 and 10.3 (reproduced from Figure 7.5 and 7.6, Chapter 7).

**Stribeck Curve-ZDDP(0.02%P)**
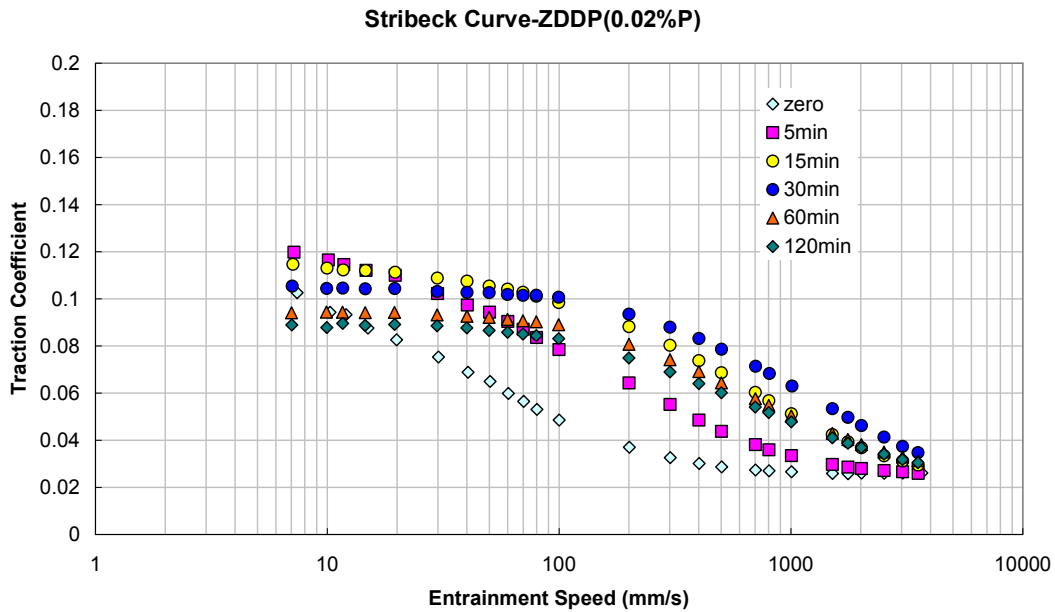


**Figure 10.2 Stribeck Curves of ZDDP (0.02 P wt%) in Base Oil Solution**

**Stribeck Curve-ZDDP(0.08%P)**
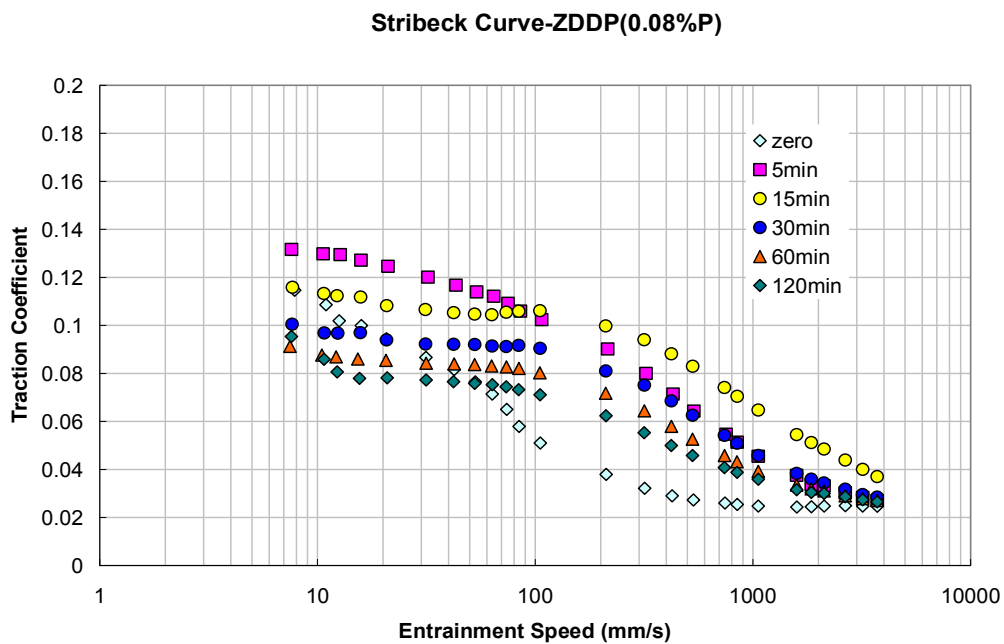


**Figure 10.3 Stribeck Curves of ZDDP (0.08 P wt%) in Base Oil Solution**

The friction increase and then decrease at low speeds may indicate by change in lubricity of the adsorbed boundary film. Initially the roughness increases and raises the proportion of load supported by asperity contact. If the adsorbed boundary films present are ineffective this will lead to a friction increase. The subsequent fall in friction may then represent the formation of a more effective adsorbed boundary films. It has been shown that for ZDDP and also ZDP solutions, straight long alkyl chain ZDDPs give lower friction than branched, short ones [111, 187]. Additionally, the ZDDP applied in current study is a secondary ZDDP derived from a

mixture of C4 and C6 alcohols. It is possible that the outer surface of the ZDDP film, which presumably determines the boundary friction, progressively changes in composition from an initially high friction form (based on C4) to a lower friction one based more on C6 alkyl groups. The fact that a solution with higher ZDDP concentration reaches highest friction faster than a lower concentration is consistent with this.

c) Wear

Wear tests using ZDDP solutions consistently confirm the very high effectiveness of ZDDP in reducing wear. Both HFRR and mixed rolling/sliding, reciprocating MTM tests showed negligible wear for solutions at all ZDDP concentrations tested. In addition, rubbing the formed film in base oil failed to remove a significant amount of ZDDP film. Therefore, ZDDP films can be recognized as being strong layers which are capable of resisting wear in base oil (or ZDDP-containing solution) under rubbing conditions.

## 10.1.2 Dispersants

In rolling contact EHL tests, it was shown that dispersants adsorb on specimen surfaces to form 5-10 nm thick layers. However these layers could not be detected using SLIM, probably because they are squashed to less than 2 nm thickness in static contact. Low and stable friction was seen for two post-treated dispersants, but not for the non-post-treated one. EC-treated dispersant increased wear when added to a base oil solution. There is very little, if any, published work on the friction and wear properties of dispersants alone in base oil solutions and the reason why they give this friction behaviour and increased wear are not obvious.

## 10.1.3 Lubricants Containing both ZDDP and Dispersant
a) Film formation

The rate of ZDDP film-forming was decreased by the addition of different types of dispersants. This decrease was dependent on the concentration of both ZDDP and dispersant, with the N/P ratio and the overall N content both influencing the film thickness. Extremely high concentrations of dispersant stopped any measureable ZDDP film from forming.

This general tendency, that film formation is reduced when either dispersant is increased or ZDDP content is reduced, is captured by the effect of N/P ratio and suggests a possible complexation of dispersant and ZDDP (or its decomposition products) in solution. The fact

that excessive dispersant (0.3 N wt%) in the ZDDP solution leads to no measurable film being formed on the rubbing surfaces suggests adsorption competition with dispersant adsorption blocking ZDDP from the surfaces. However the effect on ZDDP film formation of the three types of dispersants differs in extent. EC-treated and borated dispersants reduce the film-forming rate and film thickness less severely than non-post-treated dispersant, which may indicate that post treating reduces the complexation between the two additives. Since these treatments weaken the activity of the N atoms in dispersant by bonding them to ethylene and boron groups, this suggests that ZDDPs complex with dispersant, at least in part, through the bonding between N atom from dispersant and an atom from ZDDP (presumably Zn or P), as suggested in the study carried out by Shiomi [136] and Inoue [131]. Figure 3.17 and 3.18 showing possible complex structures are reproduced here as Figure 10.4 and 10.5.
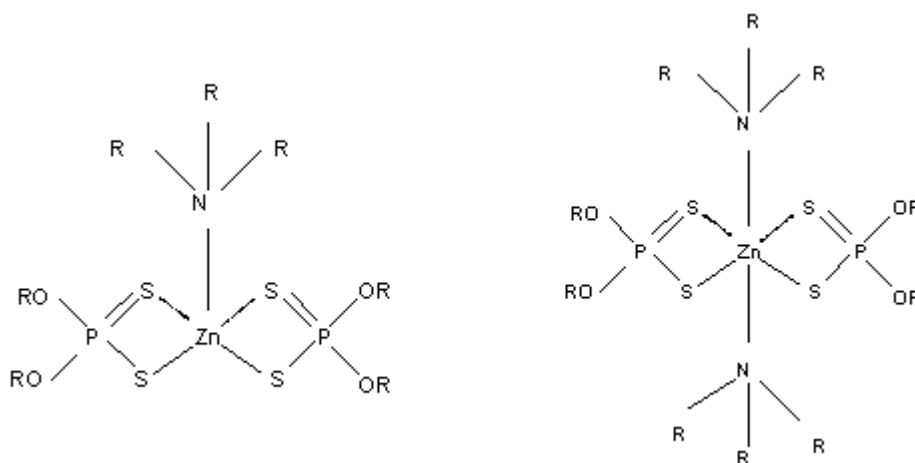


**Figure 10.4 Structures of Complex of ZDDP and Amine 1:1, complex of ZDDP and Amine 2:1 [136]**
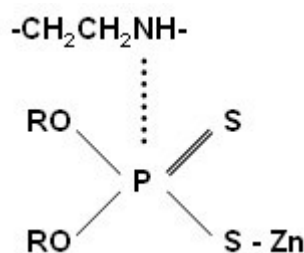


**Figure 10.5 Complexation between ZDDP and dispersant through N-P bonding [131]**

b) Friction

At first the friction behaviour of a solution containing both ZDDP and dispersant is almost the same as that of the dispersant alone. However friction increases once a ZDDP film starts

to form and it keeps increasing with the growth of this film on the rubbing surfaces. The increase in friction is slower than for ZDDP alone.

The friction behaviour of solution containing ZDDP and dispersant is believed to represent the combination of the friction behaviours of ZDDP and dispersant alone in solution. Increase in friction at intermediate speeds as seen in Figure 10.6 (reproduced from Figure 7.15 a)) results from rough ZDDP film formation. This is influenced by dispersant in so far as the dispersant reduces the thickness and thus roughness of the pad-like ZDDP films (*e.g.* Figure 10.7 reproduced from Figure 7.14 a)).
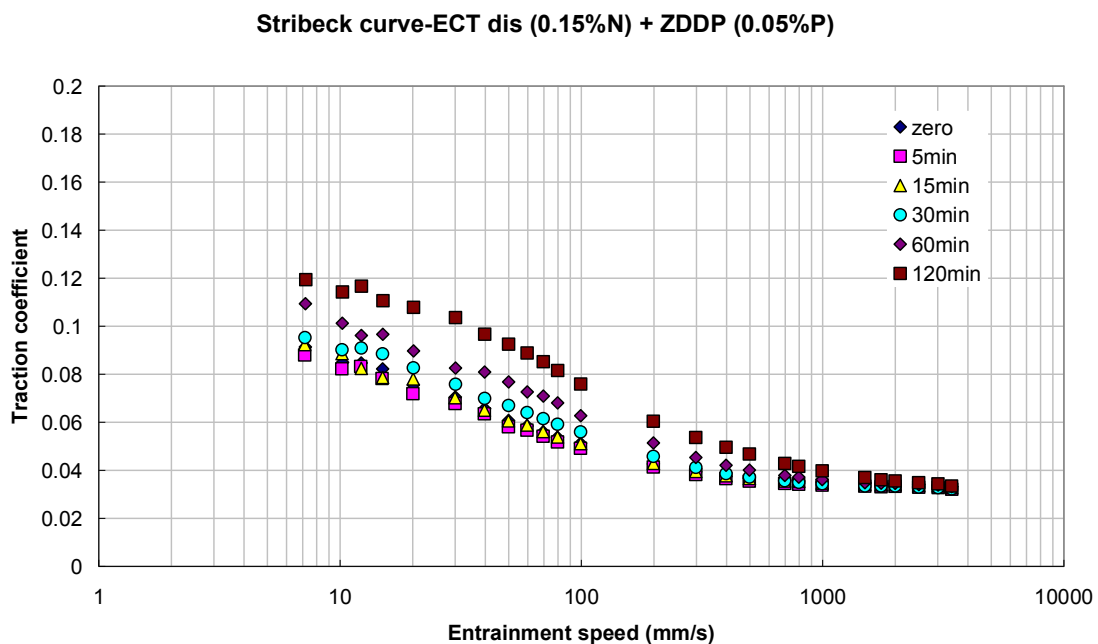


**Figure 10.6 Stribeck Curves of Solution Containing ZDDP (0.05 P wt%) and Dispersant (0.15 N wt%)**
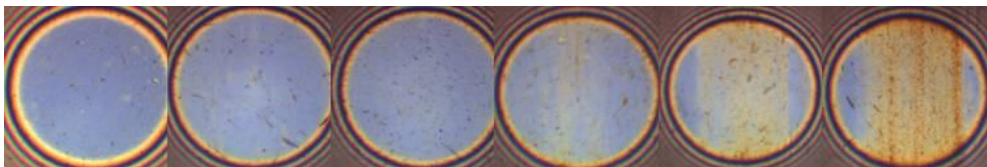


**Figure 10.7 SLIM images of solution containing ZDDP (0.05 P wt%) and dispersant (0.15 N wt%)**

For ZDDP alone in base oil solution, boundary friction behaviour is believed to represent a change in composition of the alkyl groups in the outermost part of the film. It is suggested that, after a period of film-forming, the chain length of the outer film may be greater than that

of the initially-formed film, which results in the reduction of friction. However, research has reported that in the presence of dispersant, the chain length of the polyphosphate (which is believed to be the main composition of ZDDP film) is reduced. In current study, only an increase in boundary friction is seen, which is in concert with this previous findings. Alternatively the film formed by solutions containing both ZDDP and dispersant may have shorter adsorbed hydrocarbon chains or be more branched than the film formed by ZDDP alone.

c) Wear

Wear rate varies with the P and N content for blends containing both ZDDP and dispersant, but the effect of N/P ratio shows no regular trend. There is, however, a clear trend when P content is fixed, which is that an increase in N content leads to the increase in wear rate. By contrast, changes to P content have little effect on wear at a fixed N content.

The small effect of P content on wear when N content is fixed implies that the ZDDP film is effective in protecting rubbing surfaces from wear even if this film is very thin, since thicker films formed by higher P content solution do not reduce the wear rate further. Moreover, this film, no matter whether it is thin or thick, can be removed by reacting with dispersant in solution, but re-forms rapidly and largely independently of P concentration. Alternatively, the fact that dispersant increases wear may be explained in terms of the dispersant reacting with ZDDP film, which probably consisting mainly of iron polyphosphates, resulting in loss of iron and thus wear. The rate of this iron loss and thus the wear rate increases with dispersant concentration. Wear performance of these ZDDP and dispersant solutions most likely depends on the way the film is formed and removed by dispersant.

**10.1.4 Effect of Dispersants on Pre-formed ZDDP Film**
a) Film thickness

All three types of dispersants employed in the current study partially remove a preformed ZDDP film, regardless of their concentration. The different dispersants remove ZDDP films to slightly different extents. A reduction in ZDDP film thickness is also observed after the lubricant is changed to a dispersant-containing one and then simply heated to test temperature.

The partial removal of ZDDP film by replacing lubricant and heating is observed for all these tests, which implies a complexation between dispersants and the outer layer of ZDDP film on the rubbing surfaces, followed by dissolution. The different levels of partial removal of ZDDP film by dispersants imply different extents of protection of N atoms by post-treatment. It has also been reported that, with different ZDDPs and dispersants, the extent of film removal varies with the nature of both ZDDP and dispersant [149]. Since it has been shown that the outer layer of ZDDP films consists predominantly of long chain polyphosphates with short chain ones in the bulk, it is probable that the removed part of film is mostly long chain polyphosphate. This assumption is supported by the effect of dispersant on ZDDP boundary friction.

b) Friction

When pre-formed ZDDP films are lubricated by dispersant solution, friction coefficient transition smoothly from the fluid lubrication regime to the mixed and boundary lubrication regime as the entrainment speed is reduced, which is similar to the dispersant alone in base oil solutions.

However, the friction is slightly higher than that produced by the corresponding dispersant oil, and it is also slightly different from the friction behaviour of a stabilized ZDDP film. Therefore, the overall friction behaviour is believed to be a combination effect of both the ZDDP film and the dispersant. Nevertheless, boundary friction after the replacement of lubricant is slightly higher than that of a stabilized ZDDP film. According to the relation between friction performance and different ZDDP film composition, this supports the assumption that dispersant removes the outer layer of ZDDP film which is believed to be long chain polyphosphates, and leaves the short chain polyphosphates exposed.

To summarize, the effects of dispersant on the tribological properties of ZDDP can be categorized into:

- The film thickness of a solution containing both ZDDP and dispersant is strongly dependent to the N/P ratio. Post treatment of N atoms in dispersant reduces the effect of dispersant on ZDDP film thickness.

- A reduction in film thickness occurs when ZDDP solution is replaced by a dispersant one and heated, as well as during subsequent rubbing process. (However, rubbing in base oil does not remove the stabilized ZDDP film).

- Extremely high contents of dispersant (0.3 N wt%) stop the ZDDP film forming.

## 10.2 Discussion of the Effect of other Additives on the Behaviour of ZDDP

### 10.2.1 Detergents

Overbased calcium sulfonate

Overbased calcium sulfonate detergents form thick films on rubbing surfaces, which are believed to consist of calcite [193]. This film has the effect increases intermediate speed friction, similar to the effect seen when a ZDDP antiwear film is formed. It has been suggested that, as the thick, rough calcite film grows it requires a higher entrainment speed to generate a thick fluid film to separate the contacting surfaces [193]. The initial boundary friction of this sulfonate solution is lower than that of the base oil, which indicates an effective adsorption and a friction reduction property of the detergent molecules. The boundary friction also increases with speed to reach a maximum before mixed lubrication ensues. This implies that the adsorbed films of detergent on the asperities have higher shear strength at high speed than they do at low speed.

A competition in reaching the rubbing surfaces is believed to be the main interference mechanism between this sulfonate and ZDDP when a sulfonate + ZDDP solution is tested. ZDDP at higher concentration (0.08 P wt%) dominates in this competition so the friction behaviour tends to be more similar to the behaviour of the ZDDP. Regarding wear, the sulfonate detergent is highly resistant to wear no matter whether it is blended with ZDDP, suggesting that the calcite film protects against wear.

Overbased borated calcium sulfonate

Overbased borated calcium sulfonate forms a thick film but acts antagonistically to ZDDP in film formation with mixtures of the two additives forming thinner films than the separate additives. The friction behaviour of the sulfonate solution is not changed much by the addition of ZDDP, which implies a combined effect of films formed by these two additives. It

suggests that the outer layer of the film formed by borated sulfonate and ZDDP solution is quite similar to the one formed by borated sulfonate alone, since the addition of ZDDP reduces film thickness but does not affect friction much. Wear tests show that the film formed by a borated sulfonate solution is not strong in wear resistance. This matches the assumption that the outer layer of the film formed by the mixture is similar to the one formed by borated sulfonate alone, which is weak in antiwear properties compared to a ZDDP film.

Overbased calcium salicylate

Overbased calcium salicylate forms thinner film than the other two detergents. The friction and film formation properties of salicylate solution are greatly affected by the addition of ZDDP which indicates a relatively higher activity of ZDDP than that of salicylate. However, the thin film formed by salicylate is still capable of protecting rubbing surfaces from wear. The solution containing both salicylate and ZDDP (0.08 P wt%) gives more wear than either of the two additives in base oil solution alone. The reason for this antagonistic response is not clear.

## 10.2.2 MoDTC

MoDTC forms very a thin film with a significant boundary friction-reducing effect. The tendency of film formation of a ZDDP and MoDTC-containing solution is almost the same as that of a typical ZDDP solution. However, friction stays at a low value level over a wide range of speeds. This advantageous response between MoDTC and ZDDP is believed due to the tiny $MoS_2$ sheets formed on the antiwear film. The antiwear performance of MoDTC is reasonable, and can be improved by the addition of ZDDP.

## 10.2.3 Dispersant + Detergent

The way that dispersants interact with ZDDP appears to be largely chemical, such as by complexation in solution and on surfaces, with dispersant chemically removing ZDDP films. By contrast, the sulfonate detergent probably mainly affects the ZDDP performance through adsorption competition. There is a noteworthy difference in the impact of detergent and dispersant on the boundary friction of ZDDP films. The addition of dispersant to ZDDP solution considerably increases boundary friction, which may result from partial ZDDP film removal to form a ZDDP film with different outer film composition. By contrast, the friction

of ZDDP solution is reduced by the addition of sulfonate, probably because of adsorption of the long alkyl chain detergent molecules on the film surface.

The addition of a combination of both dispersant and detergent to ZDDP reduces the ZDDP film thickness to different extents, as well as the rate of film formation. Friction of a borated dispersant + sulfonate + ZDDP (0.08 P wt%) solution is higher than that of ZDDP solution at all speeds, while EC treated dispersant gives slightly different friction behaviour. These tribological phenomena caused by three-component systems are more complicated to explain compared to two-component systems and still remains unresolved.

Solutions containing ZDDP, sulfonate, sulfonate + ZDDP and dispersant + sulfonate are all highly wear resistant, presumably due to the films formed by the ZDDP and overbased sulfonate. On the other hand, blends of dispersant and ZDDP in solution produces more wear, probably involving a ZDDP film forming and then being chemically removed by dispersant. In this process, the chemically removed (outer layer of) ZDDP film consists of iron polyphosphates with possibly other components including Fe cations, so that the film removal leads to the loss of iron from bulk material and thus wear. Therefore, a considerable amount of wear also can be seen in the three-component additive systems.

# Chapter 11 Conclusions and suggestions for future work

This chapter summarizes the conclusions which can be drawn from the results obtained in this study. It briefly describes the advantages of the newly-developed mild wear test method, and outlines the effect of dispersants and other additives on the tribological properties of ZDDP. In the end, based on the work completed in this study, some suggestions for further research are proposed.

## 11.1 Conclusions

### 11.1.1 New Mild Wear Test Method Development

A newly developed mild wear test method is described, with the following conclusions drawn:

1. Reciprocating MTM repeatedly and reliably produces localized, mild lubricated wear.

2. The combination of Wyco SWLI with EDTA treatment has proved to be accurate and convenient to measure mild wear produced by HFRR and the reciprocating MTM with ZDDP-containing oils.

3. This mild wear test method is not only capable of characterizing wear resistance of different lubricants but can also provide detailed relationships between wear and several other test parameters *e.g.* speed.

### 11.1.2 Effect of Dispersant on Friction, Film Formation and Wear Properties of ZDDP

The tribological behaviour of ZDDP- and dispersant-containing baseline lubricants and the effect of three types of dispersants on the ZDDP performance have been investigated. Notable conclusions are:

1. The secondary ZDDP employed in current study is active in film forming and effective in protecting rubbing surfaces from wear. Boundary friction behaviour and the shifting of Stribeck curves along with test time are the two friction responses of ZDDP generally observed.

2. Dispersants can act as weak boundary lubricating additives, giving relatively low friction when adsorbed on steel surfaces.

3. The film thickness of ZDDP and dispersant-containing oils increases when either N content is decreased or P content is increases. Excessive dispersant blocks ZDDP from surface.

4. The extent of mild wear produced by mixtures of ZDDP and dispersant depends on N content but less obviously on either P content or film thickness. Dispersants chemically removes part of the ZDDP film and thus increases wear, so that the wear rate increases with dispersant concentration.

5. Based upon the existing literature, on measurements of the behaviour of solutions containing ZDDP and/or dispersant and the removal of ZDDP film by dispersant solutions, several main mechanisms of the antagonism between ZDDP and dispersant are drawn:

   - Complexation of dispersant and ZDDP or its decomposition products takes place in lubricant and this complexation is likely to be through a bonding between N atom from dispersant and P and/or Zn atom from ZDDP.

   - Similar complexation happens at the rubbing surfaces, which reduces the thickness of ZDDP film not only by directly reacting with dispersant but also by rubbing in a dispersant solution.

   - Adsorption of excessive dispersant blocks ZDDP from forming films rapidly on rubbing surfaces.

   - Dispersant chemically and partially removes ZDDP film from surfaces.

**11.1.3 Effect of other Additives on Tribological Behaviour of ZDDP**

The tribological properties of solutions containing several other types of additives (in addition of ZDDP) have been investigated and results show the following:

1. Overbased calcium sulfonate forms a film on rubbing surfaces which is highly effective at preventing wear. When mixed with ZDDP, a competition in reaching surfaces occurs between these two additives, which largely depends on the concentration of both. The resultant friction behaviour is similar to that of the dominant additive.

2. The outer layer of the film formed by overbased borated calcium sulfonate and ZDDP is believed similar to the one formed by the sulfonate alone, which gives similar friction behaviour and it is weaker than the one formed by ZDDP in antiwear.

3. An antagonistic response in wear is found when blending ZDDP with overbased calcium salicylate, since this results in more wear than either of these two additives alone in base oil solution.

4. MoDTC forms very thin films and provides low boundary friction. A synergistic response is observed with ZDDP in that the addition of MoDTC reduces friction but does not affect film thickness and wear resistance of ZDDP solutions. This is believed to be due to $MoS_2$ forming on ZDDP antiwear film.

5. The relative ability of the additives in reaching rubbing surfaces determines the film formation and friction properties of three-additive systems. Generally, the film-forming and friction behaviour of these systems is similar to that of the dominant additive in base oil solution.

6. Wear produced by the solutions containing both ZDDP and dispersant is severer than any other combination, since the chemical removal of ZDDP film by dispersant involves the consumption of iron from bulk material. Negligible wear cause by the solutions containing ZDDP, sulfonate, sulfonate + ZDDP and sulfonate + dispersant indicates the films formed are either sacrificial or highly wear resistant.

## 11.2 Suggestions for Future Work

### 11.2.1 New Mild Wear Test Method Development

As described in Chapter 6, the new mild wear test method developed in current study is repeatable and reliable to characterize wear caused by ZDDP-containing oils; however to be faultless it still needs considerable further developments.

1. Application of different contact models, *e.g.* line contact and area contact, to produce mild wear and thus simulate more practical conditions.

2. Take running-in processes into consideration.

3. Carry out further investigation to explore the reason for different wear on the disc and ball

4. Employ this method to test other functional additives and formulated oils to verify its practical feasibility, *e.g.* whether EDTA can remove film formed by other additives.

**11.2.2 Effect of Dispersants on the Tribological Properties of ZDDP**

The mechanisms of the antagonistic response between ZDDP and dispersants have been investigated in respect of tribological behaviour but further study and more detailed analysis are also needed.

1. Explore the mechanisms of ZDDP film formation, *e.g.* whether ZDDP film initially forms on the asperities of steel surfaces, whether atmosphere affects ZDDP film formation, the effect of temperature on ZDDP film formation, why ZDDP film stabilizes when it reaches certain thickness, *etc.*

2. Carry out further surface analysis to compare the chemical composition and structure of a ZDDP film before and after its partial removal by dispersant, and thus confirm the compound removed from ZDDP film, as well as the remaining part.

3. Characterize the complexation between dispersant and ZDDP and/or its decomposition products using modern spectroscopes both on the surfaces and in the solution.

4. Apply advanced techniques to clarify whether there is any relation between film thickness and wear for the solutions containing both ZDDP and dispersant.

**11.2.3 Effect of other Additives on the Tribological Properties of ZDDP**

In current study, a limited number of representative additives have been employed to preliminarily investigate their effects on tribological properties of ZDDP. Considerable amount of future work should be carried out.

1. Characterize the composition and structure of films formed by different types of detergents, friction modifiers and other additives

2. Compare the films formed by these additives and the ones formed by solutions containing these additives and ZDDP to see whether the competition in reaching rubbing surfaces happens between these additives and ZDDP

3. Apply MTM-SLIM and the new mild wear test method to some other additives (*e.g.* antioxidants, viscosity modifiers) to examine their effects on film formation, friction and wear properties of ZDDP

4. Evaluate the tribological properties of full-formulated oils using MTM-SLIM and the new mild wear test method.

# References

1.      Ph. Kapsa and J.M. Martin. Boundary lubricant films: a review. Trib. Int. 1982; 15 (1), 37-42.

2.      Stribeck, R. Die Wesentlichen Eigneschaften der Gleit und Rollenlager. Z. Ver. Dt. Ing. 1902; 46 (38), 1341-1348, 46 (39), 1463-1470.

3.      Hardy, H.B. and Doubleday, I. Boundary Lubrication, - The Paraffin Series. Proc. Roy. Soc. Lond. 1922; A100, 550-757.

4.      Spikes H.A. Boundary Lubrication and Boundary Films. Proceedings of 19th Leeds-Lyon Symposium on Tribology: Thin Films in Tribology, 1993; 331-346.

5.      Spikes, H.A. The Borderline of Elastohydrodynamic and Boundary Lubrication. Proceedings of the Institution of Mechanical Engineers Part C- J Mech. Eng. Sci. 2000; 214, 23-37.

6.      T.E. Stanton. Friction. Publ. Longmans, Green & Co., London, 1923.

7.      Daniel, S.G. The Adsorption on Metal Surfaces of Long Chain Polar Compounds from Hydrocarbon Solutions. Trans. Farad. Soc. 1951; 47, 1345-1359.

8.      Gaines, G.L. Jr. Some Observation on Monolayers of Carbon-14 Labelled Stearic Acid. J. Coll. Sci. 1960; 15, 321-339.

9.      Haydon, D.A. Boundary Potentials and Adsorption at the Oil-Metal Interface. Koll. Zeit. 1963; 188, 141-147.

10.     Allen, C.M. and Drauglis, E. Boundary Layer Lubrication: Monolayer or Multilayer. Wear. 1969; 14, 363-384.

11.     Mougey, H.C. and Almen, J.O. Extreme Pressure Lubricants. Auto. Ind. 1931; 65 (26), 758-761.

12.     Evans, A.E. Extreme Pressure Lubricants. I. Mech. E. Proceedings of the General Discussion on Lubrication and Lubricants. 1937; 2, 55-59.

13.     Southcombe, J.E., Wells, J.H. and Waters, J.H. An Experimental Study of Lubrication under Conditions of Extreme Pressure. I. Mech. E. Proceedings of the General Discussion on Lubrication and Lubricants. 1937; 2, 400-411.

14.     Thorpe, R.E. and Larsen, G.G. Antiseizure Properties of Boundary Lubricants. Ind. Eng. Chem. 1949; 41, 938-943.

15.     Rabinowicz, E. and Tabor, D. Metallic Transfer between Sliding Metals: An Autoradiographic Study. Proc. Roy. Soc. Lond. 1951; A208, 455-475.

16.     Clark, G.L. Sterrett, R.R. and Lincoln, B.H. X-ray Diffraction Studies of Lubricants. Ind. Eng. Chem. 1936; 28, 1318-1328.

17.     Andrew, L.T. Electron Diffraction Analysis of the Orientation of the Molecules of Lubricating Oils. Trans. Farad. Soc. 1936; 32, 607-616.

18.     Brockway, L.O. and Karle, J. Electron Diffraction Studies of the Oleophobic Films on Copper, Iron and Aluminium Surfaces. J. Coll. Sci. 1947; 2, 277-287.

19.     Francis, S.A. and Ellison, A.H. Reflection Infrared Studies of Zinc Dialkyldithiophosphate Films Adsorbed on Metal Surfaces. J. Chem. Eng. Data. 1961; 16, 83-86.

20.     Rounds, F.G. Effect of Additives on the Friction of Steel on Steel. (I) Surface Topographic and Film Composition Studies. ASLE Trans. 1964; 7, 11-23.

21.     Sheasby, J.S., Caughlin, T.A. and Habeeb, J.J. Observation of the Antiwear Activity of Zinc Dialkyldithiophosphate Additives. Wear. 1991; 150, 247-257.

22.     Cann, P.M. and Spikes. H.A. In Lubro Studies of Lubricants in EHD Contacts Using FTIR Absorption Spectroscopy. STLE Trans. 1991; 34, 248-256.

23.     Bell, J., Coy, R. and Spikes, H.A. Cryogenic Studies of Zinc Dialkyl Dithiophosphate Anti-wear Films. Proc Jap. Int. Tribology Conf, Nagoya, 1990; 505-510.

24.     Andoh, Y., Oguchi, S., Kaneko, R. and Miyamoto, J. Evaluation of Very Thin Lubricant Films. J. Phys. D. 1992; 25, A71-A75.

25.     Swalen, J.D., Allara, D.L., Andrade, J.D., Chandross, E.A., Garoff, S., Israelachvili, J., McCarthy, T.J., Murray, R., Pease, R.F., Rabolt, J.F., Wynne, K.J. and Yu, H. Molecular Monolayers and Films. Langmuir. 1987; 3, 932-950.

26.     V. Anghel, P.M. Cann and H.A. Spikes. Direct Measurement of Boundary Lubricating Films. Tribology Series. 1997; 32, 459-466.

27.     Guangteng, G. and Spikes, H.A. The Control of Friction by Molecular Fractionation of Base Fluid Mixtures at Metal Surfaces. Trib Trans. 1997; 40, 461-469.

28.     Spikes, H.A. The History and Mechanism of ZDDP. Trib. Lett. 2004; 17, 469-489.

29.     Johnson, J.C. Antioxidants: Synthesis and Applications. Noyes Data Corp., Park Ridge, N.J. 1975.

30.     Kingsbury, A. A New Oil-Testing Machine and Some of Its Results. Trans. ASME. 1903; 24, 143-160.

31.     Wells, H.M. and Southcombe, J.E. The Theory and Practice of Lubrication: The 'Germ' Process. J. Soc. of Chem. Ind. 1920; 39, 51T-61T.

32.     Hardy, W. and Bircumshaw, I. Boundary Lubrication – Plane Surface and the Limitations of Amonton's Law. Proc. Roy. Soc. Lond. 1925; A109, 1-27.

33.     T.E. Stanton. Friction. Publ. Longmans, Green &Co., London, 1923.

34.     Langmuir, I. The Mechanism of the Surface Phenomena of Flotation. Trans. Farad. Soc. 1920; 15, 62-74.

35.     Bowden, F.P. and Leben, L. The Friction of Lubricated Metals. Phil. Trans. Roy. Soc. 1940; A239, 1-27.

36.     Bailey, A. and Courtenay Pratt, J.S. The Area of Real Contact and the Shear Strength of Monomolecular Layers of a Boundary Lubricant. Proc. Roy. Soc. Lond. 1955; A227, 500-515.

37.     Fein, R.S. and Kreuz, K.L. Chemistry of Boundary Lubrication of Steel by Hydrocarbons. ALSE Trans. 1965; 8, 29-38.

38.     Foord, C.A. Hamman, W.C. and Cameron, A. Evaluation of Lubricants Using Optical Elastohydrodynamics. ASLE Trans. 1968; 11, 31-43.

39.     Johnston, G.J., Wayte, R. and Spikes, H.A. The Measurement and Study of Very Thin Lubricant Film in Concentrated Contacts. STLE Trans. 1991; 34, 187-194.

40.     Gunsel, S., Spikes, H.A. and Aderin, M. In-situ Measurement of ZDDP Films in Concentrated Contacts. Trib. Trans. 1993; 36, 276-282.

41.     Cann, P.M., Huthcinson, J. and Spikes, H.A. Development of a Space Layer Imaging Method (SLIM) for Mapping Elastohydrodynamic Contacts. Trib. Trans. 1996; 39, 915-921.

42.     Spikes, H.A. Direct Observation of Boundary Layers. Langmuir. 1996; 12, 4567-4573.

43.     Spikes, H.A. Thin Films in Elastohydrodynamic Lubrication: The Contribution of Experiment. Proc. I Mech Eng J - J Eng. Trib. 1999; 213, 335-352.

44.     Spikes, H.A. and Cann, P.M. The Development and Application of the Spacer Layer Imaging Method for Measuring Lubricant Film Thickness. Proc. I Mech Eng J - J Eng. Trib. 2001; 215, 261-277.

45. Vilalta-Clemente, A. and Gloystein, K. Principles of Atomic Force Microscopy. Physics of Advanced Materials Winter School 2008. Based on the Lecture of Prof. Nikos Frangis. Aristotle University, Greece.

46. Binnig, G., Rohrer, H., Gerber, Ch. and Weibel, E. Surface Studies by Scanning Tunneling Microscopy. Phys. Rev. Lett. 1982; 49, 57-61.

47. Andoh, Y., Ogchi, S., Kaneko, R. and Miyamoto, J. Evaluation of Very Thin Lubricant Films. J. Phys. D. 1992; 25, A71-A75.

48. Fuller, M., Yin, Z., Kasrai, M., Bancroft, G.M., Yamaguchi, E.S., Ryason, P.R., Willermet, P.A. and Tan, K.H. Chemical Characterization of Tribochemical and Thermal Films Generated from Neutral and Basic ZDDP Using X-ray Absorption Spectroscopy. Trib. Int. 1997; 30, 305-315.

49. Israelachvili, J.N. and Tabor, D. The Measurement of Van der Waals Dispersion Forces in the Range 1.5 to 130 nm. Proc. Roy. Soc. Lond. 1972; A331, 19-38.

50. Cavdar, B. and Ludema, K.C. Dynamics of Dual Films Formation in Boundary Lubrication of Steels. Part III: Real Time Monitoring and Ellipsometry. Wear. 1991; 148, 347-361.

51. http://EnvironmentalChemistry.com/yogi/chemicals/cn/Zinc%A0Dialkyl%A0Dithiophosphates%A0(ZDDP).html. Accessed June 28th 2008.

52. Lawton, S.L. and Kokotailo, G.T. Crystal and Molecular Structures of Zinc and Calcium O, O-diisopropyl Phosphorodithioates. Inorg. Chem. 1969; 8(11), 2410-2421.

53. Brazier, AD, Elliott, JS. The Thermal Stability of Zinc Dithiophosphates. J Inst Petrol. 1967; 53(518), 63-76.

54. Armstrong, D.R., Ferrari, E.S., Roberts, K.J. and Adams, D. An Investigation into the Molecular Stability of Zinc Dialkyl Dithiophosphates in Relation to Their Use as Antiwear and Anticorrosion Additives in Lubricating Oils. Wear. 1997; 208, 138-146.

55. Armstrong, D.R., Ferrari, E.S., Roberts, K.J. and Adams, D. An Examination of the Reactivity of Zinc Dialkyl Dithiophosphate in Relation to Its Use as an Antiwear and Anticorrosion Additive in Lubricating Oils. Wear. 1998; 217, 276-287.

56. Harrison, P.G. and Kikabhai, T. Proton and Phosphorus-31 Nuclear Magnetic Resonance Study of Zinc II O, O-dialkyldithiophosphates in Solution. J. Chem. Soc. Dalton Trans. 1987; 4, 807-814.

57.     Yamaguchi, E.S. The Relative Wear Performance of Neutral and Basic ZnDTP in Engines. Trib. Trans. 1999; 42(1), 90-95.

58.     Fuller, M., Yin, Z., Kasrai, M., Bancroft, G.M., Yamaguchi, E.S., Ryason, P.R., Willerme, R.A. and Tan, K.H. Chemical Characterization of Tribochemical and Thermal Films Generated from Neutral and Basic ZDDPs Using X-ray Absorption Spectroscopy. Trib. Int. 1997; 30, 305-315.

59.     Gallopoulos N.E. Infrared Spectra and Structural Features of Salts of O, O'-Dialkylphosphorodithioic Acid. Am. Chem. Soc., Div. Petrol. Chem., Preprints. 1966; 11, 21-38.

60.     Heilweil, I.J. Association Studies of Metal O, O'-Dialkylpliospl-oro-dithioates. Am. Chem. Soc., Div. Petrol. Chem., Preprints 1965; 10, 4-D 19-31.

61.     Fang, H.L. and Milar, J.M. Characterization of the Dimer Formation of ZDDP Neutral Salt. 14th Int. Symp. Performance Evaluation of Automotive Fuels and Lubes. B'ham UK, May 1993, CEC/93/EL15.

62.     Kennerly, G.W., Patterson, W.L. Kinetic Studies of Petroleum Antioxidants. Industrial and Engineering Chemistry. 1956; 48, 1917-1924.

63.     Almalaika, S., Coker, M. and Scott, G. Polymer Degradation and Stability. 1988; 22, 147-159.

64.     Willermet, R.A., Carter, R.O., Schmitz, P.J. Everson, M., Scholl, D.J. and Weber, W.H. Formation, Structure, and Properties of Lubricant-Derived Antiwear Films. Lubr. Sci. 1997; 9(4), 325-348.

65.     Burn, A.J. The Mechanism of the Antioxidant Action of Zinc Dialkyl Dithiophosphates. Tetrahedron. 1966; 22 (7), 2153-2161.

66.     Burn AJ, Cecil R, Young VO. Peroxide-decomposing Antioxidants. Mechanisms of the Decomposition of Cumene Hydroperoxide in the Presence of Zinc Diisopropyldithiophosphate. J Inst Petrol. 1971; 57(558), 319-330.

67.     Paddy JL, Brook PS, Waters DN. Oxidation of Basic Zinc Dibutyldithiophosphate by Cumyl Hydroperoxide at 25℃: Kinetic Studies by HPLC. J Chem Soc Perkin Trans II. 1989; 1703-1706.

68.     Paddy JL, Lee NCJ, Waters DN, Trott W. Zinc Dialkyldithiophosphates Oxidation by Cumene Hydroperoxide: Kinetic Studies by Raman and 31P NMR Spectroscopy. Trib. Trans. 1990; 33(1), 15-20.

69.     Johnson M.D., Korcek S. and Zinbo M. Inhibition of Oxidation by ZDTP and Ashless Antioxidants in the Presence of Hydroperoxides at 160°C — Part 1. SAE Paper 831684, 1983, 71-81.

70.     Johnson, M.D., Korcek S. and Zinbo M., Inhibition of Oxidation by ZDTP and Ashless Antioxidants in the Presence of Hydroperoxides at 160°C. ASLE Trans. 1986; 29, 136–140.

71.     Sieber, I., Meyer, K. and Kloss, H. Characterization of Boundary Layers Formed by Different Metal Dithiophosphates in a Four-Ball Machine. Wear. 1983; 85, 43-56.

72.     Stachowiak, G.W. and Batchelor, A.W. Engineering Tribology, 2nd ed. (Publ. Butterworth-Heinemann, Boston, 2001).

73.     Masuko, M., Hanada, T. and Okabe, H. Distinction in Antiwear Performance between Organic Sulfide and Organic Phosphate as EP Additives for Steel under Rolling with Sliding Partial EHD Conditions. Lubr. Eng. 1994; 50(12), 972-977.

74.     Coy, R.C. and Jones, R.B. The Thermal Degradation and EP Performance of Zinc Dialkyldithiphosphate Additives in White Oil. ASLE Transactions. 1979; 24(1), 77-90.

75.     Habeeb, J.J. and Stover, W.H. The Role of Hydroperoxides in Engine Oil and the Effect of Zinc Dialkylthiophosphates. ASLE Trans. 1987; 30, 419-426.

76.     Rounds, F. Effects of Hydroperoxides on Wear as Measured in Four-Ball Wear Tests. Trib. Trans. 1993; 36(2), 297-303.

77.     Martin, J.M., Belin, M., Mansot, J.L., Dexpert, H. and Lagarde, P. Friction-Induced Amorphization with ZDDP: An EXAFS Study. ASLE Trans. 1986; 29, 523-531.

78.     Belin, M., Martin, J.M. and Mansot, J.L. Role of Iron in the Amorphization Process in Friction Induced Phosphate Glasses. Trib. Trans. 1989; 32, 410-413.

79.     Luther,          H.          and          Sinha,          SK. www.sciencedirect.com/science?_ob=ArticleURL&_udi=B6V57-3W07WC2-9&_user=6390781&. Erdol u Kohle-Erdgas-Perichemie. 1964; 17, 91-97.

80.     Hanneman, W.W. and Porter, R.S. The Thermal Decomposition of Dialkyl Phosphates and O, O-dialkyl Dithiophosphates. J of Org. Chem. 1964; 29, 2996-2998.

81.     Gallopoulos, N.E. Thermal Decomposition of Metal Dialkyldithiophosphate Oil Blends. ASLE Trans. 1964; 7, 55-63.

82.  Ashford, J.S., Bretherick, L. and Gould, P. J. of Appl Chem. 1965; 15, 170-178.

83.  Dickert, J.J. and Rowe, C.N. The Thermal Decomposition of Metal O,O-Dialkylphosphorodithiolates. J. of Org. Chem. 1967; 32, 647-653.

84.  Brazier, A.D. and Elliot, J.S. The Thermal Stability of Zinc Dithiophosphates. J.Inst. Petrol. 1967; 53, 63-76.

85.  Fuller, M.L., Kasrai, M., Bancroft, G.M., Fyfe, K. and Tan, K.H. Solution Decomposition of Zinc Dialkyl Dithiophosphate and Its Effect on Antiwear and Thermal Film Formation Studied by X-ray Absorption Spectroscopy. Trib. Int. 1998; 31, 627-644.

86.  Yamaguchi, E.S., Tyason, P.R. and Labrador, E.Q. Inelastic Electron Tunneling Spectra of Lubricant Oil Additives on Native Aluminium Oxide Surfaces. Trib. Trans. 1993; 36(3), 367-374.

87.  Colclough, T. and Cunneen, J.I. Oxidation of Organic Sulphides. Part XV. The Antioxidant Action of Phenothiazine, Zinc Isopropylxanthate, Zinc Di-isopropyldithiophosphate, and Zinc Dibutyldithiocarbamate, in Squalene. J. of Chem.l Soc. 1964; 4790-4793.

88.  Howard, J.A., Ohkatsu, Y., Chenier, J.H.B. and Ingold, K.U. Metal Complexes as Antioxidants. The Reaction of Zinc Dialkyldithiophosphates and Related Compounds with Peroxy Radicals. Canadian J of Chem. 1973; 51(10), 1543-1553.

89.  Willermet, P.A., Mahoney, P.A. and Haas, C.M. The Effects of Antioxidant Reactions on the Wear Behaviour of a Zinc Dialkyldithiophosphate. ASLE Trans. 1979; 22, 301-306.

90.  Willermet, P.A., Mahoney, P.A. and Bishop, C.M. Lubricant Degradation and Wear III. Antioxidant Reaction and Wear Behaviour of a Zinc Dialkyldithiophosphate in a Fully Formulated Lubricant. ALSE Trans. 1980; 23(3), 225-231.

91.  Willermet, P.A., Kandah, S.K., Siegl, W.O. and Chase, R.E. The Influence of Molecular Oxygen on Wear Protection by Surface-active Compounds. ASLE Trans. 1983; 26(4), 523-531.

92.  Spedding, H. and Watkins, R.C. The Antiwear Mechanism of ZDDPs Part I & II. Trib. Int. 1982; 2, 9-15.

93.  Glaeser, W.A., Baer, D. and Engelhardt, M. In Situ Wear Experiments in the Scanning Auger Spectrometer. Wear. 1993; 162-164, 132-138.

94.     Bell, J.C., Delargy, K.M. and Seeney, A.M. The Removal of Substrate Material through Thick Zinc Dithiophosphate Antiwear Film. Wear Particles. Tribology Series. 1992; 2, 387-396.

95.     Dacre, B. and Bovington, C.M. The Adsorption and Desorption of ZDDP on Steel. Am. Soc. Lub. Eng. Trans. 1982; 25, 546-554.

96.     Willermet, P.A., Dailey, D.P., Carter III, R.O., Schmitz, P.J. and Zhu, W. Mechanism of Formation of Antiwear Films from Zinc Dialkyldithiophosphates. Trib. Int. 1995; 28(3), 177-187.

97.     Yin, Z., Kasrai, M., Fuller, M., Bancroft, G.M., Fyfe, K. and Tan, K.H. Application of Soft X-ray Absorption Spectroscopy in Chemical Characterization of Antiwear Films Generated by ZDDP Part I: The Effect of Physical Parameters. Wear. 1997; 202, 172-191.

98.     Ferrari, E.S., Roberts, K.J., Sansone, M. and Adams, D. A Multi-edge X-ray Absorption Spectroscopy Study of the Reactivity of Zinc Dialkyldithiophosphates Antiwear Additives 2. In Situ Studies of Steel/Oil Interfaces. Wear. 1999; 236, 259-275.

99.     Pearson, R.G. The HSAB Principle. Chemical Hardness. Wiley-VCH; 1997; 1-27.

100.    H. von Luther and D.Staeck, Erdol u Kohle-Erdgas-Petrochemie. 1969; 22, 530-533.

101.    Jensen R.K., Johnson, M.D., Korcek, S. and Rokosz, M.J. Friction Reducing and Antioxidant Capabilities of Engine Oil Additive Systems under Oxidative Conditions. Lubr. Sci. 1998; 10, 99-120.

102.    Molina, A. Isolation and Chemical Characterization of a Zinc Dialkyldithiophosphate-derived Antiwear Agent. ASLE Trans. 1987; 30(4), 479-485.

103.    Willermet, P.A., Carter III, R.O. and Boulos, E.N. Lubricant-derived Tribochemical Films-An Infra-red Spectroscopic Study. Trib. Int. 1992; 25(6), 371-380.

104.    Bancroft, G.M., Kasrai, M., Fuller, M., Yin, Z., Fyfe, K. and Tan, K.H. Mechanism of Tribochemical Film Formation: Stability of Tribo- and Thermally-Generated ZDDP Films. Trib. Lett. 1997; 3, 47-51.

105.    Cann, P.M. and Spikes, H.A. In-Contact IR Spectroscopy of Hydrocarbon Lubricants. Trib. Lett. 2005; 19, 289-297.

106. Topolovec-Miklozic, K., Forbus, T.J. and Spikes, H.A. Film Thickness and Roughness of ZDDP Antiwear Films. Trib. Lett. 2007; 26(2), 161-171.

107. Smith, G.C. and Bell, J.C. Multi-technique Surface Analytical Studies of Automotive Antiwear Films. Appl. Surf. Science. 1999; 144-145, 222-227.

108. Bec, S., Tonck, A., Georges, J.M., Coy, R.C., Bell, J.C. and Roper G.W. Relationship between Mechanical Properties and Structures of Zinc Dithiophosphate Antiwear Films. Proc. Roy Soc. London A. 1999; 455, 4181-4203.

109. Minfray, C., Martin, J.M., Esnouf, C., Le Mogne, T., Kersting, R. and Hagenhoff, B. A Multi-technique Approach of Tribofilm Characterization. Thin Solid Films. 2004; 447-448, 272-277.

110. Kennedy, S. and Moore, L.D. Additive Effects on the Lubricant Fuel Economy. SAE Technical Paper Series 1987, 872121.

111. Tripaldi, G., Vettor, A. and Spikes, H.A. Friction Behaviour of ZDDP Films in the Mixed, Boundary/EHD Regime. SAE Technical Paper Series 1996; 962036, 73-84.

112. Taylor, L., Dratva, A. and Spikes, H.A. Friction and Wear Behaviour of Zinc Dialkyldithiophosphate Additive. Trib. Trans. 2000; 43(3), 469-479.

113. Palacios, J.J. Thickness and Chemical Composition of Films Formed by Antimony Dithiocarbamate and Zinc Dithiophosphate. Trib. Int. 1986; 19(1), 35-39.

114. Graham, J.F., McCague, C. and Norton, P.R. Topography and Nanomechanical Properties of Tribochemical Films Derived from Zinc Dialkyl and Diaryl Dithiophosphates. Trib. Lett. 1999; 6, 149-157.

115. Warren, O.L., Graham, J.F., Norton, P.R., Houston, J.E. and Michalske, T.A. Nanomechanical Properties of Films Derived from Zinc Dialkyldithiophosphate. Trib. Lett. 1998; 4, 89-98.

116. Mortier RM. In Orszulik in Chemistry and Technology of Lubricants. Colyer CC and Gergel WC. Eds. Blackie academic and professional. New York. 1993; 75.

117. Endo K and Inoue K. in 7th Int. Colloq Automotive Lubrication, Techn. Akad. Essligen. 1990.

118. Mang, T. and Dresel, W. Lubricants and Lubrication, Wiley-VCH GmbH, Weinheim, 2001.

119.    Kreuz, K.L. Diesel Engine Chemistry as Applied to Lubricant Problems. Lubrication. 1970; 56, 77-88.

120.    Rizvi, S.Q.A. Chapter 5 Dispersants. Lubricant Additives: Chemistry and Applications. 2003; 137-170.

121.    Fotheringham, J.D. Polybutenes. In LR Rudnick, RL Shubkin, eds. Synthetic Lubricants and High-Performance Functional Fluids. 2nd ed. New York: Marcel Dekker, 1999.

122.    Randles, S.J. *et al.* Synthetic Base Fluids. In RM Mortier, ST Orszulik, eds. Chemistry and Technology of Lubricants. New York: VCH Publishers, 1992; 32–61.

123.    Colyer, C.C., Gergel, W.C. Detergents/dispersants. In RM Mortier, ST Orszulik, eds. Chemistry and Technology of Lubricants. New York: CH Publishers, Inc., 1992; 62-82.

124.    Ethylene Amines. In Kirk Othmer's Encyclopedia of Chemical Technology, 2nd ed. vol.7. New York: Interscience Publishers, 1965; 22–37.

125.    Ingold, K.U. Inhibition of Autoxidation of Organic Substances in Liquid Phase. Chem. Rev 1961; 61, 563–589.

126.    Cochrac, G.J. and Rizvi, S.Q.A. Oxidation of Lubricants and Fuels. In: Totten GE (ed) Fuels and Lubricant Handbook: Technology, Properties, Performance, and Testing. ASTM International, West Conshohocken, PA, 2003; 787–824.

127.    Chamberlin, W.B. and Saunders, J.D. Automobile Engines. In RE Booser, ed. CRC Handbook of Lubrication, Vol. I, Theory and Practice of Tribology: Applications and Maintenance. Boca Raton, FL: CRC Press, 1983; 3–44.

128.    Obert, E.F. Basic Engine Types and Their Operation. In Internal Combustion Engines and Air Pollution. New York: Intext Educational Publishing, 1968; 1–25.

129.    Forbes, E.S. and Wood, J.M. Proc. Int. Congr. Surface Activity 5th Barcelona 1968.

130.    Egorova, K.A., Bauman, V.N. and Lashkhi, V.L. Neftepererabotkai Neftekhimiya, No. 9, 1974.

131.    Inoue, K. and Watanabe, H. Interactions of Engine Oil Additives. ASLE Trans. 1983; 26, 189-199.

132.    Rounds, F. G. Changes in Frictions and Wear Performance Caused by Interactions among Lubricant Additives. Proc. 5th Int. Colloq. Esslingen, Additives for Lubricants and Operational Fluids. 1986.

133. Plaza, S. The Effect of Other Lubricating Oil Additives on the Adsorption of Zinc Dialkyl Dithiophosphate on Fe and $\gamma$-Fe2O3 Powders. ASLE Trans. 1987; 30, 241-247.

134. Shirahama, S. and Hirata, M. The Effect of Engine Oil Additives on Valve Train Wear. Proc. 5th Int. Colloq. Esslingen. Additives for Lubricants and Operational Fluids. 1986.

135. Ramakumar, S.S., Madhusudhana Rao, A. and Srivastava, S.P. Studies on Additive-additive Interactions: Formulation of Crankcase Oils towards Radionalization. Wear. 1992; 156, 101-120.

136. Shiomi, M. Tokashiki, M., Tomizawa, H. and Kuribayashi, T. Interaction between Zinc Dialkyl Dithiophosphate and Amine. Lubrication Science. 1989; 1 (2), 131-147.

137. Rounds, F.G. Additive Interactions and Their Effect on the Performance of a Zinc Dialkyl Dithiophosphate. ASLE Trans. 1976; 21 (2), 91-101.

138. Harrison, P.G., Brown, P., and McManus, J. 31P NMR Study of the interaction of a Commercial Succinimide-type Lubricating Oil Dispersant with Zinc (II) Bis (O, O´-di-iso-butyldithiophosphate). Wear. 1992; 156, 345-349.

139. Willermet, P.A. Some Engine Oil Additives and Their Effects on Antiwear Film Formation. Trib. Lett. 1998; 5, 41-47.

140. Barcroft, F.T., Park, D. Interactions on Heated Metal Surfaces between Zinc Dialkyldithiophosphates and other Lubricating Oil Additives. Wear. 1986; 108, 213-234.

141. Kapur, G.S., Chopra, A., Ramakumar, S.S.V., Sarpal, A.S. Molecular Spectroscopic Studies of ZDDP-PIBS Interactions. Lubr. Sci. 1998; 10, 309-321.

142. Ramakumar, S.S.V., Aggarwal, N., Rao, M., Sarpal, A.S., Srivastava, S.P., Bhatnagar, A.K. Studies on Additive-additive Interactions: Effects of Dispersant and Antioxidant Additives on the Synergistic Combination of Overbased Sulfonate and ZDDP. Lubr. Sci1994; 7 (1), 25-38.

143. Martin, J.M., Grossiord, C., Le Mogne, T., Igarashi, J. Role of Nitrogen in Tribochemical Interaction between Zinc Dithiophosphate and Succinimide in Boundary Lubrication. Trib. Int. 2000; 33 (7), 453-459.

144. Zhang, Z., Kasrai, M., Bancroft, G.M., Yamaguchi, E.S. Study of the Interaction of ZDDP and Dispersants Using X-ray Absorption near Edge Structure

Spectroscopy—Part 1: Thermal Chemical Reactions. Trib. Lett. 2003; 15 (4), 377-384.

145. Yamaguchi, E.S., Zhang, Z., Kasrai, M., Bancroft, G.M. Study of the Interaction of ZDDP and Dispersants Using X-ray Absorption near Edge Structure Spectroscopy—Part 2: Tribochemical Reactions. Trib. Lett. 2003; 15 (4), 385-394.

146. Yamaguchi, E.S., Roby, S.H., Ryason, P.R. and Yeh, S.W. Electrical Contact Resistance Bench Wear Testing: Comparison with Engine Test Results. SAE 2002; 74, 01-26.

147. Masuko, M., Ohkido, T., Suzuki, A., Ueno, T., Okuda, S. and Sagawa, T. Effect of Ashless Dispersant on Deterioration of Antiwear Characteristics of ZnDTP due to Decomposition during the Oxidation Inhibition Process. Trib. Trans. 2007; 50, 310-318.

148. Zhang, Z., Najman, M., Kasrai, M., Bancroft, G.M, and Yamaguchi, E.S. Study of Interaction of EP and AW Addititves with Dispersants Using XANES. Trib. Lett. 2005; 18 (1), 43-51.

149. Zhang, Z., Yamaguchi, E.S., Kasrai, M., Bancroft, G.M. Interaction of ZDDP with Borated Dispersant Using XANES and XPS. Trib. Trans. 2004; 47, 527-536.

150. Williams, J.A. Wear Modelling: Analytical, Computational and Mapping: a Continuum Mechanics Approach. Wear, 1999; 225-229, 1-17.

151. Costa, H.L. and Hutchings, I.M. Reciprocating Lubricated Sliding on Textured Steel Surfaces. Ciência e Tecnologia dos Materiais. 2005; 17, 1/2.

152. Archard, J.F. Wear Theory and Mechanisms. Wear Control Handbook, ed. M. B. Peterson and W. O. Winer, ASME, New York. 35–80.

153. Zum Gahr, K.H. Microstructure and Wear of Materials. Elsevier, Amsterdam. 1987.

154. Basic overview of ICP-AES. http://www-odp.tamu.edu/publications/tnotes/tn29/technot2.htm

155. Brown, R.D. Chapter12. Test Methods. in Boundary Lubrication, an Appraisal of World Literature. ed. Ling, F.E., Klaus, E.E. and Fein, R.S. ASME, New York. 1969; 341-392.

156. Archard, J.F. Contact and Rubbing of Flat Surfaces. J. Appl. Phys. 1953; 24, 981-988.

157. Kato, K. and Adachi, K. Chapter 7. Wear Mechanisms. in Morden Tribology Handbook. 2001.

158. Vinsbo, O. Wear and Wear Mechanisms. Proc. Wear of Materials Conf. ASME. New York. 1979; 620-638.

159. Rowe, C.N. Role of Additive Adsorption in the Mitigation of Wear. ASLE Trans. 1970; 13, 179-188.

160. Klaus, E.E. and Bieber, H.E. Effect of Some Physical and Chemical Properties of Lubricants on Boundary Lubrication. ASLE Trans. 1964; 7, 1-10.

161. Ruff, A.W. Wear Measurement. in Friction and Wear Testing Source Book of Selected References from ASTM Standards and ASM Handbooks. ASTM and ASM. West Conshohocken, PA. 1997; 22-29.

162. Jagtap, R.N. and Ambre, A.H. Overview Literature on Atomic Force Microscopy (AFM): Basics and Its Important Applications for Polymer Characterization. Indian Journal of Engineering & Materials Sciences. 2006; 13, 368-384.

163. Cameron, A. and Gohar, R. Theoretical and Experimental Studies of the Oil Film in Lubricated Point Contact. Proceedings of Royal Society. 1966; 291, 520-536.

164. Gahlin, R. and Jacobson, S. A Novel Method to Map and Quantify Wear on a Micro-scale. Wear. 1998; 222, 93-102.

165. Benedet, J., Green, J.H., Lamb, G.D. and Spikes, H.A. Spurious Mild Wear Measurement Using White Light Interference Microscopy in the Presence of Antiwear Films. Trib. Trans. 2009; 52 (6), 841-846.

166. Fan, J.Y. and Spikes, H.A. New Test for Mild Lubricated Wear in Rolling-Sliding Contacts. Trib. Trans. 2007; 50, 145-153.

167. N. P. Suh. http://ocw.mit.edu/NR/rdonlyres/Mechanical-Engineering/2-800Fall-2004/3EB7EE5A-43BF-4B4B-860B-FD57DD8207F/0/ch4a_wear_intro.pdf.

168. Archard, J.F. and Hirst, W. Wear of Metals under Unlubricated Conditions. Proc. Roy. Soc. London. A, Mathematical and Physical Sciences. 1956; 256 (1206), 397-410.

169. Lim, S.C. and Ashby, M.F. (1987), Wear-mechanism Maps, Acta Metall. 1987; 35(1), 1-15.

170. Lim SC. Recent Developments in Wear-mechanism Maps. Trib. Int. 1998; 31, 87–97.

171. Beerbower, A. Boundary Lubrication. U.S. Army, Office of the Chief of Research and Development. Alexandria, VA, June 1972.

172. Dowson, D. and Higginson, G.R. A Numerical Solution to the Elastohydrodynamic Problem. J. Mech. Eng. Sci. 1959; 1 (1), 7-15.

173.    Ramsey, P.M. and Page, T.F. A New Approach to Predicting the Wear Behaviour of Ceramic Surfaces. Br. Ceram. Trans. J. 1988; 87, 74–80.

174.    Wang, D.Z., Peng, H.X., Liu, J. and Yao, C.K. Wear Behaviour and Microstructural Changes of SiCw–Al Composite under Unlubricated Sliding Friction. Wear. 1995; 184, 187–192.

175.    Crease, A.B. Design Data for the Wear Performance of Rubbing Bearing Surfaces. Tribology 1973; 6, 15–20.

176.    Borel, M.O., Nicoll, A.R., Schla¨pfer, H.W. and Schmid, R.K. The Wear Mechanisms Occurring in Abradable Seals of Gas Turbines. Surf. Coat. Technol. 1989; 39/40, 117–126.

177.    Yen, D.W. and Wright, P.K. Adaptive Control in Machining—a New Approach Based on the Physical Constraints of Tool Wear Mechanisms. Trans. ASME, J. Eng. Ind., 1983; 105, 31–38.

178.    Taylor, L.J. and Spikes, H.A. Friction-enhancing Properties of ZDDP Antiwear Additive: Part I - Friction and Morphology of ZDDP Reaction Films, Trib. Trans. 2003; 46, 303-309.

179.    Taylor, L.J. and Spikes, H.A. Friction-enhancing Properties of ZDDP Antiwear Additive: Part II - Influence of ZDDP Reaction Films on EHD Lubrication, Trib. Trans. 2003; 46, 310-314.

180.    Taylor, L., Dratva, A. and Spikes, H.A. Friction and Wear Behaviour of Zinc Dialkyldithiophosphate Additive, Trib. Trans. 2000; 43, 469-479.

181.    Mate, C.M., McClelland, G.M., Erlandsson, R. and Chiang, S. Atomic-scale Friction of a Tungsten Tip on a Graphite Surface. Phys. Rev. Lett. 1987; 59, 1942-1945.

182.    Binnig, G., Quate, C.F. and Gerber, Ch. Atomic Force Microscopy. Phys. Rev. Lett. 1986; 56, 930-936.

183.    Kumar, R., Prakash, B. and Sethuramiah, A. A systematic Methodology to Characterize the Running-in and Steady-state Wear Process. Wear. 2002; 252, 445-453.

184.    Zheng, M., Naeim, A.H., Walter, B. and John, G. Break-in Liner Wear and Piston Ring Assembly Friction in a Spark-ignited Engine. Trib. Trans. 1998; 41 (4), 497-504.

185. Fujita, H., Glovnea, R.P. and Spikes, H.A. Study of Zinc Dialkyldithiophosphate Antiwear Film Formation and Removal Processes, part I: Experimental, Trib. Trans. 2005; 48, 558-566.

186. Fujita, H. and Spikes, H.A. Study of Zinc Dialkyldithiophosphate Antiwear Film Formation and Removal Processes, part II: Kinetic Model, Trib. Trans. 2005; 48, 567-575.

187. Aoki, S., Suzuki, A. and Masuko, M. Comparison of Sliding Speed Dependency of Friction between Steel Surfaces Lubricated with Several ZnDTPs with Different Hydrocarbon Moieties. Proc. I Mech E. 2006; J220, 343-351.

188. Palermo, T., Giasson, S., Buffeteau, T., Desbat, B., Turlet, J.M. Study of Deposit and Friction Films of Overbased Calcium Sulphonate by PM-IRRAS Spectroscopy. Lubr. Eng. 1995; 8, 119–127.

189. Hong, H., Riga, A.T., Cahoon, J.M., Vinci, J.N. Evaluation of Overbased Sulfonates as Extreme Pressure Additives in Metalworking Fluids. Lubr. Eng. 1993; 49, 19–24.

190. Cizaire, L., Martin, J.M., Gresser, E., Truong Dinh, N., Heau, C. Tribochemistry of Overbased Calcium Detergents Studied by ToF-SIMS and Other Surface Analysis. Trib. Lett. 2004; 17, 715–721.

191. Kubo, T., Fujiwara, S., Nanao, H., Minami, I., Mori, S. ToF-SIMS Analysis of Boundary Films Derived from Calcium Sulfonates. Trib. Lett. 2006; 23, 171–176.

192. Costello, M.T., Kasrai, M. Study of Surface Films of Overbased Sulfonates and Sulfurized Olefins by X-ray Absorption near Edge Structure (XANES) Spectroscopy. Trib. Lett. 2006; 24, 163–169.

193. Topolovec-miklozic, K., Forbus, T., Spikes, H.A. Film Forming and Friction Properties of Overbased Calcium Sulphonate Detergents. Trib. Lett. 2008; 29, 33-44.

194. Yamada, Y., Igarashi, J., and Inoue, K. Effects of Metallic Detergents on the Antioxidant and Antiwear Properties of Zinc Dialkyldithiophosphates. Lubr. Eng. 1992; 48, 511-517.

195. Rounds, F.G. Effect of Detergents on ZDP Antiwear Performance as Measured in Four-Ball Wear Tests. Lubr. Eng. 1989; 45, 761-769.

196. Yamaguchi, E.S., Roby, S.H., Francisco, M.M., Ruelas, S.G. and Godfrey, D. Antiwear Film Formation by ZDDP, Detergent, and Dispersant Components of Passenger Car Motor Oils. Trib. Trans. 2002; 45, 425-429.

197. Yamaguchi, E.S., Ryason, P.R., Yeh, S.W. and Hasen, T.P. Boundary Film Formation by ZDDPs and Detergents Using ECR. Trib. Trans. 1998; 41, 262-272.

198. Wu, Y.L. and Dacre, B. Effects of Lubricant-Additives on the Kinetics and Mechanisms of ZDDP Adsorption on Steel Surfaces. Trib. Int. 1997; 30, 445-453.

199. Kubo, T., Nanao, H., Minami, I., Ichihashi, T. ToF-SIMS Analysis of Boundary Film Derived from Multi-Additives. Journal of Japanese Society of Tribologists. 2006; 51, 819-825.

200. Najman, M., Kasrai, M., Bancroft, G.M. and Davidson, R. Combination of Ashless Antiwear Additives with Metallic Detergents: Interactions with Neutral and Overbased Calcium Sulfonates. Trib. Int. 2006; 39 (4), 342-355.

201. Ingram, M., Noles, J., Watts, R., Harris, S. "Frictional Properties of Automatic Transmission Fluids: Part I – Measurement of Friction-Sliding Speed Behaviour" Trib. Trans. 2011; 54 (1), 145-153.

202. Ingram, M. Noles, J., Watts, R., Harris, S. "Frictional Properties of Automatic Transmission Fluids: Part II – Origins of Friction-Sliding Speed Behaviour" Trib. Trans. 2011; 54 (1), 154-167.

203. De Barros Bouchet, M.I., Martin, J.M., Le Mogne, Th., Bilas, P. Vache, B., Yamada, Y. Mechanisms of MoS2 Formation by MoDTC in Presence of ZnDTP: Effect of Oxidative Degradation. Wear, 2005; 258, 1643-1650.

204. Muraki, M., and Wada, H. Influence of the Alkyl Group of Zinc Dialkyldithiophosphate on the Frictional Characteristics of Molybdenum Dialkyldithiocarbamate under Sliding Conditions. Trib. Int. 2002; 35, 857-863.

205. Topolovec-Miklozic, K., Forbus, T., Spikes, H.A. Performance of Friction Modifiers on ZDDP-generated Surfaces. Trib. Trans. 2007; 50, 328-335.

206. Morina, A., and Neville, A. Understanding the Composition and Low Friction Tribofilm Formation/Removal in Boundary Lubrication. Trib. Int. 2007; 40, 1696-1704.

207. Morina, A., Neville, A., Priest, M. and Green, J.H. ZDDP and MoDTC Interactions and Their Effect on Tribological Performance – Tribofilm Characteristics and Its Evolution. Trib. Lett. 2006; 24, 243-256.

208. Muraki, M. and Wada, H. Frictional Properties of Organomolybdenum Compounds in the Presence of ZDTPs under Sliding Conditions. Tribology Series. 1995; 30, 409-422.

209. Spikes, H.A. Additive-Additive and Additive-Surface Interactions in Lubrication. Lubr. Sci. 1989; 2 (1), 3-23.

210. Larson, R. The Performance of Zinc Dithiophosphates as Lubricants. Scient. Lubr. 1958; 10 (8), 12-20.

211. Lin. Y.C. and So. H. Limitation of Use of ZDDP as an Antiwear Additive in Boundary Lubrication. Trib. Int. 2004; 37(1), 25-33.

# Appendix A. Wear Measurements on the Specimens

In this section, a way of accurately measuring wear on specimens is described.

The main function of the white light interferometry microscopy Wyko NT9100 is to profile the measured surface topography. In current study, the surface of the ball specimens is spherical which makes the volume measurements more complicated. Furthermore, the stage on which the specimens are measured is probably not perfectly horizontal, which may result in error in the following analysis and calculations. In this appendix, it therefore introduces a way of accurately measuring the wear volume on the tested ball specimens and strip area on the tested disc specimens of both HFRR and reciprocating MTM tests. However, the way of measuring the surface topography is not described here.

In the case that the advanced analysis software of this Wyko NT9100 is installed in advance, this introductory section starts with the opened surface profile of the worn region of a HFRR ball. The dialog box is shown as in Figure A.1. Then a protocol of this measurement is demonstrated by successively presenting graphs of the dialog boxes and the descriptive texts on the right side, through which the required wear volume and strip area values can be accurately obtained.

Regarding the way this software estimates volume, the function named 'term mask' is required in the volume measurements. In the programme, the volume measurement counts the volume occupied by the space between the sample surface and a plane—zero level and this zero level is automatically set by the software as the average height of the sample surface. The 'term mask' function defines an area over which the tilt fit or curvature fit performs, and then applies this fit to the whole measured surface. The measurement of the wear volume and area is then can be achieved by combining these two functions, which is shown below in the protocol.
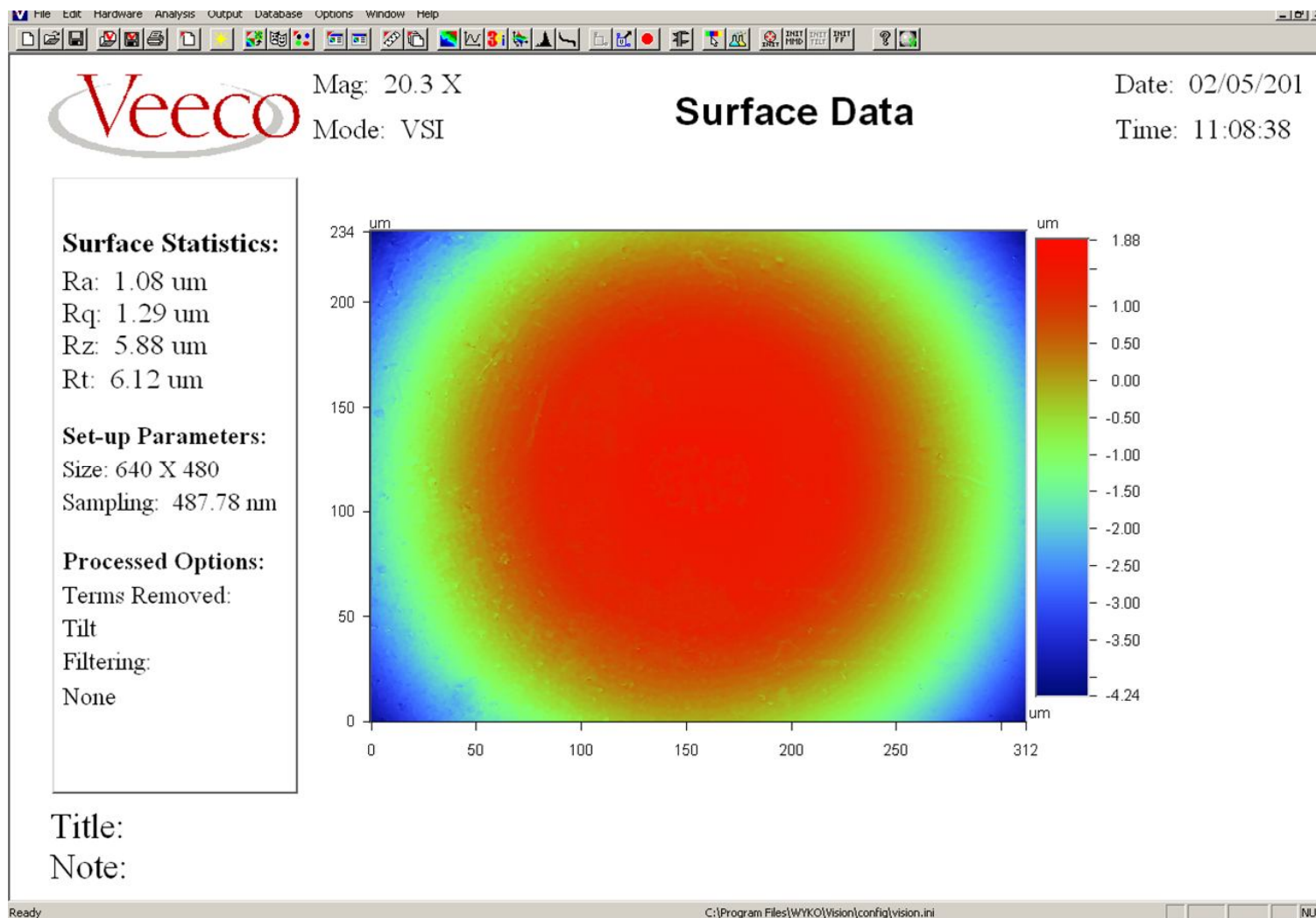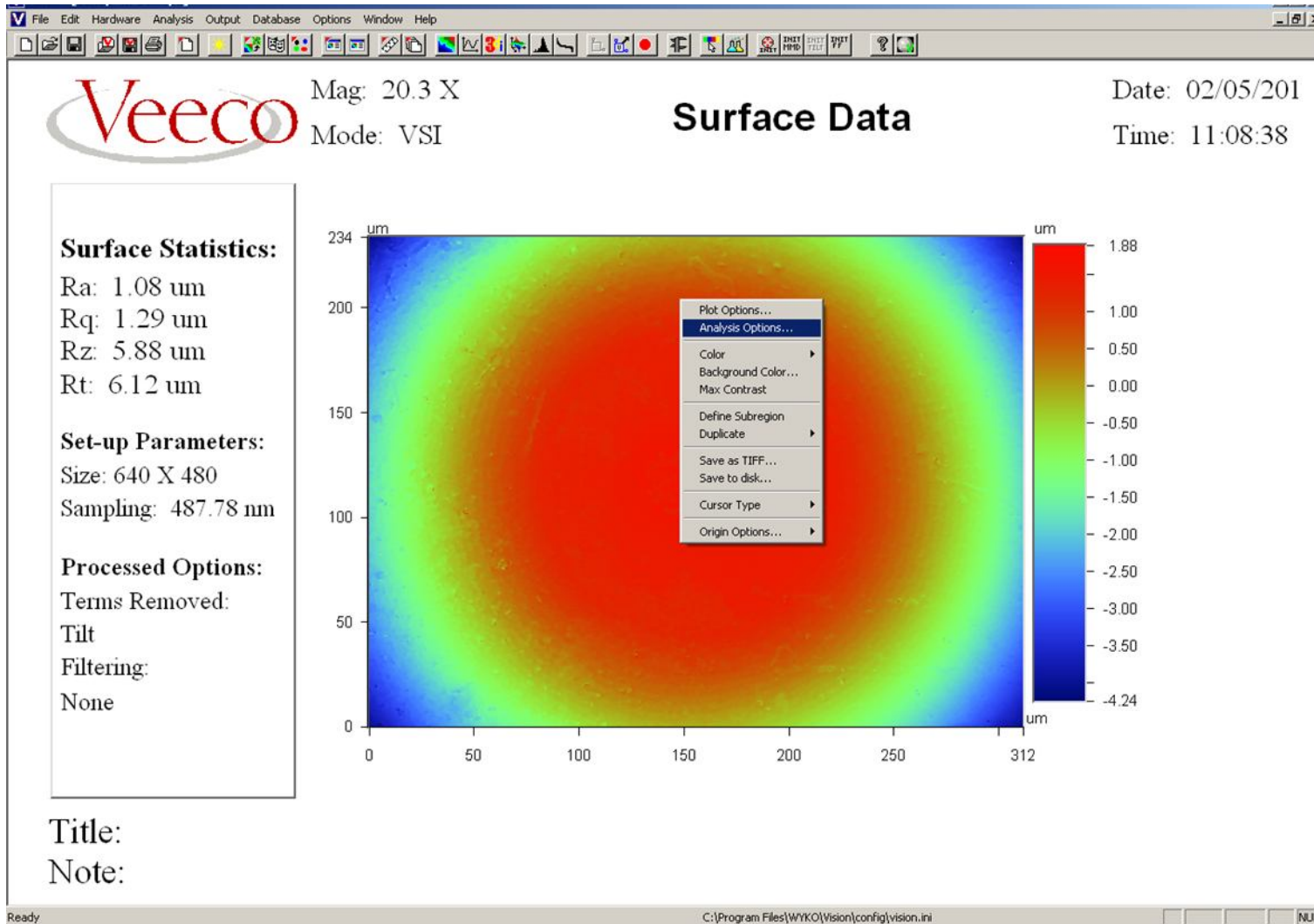
Figure A.1 is showing an original surface topography of the wear scar region on a HFRR ball.

**Figure A.1 Original Surface Topography**

215

The functions supplied by Wyko software can be used to analyze surfaces in different shape such as this spherical HFRR ball.

Right click in the image region; a dialog box appears as shown in Figure A.2. Select 'Analysis option'.

**Figure A.2 Functional Analysis**

**Figure A.3 Surface Curvature Definition**
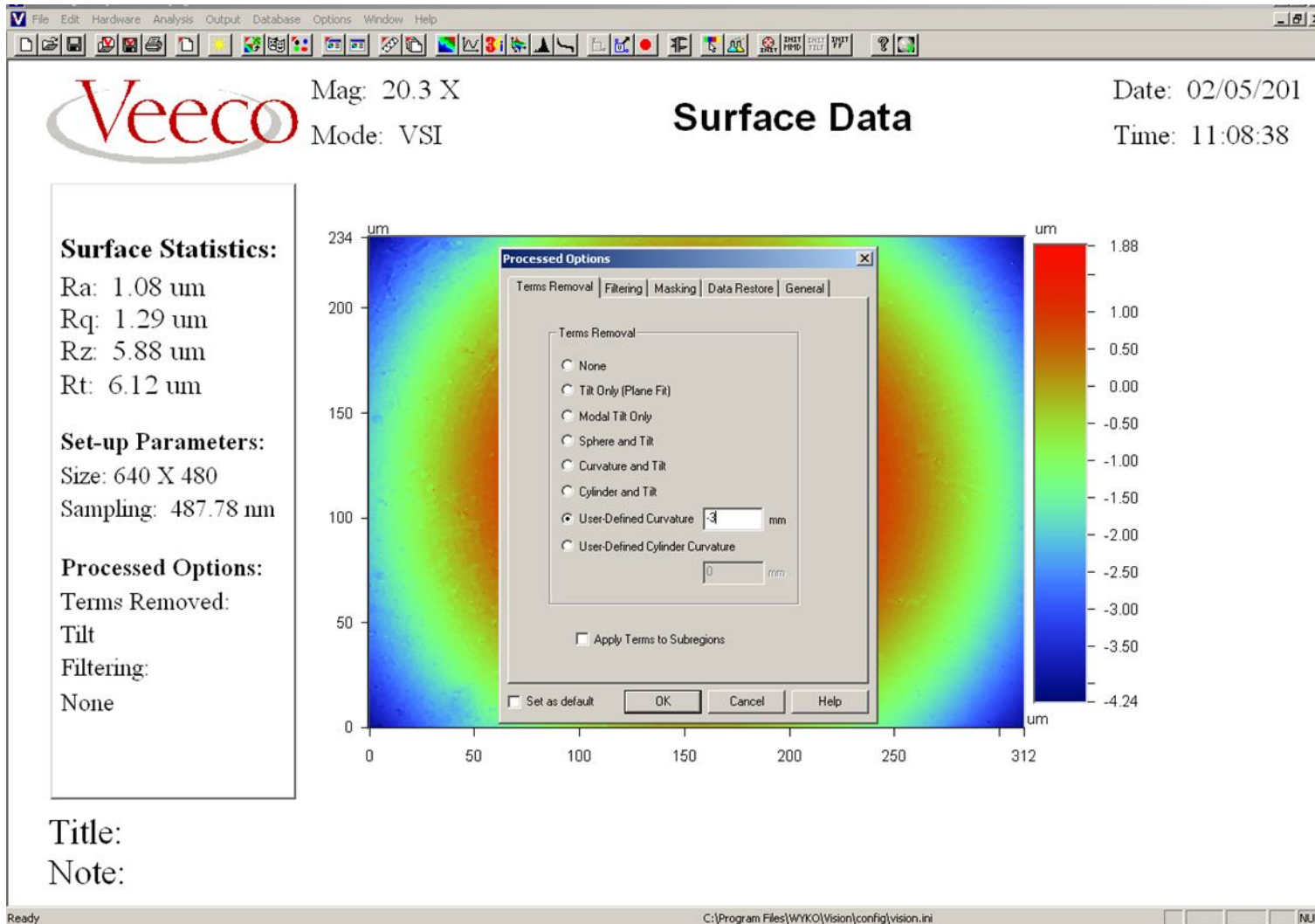
Define curvature to a minus value of the radius of the HFRR ball, which is -3.

This function is to remove tilt and natural curvature of the ball, which causes this spherical ball to appear flat.

In the case of MTM balls, defined curvature should be set to '-9.525'; while for flat disc surface 'Tilt only' should be selected.
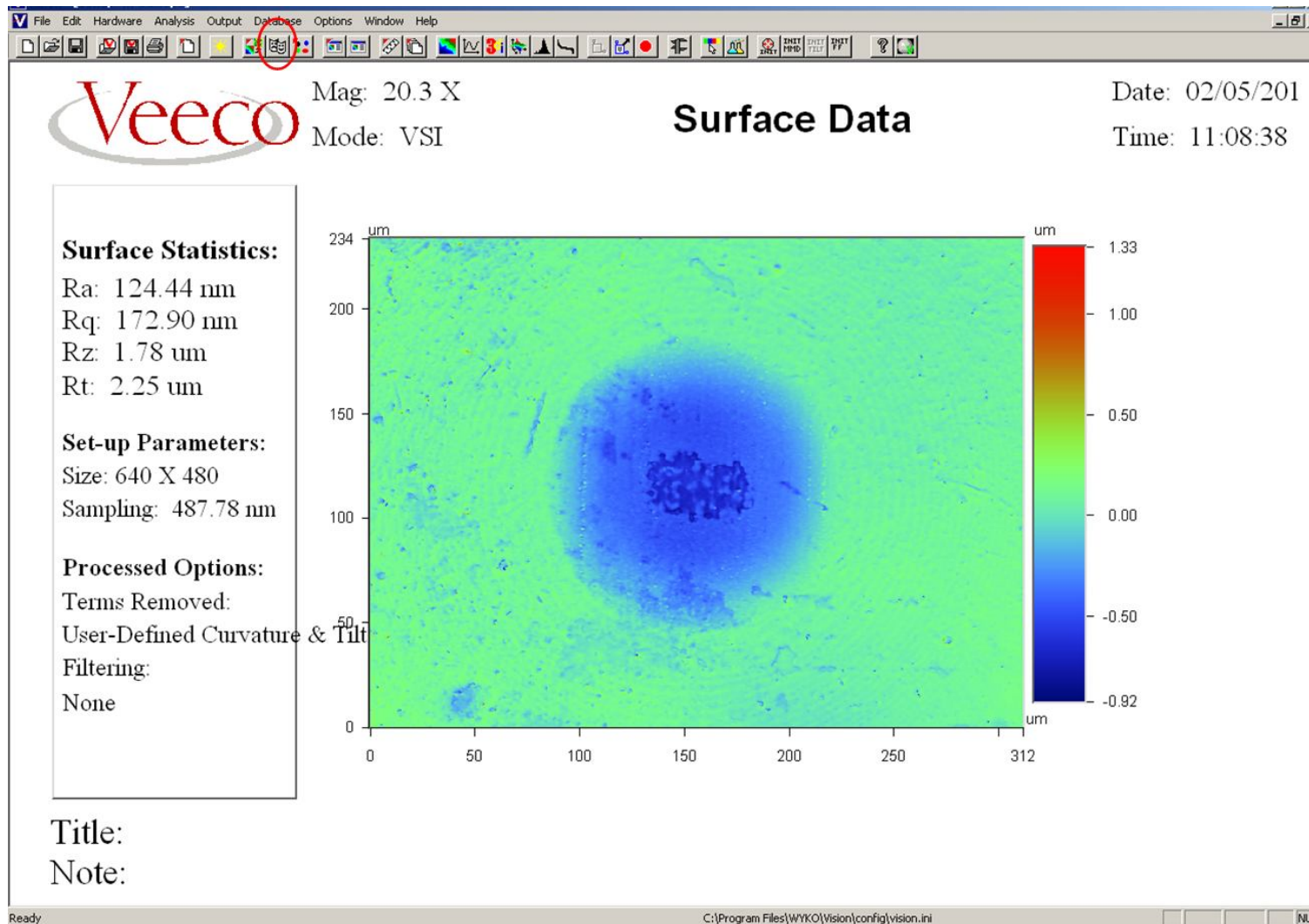
A flat presented surface of a HFRR ball is as shown in Figure A.4.

To obtain the wear volume, function named 'term mask' is required here. Click the red circled icon to complete this function.

**Figure A.4 Curvature-defined Surface Topography**

**Figure A.5 Masking Wear Scar**
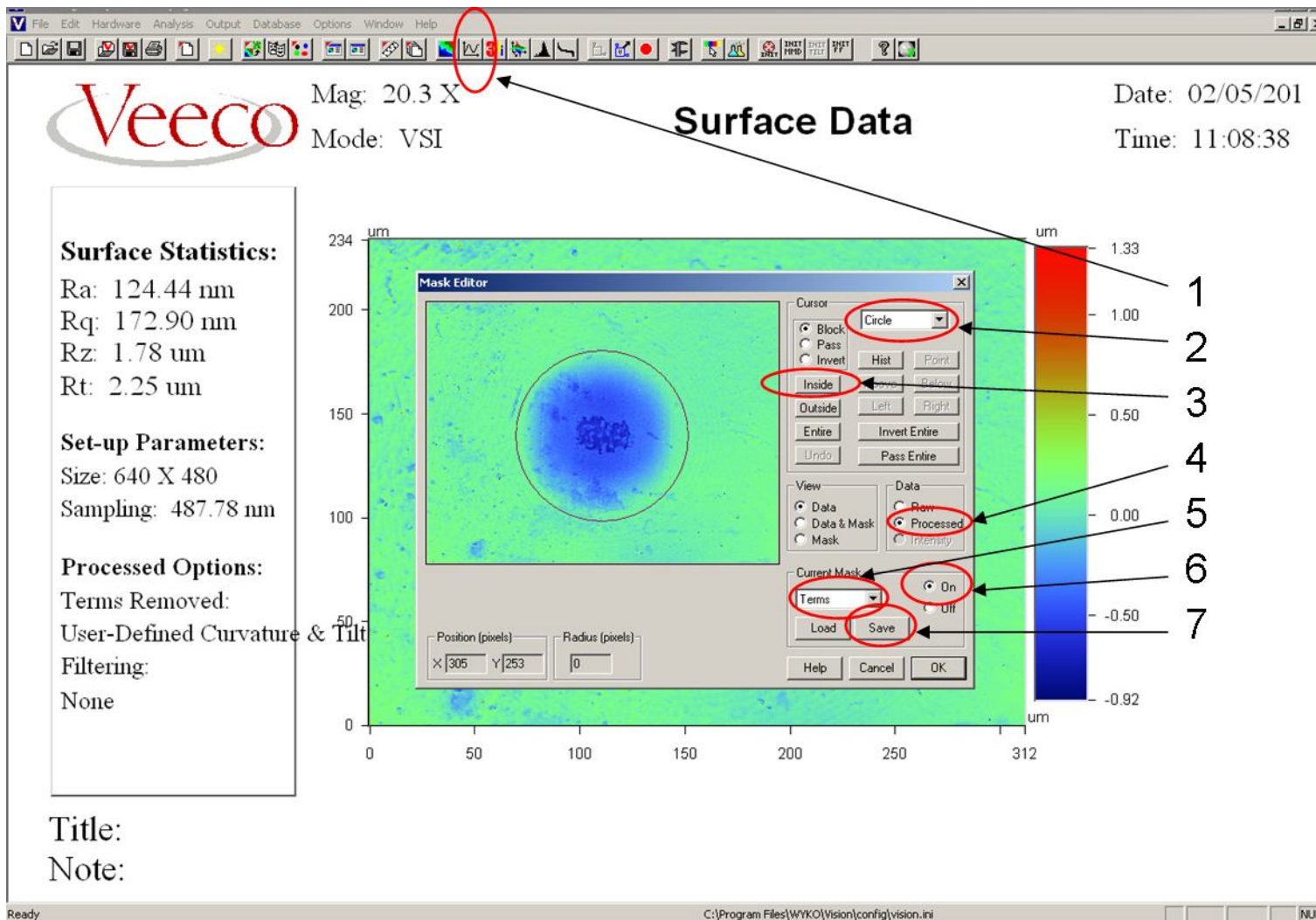
Click the 'Processed' icon in red circle 4 to apply masking on the processed image.

Select 'Circle' from the pull down menu in red circle 2. Draw a circle which can surround the whole wear scar region.

Click the 'Inside' icon to block the area inside the previously defined circle.

Select 'Terms' in red circle 5, turn on the term mask by clicking 'On' in red circle 6 and click 'save' in red circle 7.

Click the icon in red circle 1 to check 2D analysis.

**Figure A.6 2D Analysis on the Processed Surface Height Distribution Data**

Figure A.6 shows the 2D analysis result of the HFRR ball which is processed in advance. X and Y profiles show the height distribution along the red and blue line.

The height of the area out of the wear scar is roughly zero, which indicates that the 'mask' function has set the plane outside of the wear scar to the zero level. Then the accurate volume measurement can be completed by clicking the icon in the red circle.

**Figure A.7 Volume Calculations**

In Figure A.7, it shows several volume calculations, in which the negative volume is the volume occupied by the space between the zero level which is the outside of the wear scar, and the wear scar surface. Therefore, this negative volume is the required wear volume.
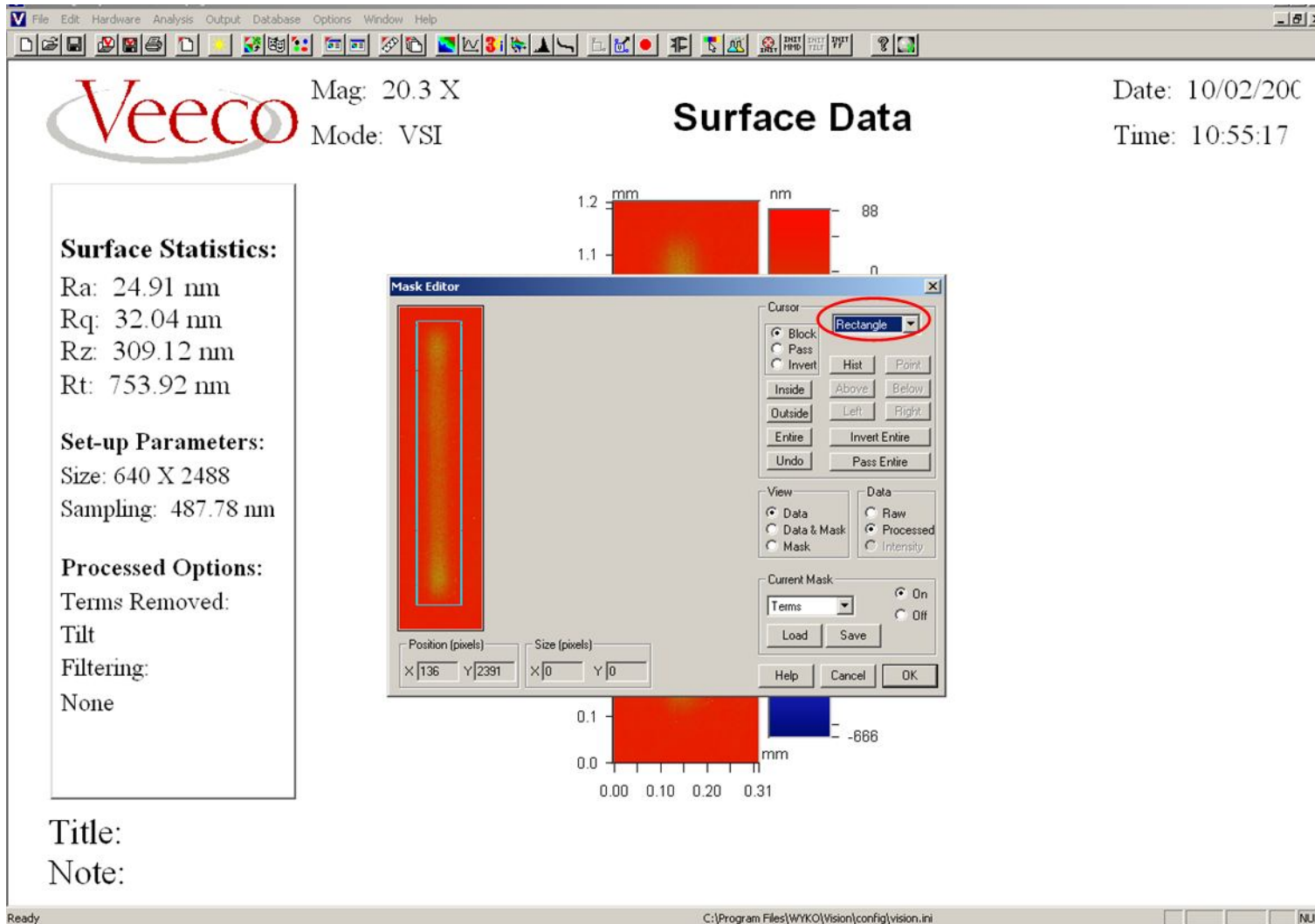
When it applies to a HFRR disc, the differences are mainly in two parts. One is choosing 'Tilt only' in the 'Analysis options' menu, while the other one is using rectangle to mask the worn area.
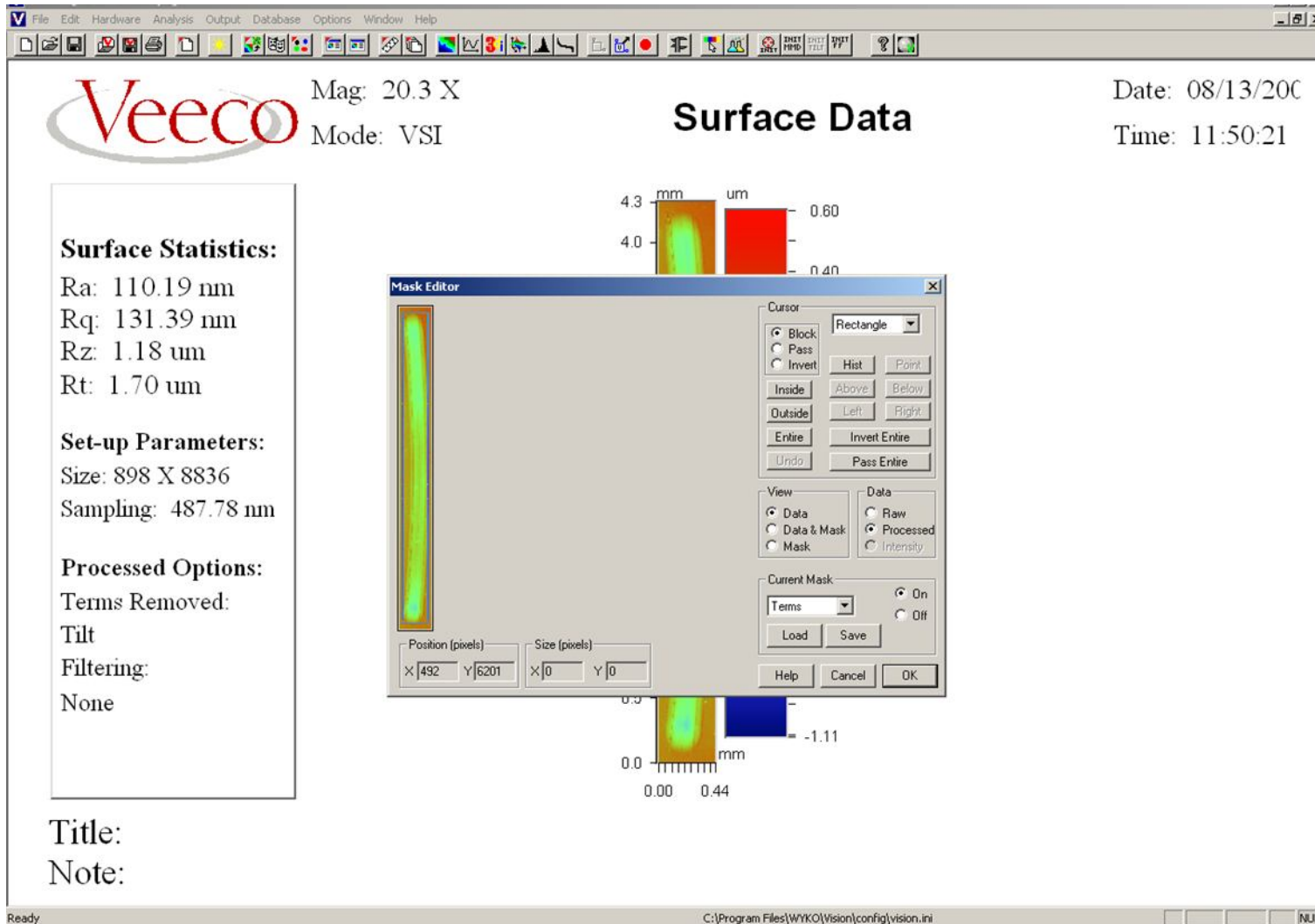
**Figure A.8 Analysis on HFRR Disc**

**Figure A.9 Analysis on MTM Ball**
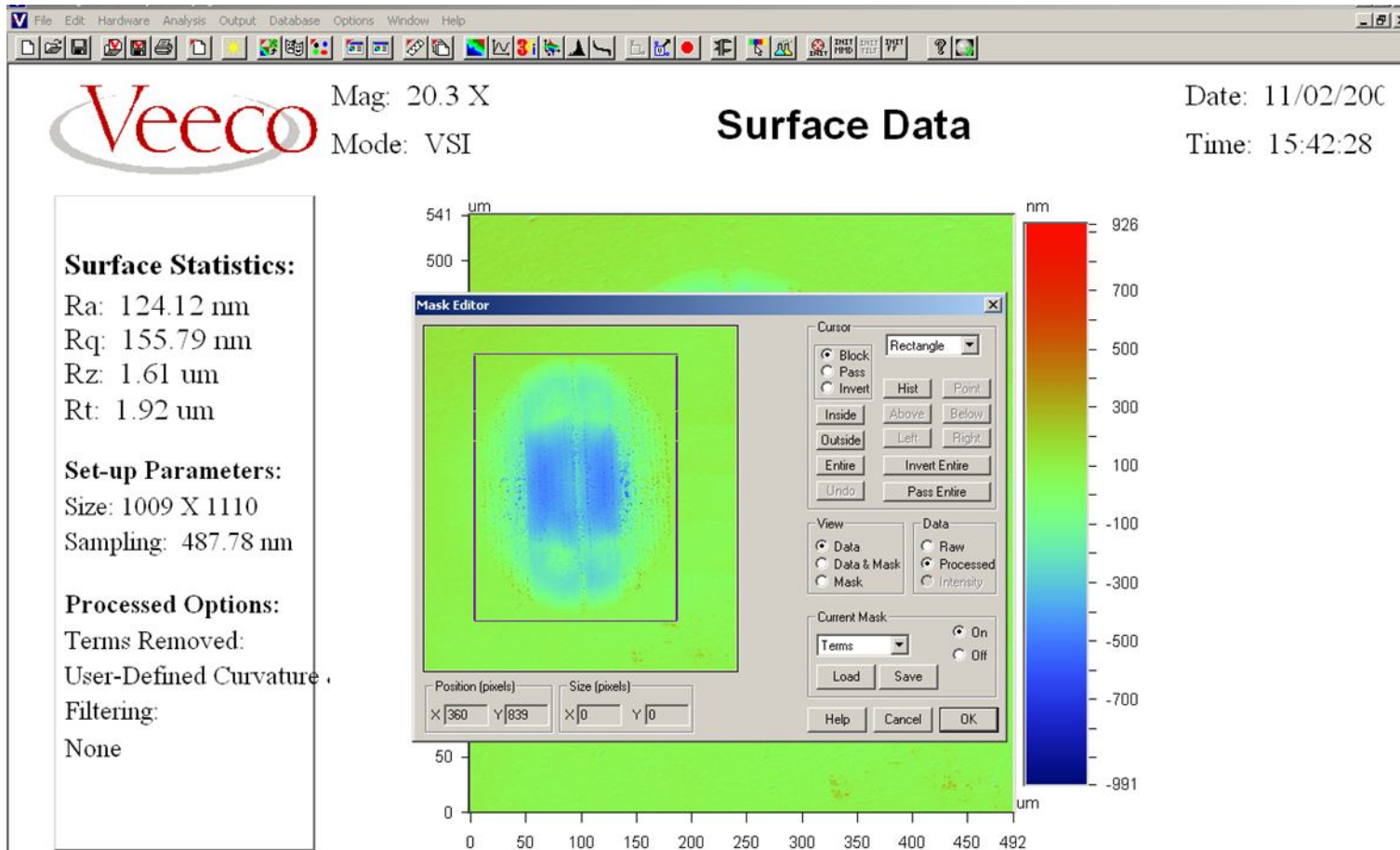
In the case that the worn area is irregular, appropriate shape should be selected to mask the whole worn area; otherwise the zero level will be mistakenly set, thus a wrong wear volume will be obtained.
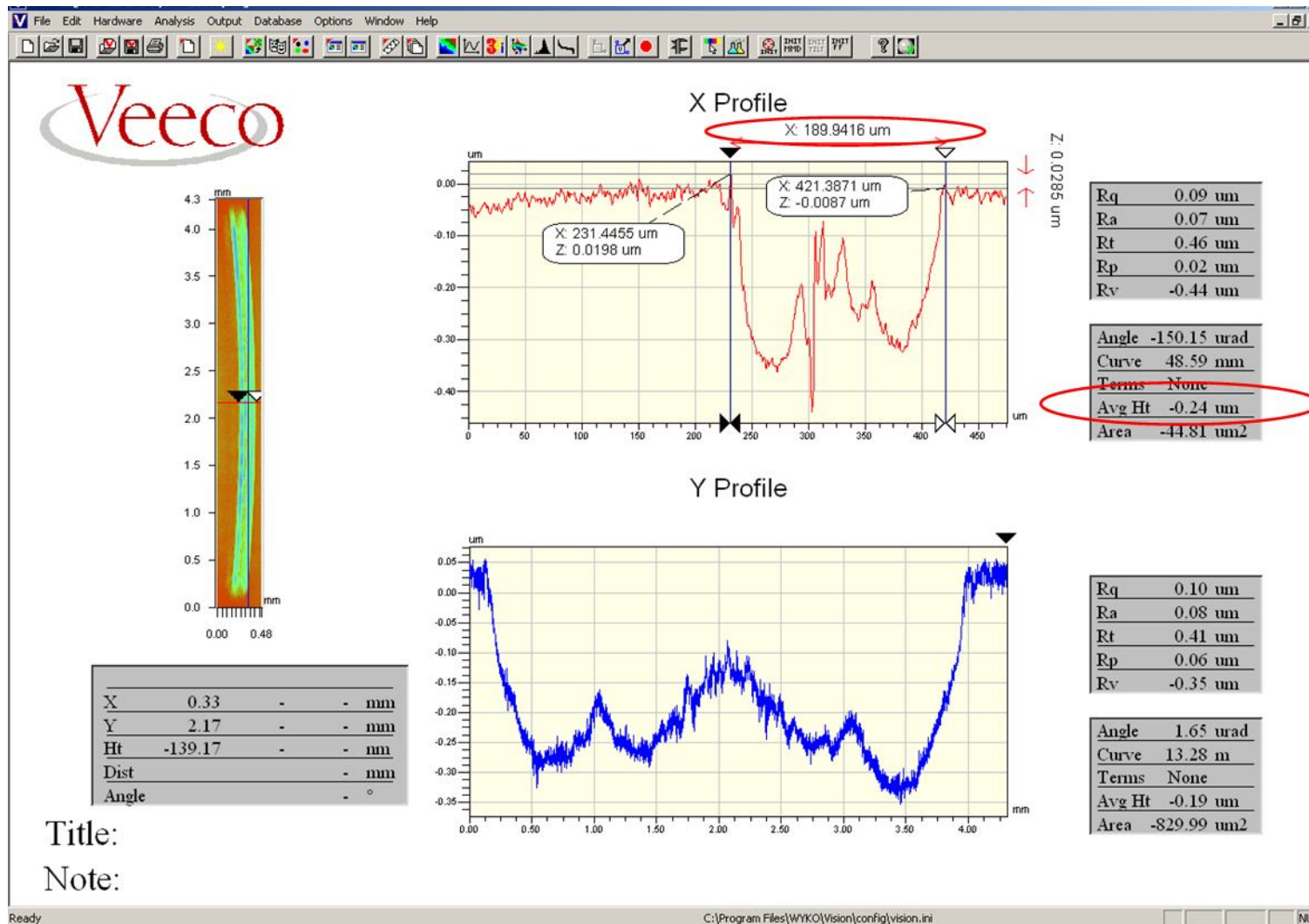
223

For curvy wear scar on the reciprocating MTM discs, rectangle can also be selected to block the worn area.

**Figure A.10 2D Masking wear track on MTM Disc**

**Figure A.11 2D Analysis on MTM Disc**

Besides the wear volume, the area of the worn strip on the disc can be calculated by further analyzing the 2D profiles.

After the zero level is set in advance, drag the two cursors in the X profile to both edges of the wear track. The area then can be calculated by multiplying the two absolute values in the two red circles, which are the average height and the width of the worn area.